

**Forest canopies and tree diversity:
from stands to tree-tree interactions**

Dissertation

zur Erlangung des
Doktorgrades der Naturwissenschaften (Dr. rer. nat.)

Der

Naturwissenschaftlichen Fakultät I
- Biowissenschaften -

der Martin-Luther-Universität Halle-Wittenberg,

vorgelegt

von Frau Maria D. Perles-Garcia

verteidigt am 14.11.2022

geprüft von

Goddert von Oheimb

Helge Bruelheide

Dominik Seidel

Trying to see the forest for the trees

Copyright notice

Chapters 3 and 4 have been either published in or submitted to international journals. Copyright is with the authors. Reprint of the presented material requires the authors' permissions, except for chapters 1 and 2, which have been published open access under the terms of the Creative Commons Attribution-NonCommercial License.

Table of contents

SUMMARY	9
ZUSAMMENFASSUNG	11
RESUMEN	13
INTRODUCTION	15
FOREST BIODIVERSITY AND ECOSYSTEM FUNCTIONING	15
REMOTE SENSING AS TOOL FOR FOREST RESEARCH – THE CASE OF TERRESTRIAL LASER SCANNER	18
BEF EXPERIMENTS	23
FIELD CAMPAIGN AND THESIS SCOPE	25
REFERENCES	28
CHAPTER I. TREE SPECIES RICHNESS PROMOTES AN EARLY INCREASE OF STAND STRUCTURAL COMPLEXITY IN YOUNG SUBTROPICAL PLANTATIONS	32
ABSTRACT	33
KEYWORDS	33
1. INTRODUCTION	33
2. MATERIAL AND METHODS	36
2.1. <i>Study site</i>	36
2.2. <i>Terrestrial laser scanning data</i>	37
2.3. <i>SSCI</i>	37
2.4. <i>Inventory-based structural indices</i>	38
2.5. <i>Statistical analyses</i>	38
3. RESULTS	39
4. DISCUSSION	42
4.1. <i>Temporal changes in TSR-stand structural complexity relationships</i>	43
4.2. <i>Relationship between TSR and inventory-based stand structural complexity indices</i>	44
4.3. <i>Role of density (MeanFrac) vs. vertical stratification (ENL) in the relationship between TSR and SSCI</i>	45
5. MANAGEMENT IMPLICATIONS AND CONCLUSIONS	45
ACKNOWLEDGEMENTS	46
CONFLICT OF INTEREST	46
AUTHORS' CONTRIBUTIONS	46
DATA AVAILABILITY STATEMENT	47
REFERENCES	48

CHAPTER II. NEIGHBOURHOOD SPECIES RICHNESS REDUCES CROWN ASYMMETRY OF SUBTROPICAL TREES IN SLOPING TERRAIN _____ 52

ABSTRACT _____	53
KEYWORDS _____	53
1. INTRODUCTION _____	53
2. MATERIALS AND METHODS _____	55
2.1. <i>Study Site</i> _____	55
2.2. <i>Terrestrial Laser Scanning Data</i> _____	57
2.3. <i>TLS Data Processing and Calculation of Crown Displacement</i> _____	57
2.4. <i>Explanatory Variables</i> _____	60
2.5. <i>Statistical Analyses</i> _____	62
3. RESULTS _____	62
4. DISCUSSION _____	64
5. CONCLUSIONS _____	66
INFORMATION ABOUT SUPPLEMENTARY MATERIALS _____	67
AUTHOR CONTRIBUTIONS _____	68
FUNDING _____	68
DATA AVAILABILITY STATEMENT _____	68
ACKNOWLEDGMENTS _____	68
CONFLICTS OF INTEREST _____	68
REFERENCES _____	68

CHAPTER III. TREE-TREE INTERACTIONS AND CROWN COMPLEMENTARITY: THE ROLE OF FUNCTIONAL DIVERSITY AND BRANCH TRAITS FOR CANOPY PACKING _____ 73

ABSTRACT _____	74
1. INTRODUCTION _____	74
2. MATERIALS AND METHODS _____	77
2.1. <i>Study area and experimental design</i> _____	77
2.2. <i>Scan design</i> _____	79
2.3. <i>TLS data processing</i> _____	80
2.4. <i>Quantitative structure modelling</i> _____	80
2.5. <i>Calculation of crown complementarity and explanatory variables</i> _____	81
2.6. <i>Statistical analysis</i> _____	82
3. RESULTS _____	83
4. DISCUSSION _____	85
DECLARATION OF COMPETING INTEREST _____	87
ACKNOWLEDGEMENTS _____	87
AUTHORSHIP _____	88

INFORMATION ABOUT SUPPLEMENTARY MATERIALS _____	88
REFERENCES _____	88
CHAPTER IV. BIOMASS ALLOCATION OF TREES IN RESPONSE TO MONO- AND HETEROSPECIFIC	
NEIGHBOURHOODS _____	93
ABSTRACT _____	94
KEYWORDS _____	94
1. INTRODUCTION _____	94
2. MATERIAL AND METHODS _____	96
2.1. <i>Greenhouse experiment</i> _____	96
2.2. <i>Field experiment (BEF China)</i> _____	97
2.3. <i>Statistical analysis</i> _____	100
3. RESULTS _____	100
4. DISCUSSION _____	103
ACKNOWLEDGEMENTS _____	105
REFERENCES _____	105
SYNTHESIS _____	110
MAIN FINDINGS _____	110
DISCUSSION _____	113
<i>Potential drivers of complexity on forest structure</i> _____	113
<i>Forest structure and ecosystem functioning</i> _____	115
<i>Limitations</i> _____	117
<i>Future implications</i> _____	117
REFERENCES _____	119
ACKNOWLEDGEMENTS _____	122
SUPPORTING INFORMATION _____	124
CHAPTER 1. TREE SPECIES RICHNESS PROMOTES AN EARLY INCREASE OF STAND STRUCTURAL COMPLEXITY IN YOUNG SUBTROPICAL PLANTATIONS _____	124
<i>Supporting Methods</i> _____	125
<i>Supporting Tables</i> _____	127
<i>Supporting Figures</i> _____	132
<i>References</i> _____	137
CHAPTER 2. NEIGHBOURHOOD SPECIES RICHNESS REDUCES CROWN ASYMMETRY OF SUBTROPICAL TREES IN SLOPING TERRAIN _____	138
<i>Supporting Methods</i> _____	139
<i>Supporting Tables</i> _____	140
<i>Supporting Figures</i> _____	144

CHAPTER 3. TREE-TREE INTERACTIONS AND CROWN COMPLEMENTARITY: THE ROLE OF FUNCTIONAL DIVERSITY AND BRANCH TRAITS FOR CANOPY PACKING	147
<i>Supporting Tables</i>	148
<i>Supporting Figures</i>	151
CHAPTER 4. BIOMASS ALLOCATION OF TREES IN RESPONSE TO MONO- AND HETEROSPECIFIC NEIGHBOURHOODS	153
<i>Supporting Tables</i>	154
<i>Supporting Figures</i>	156
APPENDICES	158
CURRICULUM VITAE	159
LIST OF PUBLICATIONS AND CONFERENCE CONTRIBUTIONS	161
DECLARATION OF ORIGINALITY - EIGENSTÄNDIGKEITSERKLÄRUNG	164

Summary

Subtropical forests represent a hotspot of terrestrial biodiversity on our planet, which is sustained by their physical structure. Stand and individual tree structure affects forest ecosystem functioning, as do the landscape conditions. How biodiversity affects ecosystem functioning has been studied for decades, but the pathways through which biodiversity (here understood as tree species richness) can alter stand and individual tree structure remain unclear.

In this thesis, I investigated the effects of tree species richness on three-dimensional (3D) stand and individual tree structure. To this end, I conducted a field campaign using terrestrial laser scanning (TLS) in the Biodiversity - Ecosystem Functioning plantation experiment "BEF China". I collected TLS point clouds from plots ranging from monocultures to 24-species mixtures, and from individual trees whose species richness ranged from monocultures to seven different tree species in the immediate neighbourhood. In the following four studies I related tree species richness or functional diversity to various stand and individual tree structure characteristics:

Chapter I. Here I examined how and why tree species richness affected the 3D structural complexity of stands over time. Tree species richness promoted structural complexity regardless of tree species identity by increasing vertical heterogeneity even in young plantations, and this effect became stronger over time. Based on these results, it is recommended that afforestation projects in subtropical areas use a large number of native species to promote structural complexity in these stands (and thus ecosystem functioning) from the beginning.

Chapter II. In the second chapter, I aimed to explain the reasons for the asymmetry of tree crowns. I found that, in addition to tree size, crown asymmetry was mainly influenced by competitive pressure from immediate neighbours. However, the neighbourhood tree species richness could stabilise this asymmetry, and this effect became stronger as the slope became steeper. Therefore, the study concludes that the use of a high tree species diversity can increase the mechanical stability of trees by avoiding canopy asymmetry, especially in plantations on steep slopes.

Chapter III. I then focused on the interactions between two individual trees (so-called tree species pairs (TSPs)) and tried to find out which tree traits increase crown complementarity. Functional dissimilarity as such, understood as differences in outer crown plasticity, showed

no effect on the crown complementarity index. However, the influence of heterospecific neighbours on crown complementarity was determined by differences in branch traits and by their interaction with functional dissimilarity. This study suggests that to understand crown complementarity one must consider not only at the differences in outer crown plasticity, but also at differences in inner crown plasticity.

Chapter IV. Finally, I wanted to consider the tree as a whole, and in the fourth study, I examined the patterns of above- and belowground biomass allocation between monospecific and heterospecific TSPs. To do this, first, in an *ex situ* experiment the above- and belowground biomass was destructively quantified one year after planting. A significant positive difference in both compartments was found for those trees planted in heterospecific pairs. Root to shoot ratios were also significantly higher in heterospecific pairs. Second, by estimating biomass density *in situ* over three years, I was able to observe how the root to shoot ratio changed: this decreased in heterospecific pairs due to a greater increase in aboveground biomass, while it increased in monospecific pairs due to a greater increase in belowground biomass. This study underscores the importance of tree-tree interactions and gives us clues to the mechanisms by which overyielding occurs in mixtures.

This thesis contributes to a deeper understanding of those mechanisms by which tree species richness affects forest structure and biomass allocation patterns. I show how increasing tree species richness in plantations can increase their complexity, stability, complementarity and productivity. These insights can help inform future planning for afforestation and reforestation projects, which are essential in the face of the ongoing climate crisis.

Zusammenfassung

Subtropische Wälder stellen einen Hotspot der terrestrischen biologischen Vielfalt auf unserem Planeten dar, die durch ihre physische Struktur aufrechterhalten wird. Die Struktur der Bestände und der einzelnen Bäume wirkt sich auf die Funktionsweise der Waldökosysteme aus, ebenso wie die Landschaftsbedingungen. Die Auswirkungen der biologischen Vielfalt auf das Funktionieren von Ökosystemen werden seit Jahrzehnten untersucht, aber die zugrundeliegenden Mechanismen, über die die biologische Vielfalt (hier verstanden als Baumartenreichtum) die Struktur von Beständen und Einzelbäumen verändern kann, sind noch unklar.

In dieser Arbeit habe ich die Effekte des Baumartenreichtums auf die dreidimensionale (3D) Bestandes- und Einzelbaumstruktur untersucht. Zu diesem Zweck führte ich eine Feldkampagne mit terrestrischem Laserscanning (TLS) im *Biodiversity - Ecosystem Functioning* (BEF)-Experiment "BEF China" durch. Ich sammelte TLS-Punktwolken von Untersuchungsflächen, die von Monokulturen bis zu Mischungen aus 24 Arten reichten, und von Einzelbäumen, bei denen der Artenreichtum in der unmittelbaren Nachbarschaft von einer bis zu sieben verschiedenen Baumarten reichte. In den folgenden vier Studien setzte ich den Baumartenreichtum oder die funktionelle Vielfalt mit verschiedenen Merkmalen der Bestandes- und Einzelbaumstruktur in Beziehung:

In Kapitel I untersuchte ich, wie und warum der Baumartenreichtum die strukturelle 3D-Komplexität von Beständen im Laufe der Zeit beeinflusst. Der Baumartenreichtum förderte die strukturelle Komplexität unabhängig von der Baumartenidentität, indem er die vertikale Heterogenität bereits in jungen Plantagen erhöhte, und dieser Effekt verstärkte sich mit der Zeit. Auf der Grundlage dieser Ergebnisse wird empfohlen, bei Aufforstungsprojekten in subtropischen Gebieten eine große Anzahl einheimischer Baumarten zu verwenden, um die strukturelle Komplexität in diesen Beständen (und damit die Funktionsweise des Ökosystems) von Anfang an zu fördern.

Kapitel II. Das zweite Kapitel zielt darauf ab, die Gründe für die Asymmetrie der Baumkronen zu erklären. Ich fand heraus, dass die Kronenasymmetrie neben der Baumgröße vor allem durch den Konkurrenzdruck der unmittelbaren Nachbarn beeinflusst wird. Der Baumartenreichtum in der Nachbarschaft konnte diese Asymmetrie jedoch stabilisieren, und dieser Effekt wurde umso stärker, je steiler der Hang wurde. Die Studie kommt daher zu dem Schluss, dass eine hohe Baumartenvielfalt die mechanische Stabilität

von Bäumen erhöhen kann, indem sie die Ausbildung einer stärkeren Asymmetrie der Baumkronen reduziert, insbesondere bei Anpflanzungen an steilen Hängen.

Kapitel III. Anschließend konzentrierte ich mich auf die Wechselwirkungen zwischen zwei Einzelbäumen (so genannte Baumartenpaare (*tree species pair* (TSP)) und versuchte herauszufinden, welche Baumeigenschaften die Komplementarität der Baumkronen erhöhen. Funktionale Unähnlichkeit als solche, verstanden als Unterschiede in der äußeren Kronenplastizität, zeigte keine Auswirkungen auf das Ausmaß der Kronenkomplementarität. Der Einfluss heterospezifischer Nachbarn auf die Kronenkomplementarität wurde jedoch durch Unterschiede in den Astmerkmalen und durch deren Wechselwirkung mit der funktionellen Unähnlichkeit bestimmt. Diese Studie legt nahe, dass man zum Verständnis der Kronenkomplementarität nicht nur die Unterschiede in der äußeren Kronenplastizität, sondern auch die Unterschiede in der inneren Kronenplastizität berücksichtigen muss.

Kapitel IV. Schließlich habe ich den Baum als Ganzes betrachtet, und in der vierten Studie untersuchte ich die Muster der ober- und unterirdischen Biomasseverteilung zwischen monospezifischen und heterospezifischen TSPs. Zu diesem Zweck wurde zunächst in einem ex situ-Experiment die ober- und unterirdische Biomasse ein Jahr nach der Pflanzung destruktiv quantifiziert. Es wurde ein signifikant positiver Unterschied in beiden Kompartimenten bei denjenigen Bäumen gefunden, die in heterospezifischen Paaren gepflanzt wurden. Auch das Verhältnis von unter- zu oberirdischer Biomasse war bei heterospezifischen Paaren signifikant höher. Zweitens konnte ich durch die Schätzung der Biomassedichte in situ über drei Jahre hinweg beobachten, wie sich das Verhältnis von unter- zu oberirdischer Biomasse veränderte: Es nahm bei heterospezifischen Paaren aufgrund einer größeren Zunahme der oberirdischen Biomasse ab, während es bei monospezifischen Paaren aufgrund einer größeren Zunahme der unterirdischen Biomasse zunahm. Diese Studie unterstreicht die Bedeutung von Baum-Baum-Interaktionen und gibt uns Hinweise auf die Mechanismen, durch die Überschusserträge in Mischungen entstehen.

Diese Arbeit trägt zu einem tieferen Verständnis derjenigen Mechanismen bei, durch die Baumartenreichtum die Bestandes- und Einzelbaumstruktur sowie die Verteilung der Baumbiomasse beeinflusst. Ich zeige, wie eine Erhöhung des Baumartenreichtums in Plantagen deren Komplexität, Stabilität, Komplementarität und Produktivität steigern kann. Diese Erkenntnisse können bei der künftigen Planung von Aufforstungs- und Wiederaufforstungsprojekten helfen, die angesichts der anhaltenden Klimakrise unerlässlich sind.

Resumen

Los bosques subtropicales representan una gran parte de la biodiversidad terrestre de nuestro planeta, el cual se sustenta en la estructura física de los mismos. La estructura de los árboles y las masas forestales afecta al funcionamiento del ecosistema del bosque, al igual que las condiciones del terreno. El modo en que la biodiversidad afecta al funcionamiento de los ecosistemas se ha estudiado durante décadas, pero los mecanismos por los que la biodiversidad (entendida aquí como riqueza de especies arbóreas) puede modificar la estructura de los árboles y los bosques siguen sin estar claros.

En esta tesis, he investigado los efectos de la riqueza de especies arbóreas en la estructura tridimensional de las plantaciones forestales y en la arquitectura de los árboles. Para ello, llevé a cabo trabajo de campo escaneando con un escáner de laser LiDAR terrestre (TLS) el experimento de Biodiversidad y Funcionamiento del Ecosistema "BEF China". Los datos recogidos, en forma de nube de puntos, incluían parcelas desde monocultivos hasta mezclas de 24 especies arbóreas, y árboles individuales cuyos árboles colindantes tenían una diversidad entre monocultivos hasta siete especies de árboles diferentes. Así, he investigado el efecto de la riqueza de especies arbóreas o la diversidad funcional en varias características de las plantaciones forestales y de la estructura arbórea:

Capítulo I. En este capítulo investigué cómo y por qué la diversidad arbórea afectaba a la complejidad estructural tridimensional de las plantaciones forestales a lo largo del tiempo. La diversidad de especies arbóreas, independientemente de la especie de los árboles, promovió la complejidad estructural mediante el aumento de la heterogeneidad vertical ya en las plantaciones jóvenes, y este efecto se fortaleció con el tiempo. Basándonos en estos resultados, recomendamos el uso de un gran número de especies nativas para los proyectos de forestación en zonas subtropicales, con el fin de promover su complejidad (y con ello, fomentar el funcionamiento del ecosistema) desde el inicio.

Capítulo II. En este segundo capítulo, me propuse explicar las razones de la asimetría en las copas de los árboles. Descubrí que, además del tamaño de los árboles, la asimetría de las copas estaba fomentada principalmente por la presión competitiva de los árboles colindantes. Sin embargo, la riqueza de especies en los árboles colindantes era capaz de estabilizar esta asimetría, y este efecto se hacía más fuerte a medida que la pendiente era más pronunciada. Por lo tanto, el estudio concluye que el uso de altos gradientes de diversidad de árboles puede aumentar la estabilidad mecánica de los mismos evitando la asimetría de las copas, especialmente en plantaciones en pendientes pronunciadas.

El capítulo III. A continuación, me centré en las interacciones entre dos árboles (llamados parejas de árboles, *tree species pairs* (TSPs)) e intenté desentrañar qué rasgos de los árboles aumentan la complementariedad de las copas. La disimilitud funcional per se, entendida como diferencias en la plasticidad de la copa exterior, no mostró ningún impacto en el índice de complementariedad entre las copas. Sin embargo, el impacto de las parejas heteroespecíficas en la complementariedad de la copa vino dado por diferencias en las características de las ramas, y por su interacción con la disimilitud funcional. Este estudio sugiere que para entender la complementariedad de la copa hay que fijarse no solo en las diferencias de plasticidad de la copa exterior, sino también en diferencias en la plasticidad interna.

Capítulo IV. Por último, quise investigar el árbol en su totalidad, y en este capítulo estudié los patrones de distribución de biomasa superficial y subterránea en parejas de especies arbóreas monoespecíficas y heteroespecíficas. Para ello, primero, en un experimento ex situ, medimos la biomasa superficial y subterránea mediante métodos destructivos tras un año de su plantación. Una significativa diferencia positiva fue encontrada tanto en la biomasa superficial como en la subterránea en aquellos árboles plantados en parejas heteroespecíficas. El ratio entre biomasa de raíces y superficial fue también significativamente mayor en parejas heteroespecíficas. Después, mediante la estimación de la densidad de biomasa in situ durante 3 años, pude observar cómo el ratio entre biomasa de raíces y superficial cambiaba: disminuyó en parejas heteroespecíficas debido a un mayor aumento de la biomasa superficial, mientras que en las parejas monoespecíficas aumentó debido a un mayor aumento de la biomasa subterránea. Este estudio pone de manifiesto la importancia de las interacciones árbol-árbol y nos da pistas sobre los mecanismos por los que se observa un aumento de rendimiento en los bosques mixtos.

Esta tesis contribuye a una mayor comprensión de aquellos mecanismos por los que la diversidad de especies arbóreas afecta a la estructura forestal y a los patrones de distribución de la biomasa del árbol. He mostrado evidencias de cómo aumentar la riqueza de especies arbóreas en una plantación puede incrementar su complejidad, estabilidad, complementariedad y productividad. Este conocimiento puede ayudar en la futura planificación de proyectos de plantación y reforestación, esenciales ante la actual crisis climática.

Introduction

Forest Biodiversity and ecosystem functioning

“Ten years to cultivate wood, a hundred years to cultivate a man” says a Chinese proverb. We need forests, but above all, we need to raise awareness for their conservation and for that, we need to study the effects of what we are doing to our world. We are facing the sixth mass extinction, and we are causing it (Ceballos et al., 2015). We are nearly eight billion people who depend on the ecosystem services we destroy. We have fragmented habitats, polluted water and soil, and released greenhouse gases into the atmosphere reaching, in the case of CO₂, 149% of the pre-industrial level (WMO - World Meteorological Organization, 2021). Biodiversity, understood as diversity within species, between species, and of ecosystems (Cooper & Noonan-Mooney, 2013), has traditionally been viewed as a response to ecosystem functioning, such that threats to ecosystems lead to biodiversity loss. And how does this loss affect the ecosystem functioning? In the last 30 years, many scientists have begun to study biodiversity not as a response but as a driver of the ecosystem functions, and this is how the so-called Biodiversity - Ecosystem Functioning (BEF) research have emerged.

Forest ecosystems are usually defined as areas with a minimum of 10% of tree crown cover (Chazdon et al., 2016) and represent 31% of the total land area of the planet (FAO, 2020). Forests provide us with multiple benefits, called ecosystem services. A remarkable one is carbon sequestration, since forests harbour 80% of the total biomass of terrestrial ecosystems (Fichtner & Härdtle, 2021). But forests also offer provisioning services, regulating services, and cultural services (Millenium Ecosystem Assessment, 2005). And, above all, they are the habitat for more than half of the Earth’s terrestrial biota (Latimer & Zuckerberg, 2017).

Depending on climatic conditions, forest ecosystems are classified into four main biomes: tropical, boreal, temperate, and subtropical, representing 45%, 27%, 16% and 11% of the total forest area, respectively (FAO, 2020). Tropical and subtropical forest constitute a hotspot of biodiversity. It is estimated that tropical forests host two thirds of the global biodiversity, and that species richness decline with latitude, reaching its maximum in the tropics and then in subtropical regions (Fichtner & Härdtle, 2021). However, they are also the biomes with the highest deforestation rates: the latest FAO report (2020) shows that, although the rate of deforestation has decreased compared to previous decades, it represents a global loss of 10.2 million hectares per year, 9.8 million hectares of which are in tropical and subtropical regions.

In this report, data on forest degradation was also processed for the first time. Some of the drivers that led to degraded forests included in the report were fires, plagues, and extreme weather events. Data from 2015 show that 3% of the global forest areas were reported as burned, 1.4% was affected by insects, 0.4% by diseases, and 0.3% by extreme weather events. Unfortunately, not all countries monitored this data, so the percentage affected is even higher. Knowing that due to climate change these events will proliferate, the need for global and multi-temporal monitoring is evident.

So, what can we do?

Conservation measures are important, especially in tropical and subtropical regions. Deforestation of these forests leads to large losses of biodiversity and ecosystem functioning, and it is not clear whether reforestation can counteract this (Lewis, Wheeler, et al., 2019; Veldkamp et al., 2020). Besides of conserving the primary forests, there may be potential on the planet for an additional 0.9 billion ha of canopy cover (Bastin et al., 2019). This number is controversial, and it is considered overrated, among other things because of land-use conflicts (Lewis, Mitchard, et al., 2019; Skidmore et al., 2019). Sloping areas tend to have low land-use conflicts, and establishing or restoring forests there contributes, apart from the economic benefits, to protect against erosion and for watershed preservation (Hou et al., 2020; Jagger & Pender, 2003; Lamb et al., 2005; Wenhua, 2004). For the moment, it appears that reforestation and afforestation policies are widely accepted, and the Bonn Challenge (2011) pretend to restore 350 million ha by 2030 in the context of combating climate change.

Letting forests regenerate naturally is the easiest way to restore degraded forests. To accelerate this process, protection policies can be applied to the area and native species can be planted. But how do we select the species?

Increasing evidence shows the positive effects of tree diversity on ecosystem functions of forests. Multiple studies from different biomes have reported aboveground overyielding in tree species mixtures compared to monocultures (Huang et al., 2018; van der Plas, 2019). The mechanisms leading to this overyield may have to do with changes in tree architecture that facilitate canopy packing (Guillemot et al., 2020; Kunz et al., 2019; Van de Peer et al., 2017; Williams et al., 2017). Tree species richness also improves resilience (Messier et al., 2021) and stability (Schnabel et al., 2021) of the forests. Much less is known about the effects of tree species richness on belowground biomass, and although a positive effect seems to be observed, there is no consensus on this (Trogisch et al., 2021).

However, plantations usually consist of one or two introduced tree species, planted in a regular grid and belonging to the same age class. The area of plantations is growing year by year. More than 290 million ha, a 7% of the world forest area, were estimated as planted forest in 2020. This is an area 70% larger than in the early 1990s (FAO, 2020). There are several advantages associated with this approach: usually a focus is on fast-growing species with short rotation period, all resources can focus in the desired service (for instance growth rate or wood quality), and such plantations are easier to establish, maintain and harvest (Liu et al., 2018).

Liu et al. (2018) also mention the negative effects: Because of this ease of harvesting, usually carried out with (heavy) machinery, it is common that soil compaction occurs. Other disadvantages include increased risk of plagues and adverse effects of extreme weather events. In addition, many of the tree species most commonly used in these plantations modify soil pH and have high water requirements, which can affect water supply. They also harbour less biodiversity, not only because of homogeneity in tree species, but also in stand structure: regularly planted, even-aged plantations show low stand structural complexity (Ehbrecht et al., 2017). Lewis et al. (2019) estimated that natural forests store 40 times more carbon than plantations. However, they also stated that carbon storage in plantations can be increased by using different tree species, but research on this topic is scarce.

Diversity has an impact on ecosystem functioning not only because of species or functional diversity, but also due to the diversity of structural elements. Branching patterns affect productivity, and structural diversity has also shown effects in microclimate and species interactions across the trophic levels (Forrester & Bauhus, 2016; Schuldt et al., 2019). In European forests, heterogeneous stands have shown more resistance against extreme weather events (Dobbertin, 2002), and increasing structural diversity seems one of the pathways to increase resilience to address the impacts of climate change (Seidl et al., 2016). Fahey et al. (2018) also related structural complexity to resilience and adaptive behaviour comparing silvicultural experiments from temperate zones. However, studies about structure of tropical and subtropical plantations are scarce.

Therefore, for afforestation projects and reforestation of degraded forests, it is important to manage for complexity. But what makes a complex forest?

Unmanaged stands can develop greater structural complexity as a response of the changes affecting the forest (Puettmann et al., 2003). An unmanaged forest can develop in many ways, while the structural development of managed forests is more limited (Jandl et al., 2019). However, Ehbrecht et al. (2017) found higher complexity values in uneven-aged

managed stands, which may be due to the difference in tree sizes both in height and diameter. This suggests that managed plantations can harbour the same or higher structural complexity than unmanaged forests. In their case, which were temperate forests, the immature forests were less complex, perhaps due to less presence of branches along the vertical profile. However, these studies focus on already developed natural forests, mostly from temperate zones. Then, how do we promote complexity in new plantations?

Trees are long-lived structural elements, and therefore it is important to understand how complexity evolves over time and what factors promoted it in early stages. Ehbrecht et al. (2017) showed that tree diversity foster structural complexity. This could be due to the different shapes of the trees or optimisation of canopy spacing due to complementarity, which would lead to the overyielding of the above-mentioned mixtures. However, the mechanisms by which diversity affects the three-dimensional (3D) structure of trees remain unclear. Does diversity modify vertical or horizontal stand structure? How do trees change shape in relation to their neighbours? Do branch traits affect complementarity? Do trees change their biomass allocation patterns depending on their direct neighbours? And, to understand it, how can we measure the 3D architecture of the forest?

Remote sensing as tool for forest research – the case of terrestrial laser scanner

Forest inventories provide accurate and up-to-date information on forest resources that are essential for the sustainable management of the forest. The problem of traditional forest inventories is that they are costly, tedious, and it cannot be applied to some areas because they are inaccessible. Furthermore, some values relevant to the understanding of the forest, such as the volume of a tree, can only be measured accurately by destructive methods. Remote sensing englobes state of the art technologies with the only common characteristic of non-contact recording from the ultraviolet, visible, infrared, and microwave regions of the electromagnetic spectrum (Fussell et al., 1986). The term emerged in the early 1960s to speak about interpretation of aerial pictures by multispectral cameras. Since then, it has been widely used in ecology: changes in land cover (deforestation, quantification of crop growth), estimation of the biomass of forest stands, spatio-temporal variation in ecosystem services values are some of the examples offered in the review from de Araujo Barbosa (2015), sometimes in combination with machine learning algorithms.

One of the biggest role of remote sensing for forest research is its contribution to the temporal and the spatial scale. Time series allow to study the changes across ecosystems,

and the remote sensing can records from near global scales to really close regional scales at very high resolutions (Kerr & Ostrovsky, 2003).

Remote sensing has been widely used in the estimation of ecosystem carbon fluxes, even succeeding in estimating soil organic carbon by applying indices to multispectral images or by direct classification of belowground photographs acquired thanks to the installation of a minirhizotron (Rewald & Ephrath, 2013; Xiao et al., 2019).

When it comes to carbon fluxes and, in particular, the estimation of aboveground biomass, it is worth highlighting the emergence of light detection and ranging (LiDAR) technology. Since Lefsky et al. (1999) first used a laser scanner LiDAR on an unmanned aerial vehicle (UAV) to quantify forest biomass on a regional scale, research with this technique has grown in popularity. This is not surprising: Zolkos et al. (2013) showed in a meta-analysis that LiDAR estimations of aboveground biomass were significantly more accurate than metrics derived from optical or radar sensors.

LiDAR sensors are active remote sensing devices that emit laser pulses to determine the distance between the sensor and the surfaces. They collect georeferenced points with x, y, and z coordinates and the reflectance intensity of the laser beam in the object (Rashidi et al., 2020). Therefore, it provides precise 3D information. The point clouds can be acquired from spacecraft, aircraft, mobile and terrestrial laser scanner. Airborne laser scanners (ALS) have been widely used for biomass estimation, however, they deal with some inaccuracies recording the inner structure of the tree and its branches due to occlusion. Here, I will focus on close range LiDAR: Terrestrial Laser Scanning (TLS).

TLS was developed in the 1990s as a survey method, as it gives structural information on a millimetre scale. Since then, several commercial brands have contributed to its development, such as RIEGEL, FARO or Leica (Disney et al., 2019). The devices have improved in terms of portability in particular. For example, the FARO Photon Scanner used in the 2012 and 2013 campaigns has the same resolution as the FARO Focus S120, but weighed 10 kg more (Supplementary Table from Chapter II). Another important breakthrough, especially for forestry, is the speed: These devices were designed for the study of fixed structures, but in the case of forests, the speed of the scanner will reduce the noise caused by the movement of branches and leaves due to the wind. Fig. 1 shows the 3 scanners that were considered for this study (Riegl VZ400i, FARO Focus 3D S120, and Leica BLK360), a table with the main characteristics of each one, and a sample of the point cloud of a tree derived from each of them. Despite being the most portable, more ghost points are observed in the Leica compared to the FARO and to the RIEGEL, which gives the most accurate results. For this

study, the FARO scanner was chosen based on criteria of portability and consistency with previous campaigns.

Applications of TLS to forestry can be classified into three categories: (i) measurements that can be taken by traditional inventories but for which TLS can be faster and more accurate, such as height or DBH; (ii) measurements that would require very indirect or destructive methods, such as crown area and shape or volume; and (iii) measurements that can only be made with TLS, such as branch interactions or characterisation of the surroundings (Disney, 2019).

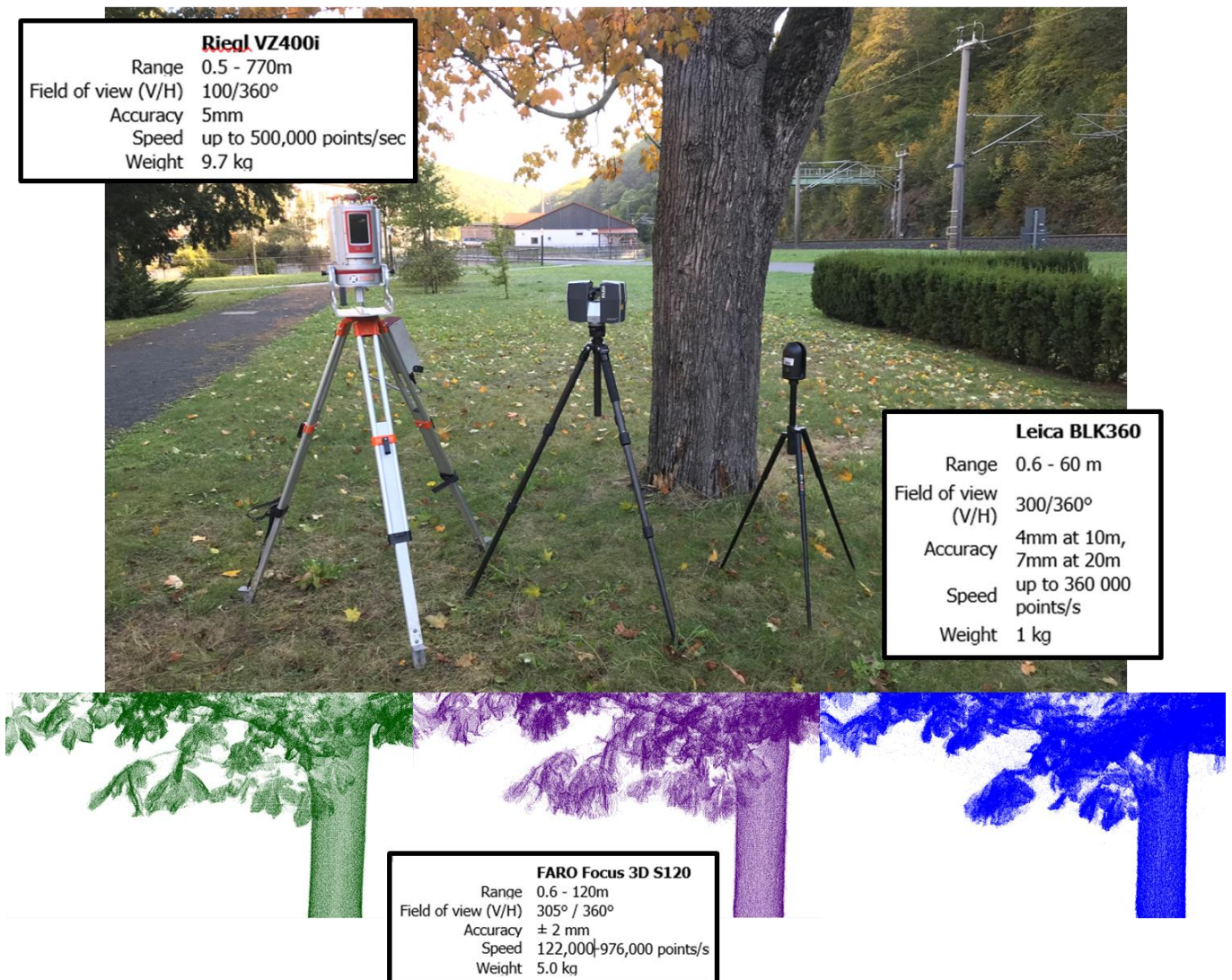


Figure 1. From left to right, Riegl VZ400i, FARO Focus 3D S120, and Leica BLK360 scanners (above) and the derived point cloud from a chestnut of each of them (below). Tables show the main characteristics of the scanners.

However, the processing of this data is very time-consuming: point clouds are large tables of points, which require specific software to process them. Although algorithms exist to automate tree extraction automatically, it is more accurate manually. The most accurate

models for deriving volume and exact shape of branches, quantitative structure models (QSM), require long and complex rendering. Figure 2 shows the workflow that was used for the different chapters of this study.

All of the above applications have been used in natural forests, but very rarely in plantations. But how do we isolate the effect of diversity on forest structure?

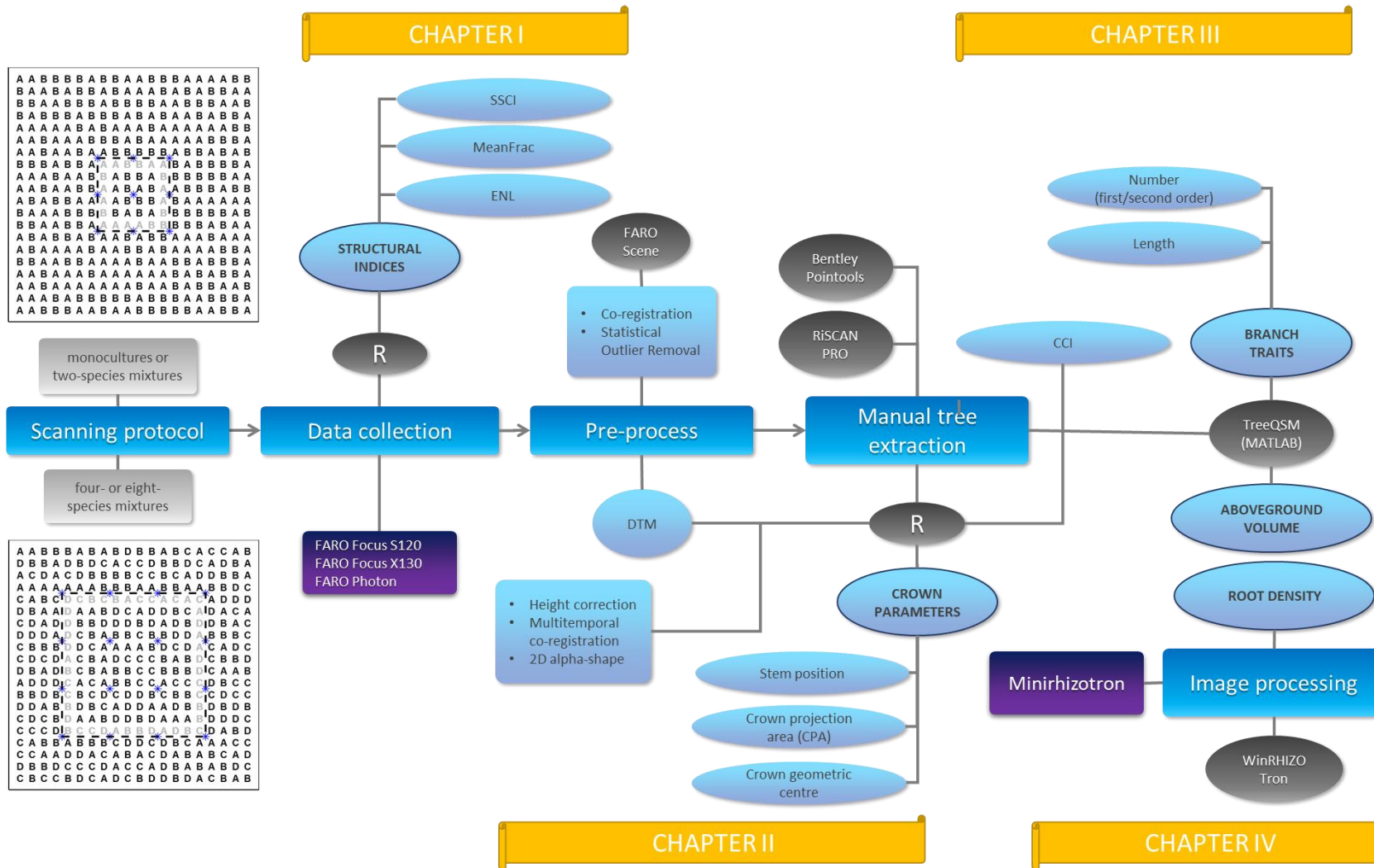


Figure 2. Workflow of data preparation. Schematic representation of the scanning protocol is adapted from Kunz et al. (2019). There, blue asterisks represent scanning positions, and letters indicate different tree species. Black circles show the used software. Outcomes are in light blue circles. Main processes are in blue squares and the instruments used are in a purple square.

BEF Experiments

To understand effects of diversity and advance in BEF research, BEF experiments manipulate species richness by comparing high levels of diversity with communities where richness is gradually reduced. The first experiments were carried out in microcosms and grasslands, but interest quickly expanded to other ecosystems (Bruehlheide et al., 2014). Thus, two decades ago, the first experiments to study the effects of tree diversity, in terms of species, genetic, or functional diversity, on ecosystem functioning started to be established. These experiments usually consists of even-aged stands of trees planted in regular rows on different plots, ranging from monocultures to high levels of diversity, sometimes in combination with shrubs (Grossman et al., 2018).

TreeDivNet is a global experimental network including tree BEF experiments of boreal, temperate, Mediterranean, tropical and subtropical biomes. These tree experiments cover more than 800 ha around the globe, and more than one million trees have been planted (Grossman et al., 2018). The results of these experiments have been published in hundreds of peer-reviewed papers, and the number continues to increase over the years. The effects of diversity in the ecosystem functioning become more noticeable over time (Jucker et al., 2020), especially in slow-growing organisms as trees, so to understand them it is important to monitor these experiments over time, especially now that these plantations are reaching maturity.

Here I will focus on an experiment established in the subtropical biome of Asia, which represents the highest net productivity of the Asian biomes (Yu et al., 2014). Specifically, this study was conducted in BEF China.

BEF China is located in Jianxi province, in the southeast of China, in the town of Xingangshan (Fig. 3). It was planted in a hilly area with slopes up to 45 degrees, to also study the effects of diversity to erosion. The main soil types are Cambisols and Regosols. It also presents Acrisols through the slopes and Regosols in the valleys (Scholten et al., 2017). It has subtropical climate, with a dry season and a monsoon season, and, averaging from 1971 to 2000, a mean annual temperature of 16.7°C and mean precipitation of 1,821 mm/year (Yang et al., 2013)

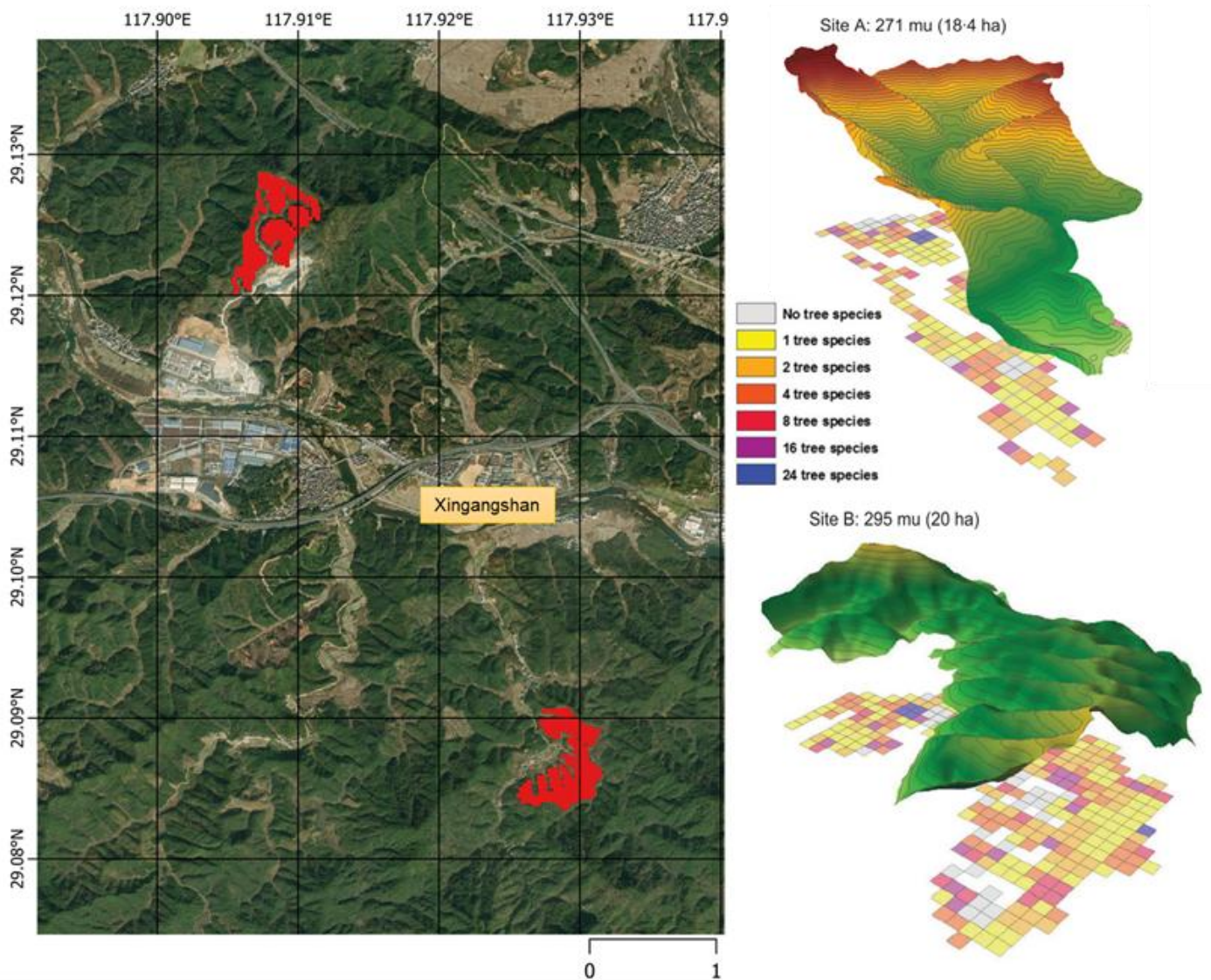


Figure 3. Location of BEF China (left) and representation of sites A and B showing the arrangement of plots with different tree species levels, adapted from Perles-Garcia et al (2022) and Bruelheide et al (2014)

Bruelheide et al. (2014) described in detail the design of the experiment: In total, it comprises 38.4 ha distributed over two sites. Site A was planted in 2009 and site B in 2010. Trees were planted in plots of 20 x 20 with a distance of 1.29m between them. It is divided in 566 plots of 25.8 x 25.8 m, in each plot 400 trees were planted in a regular grid with a distance of 1.29 m between them. This high density increases opportunities for early interactions.

It is the tree BEF experiment with the largest species pool so far: 40 native broadleaved tree species that were planted in plots ranging from monoculture to 24 species mixtures. Richness levels were randomly assigned to the plots, and to ensure a balanced design, species mixture models were established following the broken-stick model with a 16 species pool in random and non-random extinction scenarios. Species were also randomly assign to

planting positions within the plot. Here we mainly analysed the “very intensively studied plots” (vip) from the random extinction scenario, which comprises the species shown in Figure 4, and the replicates of these plots.

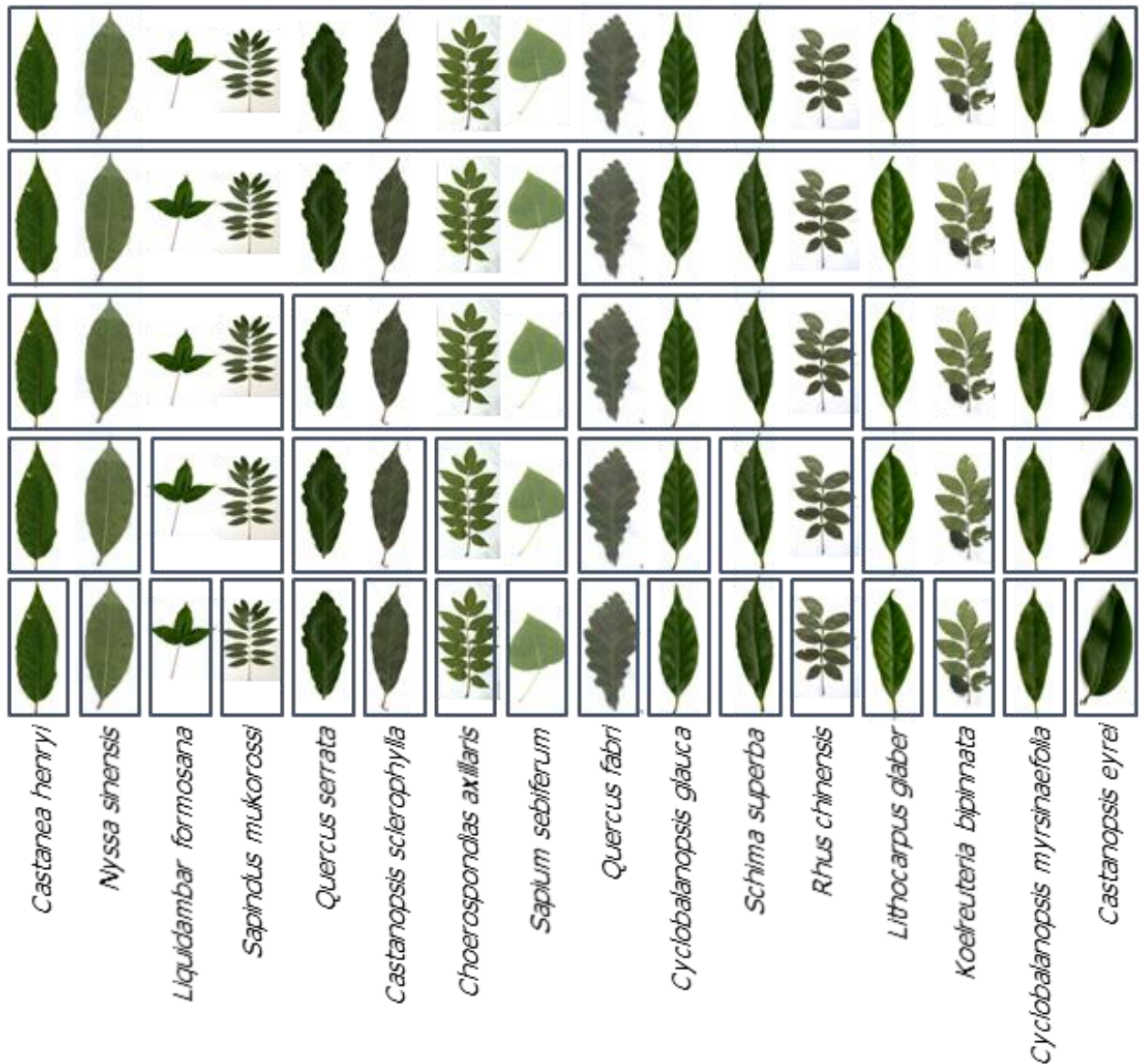


Figure 4. Random extinction scenario partition design, following the broken-stick procedure. Adapted from Bruelheide et al. (2014)

Field campaign and thesis scope

In this dissertation, I have investigated the effects of tree diversity on the 3D structure of an even-age subtropical plantation planted on steep slopes on a regular grid. I used different spatial resolutions, analysing from the plot level of the stand structure to the architecture of the tree and how it is shaped by the tree-tree interactions. I also studied the effect of slope on crown asymmetry, how functional dissimilarity affects complementarity, and the biomass

allocation patterns above- and belowground, both, under control conditions in an ex-situ greenhouse experiment, and the development over time in-situ in the plantation. To do so, I conducted a TLS field campaign in February 2019. Together with two student assistants and two local workers, we went to 96 plots. We carried a FARO Focus S120 and a FARO Focus X139 laser scanner. In addition, we brought reflectance reference targets for the co-registration of the scanners: 16 polystyrene spheres ($r = 7\text{cm}$), and three quadratic checkerboards of 45 cm edge length.

Between February, March and April 2019, we conducted scans to measure the structural complexity of 96 plots of which 49 were analysed in the Chapter I. We scanned the structure of all trees in the core area of 52 plots, 15 of which had high tree diversity (see difference in scanning protocol in Fig. 2). From them, the trees from 30 plots were analysed in Chapter II. In addition, to study tree-tree interactions we went to scan 467 tree species pairs (TSPs), from which 182 were analysed in Chapter III. In this case, we followed a closer range scanning protocol, performing from three to six scans per TSP. Furthermore, I analysed TLS data from previous years (Chapters I, II, and IV), and data from an ex-situ experiment (Chapter IV). These data were used to unravel the mechanisms by which tree richness affects stand structure.

First, in Chapter I, I and my colleagues tested whether increasing the tree species richness affects stand structural complexity over time, and if this effects are mediated by changes in density of structural elements or in the vertical stratification. In Chapter II we focused on tree crown asymmetry from a two-dimensional perspective and analysed whether it was a response to slope, to pressure from direct neighbours, and whether tree richness was able to modify these effects. In Chapter III we wanted to understand tree crown interactions from a 3D perspective, so we focused on tree-tree complementarity and tried to disentangle how it was affected by functional dissimilarity between species. Finally, in Chapter IV we aimed to look at the whole tree structure, including belowground biomass. We wanted to explore whether tree-tree interactions could affect biomass production or modify the biomass allocation patterns between above- and belowground structures. These research questions are summarize in Fig. 5.

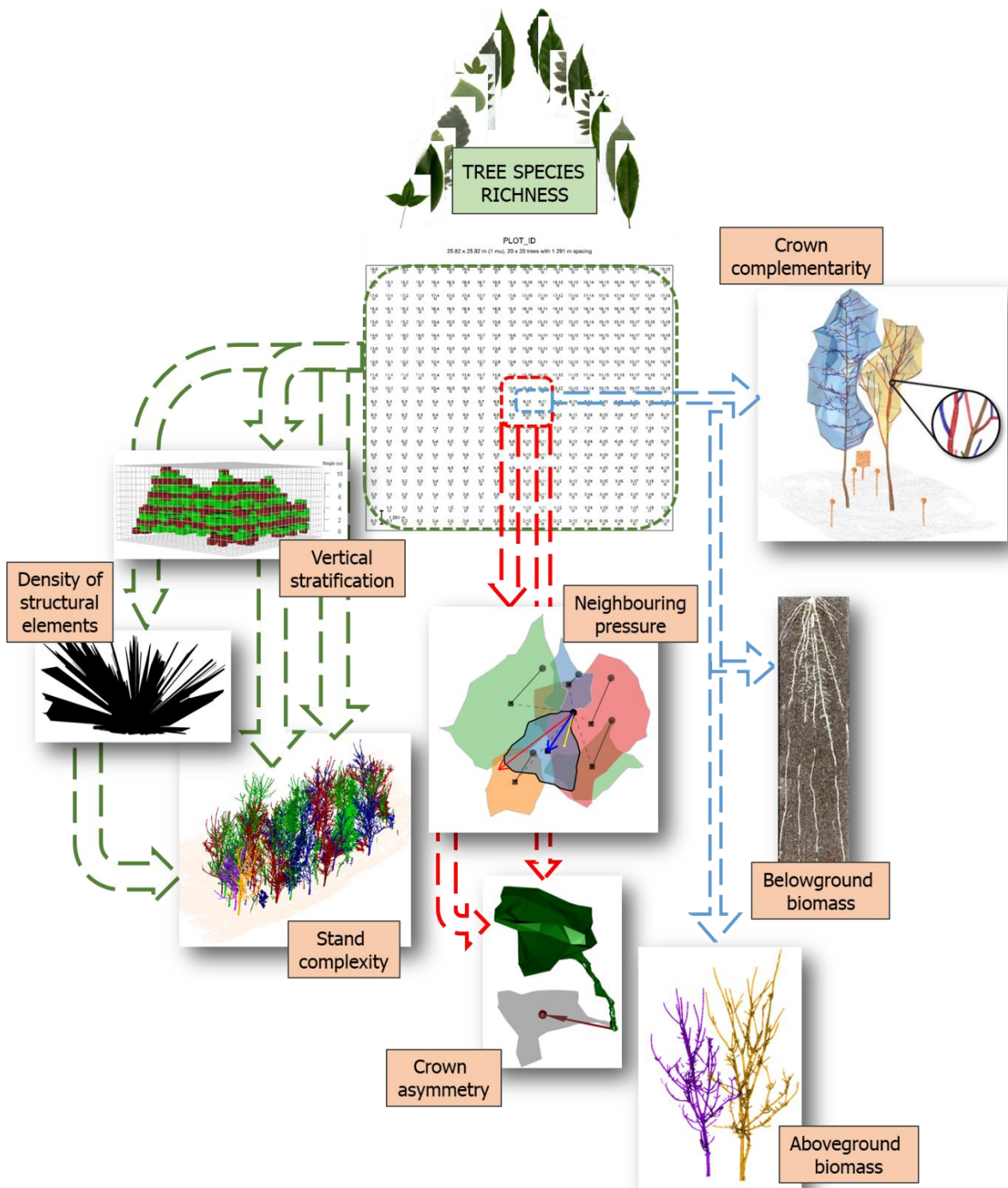


Figure 5. Conceptual figure: Research questions of the effects of tree species richness (TSR) on different structural parameters. Green arrows represent the path between TSR and structure complexity (vertical stratification and density of structural elements, Chapter I); red arrows represent the path way between TSR, neighbourhood pressure and crown asymmetry (Chapter II); blue arrows represent the path way between TSR and crown complementarity (Chapter III), and above- and belowground biomass (Chapter IV).

References

- Bastin, J.-F., Finegold, Y., Garcia, C., Mollicone, D., Rezende, M., Routh, D., Zohner, C. M., & Crowther, T. W. (2019). The global tree restoration potential. *Science*, *365*(6448), 76–79. <https://doi.org/10.1126/science.aax0848>
- Bruehlheide, H., Nadrowski, K., Assmann, T., Bauhus, J., Both, S., Buscot, F., Chen, X. Y., Ding, B., Durka, W., Erfmeier, A., Gutknecht, J. L. M., Guo, D., Guo, L. D., Härdtle, W., He, J. S., Klein, A. M., Kühn, P., Liang, Y., Liu, X., ... Schmid, B. (2014). Designing forest biodiversity experiments: General considerations illustrated by a new large experiment in subtropical China. *Methods in Ecology and Evolution*, *5*(1), 74–89. <https://doi.org/10.1111/2041-210X.12126>
- Ceballos, G., Ehrlich, P. R., Barnosky, A. D., García, A., Pringle, R. M., & Palmer, T. M. (2015). Accelerated modern human-induced species losses: Entering the sixth mass extinction. *Science Advances*, *1*(5), 9–13. <https://doi.org/10.1126/sciadv.1400253>
- Chazdon, R. L., Brancalion, P. H. S., Laestadius, L., Bennett-Curry, A., Buckingham, K., Kumar, C., Moll-Rocek, J., Vieira, I. C. G., & Wilson, S. J. (2016). When is a forest a forest? Forest concepts and definitions in the era of forest and landscape restoration. *Ambio*, *45*(5), 538–550. <https://doi.org/10.1007/s13280-016-0772-y>
- Cooper, D. H., & Noonan-Mooney, K. (2013). Convention on Biological Diversity. In *Encyclopedia of Biodiversity* (pp. 306–319). Elsevier. <https://doi.org/10.1016/B978-0-12-384719-5.00418-4>
- De Araujo Barbosa, C. C., Atkinson, P. M., & Dearing, J. A. (2015). Remote sensing of ecosystem services: A systematic review. *Ecological Indicators*, *52*, 430–443. <https://doi.org/10.1016/j.ecolind.2015.01.007>
- Disney, M. (2019). Terrestrial LiDAR: a three-dimensional revolution in how we look at trees. *New Phytologist*, *222*(4), 1736–1741. <https://doi.org/10.1111/nph.15517>
- Disney, M., Burt, A., Calders, K., Schaaf, C., & Stovall, A. (2019). Innovations in Ground and Airborne Technologies as Reference and for Training and Validation: Terrestrial Laser Scanning (TLS). *Surveys in Geophysics*, *40*(4), 937–958. <https://doi.org/10.1007/s10712-019-09527-x>
- Dobbertin, M. (2002). Influence of stand structure and site factors on wind damage comparing the storms Vivian and Lothar. *Forest Snow and Landscape Research*, *77*(1–2), 187–205.
- Ehbrecht, M., Schall, P., Ammer, C., & Seidel, D. (2017). Quantifying stand structural complexity and its relationship with forest management, tree species diversity and microclimate. *Agricultural and Forest Meteorology*, *242*(April), 1–9. <https://doi.org/10.1016/j.agrformet.2017.04.012>
- Fahey, R. T., Alvshere, B. C., Burton, J. I., D'Amato, A. W., Dickinson, Y. L., Keeton, W. S., Kern, C. C., Larson, A. J., Palik, B. J., Puettmann, K. J., Saunders, M. R., Webster, C. R., Atkins, J. W., Gough, C. M., & Hardiman, B. S. (2018). Shifting conceptions of complexity in forest management and silviculture. *Forest Ecology and Management*, *421*(January), 59–71. <https://doi.org/10.1016/j.foreco.2018.01.011>
- FAO. (2020). *Global Forest Resources Assessment 2020: Main report*. <https://doi.org/10.4324/9781315184487-1>
- Fichtner, A., & Härdtle, W. (2021). Forest Ecosystems: A Functional and Biodiversity Perspective. In C. Hobohm (Ed.), *Perspectives for Biodiversity and Ecosystems* (pp. 383–405). Springer International Publishing. https://doi.org/10.1007/978-3-030-57710-0_16

- Forrester, D. I., & Bauhus, J. (2016). A Review of Processes Behind Diversity—Productivity Relationships in Forests. *Current Forestry Reports*, 2(1), 45–61. <https://doi.org/10.1007/s40725-016-0031-2>
- Fussell, J., Rundquist, D., & Harrington, J. A. (1986). On defining remote sensing. *Photogrammetric Engineering & Remote Sensing*, 52(9), 1507–1511.
- Grossman, J. J., Vanhellemont, M., Barsoum, N., Bauhus, J., Bruelheide, H., Castagneyrol, B., Cavender-Bares, J., Eisenhauer, N., Ferlian, O., Gravel, D., Hector, A., Jactel, H., Kreft, H., Mereu, S., Messier, C., Muys, B., Nock, C., Paquette, A., Parker, J., ... Verheyen, K. (2018). Synthesis and future research directions linking tree diversity to growth, survival, and damage in a global network of tree diversity experiments. *Environmental and Experimental Botany*, 152(December 2017), 68–89. <https://doi.org/10.1016/j.envexpbot.2017.12.015>
- Guillemot, J., Kunz, M., Schnabel, F., Fichtner, A., Madsen, C. P., Gebauer, T., Härdtle, W., von Oheimb, G., & Potvin, C. (2020). Neighbourhood-mediated shifts in tree biomass allocation drive overyielding in tropical species mixtures. *New Phytologist*, 228(4), 1256–1268. <https://doi.org/10.1111/nph.16722>
- Hou, G., Delang, C. O., & Lu, X. (2020). Afforestation changes soil organic carbon stocks on sloping land: The role of previous land cover and tree type. *Ecological Engineering*, 152(November 2019), 105860. <https://doi.org/10.1016/j.ecoleng.2020.105860>
- Huang, Y., Chen, Y., Castro-Izaguirre, N., Baruffol, M., Brezzi, M., Lang, A., Li, Y., Härdtle, W., Von Oheimb, G., Yang, X., Liu, X., Pei, K., Both, S., Yang, B., Eichenberg, D., Assmann, T., Bauhus, J., Behrens, T., Buscot, F., ... Schmid, B. (2018). Impacts of species richness on productivity in a large-scale subtropical forest experiment. *Science*, 362(6410), 80–83. <https://doi.org/10.1126/science.aat6405>
- Jagger, P., & Pender, J. (2003). The role of trees for sustainable management of less-favored lands: The case of eucalyptus in Ethiopia. *Forest Policy and Economics*, 5(1), 83–95. [https://doi.org/10.1016/S1389-9341\(01\)00078-8](https://doi.org/10.1016/S1389-9341(01)00078-8)
- Jandl, R., Spathelf, P., Bolte, A., & Prescott, C. E. (2019). Forest adaptation to climate change—is non-management an option? *Annals of Forest Science*, 76(2), 48. <https://doi.org/10.1007/s13595-019-0827-x>
- Jucker, T., Koricheva, J., Finér, L., Bouriaud, O., Iacopetti, G., & Coomes, D. A. (2020). Good things take time—Diversity effects on tree growth shift from negative to positive during stand development in boreal forests. *Journal of Ecology*, 108(6), 2198–2211. <https://doi.org/10.1111/1365-2745.13464>
- Kerr, J. T., & Ostrovsky, M. (2003). From space to species: Ecological applications for remote sensing. *Trends in Ecology and Evolution*, 18(6), 299–305. [https://doi.org/10.1016/S0169-5347\(03\)00071-5](https://doi.org/10.1016/S0169-5347(03)00071-5)
- Kunz, M., Fichtner, A., Härdtle, W., Raunonen, P., Bruelheide, H., & Oheimb, G. von. (2019). Neighbour species richness and local structural variability modulate aboveground allocation patterns and crown morphology of individual trees. *Ecology Letters*. <https://doi.org/10.1111/ele.13400>
- Lamb, D., Erskine, P. D., & Parrotta, J. A. (2005). Restoration of degraded tropical forest landscapes. *Science*, 310(5754), 1628–1632. <https://doi.org/10.1126/science.1111773>
- Latimer, C. E., & Zuckerberg, B. (2017). Forest fragmentation alters winter microclimates and microrefugia in human-modified landscapes. *Ecography*, 40(1), 158–170. <https://doi.org/10.1111/ecog.02551>
- Lefsky, M. A., Harding, D., Cohen, W. ., Parker, G., & Shugart, H. . (1999). Surface Lidar Remote Sensing of

- Basal Area and Biomass in Deciduous Forests of Eastern Maryland, USA. *Remote Sensing of Environment*, 67(1), 83–98. [https://doi.org/10.1016/S0034-4257\(98\)00071-6](https://doi.org/10.1016/S0034-4257(98)00071-6)
- Lewis, S. L., Mitchard, E. T. A., Prentice, C., Maslin, M., & Poulter, B. (2019). Comment on “The global tree restoration potential.” *Science*, 366(6463), 5–8. <https://doi.org/10.1126/science.aaz0388>
- Lewis, S. L., Wheeler, C. E., Mitchard, E. T. A., & Koch, A. (2019). Restoring natural forests is the best way to remove atmospheric carbon. *Nature*, 568(7750), 25–28. <https://doi.org/10.1038/d41586-019-01026-8>
- Liu, C. L. C., Kuchma, O., & Krutovsky, K. V. (2018). Mixed-species versus monocultures in plantation forestry: Development, benefits, ecosystem services and perspectives for the future. *Global Ecology and Conservation*, 15, e00419. <https://doi.org/10.1016/j.gecco.2018.e00419>
- Messier, C., Bauhus, J., Sousa-Silva, R., Auge, H., Baeten, L., Barsoum, N., Bruelheide, H., Caldwell, B., Cavender-Bares, J., Dhiedt, E., Eisenhauer, N., Ganade, G., Gravel, D., Guillemot, J., Hall, J. S., Hector, A., Hérault, B., Jactel, H., Koricheva, J., ... Zemp, D. C. (2021). For the sake of resilience and multifunctionality, let’s diversify planted forests! *Conservation Letters*, June, 1–8. <https://doi.org/10.1111/conl.12829>
- Millenium Ecosystem Assessment. (2005). *Ecosystem and Human Well-Being - Opportunities and Challenges for Business and Industry*. 36. <http://hdl.handle.net/20.500.11822/8780>
- Puettmann, J. K., Coates, K. D., & Messier, C. (2003). *A critique of silviculture: Managing for complexity*.
- Rashidi, M., Mohammadi, M., Kivi, S. S., Abdolvand, M. M., Truong-Hong, L., & Samali, B. (2020). A decade of modern bridge monitoring using terrestrial laser scanning: Review and future directions. *Remote Sensing*, 12(22), 1–34. <https://doi.org/10.3390/rs12223796>
- Rewald, B., & Ephrath, J. E. (2013). Minirhizotron techniques. *Plant Roots: The Hidden Half, Fourth Edition, 1937*, 735–750. <https://doi.org/10.1201/b14550-53>
- Schnabel, F., Liu, X., Kunz, M., Barry, K. E., Bongers, F. J., Bruelheide, H., Fichtner, A., Härdtle, W., Li, S., Pfaff, C., Schmid, B., Schwarz, J. A., Tang, Z., Yang, B., & Bauhus, J. (2021). Species richness stabilizes productivity via asynchrony and drought-tolerance diversity in a large-scale tree biodiversity experiment. *Science Advances*, 7(51), 11–13. <https://doi.org/10.1126/sciadv.abk1643>
- Scholten, T., Goebes, P., Kuhn, P., Seitz, S., Assmann, T., Bauhus, J., Bruelheide, H., Buscot, F., Erfmeier, A., Fischer, M., Hartle, W., He, J. S., Ma, K., Niklaus, P. A., Scherer-Lorenzen, M., Schmid, B., Shi, X., Song, Z., Von Oheimb, G., ... Schmidt, K. (2017). On the combined effect of soil fertility and topography on tree growth in subtropical forest ecosystems—a study from SE China. *Journal of Plant Ecology*, 10(1), 111–127. <https://doi.org/10.1093/jpe/rtw065>
- Schuldt, A., Ebeling, A., Kunz, M., Staab, M., Guimarães-Steinicke, C., Bachmann, D., Buchmann, N., Durka, W., Fichtner, A., Fornoff, F., Härdtle, W., Hertzog, L. R., Klein, A. M., Roscher, C., Schaller, J., von Oheimb, G., Weigelt, A., Weisser, W., Wirth, C., ... Eisenhauer, N. (2019). Multiple plant diversity components drive consumer communities across ecosystems. *Nature Communications*, 10(1). <https://doi.org/10.1038/s41467-019-09448-8>
- Seidl, R., Spies, T. A., Peterson, D. L., Stephens, S. L., & Hicke, J. A. (2016). Searching for resilience: Addressing the impacts of changing disturbance regimes on forest ecosystem services. *Journal of Applied Ecology*, 53(1), 120–129. <https://doi.org/10.1111/1365-2664.12511>

- Skidmore, A. K., Wang, T., de Bie, K., & Pilesjö, P. (2019). Comment on "The global tree restoration potential." *Science*, *366*(6469), 134–151. <https://doi.org/10.1126/science.aaz0111>
- Trogisch, S., Liu, X., Rutten, G., Xue, K., Brose, U., Bu, W., Cesarz, S., Chesters, D., Connolly, J., Cui, X., Eisenhauer, N., Guo, L., Haider, S., Werner, H., Kunz, M., Liu, L., Dam, N. M. Van, Oheimb, G. Von, Wang, M., ... Bruelheide, H. (2021). The significance of tree-tree interactions for forest ecosystem functioning. *Basic and Applied Ecology*, *00*, 1–20. <https://doi.org/10.1016/j.baae.2021.02.003>
- Van de Peer, T., Verheyen, K., Kint, V., Van Cleemput, E., & Muys, B. (2017). Plasticity of tree architecture through interspecific and intraspecific competition in a young experimental plantation. *Forest Ecology and Management*, *385*, 1–9. <https://doi.org/10.1016/j.foreco.2016.11.015>
- van der Plas, F. (2019). Biodiversity and ecosystem functioning in naturally assembled communities. *Biological Reviews*, *94*(4), 1220–1245. <https://doi.org/10.1111/brv.12499>
- Veldkamp, E., Schmidt, M., Powers, J. S., & Corre, M. D. (2020). Deforestation and reforestation impacts on soils in the tropics. *Nature Reviews Earth & Environment*, *1*(11), 590–605. <https://doi.org/10.1038/s43017-020-0091-5>
- Wenhua, L. (2004). Degradation and restoration of forest ecosystems in China. *Forest Ecology and Management*, *201*(1), 33–41. <https://doi.org/10.1016/j.foreco.2004.06.010>
- Williams, L. J., Paquette, A., Cavender-Bares, J., Messier, C., & Reich, P. B. (2017). Spatial complementarity in tree crowns explains overyielding in species mixtures. *Methods in Ecology and Evolution*, *1*(February). <https://doi.org/10.1038/s41559-016-0063>
- WMO - World Meteorological Organization. (2021). WMO Greenhouse Gas Bulletin (GHG Bulletin) - No. 17. *WMO Greenhouse Gas Bulletin*, *17*(17), 1–10. https://library.wmo.int/doc_num.php?explnum_id=10904
- Xiao, J., Chevallier, F., Gomez, C., Guanter, L., Hicke, J. A., Huete, A. R., Ichii, K., Ni, W., Pang, Y., Rahman, A. F., Sun, G., Yuan, W., Zhang, L., & Zhang, X. (2019). Remote sensing of the terrestrial carbon cycle: A review of advances over 50 years. *Remote Sensing of Environment*, *233*(August). <https://doi.org/10.1016/j.rse.2019.111383>
- Yang, X., Bauhus, J., Both, S., Fang, T., Härdtle, W., Kröber, W., Ma, K., Nadrowski, K., Pei, K., Scherer-Lorenzen, M., Scholten, T., Seidler, G., Schmid, B., von Oheimb, G., & Bruelheide, H. (2013). Establishment success in a forest biodiversity and ecosystem functioning experiment in subtropical China (BEF-China). *European Journal of Forest Research*, *132*(4), 593–606. <https://doi.org/10.1007/s10342-013-0696-z>
- Yu, G., Chen, Z., Piao, S., Peng, C., Ciais, P., Wang, Q., Lia, X., & Zhu, X. (2014). High carbon dioxide uptake by subtropical forest ecosystems in the East Asian monsoon region. *Proceedings of the National Academy of Sciences of the United States of America*, *111*(13), 4910–4915. <https://doi.org/10.1073/pnas.1317065111>
- Zolkos, S. G., Goetz, S. J., & Dubayah, R. (2013). A meta-analysis of terrestrial aboveground biomass estimation using lidar remote sensing. *Remote Sensing of Environment*, *128*, 289–298. <https://doi.org/10.1016/j.rse.2012.10.017>

Chapter I. Tree species richness promotes an early increase of stand structural complexity in young subtropical plantations

Maria D. Perles-Garcia^{1,2*}, Matthias Kunz³, Andreas Fichtner⁴, Werner Härdtle⁴, Goddert von Oheimb^{3,2}

¹ Institute of Biology / Geobotany and Botanical Garden, Martin Luther University Halle-Wittenberg, 06108 Halle (Saale), Germany

² German Centre for Integrative Biodiversity Research (iDiv), Halle-Jena-Leipzig, 04103 Leipzig, Germany

³ Institute of General Ecology and Environmental Protection, Technische Universität Dresden, 01737 Tharandt, Germany

⁴ Institute of Ecology, Leuphana University of Lüneburg, 21335 Lüneburg, Germany

* Correspondence: maria_dolores.perles@idiv.de, German Centre for Integrative Biodiversity Research (iDiv), Halle-Jena-Leipzig, 04103 Leipzig, Germany.

Editorial status: Published in *Journal of Applied Ecology* (April 2021)

DOI: [10.1111/1365-2664.13973](https://doi.org/10.1111/1365-2664.13973)

Abstract

1. Forest structural complexity has been identified as an important driver for promoting simultaneously biodiversity across trophic levels and multiple ecosystem services. However, we still have a limited understanding of the processes that lead to structural complex stands and how they evolve over time.
2. Using terrestrial laser scanning (TLS), we quantified a three-dimensional (3D) stand structural complexity index (SSCI) in an experimental plantation with a long gradient of tree species richness (1 to 24 species). The plantation was established in 2009, and we made use of a multi-temporal TLS dataset recorded during the period 2012 to 2019.
3. We found a positive relationship between tree species richness and structural complexity. This relationship became stronger over time. Ten years after planting, SSCI was on average two-fold higher in 16- and 24-species mixtures than in monocultures. Furthermore, we demonstrate that tree species richness promotes 3D stand structural complexity indirectly by fostering a high vertical heterogeneity and thus greater spatial complementarity in canopy space.
4. *Synthesis and applications.* Our findings indicate that tree species richness plays a crucial role in promoting stand structural complexity in young plantations, and this role becomes more important already during early stand development. Thus, afforestation measures would benefit from planting multiple native tree species to initiate structurally complex stands.

Keywords

BEF-China, biodiversity-ecosystem functioning, restoration, stand structural complexity, terrestrial laser scanning, tree diversity, tree species mixtures

1. Introduction

Forest plantations are established globally to provide multiple ecosystem services such as the production of timber, fuel, and pulpwood (FAO, 2010). Specifically, global afforestation and reforestation efforts are among the major nature-based solutions employed to combat the adverse impacts of climate change. Currently, 168 Mha of degraded and deforested land, mainly located in the tropics and subtropics, has been pledged as restoration areas under the "Bonn Challenge" (IUCN, 2020). A large part of this area is intended for plantations of commercial trees, mostly as monocultures (Lewis, Wheeler, Mitchard, & Koch, 2019). In

recent years, however, there has been increasing criticism of monospecific stands due to their great susceptibility to adverse environmental conditions (e.g. storm, fire), pests, diseases, and invasive species, and their negative effects on soil productivity and fertility (Liu, Kuchma, & Krutovsky, 2018; Piotta, 2008). Moreover, there is robust evidence of a strong positive relationship between tree species diversity and ecosystem services (e.g., primary productivity, carbon sequestration, nitrogen retention; Chen et al., 2020; Felipe-Lucia et al., 2018; Huang et al., 2018; Lang et al., 2014; Zemp et al., 2019b). Diverse tree mixtures are also expected to promote species-rich communities across trophic levels (Schuldt et al., 2018) and have been found to show higher resistance to environmental stressors such as climate change (Fichtner et al., 2020). Importantly, Forrester & Bauhus (2016) and Schuldt et al. (2019) found that not only species richness and functional diversity, but also the structural diversity of tree stands is a highly relevant mediator of these beneficial diversity effects. This is because growth characteristics, branching architecture, and space occupation of trees affect the spatial complexity of the canopy space, microclimates, and species interactions. Furthermore, the idea of “resilience” or “adaptive” complexity has been introduced into forest and plantation management in recent years in order to promote the resilience or adaptive capacity of managed stands to current and future environmental changes and stressors (Fahey et al., 2018). Management recommendations should therefore include measures to preserve and enhance structural complexity. From a scientific perspective, it is essential that we obtain a deeper understanding of the role of tree species richness in the restoration of stand structural complexity.

Species mixing has the potential to influence the canopy structure of tree communities because tree crown complementarity (i.e. the physical niche partitioning in canopy space) increases with tree species richness (Kunz et al., 2019; Williams, Paquette, Cavender-Bares, Messier, & Reich, 2017). Crown complementarity can be explained by the functional diversity of tree mixtures and by the diversity-driven plasticity of tree crowns. Recent work has shown that changes in crown morphological plasticity may be the result of shifts in tree biomass allocation induced by neighbourhood interactions in mixed-species tree communities (Guillemot et al., 2020; Kunz et al., 2019). Notably, species mixing also leads to differences in the inner crown properties (Pretzsch, 2014). Trees growing in mixtures may have significantly more branches of the first orders and a higher sum of branch lengths than those in monocultures (Bayer, Seifert, & Pretzsch, 2013; Guillemot et al., 2020; Kunz et al., 2019). As a result, these differences in the crown structure of individual trees enhance

canopy space-use efficiency and, thus, aboveground resource utilisation in mixed-species stands. At the same time, the canopy space is more heterogeneously structured and more complex (Hess, Härdtle, Kunz, Fichtner, & von Oheimb, 2018).

Stand structural complexity can be defined as the degree of heterogeneity of the three-dimensional (3D) distribution of biomass (Ehbrecht et al. 2021 and the conceptual framework therein). It has been described in various ways, covering both indices that include only single stand structural attributes (e.g. horizontal tree distribution, stand density, tree size differentiation) and indices that combine several attributes (so-called "structural complexity indices"; McElhinny, Gibbons, Brack & Bausch, 2005; Juchheim, Ehbrecht, Schall, Ammer & Seidel 2020). Previous studies found varying relationships between tree diversity and stand structural complexity, ranging from positive to neutral responses (Hakkenberg, Song, Peet, & White, 2016; Neumann & Starlinger, 2001). All these measures of structural complexity using conventional approaches, however, are based on one- or two-dimensional attributes but do not consider the 3D nature of forest (stand) structures in detail. This lack might be a particular shortcoming when considering mixed-species stands, given the importance of diversity-induced tree crown architectural changes and plasticity-driven canopy space exploitation. Furthermore, complex 3D stand structures emerge through time. Trees store carbon in long-lived structural elements, such as trunks and branches, and therefore can be considered 'long-term records' of the effects of tree-tree interactions and growth responses of the past. In addition to patterns of species richness and composition, such tree-tree interactions might be shaped by the extent of tree age-disparity within a stand (i.e. even- vs. uneven-aged stands alongside with demographic variation and development). Analyses of stand structural complexity thus need to consider the temporal dynamics.

Terrestrial laser scanning (TLS) technology has proved to be an appropriate tool to quantify both the spatial and temporal dynamics of forest structural complexity (Liang et al., 2016). TLS is a time-efficient and non-destructive surveying technique for the measurement of the 3D structural elements of trees and delivers a fully 3D representation of tree stands. As such, it is a state-of-the-art technique that allows the study of forest structure in great detail and at high spatio-temporal resolution.

Ehbrecht, Schall, Ammer and Seidel (2017) developed a stand structural complexity index (SSCI) that is based on TLS data and measures forest structural complexity according to the 3D spatial arrangement of all visible vegetation objects within a single laser scan. The index is comprised of two elements, the mean fractal dimension (MeanFrac, Fig. S1 in Supporting

Information) scaled by the effective number of layers (ENL, Fig. S2). MeanFrac depends on the density of structural elements (e.g. branches, twigs), whereas ENL describes the vertical stratification. Applying the SSCI to mature temperate forests of Germany, Ehbrecht et al. (2017) and Juchheim et al. (2020) observed a positive, but saturating relationship between the SSCI and tree diversity. These forests are species-poor with one dominant tree species per plot and a few admixed species, with a maximum value of the exponential Shannon-Index of about four. In a very young experiment (three years after planting) with six tree species planted in a tropical oil palm plantation, Zemp et al. (2019a) found the same relationship. At this very early stage of the experiment, MeanFrac showed the same pattern as SSCI, whereas no significant relation between ENL and tree diversity was observed. In all three studies, however, the diversity gradient was rather short (exponential Shannon-Index mainly lower than three and max. tree species richness of six), and the question remains as to whether these findings hold in a highly diverse system spanning a long tree diversity gradient under experimentally controlled conditions. Furthermore, as only one-time measurements were made and no time series analyses were conducted, the dynamics of tree interactions remained unexplored.

Here, we made use of TLS technology to analyse 3D stand structural complexity at a high resolution over multiple years in a large-scale forest biodiversity-ecosystem functioning (BEF) experiment established in 2009 in the Jiangxi Province in subtropical China (BEF-China; Bruelheide et al., 2014). We quantified the SSCI based on six annual TLS data recordings conducted during the period 2012 to 2019 in plots covering a diversity gradient of tree species richness (TSR) ranging from monocultures to 24-species mixtures. We hypothesised that (i) TSR positively affects stand structural complexity, (ii) TSR effects on stand structural complexity increase over time, and (iii) TSR effects on stand structural complexity are mainly mediated by changes of one of its elements, MeanFrac or ENL. We thus strive to determine to what extent and over what timescale TSR can foster 3D structural complexity in forest plantations.

2. Material and methods

2.1. Study site

The BEF-China tree diversity experiment is located in Jiangxi province in southeast subtropical China (29.08°-29.11°N, 117.90°-117.93°E, 100–300 m a.s.l.; Bruelheide et al., 2014). The natural forest around the study site consists of subtropical mixed broad-leaved

species, both deciduous and evergreens. The mean annual temperature is 16.7 °C and mean precipitation is 1821 mm year⁻¹ (averaged from 1971 to 2000; Yang et al., 2013).

The experiment consists of two sites (A and B), established in 2009 and 2010, respectively, with a total of 566 plots comprising tree species richness levels from 1 to 24 and different species compositions (with a random allocation of richness levels and composition to plots; see Bruelheide et al. 2014 for more details). On each plot, covering 25.8 × 25.8 m, 400 trees were planted in a regular grid with a planting distance of 1.29 m, with species randomly assigned to planting positions. Here, we analyse data from 49 plots of site A (for details on sample plot selection see Methods S1). Plots have an experimentally established tree species richness gradient of 1, 2, 4, 8, 16, and 24 species, on 20, 15, 6, 3, 3, and 2 plots, respectively. Each plot in our study was scanned at least twice using TLS within the period between 2012 to 2019 (see Table S1). Due to faster and lighter TLS systems, more plots have been scanned within the recent years 2015 to 2019 compared to 2012 to 2014. Because of that, we also tested our hypotheses in a subsample of 30 plots that were repeatedly scanned in 2013, 2015, and 2019. The plots included in our analyses showed tree mortality rates less than 80% (based on the inventory from 2016, see below). Further plot information is provided in Table S1.

2.2. *Terrestrial laser scanning data*

TLS data were collected using a FARO Focus S120 and a FARO Focus X130 laser scanner in 2019, a FARO Focus S120 in 2016, 2015 and 2014, and a FARO Photon Scanner in 2013 and 2012 (FARO Europe, Korntal-Münchingen, Germany; for a detailed description of scan campaigns see Kunz et al. 2019). All scan campaigns were conducted in February-March under leaf-off conditions of the deciduous tree species. A single scan was captured at the centre of each plot. We used a spatial resolution of 10240 points per 360°, corresponding to a resolution of around 6 mm at a distance of 10 m. The laser scanner was set up on a tripod at 1.3 m height. All scans were performed under clear skies and almost windless conditions. For a test on the dependency of SSCI values on scanner position and leaf conditions see Methods S2.

2.3. *SSCI*

For each single scan from the plot centre, we computed the SSCI according to Ehbrecht et al. (2017) (for detailed explanations of how the index works see Ehbrecht et al. 2021). Prior to the SSCI computation, all scans were filtered for possible noise and stray points using a statistical outlier removal filter (SOR, N=10, SD=3) in CloudCompare 2.9.1 software. To

ensure that the index only included points representing the plot structure, we restricted the point cloud to a radius of 10 m around the scan position ($\sim 315 \text{ m}^2$).

The SSCI is defined as:

$$SSCI = \text{MeanFrac}^{\ln(ENL)}$$

where "MeanFrac" is the mean fractal dimension index and "ENL" is the effective number of layers.

To calculate the MeanFrac (Ehbrecht et al., 2017), each point cloud was divided into 2560 cross-sections. The points of each cross-section were sorted by angle and combined in a polygon. The MeanFrac was calculated as the mean value of the fractal dimension of the 2560 cross-sections (cf. Fig. S1). For the calculation of ENL (Ehbrecht, Schall, Juchheim, Ammer & Seidel, 2016), we converted the 10 m radius point cloud to a voxel grid. We applied a slope correction to align the layers parallel to the ground surface. Then, we quantified the proportion of filled voxels in relation to the total voxels of each slice, and the ENL was computed using the inverse Simpson-Index (for details on the calculation of ENL and slope correction see Methods S3 and Fig. S2).

SSCI, MeanFrac and ENL were computed using R 4.0.2 (R Core Team, 2018) with the packages VoxR (Lecigne, Delagrange, & Messier, 2014) and sp (Pebesma & Bivand, 2005).

2.4. *Inventory-based structural indices*

The trees in the core area of each plot have been measured since 2010 using traditional inventory methods (Li, Hess, von Wehrden, Härdtle, & von Oheimb, 2014). Information on survival, species identity, stem diameter 5 cm above ground (ground diameter GD), and tree height were collected for each year between 2010 and 2016. We calculated inventory-based indices of structural complexity (in the vertical and horizontal domain) using the standard deviation (SD), coefficient of variation and Gini-coefficient (Cowell, 2009) of GD and tree height for each plot and tested the relationship between these indices and TSR. We also calculated the mortality per plot using the last complete inventory data available from the year 2016.

2.5. *Statistical analyses*

We fitted linear mixed-effects models (Zuur, Ieno, Walker, & Smith, 2009) to evaluate the effects of TSR and study year on stand structural complexity. To test for temporal dependency of TSR effects, we also considered the interaction TSR \times year. Tree species composition and its interaction with year (correlated random slope), as well as study plot,

were used as crossed random effects (Fig. S3). Year 0 was considered as the year of plantation, 2009. The models were fitted separately to SSCI, MeanFrac, ENL and inventory-based structural complexity indices. To test whether our results depended on the consistency of temporal measurements, we additionally fitted the models to a subsample containing those 30 plots that were consistently scanned in 2013, 2015, and 2019. Fixed factors were standardized around their mean value with a standard deviation of one before fitting the models. Prior to analyses, the dependent variables and TSR were \log_2 transformed to meet model assumptions (i.e. homogeneity, independence and normality; Zuur et al. 2009). Residuals plots showed no violation of these assumptions. To test the relationship between all the structural complexity indices applied, we calculated Pearson's correlation coefficients.

To test how the SSCI-TSR relationship varies with species identity, we separately fitted linear regression models for 16 species measured in 2019. We analysed those tree species that were present in at least four of the analysed plots from 2019 (Table S2).

Furthermore, we conducted a path analysis to explore drivers for SSCI using a piecewise approach that allows for the implementation of random effects (using the same random structure as described above; Lefcheck, 2016). We tested the hypothesis that TSR effects on SSCI were mediated by changes in MeanFrac and/or ENL. We further hypothesized that changes in MeanFrac, ENL and SSCI are driven by stand development (study year). All variables were standardized and transformed as described above and the model fit was evaluated based on Fisher's *C* statistics (Lefcheck, 2016).

All statistical analyses were performed in R 4.0.2 (R Core Team, 2018) using the packages lmerTest (Kuznetsova, Brockhoff, & Christensen, 2017), piecewiseSEM (Lefcheck, 2016), and MuMIn (Barton, 2019).

3. Results

In general, we observed a positive relationship between TSR and structural complexity (Fig. 1, Table 1, Figs. S4 and S5, Tables S3 and S4). Importantly, these effects became stronger over time for the TLS-based indices, as indicated by the significant two-way interactions (Fig. 1, Table 1). Ten years after planting we found a two-fold increase of the SSCI in 16- and 24-species mixtures compared to monocultures. MeanFrac decreased slightly with TSR during the first years, while these effects became neutral to positive over time (Fig. 1 b, Table 1). These relationships were qualitatively the same when fitting the models to those plots that were repeatedly measured in 2013, 2015 and 2019 (Table S3, Fig. S4).

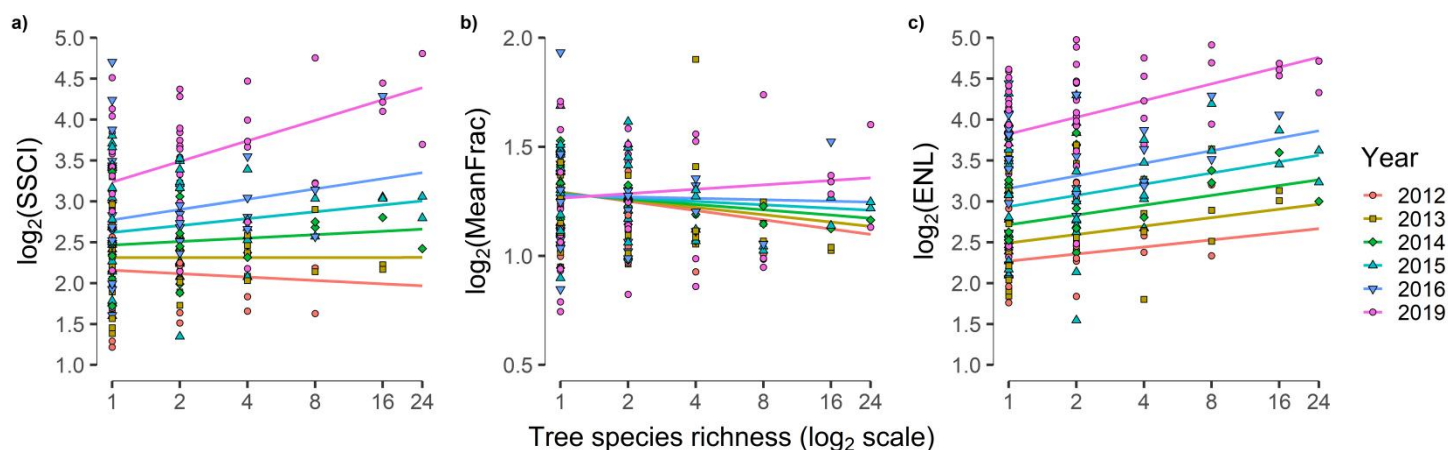


Figure 1. Temporal changes in the relationship between tree species richness and different components of stand structural complexity (a: stand structural complexity index (SSCI); b: mean fractal dimension (MeanFrac); c: effective number of layers (ENL)). Lines show predictions of linear mixed-effects models, and symbols indicate observed values.

The temporal development of TSR effects, however, differed among the inventory-based indices (Table S4, Fig. S5). The positive relationship between the SD of GD and TSR was present from the first study year and remained constant over time (i.e. no significant interaction with year), whereas the positive relationship between the SD of tree height and TSR became stronger with time (i.e. positive interaction with year). In contrast, TSR effects varied with year for the coefficient of variation and the Gini coefficient of GD, but not for those of tree height (Table S4). All inventory-based indices were closely positively correlated to each other, whereas the correlations between SSCI and the inventory-based indices were mostly non-significant (Fig. S6).

Table 1. Results of mixed-effects models for the effects of tree species richness (TSR; \log_2 -transformed), year and their interaction on different components of stand structural complexity (SSCI, MeanFrac and ENL; all \log_2 -transformed). $n=315$

Fixed effect	SSCI				MeanFrac				ENL			
	df _{num}	df _{den}	F	p	df _{num}	df _{den}	F	p	df _{num}	df _{den}	F	p
Intercept	-	-	-	< 0.001	-	-	-	< 0.001	-	-	-	< 0.001
TSR	1	92.76	6.36	< 0.05	1	103.42	12.16	< 0.001	1	66.08	0.29	0.593
Year	1	54.35	76.64	< 0.001	1	58.78	0.39	0.533	1	26.85	299.52	< 0.001
TSR*Year	1	38.74	18.63	< 0.001	1	44.57	6.09	< 0.05	1	19.16	5.75	< 0.05

df_{num}, numerator degrees of freedom; df_{den}, denominator degrees of freedom. F and P indicate F ratios and the P value of the significance test, respectively.

The positive relationship between TSR and SSCI was consistent across species: In 2019 all species showed a positive relationship between SSCI and TSR, meaning that monocultures

display lower stand structural complexity than the mixtures where they were present (Fig. 2). The relationship between TSR and SSCI was significant at $p < 0.01$ for six species (Table S2). Tree mortality did not affect SSCI ($p = 0.29$).

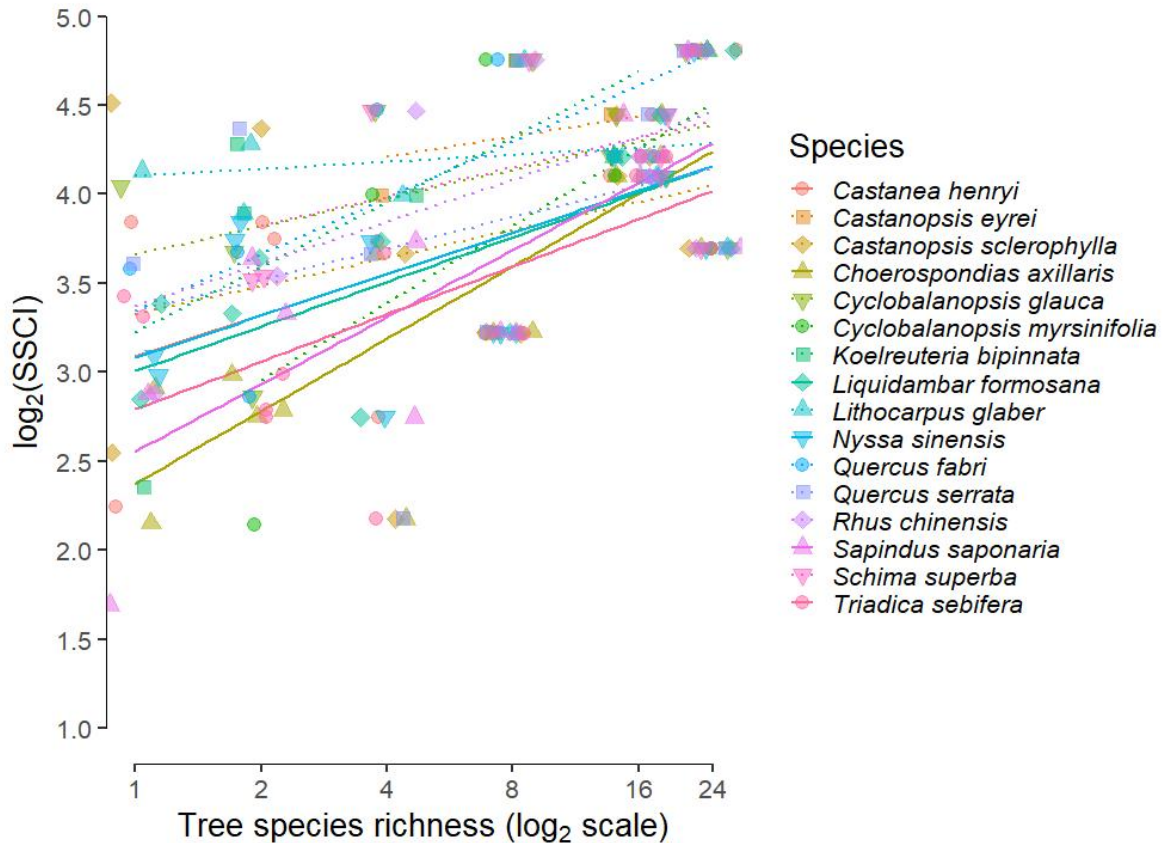


Figure 2. Relationship between tree species richness (TSR) and stand structural complexity index (SSCI) for 16 tree species measured in 2019. TSR = 1 means that the plot was planted as a monoculture. Dotted lines show non-significant ($p > 0.1$), solid lines indicate significant ($p < 0.1$) relationships. Symbols indicate observed values jittered to facilitate visibility.

The path model resulted in a good fit to the data (Fisher C = 1.25, df = 2, $p = 0.536$) and TSR, ENL, MeanFrac, and Year accounted for 97% of the variation in SSCI. ENL ($p < 0.001$) and MeanFrac ($p < 0.001$) had a positive direct effect on SSCI with ENL being the strongest driver for changes in SSCI (Fig. 3). We found no significant direct pathway between TSR and SSCI ($p = 0.375$). Instead, TSR enhanced SSCI indirectly via increasing ENL ($p = 0.020$) and not via increasing MeanFrac ($p = 0.431$), indicating that TSR effects on SSCI are mediated by changes in ENL. ENL, in turn, was positively related to stand development ($p < 0.001$), while SSCI and MeanFrac were not directly affected by changes over time (SSCI: $p = 0.849$; MeanFrac: $p = 0.486$).

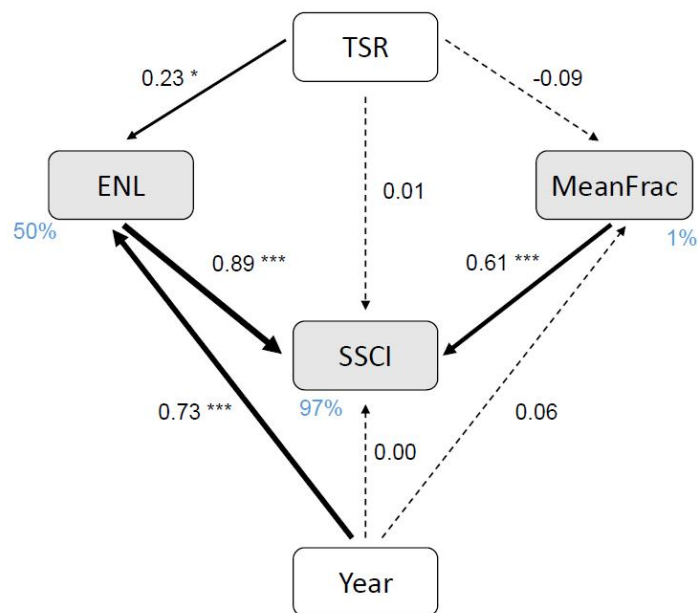


Figure 3. Path model linking the effects of tree species richness (TSR), effective number of layers (ENL), mean fractal dimension (MeanFrac), stand development (year) and stand structural complexity (SSCI). Solid arrows denote significant causal relationships (* $p < 0.05$, ** $p < 0.01$, *** $p < 0.001$), while non-significant ($p > 0.05$) relationships are indicated by dotted arrows. Numbers beside arrows (standardized path coefficients) and arrow width denote the effect size of the pathways. Percentage values (blue) are explained variances of fixed-effects only (marginal R^2 -values).

4. Discussion

Ten years after establishment we found a significant positive relationship between 3D stand structural complexity (expressed as TLS-data based SSCI) and TSR across a broad diversity gradient in a subtropical experimental tree plantation, thus confirming our first hypothesis that TSR positively affects stand structural complexity. This is an important finding because it demonstrates that, already in young plantations, management decisions can considerably contribute to the improvement of stand structural complexity. Stand structural complexity, in turn, is considered a key component of biodiversity in tree communities and an important driver of various ecosystem functions. For example, there is evidence that stand structural complexity positively affects the abundance and species richness of consumers (Schuldt et al., 2019), the robustness of multitrophic interactions (Fornoff, Klein, Blüthgen, & Staab, 2019), as well as the resilience to current and future environmental changes and stressors (Fahey et al., 2018).

Our findings are in part consistent with those from other studies using TLS-based SSCI assessments (Ehbrecht et al., 2017; Juchheim et al., 2020; Zemp, et al., 2019a), but differ with regard to an important element: While those studies observed a non-linear positive relation with saturation at relatively low tree diversity, we found that log-SSCI consistently increased with log-TSR across a long gradient of TSR (up to 24-species mixtures). This discrepancy might be partially explained by differences in the aboveground biomass of forests of different biomes, since subtropical tree species (as analysed in the present study) have the potential to accumulate significantly higher amounts of biomass in their canopy as compared to temperate tree species (Keeling & Phillips, 2007), but potentially also by the length of the diversity gradient itself and by the limited representation of plots with very high diversity levels in the studies by Ehbrecht et al. (2017), Juchheim et al. (2020) and Zemp et al. (2019a). The temperate forests of Central Europe are generally poor in tree species, and accordingly, the tree diversity gradient in the studies by Ehbrecht et al. (2017) and Juchheim et al. (2020) was narrow. A cessation of the increase of the SSCI with increasing tree diversity already occurred at exponential Shannon index values of about 2. In an experimental enrichment plantation of six native broadleaved tree species in commercial oil palm monocultures in tropical Sumatra, Indonesia, the tree species richness gradient ranged, in the majority of cases from 0 to 3, with only two 5-species and one 6-species plots (Zemp et al., 2019a). It thus remains open whether considerably longer tree diversity gradients in the temperate and the tropical biome would yield a similar linear increase in 3D stand structural complexity with increasing tree species richness, as observed in our subtropical plantation.

4.1. *Temporal changes in TSR-stand structural complexity relationships*

Another important factor that might influence the mode of the relationships between tree diversity and SSCI is the age of the trees. This is of particular relevance in communities with long-living individuals such as trees, as they record the history of past growth and interactions with the environment in long-lasting woody structures. In accordance with our second hypothesis, stand development proved to be an important predictor for structural complexity: Whereas relationships between TSR and SSCI were slightly negative at the beginning of the measurement period in 2012-2013 (i.e. in the third and fourth year after planting), they proved to be strongly positive after 10 years. This is a clear indication that the importance of positive species interactions (e.g. resource partitioning and facilitation) strengthened over time. This in turn might be a key mechanism underlying positive TSR-SSCI relationships. Due to the high planting density in BEF-China, early onset of tree-

tree interactions was observed already in the first years after planting (Li et al., 2014). However, diversity-mediated patterns in biomass allocation resulting in morphological adjustments in the 3D tree architecture and hence positive diversity – productivity relationships need time to develop (Kunz et al., 2019). Zemp et al. (2019a) conducted a single measurement three years after planting and found that the variability of SSCI was mainly explained by species identity effects rather than tree species interactions. However, the authors expected this pattern to change over time as trees develop larger, more complex and plastic crowns. In line with Zemp et al. (2019a), we observed a high variation of SSCI values in monocultures within the individual study years. This might be attributed largely to major trait differences among the planted tree species in BEF-China, which in turn result in substantial differences in growth rates (Li et al., 2014; Li, Kröber, Bruelheide, Härdtle, & von Oheimb, 2017). In our study, however, we can exclude strong species identity effects on the overall TSR–SSCI relationship, since the positive relationship between TSR and SSCI in 2019 was consistent across the 16 tree species most abundant in our study, meaning that all the species, independently of their traits, showed lower stand structural complexity in monocultures than in mixtures 10 years after planting. This also suggests that differences in mortality rates are of minor importance. Based on the findings of Bruelheide et al. (2011) we do not expect a reduction of structural complexity in species mixtures in the long term, because, in a natural forest nearby the experimental site, young and old stands did not differ with respect to species composition or richness.

4.2. Relationship between TSR and inventory-based stand structural complexity indices

Although all inventory-based indices displayed the same overall positive relation with TSR as SSCI, the development over time was different. Importantly, all TSR–inventory-based index relationships were positive from the beginning (i.e. year 2012). The indices based on the ground diameter (GD) either showed no significant (SD of GD) or a decreasing impact of TSR over time (coefficient of variation and Gini-coefficient of GD). By contrast, we found a slightly or non-significant increasing effect of TSR on all indices based on tree height over time. These observations suggest that, unlike the SSCI, the inventory-based indices showed strong species identity effects with high variability in GD and tree height due to species-specific differences in growth rates. Over time, GD appeared to be more evenly distributed across TSR levels, whereas a less even distribution in height developed. In addition, tree mixtures showed higher productivity, mainly driven by a neighbourhood-mediated enhancement of individual-tree growth (Fichtner et al., 2018; Kunz et al., 2019). We

hypothesise that a tree's height growth is of higher priority than diameter growth when light is the main growth limiting factor (Falster & Westoby, 2003; Pretzsch, 2009). In dense young plantations, like those in our study, preferential biomass investments in height growth are, therefore, to be expected (Li et al., 2017). For the tree species mixtures, competitive reduction has been found to be the main driving mechanism of positive diversity effects for fast-growing species (Fichtner et al., 2017).

4.3. Role of density (MeanFrac) vs. vertical stratification (ENL) in the relationship between TSR and SSCI

Our finding that the positive effects of TSR on SSCI are mediated by ENL rather than MeanFrac suggests that TSR promotes stand structural complexity indirectly by allowing for greater complementarity in canopy space (i.e. vertical stratification). The lack of a strong impact of TSR on MeanFrac may be partly explained by the regular (rasterised) pattern in which the trees were planted in the BEF-China experiment. Nevertheless, there is a temporal trend that might lead towards a positive relation between TSR and MeanFrac in the future, probably due to differences in mortality rates (i.e., self-thinning with a loss of the suppressed individuals). In contrast, ENL was a strong mediator of the TSR effects on SSCI, and was also significantly positively related to stand development. This coincides with our finding of a highly variable height growth of the trees analysed, which then fosters a strong vertical differentiation of crown elements (i.e. branches) in higher mixtures. Species mixtures often show a higher crown complementarity than monocultures (Williams et al., 2017), in particular as a result of neighbourhood-driven changes in crown architecture (Guillemot et al., 2020; Kunz et al., 2019). Specifically, diversity-mediated changes may lead to a higher biomass allocation to branches, increased crown size, more sinuous crowns, higher branch ramification and more even vertical distribution of crown volume (Bayer et al., 2013; Guillemot et al., 2020; Kunz et al., 2019; Lang et al., 2012; Martin-Ducup, Schneider, & Fournier, 2016). As a result, canopy space is more complex (and partly more heterogeneously structured), which in turn may cause increased canopy packing (Ehbrecht et al., 2016; Morin, Fahse, Scherer-Lorenzen, & Bugmann, 2011; Pretzsch, 2014; Williams et al., 2017).

5. Management implications and conclusions

Given the huge area of afforestation projects currently in progress worldwide, particularly in Asia (Yang, Jia, & Ci, 2010), the selection of appropriate tree species is key to achieving the intended ecosystem functions and services (IUCN, 2020; Tang & Li, 2013). However, many

afforestation projects still utilise a limited range of the potentially available tree species typical of a respective site, and possibly miss opportunities related to such afforestation programmes (Gong, Tan, Liu, & Xu, 2020). Taking subtropical forest plantations as an example, our study provides evidence that increasing the tree species richness of plantations has a positive influence on stand structural complexity, which in turn may foster the stands' resistance or resilience to environmental stressors or natural disturbances (Seidl, Spies, Peterson, Stephens, & Hicke, 2016). In the absence of sufficient knowledge about which species should be planted in mixtures for afforestations, the best current approach is to plant a large number of species. Our study demonstrates that species richness *per se* generally supports a high stand structural complexity with all its beneficial consequences. Tree species richness mainly promotes vertical heterogeneity, which supports ecosystem functions and services such as timber production or carbon sequestration (Guillemot et al., 2020; Williams et al., 2017; Zemp, et al., 2019a), but also positively affects the species diversity or abundance of higher trophic levels (Knuff et al., 2020; Schuldt et al., 2019) as well as the robustness of multitrophic interactions (Fornoff et al., 2019). Afforestation projects should therefore use a broad range of the tree species native to a respective site in order to promote both the functioning of the newly established forests (including related services) and the biodiversity they potentially host.

Acknowledgements

We are grateful to the local workers and to M.Hildebrand and G.Hähn who assisted to conduct the scans in the field, to A.Koller and I.Frehse who contribute processing the data, and to the BEF-China coordination team for continuous logistical support. This study was supported by the International Research Training Group TreeDì jointly funded by the Deutsche Forschungsgemeinschaft (DFG, German Research Foundation) – 319936945/GRK2324 and the University of Chinese Academy of Sciences (UCAS). We are grateful to Alex Fajardo and three anonymous referees for their constructive comments on an earlier version of this article.

Conflict of interest

The authors declare no conflict of interest.

Authors' contributions

The study was conceived by MPG, GvO, WH and MK. MPG and MK performed the field work. MPG, MK and AF analysed the data. MPG wrote the first draft of the manuscript and all the authors contributed substantially to the submitted version.

Data availability statement

All data are available on the BEF-China project database: <https://data.botanik.uni-halle.de/bef-china/datasets/637> (Perles-Garcia et al., 2020).

References

- Barton, K. (2019). MuMIn: Multi-Model Inference. Retrieved from <https://cran.r-project.org/package=MuMIn>
- Bayer, D., Seifert, S., & Pretzsch, H. (2013). Structural crown properties of Norway spruce (*Picea abies* [L.] Karst.) and European beech (*Fagus sylvatica* [L.]) in mixed versus pure stands revealed by terrestrial laser scanning. *Trees - Structure and Function*, 27(4), 1035–1047. <https://doi.org/10.1007/s00468-013-0854-4>
- Bruelheide, H., Böhnke, M., Both, S., Fang, T., Assmann, T., Baruffol, M., ... Schmid, B. (2011). Community assembly during secondary forest succession in a Chinese subtropical forest. *Ecological Monographs*, 81(1), 25–41. <https://doi.org/10.1890/09-2172.1>
- Bruelheide, H., Nadrowski, K., Assmann, T., Bauhus, J., Both, S., Buscot, F., ... Schmid, B. (2014). Designing forest biodiversity experiments: General considerations illustrated by a new large experiment in subtropical China. *Methods in Ecology and Evolution*, 5(1), 74–89. <https://doi.org/10.1111/2041-210X.12126>
- Chen, Y., Huang, Y., Niklaus, P. A., Castro-Izaguirre, N., Clark, A. T., ... Schmid, B. (2020). Directed species loss reduces community productivity in a subtropical forest biodiversity experiment. *Nature Ecology & Evolution*, 4, 550–559. <https://doi.org/10.1038/s41559-020-1127-4>
- Cowell, F.A. (2009). *Measuring Inequality*. Oxford University Press. <https://doi.org/10.1093/acprof:osobl/9780199594030.001.0001>
- Ehbrecht, M., Schall, P., Ammer, C., & Seidel, D. (2017). Quantifying stand structural complexity and its relationship with forest management, tree species diversity and microclimate. *Agricultural and Forest Meteorology*, 242(April), 1–9. <https://doi.org/10.1016/j.agrformet.2017.04.012>
- Ehbrecht, M., Schall, P., Juchheim, J., Ammer, C., & Seidel, D. (2016). Effective number of layers: A new measure for quantifying three-dimensional stand structure based on sampling with terrestrial LiDAR. *Forest Ecology and Management*, 380, 212–223. <https://doi.org/10.1016/j.foreco.2016.09.003>
- Ehbrecht, M., Seidel, D., Annighöfer, P., Kreft, H., Köhler, M., Zemp, D. C., ... Ammer, C. (2021) Global patterns and climatic controls of forest structural complexity. *Nature Communications*, 12, 519. <https://doi.org/10.1038/s41467-020-20767-z>
- Fahey, R.T., Alveshere, B.C., Burton, J.I., D'Amato, A.W., Dickinson, Y.L., Keeton, W.S., ... Hardiman, B.S. (2018). Shifting conceptions of complexity in forest management and silviculture. *Forest Ecology and Management*, 421(January), 59–71. <https://doi.org/10.1016/j.foreco.2018.01.011>
- Falster, D.S., & Westoby, M. (2003). Plant height and evolutionary games. *Trends in Ecology and Evolution*, 18(7), 337–343. [https://doi.org/10.1016/S0169-5347\(03\)00061-2](https://doi.org/10.1016/S0169-5347(03)00061-2)
- FAO. (2010). Global Forest Resources Assessment 2010. *FAO Forestry Paper*, 163. Retrieved from <http://www.fao.org/3/i1757e/i1757e.pdf>
- Felipe-Lucia, M.R., Soliveres, S., Penone, C., Manning, P., van der Plas, F., Boch, S., ... Allan, E. (2018). Multiple forest attributes underpin the supply of multiple ecosystem services. *Nature Communications*, 9(1), 4839. <https://doi.org/10.1038/s41467-018-07082-4>
- Fichtner, A., Härdtle, W., Bruelheide, H., Kunz, M., Li, Y., & von Oheimb, G. (2018). Neighbourhood interactions drive overyielding in mixed-species tree communities. *Nature Communications*, 9(1), 1144. <https://doi.org/10.1038/s41467-018-03529-w>
- Fichtner, A., Härdtle, W., Li, Y., Bruelheide, H., Kunz, M., & von Oheimb, G. (2017). From competition to facilitation: how tree species respond to neighbourhood diversity. *Ecology Letters*, 20(7), 892–900. <https://doi.org/10.1111/ele.12786>
- Fichtner, A., Schnabel, F., Bruelheide, H., Kunz, M., Mausolf, K., Schuldt, A., ... von Oheimb, G. (2020). Neighbourhood diversity mitigates drought impacts on tree growth. *Journal of Ecology*, 108(3), 865–875. <https://doi.org/10.1111/1365-2745.13353>
- Fornoff, F., Klein, A. M., Blüthgen, N., & Staab, M. (2019). Tree diversity increases robustness of multi-trophic interactions. *Proceedings of the Royal Society B: Biological Sciences*, 286(1898).

<https://doi.org/10.1098/rspb.2018.2399>

- Forrester, D. I. & Bausch, J.A. (2016). Review of processes behind diversity—productivity relationships in forests. *Current Forestry Reports* 2, 45–61. <https://doi.org/10.1007/s40725-016-0031-2>
- Gong, C., Tan, Q., Liu, G., & Xu, M. (2020). Mixed-species plantations enhance soil carbon stocks on the loess plateau of China. *Plant and Soil*, (C). <https://doi.org/10.1007/s11104-020-04559-4>
- Guillemot, J., Kunz, M., Schnabel, F., Fichtner, A., Madsen, C.P., Gebauer, T., ... Potvin, C. (2020). Neighbourhood-mediated shifts in tree biomass allocation drive overyielding in tropical species mixtures. *New Phytologist*. <https://doi.org/10.1111/nph.16722>
- Hakkenberg, C.R., Song, C., Peet, R.K., & White, P.S. (2016). Forest structure as a predictor of tree species diversity in the North Carolina Piedmont. *Journal of Vegetation Science*, 27(6), 1151–1163. <https://doi.org/10.1111/jvs.12451>
- Hess, C., Härdtle, W., Kunz, M., Fichtner, A., & von Oheimb, G. (2018). A high-resolution approach for the spatio-temporal analysis of forest canopy space using terrestrial laser scanning data. *Ecology and Evolution*, in press(September 2017), 1–12. <https://doi.org/10.1002/ece3.4193>
- Huang, Y., Chen, Y., Castro-Izaguirre, N., Baruffol, M., Brezzi, M., Lang, A., ... Schmid, B. (2018). Impacts of species richness on productivity in a large-scale subtropical forest experiment. *Science*, 362(6410), 80–83. <https://doi.org/10.1126/science.aat6405>
- IUCN. (2020). The Bonn Challenge. Retrieved June 21, 2020, from <https://www.iucn.org/pt/node/18963>
- Juchheim, J., Ehbrecht, M., Schall, P., Ammer, C., & Seidel, D. (2020). Effect of tree species mixing on stand structural complexity. *Forestry*, 93(1), 75–83. <https://doi.org/10.1093/forestry/cpz046>
- Keeling H.C., Phillips O.L. (2007) The global relationship between forest productivity and biomass. *Global Ecology and Biogeography* 16, 618–631. <https://doi.org/10.1111/j.1466-8238.2007.00314.x>
- Knuff, A.K., Staab, M., Frey, J., Dormann, C. F., Asbeck, T., & Klein, A.M. (2020). Insect abundance in managed forests benefits from multi-layered vegetation. *Basic and Applied Ecology*, 48, 124–135. <https://doi.org/10.1016/j.baae.2020.09.002>
- Kunz, M., Fichtner, A., Härdtle, W., Raunonen, P., Bruelheide, H., & von Oheimb, G. (2019). Neighbour species richness and local structural variability modulate aboveground allocation patterns and crown morphology of individual trees. *Ecology Letters*, 22, 2130–2140. <https://doi.org/10.1111/ele.13400>
- Kuznetsova, A., Brockhoff, P. B., & Christensen, R.H.B. (2017). {lmerTest} Package: Tests in Linear Mixed Effects Models. *Journal of Statistical Software*, 82(13), 1–26. <https://doi.org/10.18637/jss.v082.i13>
- Lang, A.C., Härdtle, W., Baruffol, M., Böhnke, M., Bruelheide, H., Schmid, B., von Wehrden H., & von Oheimb, G. (2012). Mechanisms promoting tree species coexistence: Experimental evidence with saplings of subtropical forest ecosystems of China. *Journal of Vegetation Science*, 23(5), 837–846. <https://doi.org/10.1111/j.1654-1103.2012.01403.x>
- Lang, A.C., von Oheimb, G., Scherer-Lorenzen, M., Bo, Y., Trogisch, S., Ma, K., & Härdtle, W. (2014). Mixed afforestations of young subtropical trees promote nitrogen acquisition and retention. *Journal of Applied Ecology*, 51, 224–233. <https://doi.org/10.1111/1365-2664.12157>
- Lecigne, B., Delagrangé, S., & Messier, C. (2014). VoxR: Metrics extraction of trees from T-LiDAR data. Retrieved from <https://cran.r-project.org/package=VoxR>
- Lefcheck, J.S. (2016). piecewiseSEM: Piecewise structural equation modelling in r for ecology, evolution, and systematics. *Methods in Ecology and Evolution*, 7(5), 573–579. <https://doi.org/10.1111/2041-210X.12512>
- Lewis, S.L., Wheeler, C.E., Mitchard, E.T.A., & Koch, A. (2019). Restoring natural forests is the best way to remove atmospheric carbon. *Nature*, 568(7750), 25–28. <https://doi.org/10.1038/d41586-019-01026-8>
- Li, Y., Hess, C., von Wehrden, H., Härdtle, W., & von Oheimb, G. (2014). Assessing tree dendrometrics in young regenerating plantations using terrestrial laser scanning. *Annals of Forest Science*, 71(4), 453–462. <https://doi.org/10.1007/s13595-014-0358-4>

- Li, Y., Kröber, W., Bruelheide, H., Härdtle, W., & von Oheimb, G. (2017). Crown and leaf traits as predictors of subtropical tree sapling growth rates. *Journal of Plant Ecology*, *10*(1), 136–145. <https://doi.org/10.1093/jpe/rtw041>
- Liang, J., Crowther, T.W., Picard, N., Wiser, S., Zhou, M., Alberti, G., ... Ferreira, L.V. (2016). Positive biodiversity-productivity relationship predominant in global forests, *354*(6309). <https://doi.org/10.1126/science.aaf8957>
- Liu, C.L.C., Kuchma, O., & Krutovsky, K.V. (2018). Mixed-species versus monocultures in plantation forestry: Development, benefits, ecosystem services and perspectives for the future. *Global Ecology and Conservation*, *15*, e00419. <https://doi.org/10.1016/j.gecco.2018.e00419>
- Martin-Ducup, O., Schneider, R., & Fournier, R.A. (2016). Response of sugar maple (*Acer saccharum*, Marsh.) tree crown structure to competition in pure versus mixed stands. *Forest Ecology and Management*, *374*, 20–32. <https://doi.org/10.1016/j.foreco.2016.04.047>
- McElhinny, C., Gibbons, P., Brack, C., & Bauhus, J. (2005). Forest and woodland stand structural complexity: Its definition and measurement. *Forest Ecology and Management*, *218*(1–3), 1–24. <https://doi.org/10.1016/j.foreco.2005.08.034>
- Morin, X., Fahse, L., Scherer-Lorenzen, M., & Bugmann, H. (2011). Tree species richness promotes productivity in temperate forests through strong complementarity between species. *Ecology Letters*, *14*(12), 1211–1219. <https://doi.org/10.1111/j.1461-0248.2011.01691.x>
- Neumann, M., & Starlinger, F. (2001). The significance of different indices for stand structure and diversity in forests. *Forest Ecology and Management*, *145*(1–2), 91–106. [https://doi.org/10.1016/S0378-1127\(00\)00577-6](https://doi.org/10.1016/S0378-1127(00)00577-6)
- Pebesma, E.J., & Bivand, R.S. (2005). Classes and methods for spatial data in R. *R News*, *5*(2), 9–13. Retrieved from <https://cran.r-project.org/doc/Rnews/>
- Perles-Garcia, M.D., Kunz, M., Fichtner, A., Härdtle, W., von Oheimb, G. (2020). Data from: Tree species richness promotes an early increase of stand structural complexity in young subtropical plantations. BEF-China project database. Retrieved from <https://data.botanik.uni-halle.de/bef-china/datasets/637>
- Piotto, D. (2008). A meta-analysis comparing tree growth in monocultures and mixed plantations. *Forest Ecology and Management*, *255*(3–4), 781–786. <https://doi.org/10.1016/j.foreco.2007.09.065>
- Pretzsch, H. (2009). *Forest Dynamics, Growth and Yield. Forest Dynamics, Growth and Yield.* <https://doi.org/10.1007/978-3-540-88307-4>
- Pretzsch, H. (2014). Canopy space filling and tree crown morphology in mixed-species stands compared with monocultures. *Forest Ecology and Management*, *327*, 251–264. <https://doi.org/10.1016/j.foreco.2014.04.027>
- R Core Team. (2018). R: A Language and Environment for Statistical Computing. Vienna, Austria. Retrieved from <https://www.r-project.org/>
- Schuldt, A., Assmann, T., Brezzi, M., Buscot, F., Eichenberg, D., Gutknecht, J., ... Bruelheide, H. (2018). Biodiversity across trophic levels drives multifunctionality in highly diverse forests. *Nature Communications*, *9*(1). <https://doi.org/10.1038/s41467-018-05421-z>
- Schuldt, A., Ebeling, A., Kunz, M., Staab, M., Guimarães-Steinicke, C., Bachmann, D., ... Eisenhauer, N. (2019). Multiple plant diversity components drive consumer communities across ecosystems. *Nature Communications*, *10*(1). <https://doi.org/10.1038/s41467-019-09448-8>
- Seidl, R., Spies, T.A., Peterson, D.L., Stephens, S.L., & Hicke, J.A. (2016). Searching for resilience: Addressing the impacts of changing disturbance regimes on forest ecosystem services. *Journal of Applied Ecology*, *53*(1), 120–129. <https://doi.org/10.1111/1365-2664.12511>
- Tang, G., & Li, K. (2013). Tree species controls on soil carbon sequestration and carbon stability following 20 years of afforestation in a valley-type savanna. *Forest Ecology and Management*, *291*, 13–19. <https://doi.org/10.1016/j.foreco.2012.12.001>

- Williams, L.J., Paquette, A., Cavender-Bares, J., Messier, C., & Reich, P.B. (2017). Spatial complementarity in tree crowns explains overyielding in species mixtures. *Methods in Ecology and Evolution*, 1(February). <https://doi.org/10.1038/s41559-016-0063>
- Yang, X., Jia, Z., & Ci, L. (2010). Assessing effects of afforestation projects in China. *Nature*, 466(7304), 315–315. <https://doi.org/10.1038/466315c>
- Yang, X., Bauhus, J., Both, S., Fang, T., Härdtle, W., Kröber, W., ... Bruelheide, H. (2013). Establishment success in a forest biodiversity and ecosystem functioning experiment in subtropical China (BEF-China). *European Journal of Forest Research*, 132(4), 593–606. <https://doi.org/10.1007/s10342-013-0696-z>
- Zemp, D.C., Ehbrecht, M., Seidel, D., Ammer, C., Craven, D., Erkelenz, J., ... Kreft, H. (2019a). Mixed-species tree plantings enhance structural complexity in oil palm plantations. *Agriculture, Ecosystems and Environment*, 283(September), 106564. <https://doi.org/10.1016/j.agee.2019.06.003>
- Zemp, D.C., Gérard, A., Hölscher, D., Ammer, C., Irawan, B., Sundawati, L., ... Kreft, H. (2019b). Tree performance in a biodiversity enrichment experiment in an oil palm landscape. *Journal of Applied Ecology*, (May), 1–13. <https://doi.org/10.1111/1365-2664.13460>
- Zuur, A.F., Ieno, E.N., Walker, N.S., & Smith, G.M. (2009). *Mixed Effects Models and Extensions in Ecology with R. Smart Society: A Sociological Perspective on Smart Living*. <https://doi.org/10.4324/9780429201271-2>

Chapter II. Neighbourhood species richness reduces crown asymmetry of subtropical trees in sloping terrain

Maria D. Perles-Garcia ^{1,2,*}, Matthias Kunz ³, Andreas Fichtner ⁴, Nora Meyer ³, Werner Härdtle ⁴ and Goddert von Oheimb ³

¹ German Centre for Integrative Biodiversity Research (iDiv), 04103 Leipzig, Germany

² Institute of Biology/Geobotany and Botanical Garden, Martin Luther University Halle-Wittenberg, 06108 Halle (Saale), Germany

³ Institute of General Ecology and Environmental Protection, Technische Universität Dresden,
01737 Tharandt, Germany; matthias.kunz@tu-dresden.de (M.K.); nora.meyer@tu-dresden.de (N.M.); goddert_v_oheimb@tu-dresden.de (G.v.O.)

⁴ Institute of Ecology, Leuphana University of Lüneburg, 21335 Lüneburg, Germany; fichtner@leuphana.de (A.F.); werner.haerdtle@leuphana.de (W.H.)

*Correspondence: maria_dolores.perles@idiv.de

Editorial status: Published in *Remote Sensing* (March 2022)

DOI: [10.3390/rs14061441](https://doi.org/10.3390/rs14061441)

Abstract

Reforestation in sloping terrain is an important measure for soil erosion control and sustainable watershed management. The mechanical stability of such reforested stands, however, can be low due to a strong asymmetric shape of tree crowns. We investigated how neighbourhood tree species richness, neighbourhood pressure, tree height, and slope inclination affect crown asymmetry in a large-scale plantation biodiversity-ecosystem functioning experiment in subtropical China (BEF-China) over eight years. We took the advantage of terrestrial laser scanning (TLS) measurements, which provide non-destructive, high-resolution data of tree structure without altering tree interactions. Neighbourhood species richness significantly reduced crown asymmetry, and this effect became stronger at steeper slopes. Our results suggest that tree diversity promotes the mechanical stability of forest stands in sloping terrain and highlight the importance of TLS-data for a comprehensive understanding of the role of tree diversity in modulating crown interactions in mixed-species forest plantations.

Keywords

BEF-China; biodiversity-ecosystem functioning; crown asymmetry; crown complementarity; forestry; LiDAR; sloping terrain; terrestrial laser scanning

1. Introduction

Global forest restoration is an essential measure to counteract ongoing biodiversity loss across biomes, and thereby, promoting ecological resilience and securing multiple benefits for people [1,2]. Similarly, (re-)establishing forests on formerly degraded land is a further important measure to halt ongoing global forest loss [3]. Specifically, planting trees at sloping sites, where land-use conflicts are low, has multiple ecological and socio-economic benefits, such as soil resource (e.g., reduction of erosion), watershed protection, or forest food and wood-based energy provisioning [4–7]. Yet, in such areas, restoration, reforestation, and afforestation success largely depends on the mechanical stability of planted trees. Although there is ample evidence why mixed-species forests should be prioritised over monocultures in forest projects [8], the role of (local) tree diversity in modulating the mechanical stability of planted trees in sloping terrain remains largely unknown.

Changes in local biotic and abiotic conditions are often reflected in tree morphological adjustments. There is ample evidence that crown asymmetry is strongly related to

competitive neighbourhood interactions [9], as trees try to avoid competitive pressure by adjusting their crown size and architecture relative to neighbour size. Such plastic responses to environmental conditions are species-specific and can be considered as one aspect of crown plasticity [10–13]. In general, crown plasticity enables trees to improve their light interception by resorting to spaces where light intensity is higher [14]. Given that competition for light is size-asymmetric [15], taller neighbours induce a higher competitive pressure on smaller individuals, which in turn results in a higher crown asymmetry of the suppressed tree [16,17]. Alternatively, crown asymmetry of tall individuals can result from a low competitive neighbourhood pressure when surrounding light conditions are highly heterogeneous and tall, competitive individuals expand their crowns in adjacent canopy gaps to improve their light interception [18]. Moreover, it has been shown that light-demanding tree species exhibit a higher plastic response compared to shade-tolerant species, and that, within a given level of shade tolerance, the strength of a species' response to slope inclination depends on its phenotypic plasticity (e.g., broad-leaved vs. coniferous tree species) [19–21]. Neighbour identity is a further potential factor that alters trees' crown shape. For example, light interception was found to be higher in species-mixtures than monocultures [22], most likely due to changes in biomass allocation pattern and branching modes, which in turn result in a higher crown complementarity [13,23–25]. Crown asymmetry can also result from harsh environmental conditions, such as exposure to strong winds [26] or slope inclination. As trees grow larger, they develop larger crowns. Large-sized crowns of trees growing on steep slopes should, therefore, be more affected by gravitropism compared to those with small-sized crowns, leading to a stronger asymmetric expansion of the crown towards the downhill direction of tall trees [9,27,28]. The magnitude of crown asymmetry, however, may regulate a trees' mechanical stability and thereby determine its susceptibility to abiotic disturbances, such as blowdowns and uprooting, ice, or snow break events. As the frequency and severity of extreme weather events are increasing due to climate change, it is important to understand how environmental factors affect crown asymmetry. Particularly, the importance of tree species richness at the local neighbourhood scale in shaping crown asymmetry is not well understood. This, in turn, has high relevance for sustainable forest management, particularly in sloping terrain. Assuming that species rich neighbourhoods promote positive interactions between tree species and, thus, growth and performance of individual trees, the establishment of highly diverse reforestations would significantly improve ecosystem functioning and related services such as timber production, carbon sequestration, or erosion control.

When it comes to quantifying crown asymmetry in mixed-species forests, terrestrial laser scanning (TLS) has proven to play an important role [29]. It is a non-destructive state-of-the-art technology that allows to quantify the three-dimensional structure of a given target tree and its surrounding neighbours without altering tree-tree interactions [30]. The high accuracy of TLS data (i.e., at the level of centimetres) offers detailed, high-resolution measures in forests that are difficult to derive from traditional survey methods [31,32] or from other remote sensing technics, such as airborne or mobile/personal laser scanning [33,34]. However, this technique is still expensive and requires personnel trained in the specific software to process the point clouds, so not many long-term studies of crown interactions are available [32]. Here, we used data from a large-scale plantation biodiversity-ecosystem functioning (BEF) experiment (BEF-China; www.bef-china.com, accessed on 21 February 2022), which was performed in subtropical China and planted in 2009 and 2010. Plot species richness ranged from monocultures up to 24 species mixtures [31]. Trees were planted in a regular grid, resulting in an initial maximum of eight neighbours. In total, we evaluated TLS data of 878 trees collected over a period of 8 years to address the follow questions: (i) What are the effects of local neighbourhood conditions (i.e., neighbourhood species richness and neighbourhood pressure) on crown development and crown displacement (CD) of a target tree (considering CD as a measure of crown asymmetry)? (ii) What are the effects of site microtopography (i.e., slope inclination at the spatial scale of an individual tree) on CD of a target tree? (iii) What are the underlying mechanisms of species richness–CD relationships and the modifying impacts of abiotic site conditions? We hypothesised (i) that neighbourhood species richness reduces CD due to complementarity effects and (ii) that the strength of neighbourhood species richness and neighbourhood pressure effects depend on microtopography.

2. Materials and methods

2.1. Study Site

The study was conducted in subtropical China at the biodiversity–ecosystem functioning experiment China (BEF-China) platform (29.08°–29.11°N, 117.90°–117.93°E, 100–300 m a.s.l., Figure 1) [35]. The trees of the experiment are representative for subtropical mixed evergreen broadleaved forests. The most common soil types are Cambisols and Regosols, with Acrisols along the slopes and Gleysols in the valleys [36]. The mean precipitation of the study area is 1821 mm year⁻¹ and the mean annual temperature is 16.7 °C (averaged from 1971 to 2000; [37]). The slope inclination of the terrain ranges between 1° and 53° (2% to 133%) [36]. The BEF-China experiment covers an area of ca. 37 ha. It consists of 566 study

plots established in two sites: site A, planted in 2009, and site B, planted in 2010. In each plot, 400 trees were planted following a regular grid of 20×20 trees with a distance between them of 1.29 m, so each tree counts with eight direct neighbours. The high tree diversity gradient of BEF China allows us to study the response of the same species in a direct neighbourhood species richness (NSR) ranging from zero (monoculture, all the trees are the same species as the target tree) to six.

For this study, we used data from 878 individual trees (i.e., target trees) of the eight tree species *Castanea henryi* (Skan) Rehder & E.H. Wilson, *Castanopsis sclerophylla* (Lindley & Paxton) Schottky, *Choerospondias axillaris* (Roxburgh) B. L. Burtt & A. W. Hill, *Liquidambar formosana* Hance, *Nyssa sinensis* Oliver, *Quercus serrata* Murray, *Sapindus saponaria* Linnaeus, and *Triadica sebifera* (Linnaeus) Small. These target trees grew in 30 study plots from Site A that varied in tree species richness ranging from monoculture to mixtures of 2, 4, and 8 species. All trees were randomly assigned to planting positions before planting, and were planted in a regular grid with a distance of 1.29 m. Further plot information is provided in Table S1.

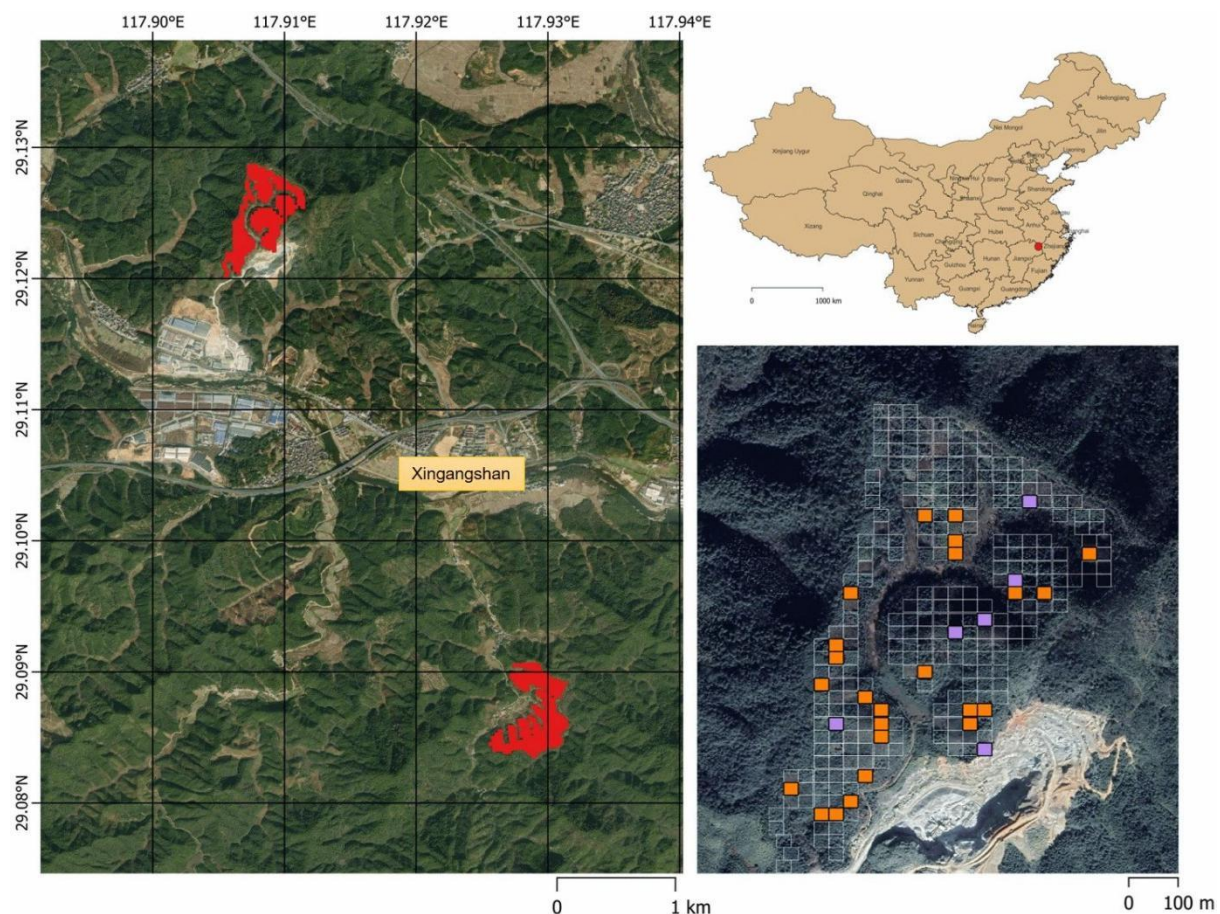


Figure 1. Location of the study site. The top right panel represents provincial boundary of China, adapted from the Stanford Geoweb service WFS (Hijmans, 2015). Location of the study area is represented with a red circle; the left panel shows the location of sites A and B (red polygons) and the closest village (Xingangshan), with the

coordinates on the ESRI ArcGIS World Imagery WMS. The bottom right panel shows the studied plots on the ESRI ArcGIS World Imagery WMS: in orange monocultures and two-species mixtures, where nine scan positions were distributed following a regular grid, and in purple the four- and eight- species mixtures, where 16 scan positions were regularly distributed in the centre of the plot.

2.2. Terrestrial Laser Scanning Data

TLS data have been collected during February–March of the years 2012, 2013, 2014, 2015, 2016, and 2019. For the whole period of time, this resulted in a total sample size of 4004 target trees. Table S2 shows an overview of the number and size of the files. Scanning was mainly done using the laser scanner FARO Focus S120, but also the FARO Focus X130 in 2019, and the FARO Photon Scanner in 2013 and 2012 (FARO Europe, Korntal-Münchingen, Germany). The technical specifications of the scanners can be found in Table S3.

The scan positions within the plot were equally distributed, recording the 6×6 central trees with 9 scan positions for the monocultures and two-species mixture plots, and the 12×12 central trees with 16 scan positions for the four- and eight-species mixture plots (Figure 2) [38]. Ten polystyrene spheres and three quadratic checkerboards were distributed in each plot and used as reflectance targets to co-register the point clouds. We used a spatial resolution equivalent of around 6 mm at a distance of 10 m. The FARO scanner was set up on a levelled tripod around 1.3 m in height. All scans were performed in almost windless conditions.

2.3. TLS Data Processing and Calculation of Crown Displacement

The calculation of CD was based on TLS measurements. To process the TLS data, we used FARO Scene software (V. 5.2.6) to co-register the point clouds of each plot. For the co-registration, mean reference tension did not exceed 0.005. Then, we used a statistical outlier removal to delete stray points and stored each point cloud in a local Cartesian coordinates system (3D coordinates: X, Y, Z). Individual trees were extracted manually using RiSCAN PRO (v2.6.2) and Bentley Pointools (v1.5 Pro). Each tree point cloud was identified by its relative position within the plot and related to the reference targets, and it was stored separately in an ASCII format.

Each of the registered point clouds of the plots in a given year exists in an arbitrary local coordinate system. This is explained by the missing GNSS capabilities of the FARO scanners. In order to compare the trees and the crowns over time, a multi-temporal co-registration into a common reference frame (here UTM Zone 50N, WGS84; EPSG:32650) was required. This was achieved in a two-step approach. First, the tree point clouds of the individual plots were registered relative to each other. The tree positions were registered using a 2D

conformal transformation with constant scale in a least squares fashion [39]. The tree positions from the year 2015 were used as references. The scanners, which have an in-built Inertial Measurement Unit (IMU), and the respective point clouds were levelled and rotated with respect to the horizontal level. In order to align the trees to the same height level, we projected the tree positions onto the respective digital terrain model (DTM) and calculated a mean height level for each plot and year. DTMs were extracted using the rasterise tool with the minimum Z coordinate at each grid cell of 5 cm. To avoid below ground points, each DTM was visually inspected before further processing. Possible gaps in the DTM were closed using the raster package in R. A height correction was then applied to the point clouds to achieve a match. In a second step, the local coordinates were transformed in the global coordinate system in the same fashion using the theoretically planned tree locations from the BEF-China data portal (<https://data.botanik.uni-halle.de/bef-china/>, accessed on 21 February 2022). All multi-temporal co-registrations of the tree positions showed a mean error around zero with normally distributed residuals (SD was between 1 and 3 cm).

For each target tree, we first determined crown projection area (CPA) from a 2D alpha shape [40] of the orthogonal projection of all tree points in the x-y plane. We also computed the geometric centre (centroid point) of the CPA. This point allows us to quantify the overall horizontal direction and magnitude of CD with respect to the planting position of the tree. Two-dimensional alpha shapes were computed in R 3.6.0 using the package [41]. The alpha-value was set to 0.5. The centroid, area, and perimeter of the enclosing polygon was computed using the sp package [42]. The stem position was computed by fitting a circle (least squares procedure) into a horizontal slice (3 cm slice thickness) of the tree point cloud at 5 cm above the ground. CD was calculated as the distance from the vector that goes from the stem position to the centre of the CPA based on the 2D polygon of the CPA (Figure 3a). The complete workflow is represented in Figure 2.

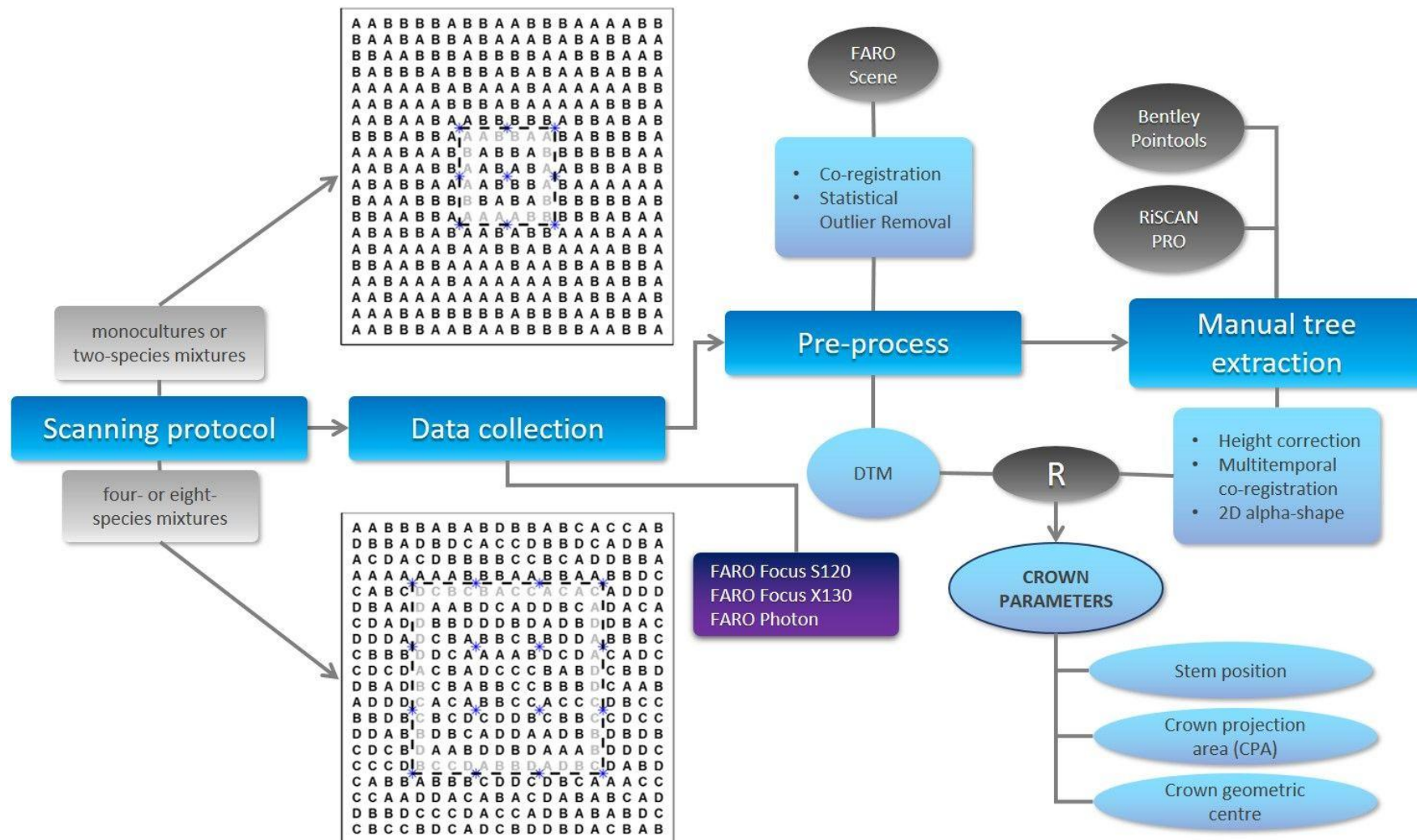


Figure 2. Workflow of data preparation. Schematic representation of the scanning protocol is adapted from Kunz et al. (2019, Figure S1) [13]. There, blue asterisks represent scanning positions, and letters indicate different tree species. Black circles show the used software, while the outcomes are in light blue circles. Main processes are in blue squares and the instruments used are in a purple square.

2.4. Explanatory Variables

To identify potential drivers of CD, we used microtopography, target tree height, neighbourhood pressure, and neighbourhood tree species richness as potential explanatory variables.

Microtopography (MT) was calculated as the distance from the stem position to the horizontal unit (one meter) in the direction of the steepest slope [11] (Figure 3b). For each plot and year, data on MT were obtained from the DTM (5 cm grid). Slope and aspect were computed for each tree with bilinear interpolation from the DTM at the respective tree location in the global coordinate system using the terrain function from the raster package in R [43]. The height of each target tree (TH) was calculated as the difference between the highest and lowest z-coordinate of the tree point cloud.

For each target tree, we calculated an index of neighbourhood pressure (NP, Equation (1)). Other studies assume a linear relation between the size of the tree and its pressure on the target tree [11,12,26,30,44]. In this study, we, therefore, developed a new parameter that scale the pressure depending on the relative canopy position in respect of the target tree: the canopy level index (C_{li} , Sup. Equation (1)). To account for the crown size of the neighbour and the direction of growth, we also include the CD of the neighbour.

$$NP = \sum_n \frac{(CD_n + CP) \times C_{li}}{CP^2} \quad (1)$$

NP was calculated using vectors: for each neighbour (n), we sum its vector of CD (CD_n , represented as a solid line in Figure 3c) to the competitive pressure (CP, represented as dotted line in Figure 3c). The resultant vector is escalated by the C_{li} (Sup. Equation (1)), and the result is divided by the squared of the CP. NP is the length of the vector that results from the sum of the individual NP from all direct neighbours (represented as a solid red arrow in Figure 3c).

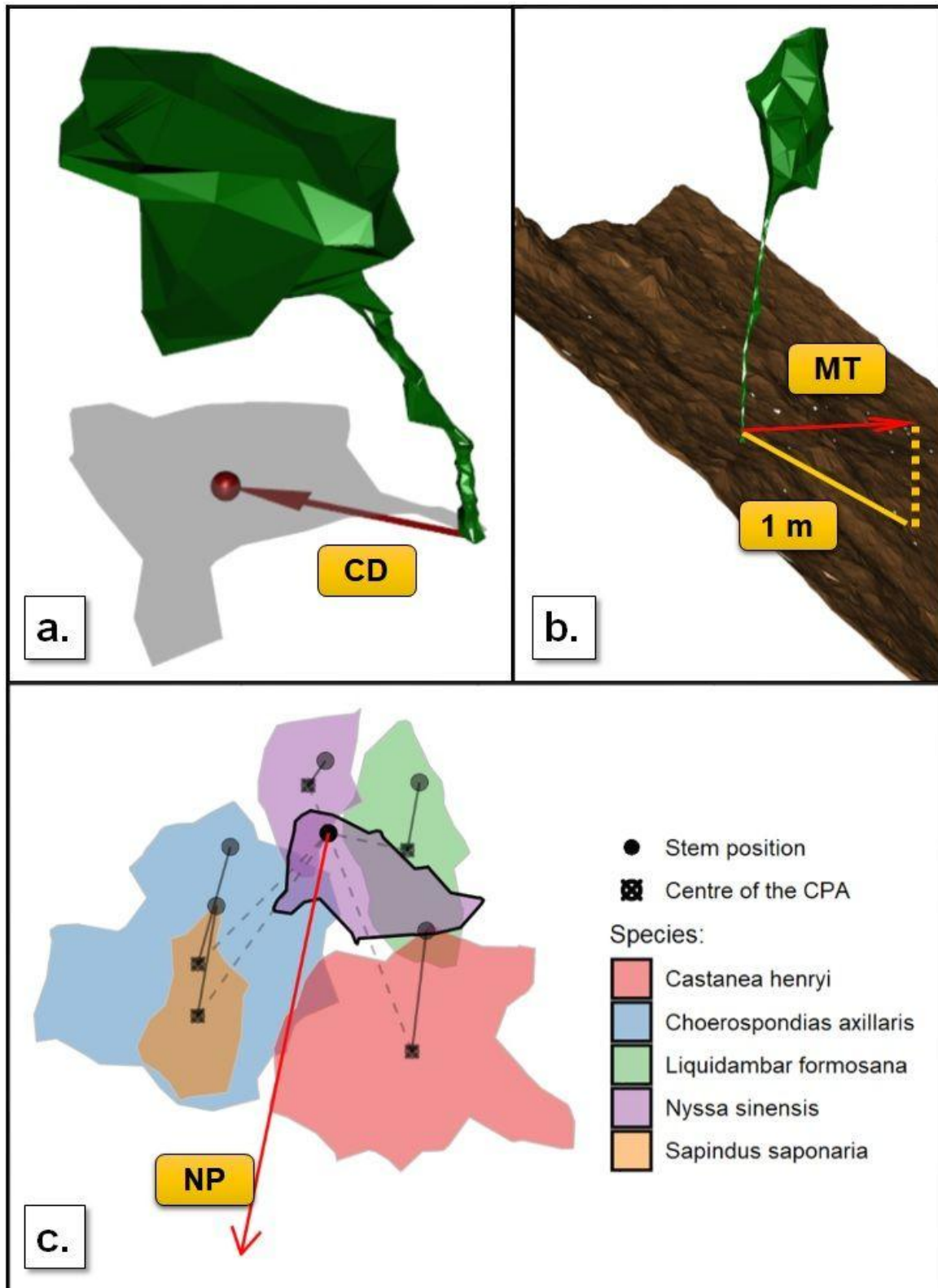


Figure 3. Graphic representation of (a) crown displacement, where the crown projection area is shown in grey, the centre is represented as a red dot, and the crown displacement is represented as a red arrow. In green is the alpha shape representation of an individual tree; (b) microtopography, showing in brown the terrain, in green the representation of an individual tree, and in red the vector of microtopography; and (c) neighbourhood pressure, showing the crown projection area of the target tree (with a black outline) and its direct neighbours. Dots represent the stem position, dots with a cross represent the centre of the crown projection area, solid lines represent the displacement of each neighbour, and dotted lines the pressure from the neighbour to the target

tree. The red arrow represents the total neighbourhood pressure. Different polygon colours indicate different tree species.

Neighbourhood tree species richness (NSR) was defined as the number of neighbours that differed in the species identity from the target tree. In this study, this resulted in a gradient of varying levels of NSR ranging from 0 (conspecific neighbours) to 6 (maximum of heterospecific neighbours). To ensure representative NSR-levels, respectively, we excluded those target trees ($n = 32$; 0.9% of the data) that were surrounded by six heterospecific neighbours (NSR = 6). Consequently, our NSR gradient ranged between zero and five.

2.5. Statistical Analyses

We applied linear mixed-effects models to test the effects of MT, tree size (TH), and neighbourhood conditions (NP and NSR) on CD. We also included the two-way interactions MT * NSR and NP * NSR in the initial model to test for potential NSR dependencies on the CD-MT and the CD-NP relationships. Given the positive relationship between TH and study year ($t: 34.97, p < 0.001$; Figure S3), TH also accounts for the temporal development of the target trees. Species identity of the target tree, neighbourhood tree species composition, and target tree nested in the study plot were used as crossed random effects. Moreover, we included target tree height as a random slope in the model structure, to test for the effect of tree ontogeny (i.e., tree height) depending on species. Including a random slope effect significantly improved the fit of the initial model ($\Delta AIC: 202.2; p < 0.001$).

Model selection (backward-approach) was based on likelihood ratio tests with maximum likelihood estimations [45]. The best-fitting model was based on restricted maximum likelihood estimation. CD and VP were square root-transformed prior to analyses to meet model assumptions, which were confirmed by the residual plots of the best-fitting model (Figure S4). Prior to analysis, all predictors were standardised (mean = 0, SD = 1). All analyses were conducted using R (version 4.0.2) and the packages circular, lm4, lmerTest, MuMIn, and sjPlot.

3. Results

The best-fitting model included microtopography (MT), target tree height (TH), neighbourhood pressure (NP), and neighbourhood tree species richness (NSR), as well as the interaction between MT and NSR, and explained 60% (fixed-effects only, marginal R^2) and 85% (fixed and random effects, conditional R^2) of the variation in CD (Table 1). As expected, TH was the strongest predictor for square root-transformed CD, followed by NP (Figure 4; Table 1). Here, CD increased as trees grew larger or experienced a higher NP

intensity (Figure 4). Moreover, the positive effect of MT on CD was modulated by NSR (two-way interaction MT * NSR: $\chi^2 = 0.40$, $p = 0.036$; Table 1). CD decreased continuously with increasing NSR, and this effect became stronger with increasing MT (Figure 5a). As a result, CD of trees growing in heterospecific neighbourhoods were 4 % (NSR: 1) to 18% (NSR: 5) lower than in conspecific neighbourhoods on average (Figure 5b). A maximum reduction of CD (33%) was observed for trees on steep slopes (i.e., 51° in our study) growing in species-rich neighbourhoods (NSR: 5; Figure 5b). In contrast, we did not find an NSR dependency of NP effects (two-way interaction NP * NSR: $\chi^2 = 0.32$, $p = 0.571$).

Table 1. Results of mixed-effects model of microtopography (MT), target tree height (TH), neighbourhood pressure (NP, square root-transformed), neighbourhood tree species richness (NSR), and the interaction between MT and NSR on crown displacement (square root-transformed). Parameter estimates are standardised and represent the effect size of the covariates in the model. $n = 4004$.

	Estimate	SE	df	F	<i>p</i>
MT	0.0109	0.0058	383.3233	3.5242	0.0609
TH	0.2119	0.0187	6.6612	127.8893	<0.001
NP	0.0578	0.0031	3909.9625	355.8978	<0.001
NSR	-0.0244	0.0090	160.9722	7.3146	0.0076
MT * NSR	-0.0111	0.0053	1125.5189	4.3397	0.0375
Marginal R ²		0.60			
Conditional R ²		0.85			
Random effects					
	SD (tree tag nested plot)			0.1022	
	SD (plot)			0.0601	
	SD (species identity)			0.0589	
	SD (neighbourhood composition)			0.0511	
	SD (tree height)			0.0516	

SE: standard error; df: degrees of freedom; SD: standard deviation.

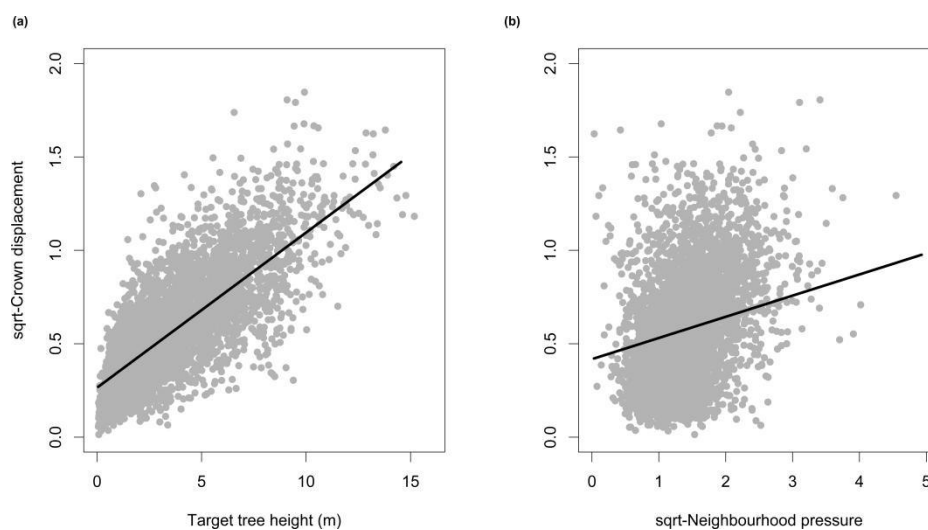


Figure 4. Differences in the strength of the effects of (a) target tree height and (b) neighbourhood pressure (square root-transformed) on crown displacement (square root-transformed). Lines represent mixed-effects model fits with microtopography and neighbourhood tree species richness kept at their means. Grey points represent observed values.

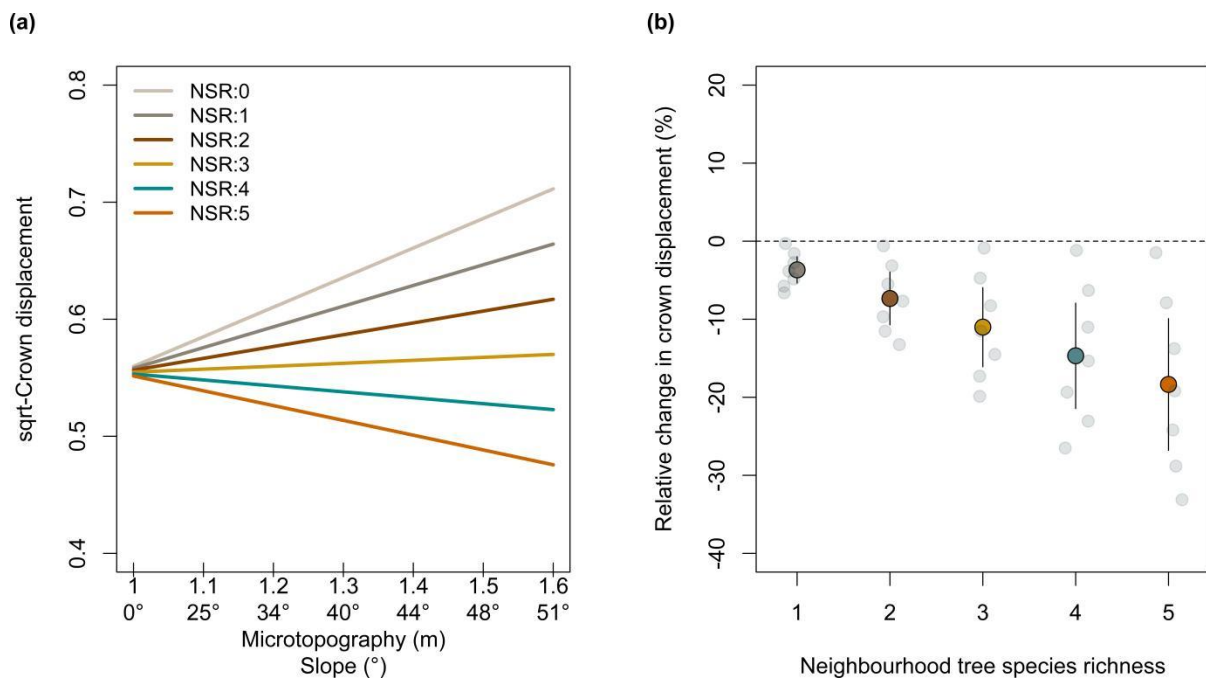


Figure 5. (a) Effects of microtopography (MT) on crown displacement (square root-transformed) with varying levels of neighbourhood tree species richness (NSR). Lines represent mixed-effects model fits (with target tree height and neighbourhood pressure kept at its mean). X-axis shows MT in meters and its conversion to slope in degrees. **(b)** Relative changes (%) in crown displacement between conspecific neighbourhoods (NSR: 0) and heterospecific neighbourhoods (NSR: 1–5). Dots represent predicted means based on a mixed-effects model (with target tree height kept at its mean), and error bars indicate the 95% confidence interval of the prediction. Grey points (slightly jittered to facilitate visibility) represent predictions for each level of the microtopography gradient ranging from 1 to 1.6 (see panel (a)).

4. Discussion

Based on an eight-year TLS measurement series on tree growth in the BEF-China experiment, our study provides evidence that NSR has the potential to significantly reduce the CD of trees growing in sloping terrain. We hypothesise that this finding is mainly attributable to the effects of interspecific niche complementarity between neighbouring trees, which increases with increasing tree NSR [46]. There is evidence that increasing NSR increases the probability of neighbouring trees to differ with regard to growth-related functional traits, which in turn affect tree–tree interactions in diverse neighbourhoods. For example, functional richness-related differences in crown traits, biomass allocation patterns, or light requirements are important drivers of crown complementarity and may, therefore, reduce interspecific competition between neighbouring trees [21,24,25,47,48]. As a result, NSR may improve tree crown complementarity (also in a physical sense) and, thus, decreases CD as an expression of decreasing competitive interactions. This interpretation is in agreement with previous studies which have shown that tree species differ in biomass allocation patterns when comparing their growth behaviour in mixtures and monocultures (increasing crown plasticity in mixtures; [23,24]). Thus, high functional diversity (with

regard to growth-related traits) allows tree canopies to complement each other without increasing asymmetry. This is particularly important in the context of forests growing on slopes, as it could potentially increase individual tree survival by reducing the risk of stem breakage, and thus, enhance stand stability.

Interestingly, we also found a significant interaction effect between MT and NSR, which negatively affects CD (partly confirming our second hypothesis). As indicated by Figure 5a, CD decreases with decreasing MT for conspecific neighbourhoods, but increases with decreasing MT for heterospecific neighbourhoods. These findings suggest that intraspecific competition (i.e., in conspecific neighbourhoods and monocultures, respectively) increases with increasing MT, which in turn forces trees to a higher crown displacement, e.g., for minimising overshading (i.e., competition for light [16,19]). In contrast, trees in heterospecific neighbourhoods benefit from a diverse neighbourhood with increasing MT, since complementarity effects (e.g., attributable to different light requirements of different tree species) may minimise neighbourhood pressure and, thus, CD [21,49]. In this context, it is important to note that the CD of trees could also increase with increasing MT due to physical displacement mechanisms, e.g., because trees might tend to overturn downslope due to unstable substrate conditions. However, this process is effective across tree species and different neighbourhood richness levels and, thus, cannot explain the negative NSR and MT*NSR effects on CD. However, our findings did not support our expectation that NSR effects on CD are mediated by NP (i.e., we found no significant NP×NSR interaction). This suggests that NP is strongly co-determined by tree height, which in turn affects CD (see below) and is effective regardless of NSR.

TH proved to be the strongest predictor of CD, with a positive relationship between CD and TH. This contradicts findings from tropical forests, according to which TH and CD were negatively correlated [16]. Our results suggest that trees growing on sloping terrain develop asymmetric crowns already at an early stage, and this asymmetry becomes stronger over time, that is, with proceeding growth of the trees. It is likely that differences in TH are a driver of overshading, particularly for trees growing downslope, which forces them to develop asymmetric crowns to improve light access. High CD, in turn, could be problematic for the survival of trees in the longer term, because a strongly asymmetric crown growing on a steep slope could challenge the trees' capability to physically stabilise its crown architecture against gravity forces [10], but also increases the risk of stem breakage.

In addition to TH, NP also proved to be an important predictor for CD, since NP strengthened CD (according to the model prediction) and was closely positively correlated

with CD ($r = 0.73$, Figure S2). This is consistent with previous studies, which also showed a strong impact of NP on CD [11,12,50,51]. Some studies found no significant effect of NP on CD, but showed a close correlation between the direction of NP and CD [30,44]. A main mechanism underlying our findings could be that competitive interactions increase with increasing NP (e.g., for resources such as light). Increasing CD, thus, indicates that trees attempt to avoid overshading (e.g., by upslope individuals), and therefore, re-position their crowns. This is accompanied by a trade-off between morphological plasticity and mechanical stability, and thus, high CD may decrease the mechanical stability of trees and forest stands. CD, therefore, could be considered as an adaptive mechanism to avoid competition for solar radiation by searching for canopy gaps. Since our refined equation for capturing neighbourhood pressure effects (Sup. methods) significantly improved the fit of the initial model ($\Delta AIC: 135$, $p < 0.001$; Table S2) compared to the index proposed by Brisson and Reynolds [52], it is likely that the relative position of the neighbour crown and its asymmetry constitute an important driver for crown asymmetry.

MT proved to be a third significant driver of CD. Even though several studies already showed that MT had a positive effect on CD [9,11,53–55], we can substantiate this based on data from a controlled experimental setting. MT strongly impacts CD, because trees tend to grow downslope to avoid overshading and to improve light availability [55]. This interpretation is supported by our finding that the direction of the CD was highly positively correlated with the direction of MT (Figure S2) Importantly, this downhill orientation of the tree crowns emerged rapidly, since it was already developed within the first study years (i.e., only a few years after planting). The consequences of our findings for sustainable forest management are discussed in the following conclusion section (see also [56–58]).

5. Conclusions

Reforestation of sloping terrain is an important measure to counteract the adverse effects of former clear-cuts and to improve ecosystem services related to the reestablishment of forest ecosystems. Forest restoration, particularly in sloping areas, improves carbon sequestration, stabilises slopes by preventing soil erosion, improves groundwater recharge, and may improve timber supply for local people. However, many forest restoration projects, particularly in the tropics and subtropics, made use of few or even only one tree species, despite a broad spectrum of native tree species typical of natural forests of these regions. Thus, resulting monocultures often show limited functions, for example in terms of productivity or stability with regard to extreme weather events, but also miss the

opportunity to support high biodiversity, which in turn stabilises food webs and contributes to improved ecosystem functioning.

The present study provides further evidence for the use of a diverse spectrum of tree species in the context of reforestation projects and sustainable forest management practices, particularly for sloping terrain. Our results suggest that tree species richness at the local neighbourhood scale also plays a crucial role for the patterns of tree crown development at sloping sites, as neighbourhood tree species richness minimises crown displacement, most likely as a result of complementarity effects increasing with an increasing neighbourhood species richness. This in turn indicates that tree diversity has the potential to physically stabilise tree growth at sloping sites, reduces the risk of stem breakage or blowdowns, and improves the quality of timber due to the formation of stems with lower CD. As a consequence, sustainable forest management should therefore use the widest possible range of tree species that are natural and representative for a given area. In this way, forestry could improve the functioning of forest plantations (e.g., in the context of reforestation projects) and related ecosystem services such as timber production, carbon sequestration, or erosion control. In summary, our findings stress the importance of tree diversity for forest stability and may encourage forest restoration projects to use a high number of native tree species, particularly in the face of ongoing global environmental shifts such as climate change.

Information about Supplementary materials

The following supporting information can be downloaded at: www.mdpi.com/xxx/s1, Supporting Methods: Neighbourhood pressure (NP); Table S1: Included plots and their characteristics; Table S2: Overview of mean file size (and standard deviation) in Mb for each year and plot. In addition, the number of scans is given for each plot; Table S3: Technical specification of the three FARO scanners based on the technical fact sheets by FARO (Korntal-Münchingen, Germany); Table S4: Model comparison using different calculations of neighbourhood pressure index; Figure S1: Representation of possible inaccuracies when using (a) crown projection area or (b) height as size measurement for the neighbourhood pressure index; Figure S2: Curve of the function for the canopy level index (c_i); Figure S3: Correlations between the direction of crown displacement (CD), microtopography (MT), and neighbourhood pressure (NP); Figure S4: Boxplot showing the relationship between tree height and study year; Figure S5: Residual plots of the best-fitting model.

Author Contributions

Conceptualisation, M.D.P.-G., G.v.O., W.H., and M.K.; methodology, M.D.P.-G., N.M., and M.K.; software, M.D.P.-G., N.M., A.F., and M.K.; validation, A.F.; formal analysis, M.D.P.-G., M.K., and A.F.; investigation, M.D.P.-G. and M.K.; resources, G.v.O. and W.H.; data curation, M.D.P.-G., M.K., and A.F.; writing—original draft preparation, M.D.P.-G.; writing—review and editing, M.D.P.-G., G.v.O., A.F., W.H., M.K., and N.M.; visualisation, M.D.P.-G. and A.F.; supervision, G.v.O.; project administration, G.v.O. and W.H.; funding acquisition, G.v.O. and W.H. All authors have read and agreed to the published version of the manuscript.

Funding

This research was funded by the Deutsche Forschungsgemeinschaft (DFG, German Research Foundation), grant number 319936945/GRK2324, and by the University of Chinese Academy of Sciences (UCAS).

Data Availability Statement

Data available under request via the BEF-China project database: <https://data.botanik.uni-halle.de/bef-china/datasets/654>, accessed on 15 March 2022 (Perles-Garcia et al., 2022).

Acknowledgments

We are grateful to the local workers and to M. Hildebrand and G. Hähn, who assisted to conduct the scans in the field, to A. Koller and I. Frehse, who contributed processing the data, to R. Vidaurre and A. Vovides, who supported the development of the methodology, and to the BEF-China coordination team for continuous logistical support.

Conflicts of Interest

The authors declare no conflict of interest. The funders had no role in the design of the study; in the collection, analyses, or interpretation of data; in the writing of the manuscript, or in the decision to publish the results.

References

1. Brancalion, P.H.S.; Niamir, A.; Broadbent, E.; Crouzeilles, R.; Barros, F.S.M.; Almeyda Zambrano, A.M.; Baccini, A.; Aronson, J.; Goetz, S.; Leighton Reid, J.; et al. Global restoration opportunities in tropical rainforest landscapes. *Sci. Adv.* 2019, 5, 1–12, doi:10.1126/sciadv.aav3223.
2. Fichtner, A.; Härdtle, W. Forest Ecosystems: A Functional and Biodiversity Perspective. In *Perspectives for Biodiversity and Ecosystems*; Hobohm, C., Ed.; Springer International Publishing: Cham, 2021; pp. 383–405 ISBN 978-3-030-57710-0.

3. FAO Global Forest Resources Assessment 2020: Main report.; Rome, 2020;
4. Lamb, D.; Erskine, P.D.; Parrotta, J.A. Restoration of degraded tropical forest landscapes. *Science* 2005, 310, 1628–1632, doi:10.1126/science.1111773.
5. Jagger, P.; Pender, J. The role of trees for sustainable management of less-favored lands: The case of eucalyptus in Ethiopia. *For. Policy Econ.* 2003, 5, 83–95, doi:10.1016/S1389-9341(01)00078-8.
6. Wenhua, L. Degradation and restoration of forest ecosystems in China. *For. Ecol. Manage.* 2004, 201, 33–41, doi:10.1016/j.foreco.2004.06.010.
7. Hou, G.; Delang, C.O.; Lu, X. Afforestation changes soil organic carbon stocks on sloping land: The role of previous land cover and tree type. *Ecol. Eng.* 2020, 152, 105860, doi:10.1016/j.ecoleng.2020.105860.
8. Lewis, S.L.; Wheeler, C.E.; Mitchard, E.T.A.; Koch, A. Restoring natural forests is the best way to remove atmospheric carbon. *Nature* 2019, 568, 25–28, doi:10.1038/d41586-019-01026-8.
9. Lang, A.C.; Härdtle, W.; Bruelheide, H.; Geißler, C.; Nadrowski, K.; Schuldt, A.; Yu, M.; von Oheimb, G. Tree morphology responds to neighbourhood competition and slope in species-rich forests of subtropical China. *For. Ecol. Manage.* 2010, 260, 1708–1715, doi:10.1016/j.foreco.2010.08.015.
10. Valladares, F.; Gianoli, E.; Gómez, J.M. Ecological limits to plant phenotypic plasticity. *New Phytol.* 2007, 176, 749–763, doi:10.1111/j.1469-8137.2007.02275.x.
11. Umeki, K. Modeling the relationship between the asymmetry in crown display and local environment. *Ecol. Modell.* 1995, 82, 11–20, doi:10.1016/0304-3800(94)00081-R.
12. Schröter, M.; Härdtle, W.; von Oheimb, G. Crown plasticity and neighborhood interactions of European beech (*Fagus sylvatica* L.) in an old-growth forest. *Eur. J. For. Res.* 2012, 131, 787–798, doi:10.1007/s10342-011-0552-y.
13. Kunz, M.; Fichtner, A.; Härdtle, W.; Raunonen, P.; Bruelheide, H.; von Oheimb, G. Neighbour species richness and local structural variability modulate aboveground allocation patterns and crown morphology of individual trees. *Ecol. Lett.* 2019, 22, 2130–2140, doi:10.1111/ele.13400.
14. Uria-Diez, J.; Pommerening, A. Crown plasticity in Scots pine (*Pinus sylvestris* L.) as a strategy of adaptation to competition and environmental factors. *Ecol. Modell.* 2017, 356, 117–126, doi:10.1016/j.ecolmodel.2017.03.018.
15. Schwinning, S.; Weiner, J. Mechanisms the degree of size asymmetry determining in competition among plants. *Oecologia* 2012, 113, 447–455.
16. Young, T.P.; Hubbell, S.P. Crown asymmetry, treefalls, and repeat disturbance of broad-leaved forest gaps. *Ecology* 1991, 72, 1464–1471.
17. Longuetaud, F.; Piboule, A.; Wernsdörfer, H.; Collet, C. Crown plasticity reduces inter-tree competition in a mixed broadleaved forest. *Eur. J. For. Res.* 2013, 132, 621–634, doi:10.1007/s10342-013-0699-9.
18. Muth, C.C.; Bazzaz, F.A. Tree canopy displacement and neighborhood interactions. *Can. J. For. Res.* 2003, 33, 1323–1330, doi:10.1139/x03-045.
19. Niinemets, Ü. A review of light interception in plant stands from leaf to canopy in different plant functional types and in species with varying shade tolerance. *Ecol. Res.* 2010, 25, 693–714, doi:10.1007/s11284-010-0712-4.
20. Böhnke, M.; Bruelheide, H. How do evergreen and deciduous species respond to shade?-Tolerance and plasticity of subtropical tree and shrub species of South-East China. *Environ. Exp. Bot.* 2013, 87, 179–190, doi:10.1016/j.envexpbot.2012.09.010.
21. Jucker, T.; Bouriaud, O.; Coomes, D.A. Crown plasticity enables trees to optimize canopy packing in mixed-species forests. *Funct. Ecol.* 2015, 29, 1078–1086, doi:10.1111/1365-2435.12428.
22. Duarte, M.M.; Moral, R. de A.; Guillemot, J.; Zuim, C.I.F.; Potvin, C.; Bonat, W.H.; Stape, J.L.; Brancalion, P.H.S. High tree diversity enhances light interception in tropical forests. *J. Ecol.* 2021, 109, 2597–2611, doi:10.1111/1365-2745.13669.

23. Guillemot, J.; Kunz, M.; Schnabel, F.; Fichtner, A.; Madsen, C.P.; Gebauer, T.; Härdtle, W.; von Oheimb, G.; Potvin, C. Neighbourhood-mediated shifts in tree biomass allocation drive overyielding in tropical species mixtures. *New Phytol.* 2020, 228, 1256–1268, doi:10.1111/nph.16722.
24. Hildebrand, M.; Perles-Garcia, M.D.; Kunz, M.; Härdtle, W.; von Oheimb, G.; Fichtner, A. Tree-tree interactions and crown complementarity: The role of functional diversity and branch traits for canopy packing. *Basic Appl. Ecol.* 2021, 50, 217–227, doi:10.1016/j.baae.2020.12.003.
25. Williams, L.J.; Paquette, A.; Cavender-Bares, J.; Messier, C.; Reich, P.B. Spatial complementarity in tree crowns explains overyielding in species mixtures. *Methods Ecol. Evol.* 2017, 1, doi:10.1038/s41559-016-0063.
26. Vovides, A.G.; Berger, U.; Grueters, U.; Guevara, R.; Pommerening, A.; Lara-Domínguez, A.L.; López-Portillo, J. Change in drivers of mangrove crown displacement along a salinity stress gradient. *Funct. Ecol.* 2018, 32, 2753–2765, doi:10.1111/1365-2435.13218.
27. Umeki, K. Importance of crown position and morphological plasticity in competitive interaction in a population of *Xanthium canadense*. *Ann. Bot.* 1995, 75, 259–265.
28. Matsuzaki, J.; Masumori, M.; Tange, T. Stem phototropism of trees: A possible significant factor in determining stem inclination on forest slopes. *Ann. Bot.* 2006, 98, 573–581, doi:10.1093/aob/mcl127.
29. Calders, K.; Adams, J.; Armston, J.; Bartholomeus, H.; Bauwens, S.; Bentley, L.P.; Chave, J.; Danson, F.M.; Demol, M.; Disney, M.; et al. Terrestrial laser scanning in forest ecology: Expanding the horizon. *Remote Sens. Environ.* 2020, 251, 112102, doi:10.1016/j.rse.2020.112102.
30. Seidel, D.; Leuschner, C.; Müller, A.; Krause, B. Crown plasticity in mixed forests—Quantifying asymmetry as a measure of competition using terrestrial laser scanning. *For. Ecol. Manage.* 2011, 261, 2123–2132, doi:10.1016/j.foreco.2011.03.008.
31. Newnham, G.J.; Armston, J.D.; Calders, K.; Disney, M.I.; Lovell, J.L.; Schaaf, C.B.; Strahler, A.H.; Danson, F.M. Terrestrial laser scanning for plot-scale forest measurement. *Curr. For. Reports* 2015, 1, 239–251, doi:10.1007/s40725-015-0025-5.
32. Liang, X.; Kankare, V.; Hyypä, J.; Wang, Y.; Kukko, A.; Haggren, H.; Yu, X.; Kaartinen, H.; Jaakkola, A.; Guan, F.; et al. Terrestrial laser scanning in forest inventories. *ISPRS J. Photogramm. Remote Sens.* 2016, 115, 63–77, doi:10.1016/j.isprsjprs.2016.01.006.
33. Bienert, A.; Georgi, L.; Kunz, M.; Maas, H.G.; von Oheimb, G. Comparison and combination of mobile and terrestrial laser scanning for natural forest inventories. *Forests* 2018, 9 (7), 395, doi:10.3390/f9070395.
34. Jung, S.E.; Kwak, D.A.; Park, T.; Lee, W.K.; Yoo, S. Estimating crown variables of individual trees using airborne and terrestrial laser scanners. *Remote Sens.* 2011, 3, 2346–2363, doi:10.3390/rs3112346.
35. Bruelheide, H.; Nadrowski, K.; Assmann, T.; Bauhus, J.; Both, S.; Buscot, F.; Chen, X.Y.; Ding, B.; Durka, W.; Erfmeier, A.; et al. Designing forest biodiversity experiments: General considerations illustrated by a new large experiment in subtropical China. *Methods Ecol. Evol.* 2014, 5, 74–89, doi:10.1111/2041-210X.12126.
36. Scholten, T.; Goebes, P.; Kuhn, P.; Seitz, S.; Assmann, T.; Bauhus, J.; et al. On the combined effect of soil fertility and topography on tree growth in subtropical forest ecosystems—a study from SE China. *J. Plant Ecol.* 2017, 10(1), 111–127, doi:10.1093/jpe/rtw065.
37. Yang, X.; Bauhus, J.; Both, S.; Fang, T.; Härdtle, W.; Kröber, W.; Ma, K.; Nadrowski, K.; Pei, K.; Scherer-Lorenzen, M.; et al. Establishment success in a forest biodiversity and ecosystem functioning experiment in subtropical China (BEF-China). *Eur. J. For. Res.* 2013, 132, 593–606, doi:10.1007/s10342-013-0696-z.
38. Li, Y.; Hess, C.; von Wehrden, H.; Härdtle, W.; von Oheimb, G. Assessing tree dendrometrics in young regenerating plantations using terrestrial laser scanning. *Ann. For. Sci.* 2014, 71, 453–462, doi:10.1007/s13595-014-0358-4.
39. Ghilani, C.D.; Wolf, P.R. Adjustment computations: Spatial data analysis; 5th ed.; 2010.

40. Edelsbrunner, H.; Kirkpatrick, D.; Seidel, R. On the shape of a set of points in the plane. *IEEE Trans. Inf. Theory* 1983, 29, 551–559, doi:10.1109/TIT.1983.1056714.
41. Pateiro-Lopez, B.; Rodriguez-Casal, A. *alphahull Generalization of the Convex Hull of a Sample of Points in the Plane* 2019.
42. Bivand, R.S.; Pebesma, E.; Gomez-Rubio, V. *Applied spatial data analysis with R*, Second edition; Springer, NY, 2013.
43. Hijmans, R.J. *raster: Geographic Data Analysis and Modeling* 2020.
44. Brisson, J. Neighborhood competition and crown asymmetry in *Acer saccharum*. *Can. J. For. Res.* 2001, 31, 2151–2159, doi:10.1139/x01-161.
45. Zuur, A.F.; Ieno, E.N.; Walker, N.S.; Smith, G.M. *Mixed Effects Models and Extensions in Ecology with R*; 2009; ISBN 9780429576966.
46. Niklaus, P.A.; Baruffol, M.; He, J.S.; Ma, K.; Schmid, B. Can niche plasticity promote biodiversity–productivity relationships through increased complementarity? *Ecology* 2017, 98, 1104–1116, doi:10.1002/ecy.1748.
47. Schmid, B.; Niklaus, P.A. Biodiversity: Complementary canopies. *Nat. Ecol. Evol.* 2017, 1, 0104, doi:10.1038/s41559-017-0104.
48. Ali, A.; Lin, S.L.; He, J.K.; Kong, F.M.; Yu, J.H.; Jiang, H.S. Tree crown complementarity links positive functional diversity and aboveground biomass along large-scale ecological gradients in tropical forests. *Sci. Total Environ.* 2019, 656, 45–54, doi:10.1016/j.scitotenv.2018.11.342.
49. Fichtner, A.; Härdtle, W.; Bruelheide, H.; Kunz, M.; Li, Y.; von Oheimb, G. Neighbourhood interactions drive overyielding in mixed-species tree communities. *Nat. Commun.* 2018, 9, 1144, doi:10.1038/s41467-018-03529-w.
50. Lang, A.C.; von Oheimb, G.; Scherer-Lorenzen, M.; Yang, B.; Trogisch, S.; Bruelheide, H.; Ma, K.; Härdtle, W. Mixed afforestation of young subtropical trees promotes nitrogen acquisition and retention. *J. Appl. Ecol.* 2014, 51, 224–233, doi:10.1111/1365-2664.12157.
51. Aakala, T.; Shimatani, K.; Abe, T.; Kubota, Y.; Kuuluvainen, T. Crown asymmetry in high latitude forests: disentangling the directional effects of tree competition and solar radiation. *Oikos* 2016, 125, 1035–1043, doi:10.1111/oik.02858.
52. Brisson, J.; Reynolds, J.F. The effect of neighbors on root distribution in a creosotebush (*Larrea Tridentata*) population. *Ecology* 1994, 75, 1693–1702, doi:10.2307/1939629.
53. Ehbrecht, M.A. *Quantifying three-dimensional stand structure and its relationship with forest management and microclimate in temperate forest ecosystems*, Georg-August-Universität Göttingen, 2018.
54. Getzin, S.; Wiegand, K. Asymmetric tree growth at the stand level: Random crown patterns and the response to slope. *For. Ecol. Manage.* 2007, 242, 165–174, doi:10.1016/j.foreco.2007.01.009.
55. Sumida, A.; Terazawa, I.; Togashi, A.; Komiyama, A. Spatial arrangement of branches in relation to slope and neighbourhood competition. *Ann. Bot.* 2002, 89, 301–310, doi:10.1093/aob/mcf042.
56. Song, Z.; Seitz, S.; Li, J.; Goebes, P.; Schmidt, K.; Kühn, P.; Shi, X.; Scholten, T. Tree diversity reduced soil erosion by affecting tree canopy and biological soil crust development in a subtropical forest experiment. *For. Ecol. Manage.* 2019, 444, 69–77, doi:10.1016/j.foreco.2019.04.015.
57. Schuldt, A.; Ebeling, A.; Kunz, M.; Staab, M.; Guimarães-Steinicke, C.; Bachmann, D.; Buchmann, N.; Durka, W.; Fichtner, A.; Fornoff, F.; et al. Multiple plant diversity components drive consumer communities across ecosystems. *Nat. Commun.* 2019, 10, 1460, doi:10.1038/s41467-019-09448-8.
58. Fichtner, A.; Härdtle, W.; Li, Y.; Bruelheide, H.; Kunz, M.; von Oheimb, G. From competition to facilitation: how tree species respond to neighbourhood diversity. *Ecol. Lett.* 2017, 20, 892–900, doi:10.1111/ele.12786.

Chapter III. Tree-tree interactions and crown complementarity: The role of functional diversity and branch traits for canopy packing

Michaela Hildebrand^{a,*}, Maria D. Perles-Garcia^{b,c}, Matthias Kunz^a, Werner Härdtle^d, Goddert von Oheimb^{a,c}, Andreas Fichtner^d

^a Institute of General Ecology and Environmental Protection, Technische Universität Dresden, 01737 Tharandt, Germany

^b Institute of Biology/ Geobotany and Botanical Garden, Martin Luther University Halle-Wittenberg, Große Steinstr. 79/80, 06108 Halle (Saale), Germany

^c German Centre for Integrative Biodiversity Research (iDiv), Halle-Jena-Leipzig, 04103 Leipzig, Germany

^d Institute of Ecology, Leuphana University of Lüneburg, Universitätsallee 1, 21335 Lüneburg, Germany

* Correspondence: michaela.hildebrand@tu-dresden.de, Technische Universität Dresden, Institute of General Ecology and Environmental Protection, Chair of Biodiversity and Nature Conservation, Piener Straße 7, 01737 Tharandt, Germany.

Editorial status: Published in *Basic and Applied Ecology* (December 2020)

DOI: [10.1016/j.baae.2021.01.010](https://doi.org/10.1016/j.baae.2021.01.010)

Abstract

Previous studies have shown that tree species richness increases forest productivity by allowing for greater spatial complementarity of tree crowns (crown complementarity), which in turn results in more densely packed canopies. However, the mechanisms driving crown complementarity in tree species mixtures remain unclear. Here, we take advantage of a high-resolution, three-dimensional terrestrial laser scanning approach in the context of a large-scale biodiversity-ecosystem functioning experiment in subtropical China (BEF-China) to quantify the extent to which functional dissimilarity and divergences in branch traits between neighbouring trees affect crown complementarity at the scale of tree species pairs (i.e., two adjacent trees). Overall, we found no support that functional dissimilarity (divergence in morphological flexibility, specific leaf area and wood density) promotes crown complementarity. However, we show that the effects of functional dissimilarity (the plasticity of the outer crown structure) on crown complementarity vary in their magnitude and importance depending on branch trait divergences. Firstly, crown complementarity tended to be highest for tree species pairs that strongly differed in their functional traits, but were similar in branch density. In contrast, heterospecific pairs with a low functional trait divergence benefitted the most from a large difference in branch density compared with pairs characterised by a large functional dissimilarity. Secondly, the positive effects of increasing divergence in branching intensity (the plasticity of the inner crown structure) on crown complementarity became most important at low levels of functional dissimilarity, i.e. when species pairs were similar in their branch packing and vice versa. This suggests that species mixing allows trees to occupy canopy space more efficiently mainly due to phenotypic changes associated with crown morphology and branch plasticity. Our findings highlight the importance of considering outer and inner crown structures (e.g. branching architecture) to deepen our understanding of tree-tree interactions in mixed-species communities.

1. Introduction

Restoration of forests is gaining global momentum in order to increase the production of timber and pulpwood, but also to improve ecosystem services such as carbon sequestration and to support biodiversity conservation (FAO, 2010; IUCN, 2020). A significant proportion of the afforested and reforested area involves the planting of monocultures of trees with high commercial value (Lewis, Wheeler, Mitchard, & Koch, 2019), even though there is ample evidence that tree species mixtures can promote numerous ecosystem functions and

services (Steur, Verburg, Wassen, & Verweij, 2020; van der Plas, 2019). In particular, tree diversity has positive effects on forest productivity and carbon storage (Guillemot et al., 2020; Huang et al., 2018; Liang et al., 2016a; Liu et al., 2018). However, the understanding of the underlying ecological mechanisms driving the biodiversity-productivity relationship in forests is still incomplete (Ammer, 2019).

The physical niche partitioning amongst tree crowns in canopy space (hereafter "crown complementarity") has been proposed as an important mechanism underlying the positive mixture effects in forests (Pretzsch, 2014; Sapijanskas, Paquette, Potvin, Kunert, & Loreau, 2014; Williams, Paquette, Cavender-Bares, Messier, & Reich, 2017). This is conceivable because light is often the major factor limiting tree growth, and the spatial arrangement of tree crowns is decisive for light-related tree interactions and, thus, primary productivity (Ishii & Asano, 2010). Different factors have been identified to be important for crown complementarity in tree species mixtures: interspecific differences in growth rates, crown architecture and leaf physiology, because this enables the occupation of different spatial niches in canopy space (also called "vertical stratification"; Ishii & Asano, 2010; Jucker, Bouriaud, & Coomes, 2015; Niinemets, 2010; Williams, Paquette, Cavender-Bares, Messier, &

Reich, 2017), and crown plasticity of individual trees (Kunz et al., 2019; Lang et al., 2010; Pretzsch, 2014). Williams, Paquette, Cavender-Bares, Messier, & Reich, 2017 introduced a crown complementarity index (CCI) by averaging pairwise vertical crown overlap between trees, representing the partitioning of canopy space in different height strata at the plot level. Applying this index to temperate-boreal species planted in a young tree diversity experiment they found that crown complementarity was enhanced in 23 out of 25 mixtures compared to their constituent monocultures. Williams, Paquette, Cavender-Bares, Messier, & Reich, 2017 conclude that the positive effects of tree species richness on crown complementarity are largely the result of species-specific differences rather than crown plasticity. Tree interactions at the local neighbourhood scale, however, have been identified as a major determinant of positive biodiversity-productivity relationships in forests, as they explain over half of the variation on average in community productivity (Fichtner et al., 2018). Consequently, Kunz et al. (2019) applied an adjusted index by calculating the local crown complementarity index (CCI_i) as the mean crown complementarity of an individual tree with all its direct neighbours. The authors found a positive relationship between neighbourhood tree species richness and CCI_i . Interestingly, a large proportion of variance in CCI_i was explained by crown shape compared to crown size in tree species mixtures,

suggesting that neighbourhood-driven shape plasticity of tree crowns is of high importance in mixed-species stands. Kunz et al. (2019) suggest that the relevance of diversity-driven crown plasticity might have been underestimated by the approaches used in previous studies (Jucker, Bouriaud, & Coomes, 2015; Williams, Paquette, Cavender-Bares, Messier, & Reich, 2017).

Crown plasticity was defined by Kunz et al. (2019) based on measures that characterise the outer crown structure (e.g. crown sinuosity or crown length to crown width ratio). However, for a given crown shape different inner crown structures might be realised, which is the result of complex mechanisms operating at lower levels of organisation, i.e. the dynamic development of branches of different orders (Lang et al., 2012; Niinemets, 2010; Van de Peer, Verheyen, Kint, Van Cleemput, & Muys, 2017). In particular, the number of branches per unit crown volume (i.e. branch density or branch packing) and the rate of branch ramification (i.e. branching intensity) are key attributes of the inner crown structure and might affect the physical niche partitioning in canopy space. Typical morphological adjustments in response to locally favourable light conditions are an increase in branching rate. Under such morphological changes at the branch level, trees modularly respond to micro-environmental light heterogeneity (Kawamura, 2010), resulting in differences in branch density and/or branching intensity amongst individual trees, which in turn might contribute substantially to crown complementarity. This assumption is based on the concept of functional differences of the axes within a tree crown: some axes are involved in space exploration and support, whereas others fulfil functions in light exploitation and carbon assimilation ("axis polymorphism"; Barthélémy & Caraglio, 2007; Bell, 1991; Hallé, Oldeman, & Tomlinson, 1978; Ishii, 2011; Normand, Bello, Trottier, & Lauri, 2009; Taugourdeau & Sabatier, 2010). However, non-destructively quantifying branching responses of tree individuals in situ tree experiments has long been logistically unfeasible (but see Guillemot et al., 2020). As a result, the underlying mechanisms of crown complementarity remain unclear.

In this study, we take advantage of the combination of two innovative approaches to deepen our understanding on how tree diversity affects aboveground spatial complementarity. Applying terrestrial laser scanning (TLS) technology to tree species pairs (TSPs; see Trogisch et al., this issue) in a tree diversity experiment enables a rigorous analysis with a very high spatial resolution, i.e. at the level of individual branches. TLS provides the means of time-efficient measurement of the 3D structural elements of trees (Calders et al., 2015; Liang et al., 2016b). In tree diversity experiments TLS has been

applied to derive several conventional (e.g., height and stem diameter), but also more complex variables (e.g., crown volume and wood volume) for individual trees (Guillemot et al., 2020; Hess, Härdtle, Kunz, Fichtner, & von Oheimb, 2018; Kunz et al., 2019; Li, Hess, von Wehrden, Härdtle, & von Oheimb, 2014a; for more details see Trogisch et al., 2017). In particular, the construction of quantitative structure models (QSMs), which are hierarchical geometric primitive models based on TLS point clouds, very accurately approximate a tree's branching structure (Calders et al., 2015; Raunonen et al., 2013).

Between-species differences in functional traits largely shape the outcome of neighbourhood interactions (Butterfield & Callaway, 2013). This is in line with experimental findings at the local neighbourhood level, where great trait dissimilarities amongst the planted tree species (Kröber, Zhang, Ehmiq, & Bruelheide, 2014) resulted in strong differences in growth rates (Li, Hess, von Wehrden, Härdtle, & von Oheimb, 2014b; Li, Kröber, Bruelheide, Härdtle, & von Oheimb, 2017). In addition, Fichtner et al. (2017) demonstrated that a target tree's functional traits largely regulate the mechanisms underlying biodiversity-productivity relationships at the local neighbourhood level (i.e. competitive reduction for species with acquisitive and facilitation for species with conservative traits). Although functional diversity has been shown to be positively linked to crown complementarity at the community level (Forrester & Bausch, 2016; Williams, Paquette, Cavender-Bares, Messier, & Reich, 2017), the importance of tree functional dissimilarity for crown complementarity in pairwise tree interactions is still unclear. Here we define functional dissimilarity based on three key traits (morphological flexibility, specific leaf area and wood density) that have been shown to be major determinants of outer crown structure plasticity (Kunz et al., 2019) and neighbour competitive effects (Kunstler et al., 2016) on tree growth.

The objective of the present study was to analyse the impact of divergences in branch traits (the differences in branch density and branching intensity) on crown complementarity at the scale of TSPs, making use of the BEF-China experiment (Bruelheide et al., 2014). We additionally considered the effects of trait dissimilarity (the difference in three key functional traits related to crown plasticity and competitive strength) to test the hypothesis that branch trait-crown complementarity relationships are mediated by functional diversity.

2. Materials and methods

2.1. Study area and experimental design

The study area is part of the BEF-China experiment, which is located close to Xingangshan township in the Jiangxi Province in southeast China (29.08°-29.11°N, 117.90°-117.93°E, 100-300 m above sea level). The climate at the site is subtropical with an annual mean temperature of 16.7 °C and annual mean precipitation of 1821 mm (Yang et al., 2013). Cambisols and Regosols (ridges, spurs, crests), Cambisols and Acrisols (slopes), colluvic Cambisols and Gleysols (footslopes, valleys) and hydragic Anthrosols (valley cuttings, lower footslopes) are prevailing soils in the study area (Scholten et al., 2017). The BEF-China experiment was established in 2009/2010 on two sloped experimental sites (A and B) with a total area of 38.4 ha. The species pool represented the local tree community and contained 40 native broad-leaved tree species, 18 shrubs, and 2 conifer species - the latter were included because they are commonly used in commercial plantations (Bruelheide et al., 2014).

A grid of square plots with a size of 667 m² (25.82 m x 25.82 m) per plot was laid out on the two experimental sites. The planting distance between the saplings was 1.29 m in horizontal projection (Bruelheide et al., 2014). For a more detailed description of the experimental design of BEF China, see Bruelheide et al. (2014). The tree species pairs (TSPs) were selected to study tree-tree interactions in diverse neighbourhoods (Trogisch et al., Fig. 3; this issue). Because the planting positions of the trees were randomly assigned to the plots, a high number of TSP combinations is realised. However, the number of TSPs was limited to 240 per site according to Trogisch et al. (this issue). In the BEF-China experiment, a “broken-stick” design was used for the establishment of plot-specific levels of tree species richness. In brief, three minimally overlapping, randomly selected compositions of 16 species (out of a pool of 24 species) were broken down into two nested, non-overlapping mixtures of eight species. Species compositions of the less diverse mixtures (four- and two-species mixtures and monocultures) followed the same partitioning process (Bruelheide et al., 2014). This random partitioning design ensures that all species are equally represented at each diversity level (for detailed information see Bruelheide et al., 2014). We chose the species of the TSPs for this study from half of the “broken-stick” (see Appendix A: Table 1) and excluded one deciduous species because of its low height growth and the absence of interactions in crown space (*Quercus serrata* Murray) and one evergreen species (*Castanopsis sclerophylla* Lindley & Paxton), since its leaves preclude a high-resolution analysis of the branches. Therefore, we examined six different tree species present in a total of 126 TSPs on site A: *Castanea henryi* (Skan) Rehder & E. H. Wilson, *Choerospondias axillaris* (Roxburgh) B. L. Burt & A. W. Hill, *Liquidambar formosana* Hance, *Nyssa sinensis*

Oliver, *Sapindus saponaria* (L.), *Triadica sebifera* (L.) Small (Table 1). Saplings were planted in spring 2009 at an age of one year, and replanting of saplings that died during the first growing season took place in November 2009. Characteristics of the study species are displayed in Table 2.

Table 1. Realised species combinations within the examined tree species pairs (TSP). The numbers indicate the number of replicates of a given TSP.

	<i>C. henryi</i>	<i>C. axillaris</i>	<i>L. formosana</i>	<i>N. sinensis</i>	<i>S. saponaria</i>	<i>T. sebifera</i>
<i>Castanea henryi</i>	13	1	4	14	2	–
<i>Choerospondias axillaris</i>	1	10	–	–	–	16
<i>Liquidambar formosana</i>	4	–	12	3	10	–
<i>Nyssa sinensis</i>	14	–	3	13	4	–
<i>Sapindus saponaria</i>	2	–	10	4	13	1
<i>Triadica sebifera</i>	–	16	–	–	1	10

Table 2. Study species characteristics (mean \pm standard error) based on terrestrial laser scanning and functional trait data for the study species obtained at our study site (the generic names of the species are abbreviated). Branch density was calculated as the total number of branches per unit, crown volume and branching intensity as the total number of second-order branches per unit length of first-order branches. Wood density (WD) and specific leaf area (SLA) were taken from Kröber et al, (2015) and morphological flexibility (MF) from Kunz et al. (2019).

	Tree height (m)	Branch density (number / l)	Branching intensity (number / m)	Crown volume (l)	WD	SLA	MF
<i>C. henryi</i>	7.87 \pm 0.36	26.12 \pm 10.41	1.46 \pm 0.12	9.77 \pm 1.20	0.61	11.83	0.67
<i>C. axillaris</i>	6.99 \pm 0.53	20.37 \pm 3.07	1.49 \pm 0.14	11.55 \pm 3.42	0.61	11.57	0.65
<i>L. formosana</i>	6.45 \pm 0.33	21.45 \pm 2.76	1.32 \pm 0.07	7.19 \pm 1.03	0.51	12.42	0.29
<i>N. sinensis</i>	7.84 \pm 0.26	15.15 \pm 2.39	1.53 \pm 0.08	11.78 \pm 1.66	0.51	13.08	0.47
<i>S. saponaria</i>	5.07 \pm 0.36	38.42 \pm 5.44	1.46 \pm 0.11	4.09 \pm 1.19	0.73	12.31	0.58
<i>T. sebifera</i>	6.03 \pm 0.57	47.74 \pm 11.28	1.87 \pm 0.18	4.22 \pm 1.19	0.50	13.25	0.36

2.2. Scan design

The data collection took place during the field campaign of 2019 in February, March and April on site A (Fig. 1B). We chose the early spring season because deciduous trees were in leaf-off condition allowing for better canopy penetration of the laser beam and therefore a better coverage of the branches and the overall woody structure of the crowns. The scanning was performed during windless and rainless days with temperatures between 3.5 °C and 22 °C (Harris, Jones, Osborn, & Lister, 2014). We collected the TLS data using a FARO Focus 3D X 130 and a FARO Focus S120 which allow for a 360° (horizontally) x 300° (vertically) field of view. The scanners operate with a wavelength of 905 nm and 1550 nm, respectively. The scanner resolution was set at 1/8 corresponding to a spatial resolution of \sim 6 mm at 10 m distance and the scan quality option was set to 3x (FARO Technologies Inc. 2012; 2015).

For scan registration we used a quadratic checkerboard reference target with 45 cm edge and four polystyrene spherical reference targets with a radius of 7 cm around the TSPs. We

conducted three to six scans per TSP, depending on tree height, stock density and canopy complexity (Fig. 1A).

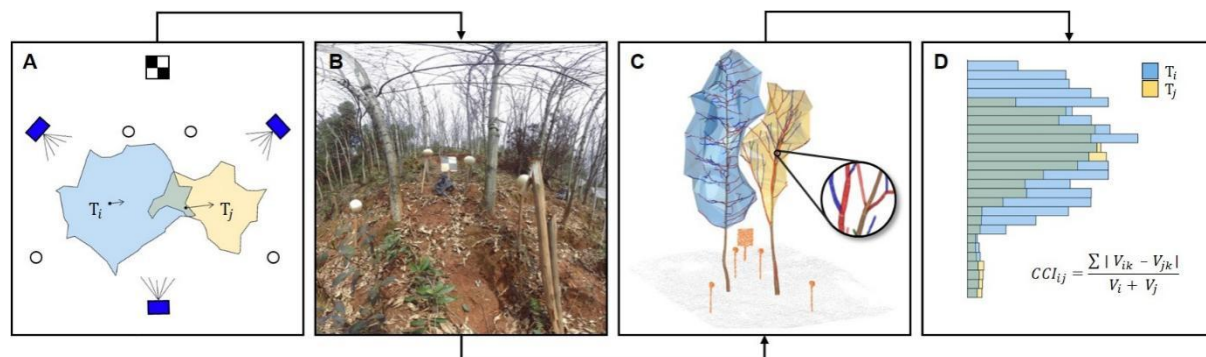


Figure 1. Presentation of field setup and the further processing steps for tree species pairs (TSP) survey. **(A)** Schematic scan design used during the field campaign: spherical reference targets, checkerboard reference target, three different scan positions. The individual trees of the TSP (T_i and T_j) are represented by their crown projection area, the arrows represent the crown displacement. **(B)** Coloured planar scan view from one scan position. Note, branches appear distorted due to two-dimensional projection of the three-dimensional image. **(C)** Quantitative structure models of the TSP colour-coded cylinders for the different branch orders of each tree. The ramification structure is shown: the trunk is coloured brown, the first order branches red, the second order branches blue and the third order branches green. Models were derived from high-resolution, three-dimensional point clouds of each tree individual. Respective tree crown volumes are visualised by coloured 3D α -shapes. Additionally, ground points of the local neighbourhood are shown in grey and reference targets in orange. **(D)** Occupied crown space volume per stratum of T_i (blue) and T_j (yellow) and shared crown space (pale green). The calculation of the crown complementarity (CCI) is based on the method of Williams, Paquette, Cavender-Bares, Messier, & Reich, 2017.

2.3. TLS data processing

With the FARO Scene software (Version 5.26), we co-registered the point clouds of the individual scans of each TSP. Each co-registered point cloud was stored in a local Cartesian coordinates system (3D coordinates X, Y, Z) in an ASCII format. We identified the tree individuals of the TSPs in the co-registered scans by their position to the reference target and information of the direction of the checkerboard and scanning protocols. We used RiSCAN Pro software (Version 2.6.2) to manually extract the individual trees of the TSP. We used a statistical outlier removal filter (with $n = 12$ and $\sigma = 2.0$) from Cloud Compare (Version 2.10.2) to remove remaining stray points and to improve the overall point cloud quality. Crown volume was computed using a 3D alpha-shape with an α -value of 0.3, computed in R 3.3.0 (R Core Team 2016) using the `alphashape3d` (Lafarge & Pateiro-Lopez, 2017) package.

2.4. Quantitative structure modelling

Using TreeQSM software (Version 2.30; Akerblom, Raunonen, Mäkipää, & Kaasalainen, 2017), running under MATLAB (Version R2018a), we computed QSMs, using five models run

for each tree of the TSPs (Fig. 1C; for further information on the method see Kunz et al., 2019). We chose the following QSM modelling parameters:

- patch size of the first uniform size cover: 3 mm
- minimum patch size of the cover sets in the second cover: 2 mm
- maximum patch size: 40 mm
- relative cylinder length: 3, 4, 6
- relative radius for outlier removal: 3, 4.5
- minimum cylinder radius: 0.5 mm.

QSMs were computed for all 252 trees of the 126 TSPs. From the QSMs we used the total number of branches, the length of the first-order branches and the total number of second-order branches for subsequent analyses (see below).

2.5. Calculation of crown complementarity and explanatory variables

Using the TLS data the crown complementarity index (CCI) was calculated as the sum of the difference in crown volume between the two trees of the TSP (T_i and T_j) in each stratum ($k = 0.3$ m) divided by the total volume (V) of both trees: $CCI_{ij} = \sum |V_{ik} - V_{jk}| / V_i + V_j$ (sensu Williams, Paquette, Cavender-Bares, Messier, & Reich, 2017; Fig. 1D). Basically, the CCI of a TSP represents the extent to which both trees occupy different strata (Williams, Paquette, Cavender-Bares, Messier, & Reich, 2017). It ranges between 0 (crowns are not complementary) and 1 (crowns are 100% complementary; Kunz et al., 2019; Williams, Paquette, Cavender-Bares, Messier, & Reich, 2017; see Appendix A: Table 2).

To explore the drivers of CCI, we used three different measures of species and structural diversity: functional dissimilarity, branch density dissimilarity and branching intensity dissimilarity.

We focused on three key functional traits to calculate the functional dissimilarity (FD) between a given TSP based on the competitive strength and crown plasticity of component species: specific leaf area (SLA), wood density (WD) and morphological flexibility (MF; Table 2), with SLA and WD taken from Kröber et al. (2015) and MF from Kunz et al. (2019). SLA and WD are closely related to a tree's competition tolerance and competitive effect on neighbours (Kunstler et al., 2016), while MF captures a species' ability to respond with crown plasticity (variation in size and shape) related to changes in biotic or abiotic factors (Kunz et al., 2019). MF is an integrative trait that incorporates various traits related to the outer crown structure: crown sinuosity, crown compactness, Gini coefficient of crown volumes per strata, and the ratios of crown-width-to-crown-length, crown-length-to-tree-height, crown-surface-area-to-crown-volume, crown-displacement-to-tree-height, and

crown-sinuosity-to-tree-height (Kunz et al., 2019). The first two axes of a principal component analysis (PCA) on standardised values of these leaf (SLA), wood (WD) and crown traits (MF) explained 92.5% of the overall trait variation amongst TSPs (see Appendix A: Fig. 1). FD therefore captures variation in crown plasticity and competition intensity amongst the study species. FD was calculated as: $FD_{i,j} = \text{sqrt}(\sum(x_{i,k} - x_{j,k})^2)$, where FD indicates the functional dissimilarity between tree i and j of a given TSP, and k is the specific functional trait value (see Appendix A: Table 3).

Based on TLS data we calculated for each tree of a given TSP the branch density (BD: the total number of branches per unit crown volume) and the branching intensity (BI; the total number of second-order branches per unit length of first-order branches). For each TSP, the dissimilarity of BD and BI (hereafter BDD and BID) were calculated as the absolute difference in BD and BI divided by the total value of BD and BI of a given TSP, respectively. BDD therefore reflects the relative degree of heterogeneity in branch packing, while BID reflects the relative degree of heterogeneity in branch architecture at the TSP level. Both indices range between 0 (no dissimilarity) to 1 (complete dissimilarity), thus quantifying the degree to which branch traits are divergent amongst the two trees. The average relative difference in tree height (median: 10%) and average terrain difference between the two individuals of a TSP was small (median: 0.2 m).

2.6. Statistical analysis

We applied generalised additive mixed models (GAMMs) with an identity link function and Gaussian distribution to assess the effects of FD, BDD and BID and their two- and three-way interactions on CCI (using tensor product interactions). To account for small-scale variation in topography, we used the local slope of a given TSP as further covariate. Study plot was used as random factor. To meet model assumptions, we included a variance function in the random structure where the residual variance is multiplied by an exponential function of FD (Zuur, Ieno, Walker, Saveliev, & Smith, 2009) that significantly improved the model ($\chi^2 = 7.87$, $P = 0.005$). Models were fitted with a thin plate regression spline and the optimal amount of smoothing was determined by the cross-validation method (Wood, 2017). For the three-way interaction between FD, BDD and BID, we used a maximum of five degrees of freedom as the initial GAMM using the cross-validation method did not converge. The importance of predictors was assessed by the Akaike Information Criterion (AIC) and the Akaike weights (Burnham & Anderson, 2002) based on maximum likelihood estimation (ML). The significance of predictors was assessed with likelihood-ratio tests (using the ML method)

when comparing nested models. The most parsimonious model was re-fitted with restricted maximum likelihood estimation. Model validation was performed following Zuur, Ieno, Walker, Saveliev, & Smith, 2009 (see Appendix A: Fig. 2). The variance inflation factors (VIFs <1.04) indicated no critical correlation between explanatory variables (collinearity).

Changes in CCI with FD along the BID gradient were assessed by predicting CCI (based on our best-fitting model) for conspecific (FD = 0) and for low and high levels of FD (using the 30% and 70% quantile of observed FD-values of heterospecific TSPs) at low and high levels of BDD (using the 30% and 70% quantile of observed BD-values). All analyses were conducted in R 3.6.3 (R Core Team, 2020) using the packages mgcv (Wood, 2017) and MuMIn (Bartoń, 2019).

3. Results

Small-scale variation in topography did not affect crown complementarity index (CCI; $\chi^2 = 0.13$, $P = 0.911$). Instead, CCI linearly increased on average with branch density dissimilarity (BDD; $\chi^2 = 48.67$, $P < 0.001$; Fig. 2A), while the relationship between branching intensity dissimilarity (BID) and CCI followed a concave-down pattern ($\chi^2 = 3.86$, $P = 0.027$; Fig. 2B). Although predicted CCI was on average 3% higher in heterospecific compared to conspecific TSPs, we found no support for a significant functional dissimilarity (FD) – CCI relationship ($\chi^2 = 0.03$, $P = 0.986$; Fig. 2C). However, the best-fitting model revealed that the BDD – CCI and BID – CCI relationships were not consistent across varying levels of FD, and that the BID – CCI relationship depended on both BDD and FD (as indicated by the significant three-way interaction; Table 3).

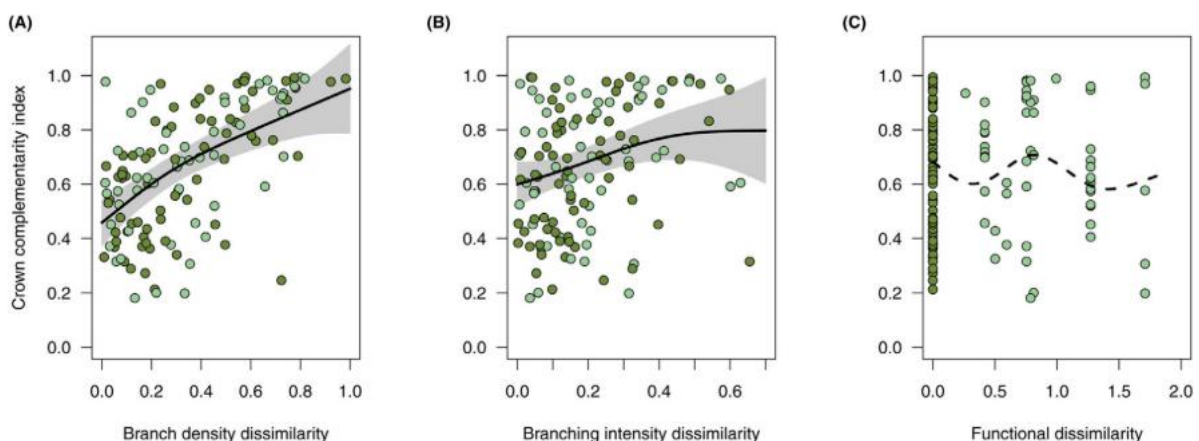


Figure 2. Partial effects of **(A)** branch density dissimilarity (BDD), **(B)** branching intensity dissimilarity (BID) and **(C)** functional dissimilarity (FD) of a tree species pair (TSP) on the crown complementarity index (CCI). The solid lines correspond to significant fitted relationships of the most parsimonious generalised additive mixed models, while keeping other covariates fixed at their means. The dashed line indicates a non-significant relationship.

Shaded areas indicate 95% confidence intervals, and dots represent the observed values (dark green: conspecific TSPs, light green: heterospecific TSPs).

Table 3. Results of the best-fitting generalised additive mixed model. edf: estimated degrees of freedom for the smoother, δ : estimated parameter for the variance covariate, functional dissimilarity (FD), SD: standard deviation, TSP: tree species pair.

	edf	F-value	P-value
Functional dissimilarity (FD)	1.00	0.02	0.888
Branch density dissimilarity (BDD)	1.00	56.26	<0.001
Branching intensity dissimilarity (BID)	1.90	3.86	0.021
FD x BDD	4.55	13.68	<0.001
FD x BID	5.93	4.50	<0.001
BDD x BID	1.00	2.42	0.123
FD x BDD x BID	2.40	5.39	0.018
SD (plot)	0.025		
δ	-0.577		
R^2 (adj.)	0.702		
n (TSP)	126		

At low BDD, CCI tended to be higher for TSPs with high FD (FD-high) compared to TSPs with low FD (FD-low) as well as conspecific TSPs (FD-0; Fig. 3A). The opposite response was evident at high levels of BDD (Fig. 3B). Overall, BID had a positive effect on CCI, but the magnitude and importance (i.e. the strength of the BID–CCI relationship) depended on FD. At low BDD, CCI increased with increasing BID by 37% for conspecific TSPs (FD-0) and by 60% (FD-high) and 193% (FD-low) for heterospecific TSPs across the common BID-gradient (Fig. 3A; note that BID values larger than 0.4 were not realised at higher levels of FD). At high BDD, the effect size of BID was almost four-times higher for FD-high (81%) than for FD-low (21%) and FD-0 (24%; Fig. 3B). Consequently, differences in CCI amongst con- and heterospecific TSPs were largest at extremely low levels of BID, regardless of BDD, but became less distinct with increasing BID (Fig. 3).

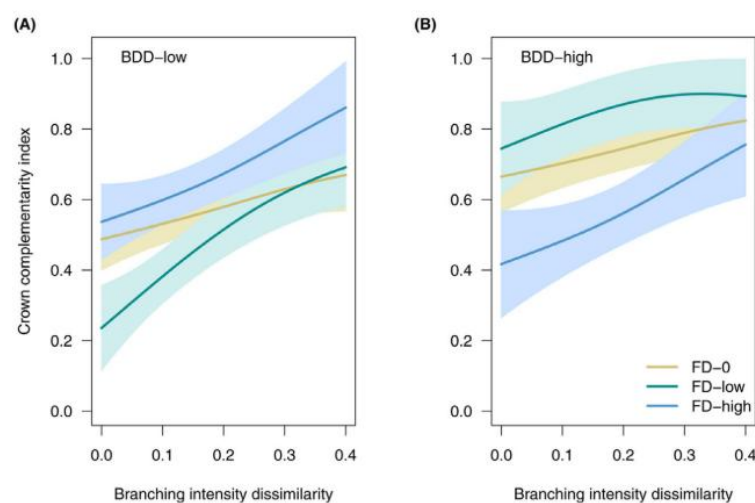


Figure 3. Non-additive effects of functional dissimilarity (FD) and divergence in branch traits (BDD: branch density dissimilarity; BID: branching intensity dissimilarity) of a tree species pair (TSP) on crown

complementarity index (CCI). Regression lines correspond to generalised additive mixed model fits for conspecific (FD-0) and heterospecific TSPs at low and high levels of FD and varying levels of BDD: (A) TSP is similar in branch density (BDD-low); (B) TSP strongly differs in branch density (BDD-high). Shaded areas indicate 95% confidence intervals.

4. Discussion

We found no evidence of a single effect of functional diversity on crown complementarity. Instead, our results support the hypothesis that crown complementarity patterns of TSPs are largely determined by non-additive effects of functional diversity and branch trait divergences (differences in branch density and branching intensity), which explained a substantial proportion of variation in CCI (70%; Table 3). We identified two processes that promote spatial complementarity of tree crowns via increasing phenotypic plasticity: differences in functional traits and branching intensity. In our study, FD was strongly associated with a trees' morphological flexibility (see Appendix A: Fig. 1) that captures the species' overall potential of phenotypic crown changes (see Kunz et al., 2019). We therefore assume that a high FD allows one tree of the TSP to use canopy space more efficiently by adjusting its outer crown structure (e.g. crown sinuosity or crown length-width ratio) in response to crown competition ("space exploration" sensu Bell, 1991). In contrast, increasing differences in branching intensity should allow one tree of the TSP to use canopy space more efficiently by optimising its inner crown structure (e.g. branch architecture) depending on crown competition intensity ("light exploitation" sensu Bell, 1991). This suggests that functional diversity does not inevitably lead to higher physical niche partitioning in canopy space between two trees. Instead, branch adjustments (e.g. higher branching intensities) can compensate for a lower plasticity of the outer crown associated with decreasing functional diversity. On average, crown complementarity was 23% higher at high BDD compared to low BDD, regardless of differences in functional traits or branching intensity (Fig. 3). This can be largely attributed to variation in tree height, which drives competitive exclusion, but not to FD or BID which promote morphological plasticity. The strong negative relationship between log-BD and tree height in our study ($r = -0.75$, $P < 0.001$) suggests that TSPs becoming more divergent in BD are associated with larger differences in tree height ($r = 0.58$, $P < 0.001$; see Appendix A: Fig. 3A). Note that BID was not significantly correlated to differences in tree height ($r = 0.08$, $P = 0.376$; see Appendix A: Fig. 3B). Given that canopy space is limited, similar BDs (i.e. low levels of BDD) will lead to increasing competition for space and light compared to TSPs that are more divergent in their branch packing (i.e. high BDD). Thus, TSPs characterised by high functional and thus crown plasticity dissimilarity can more efficiently respond to increasing competition in canopy space

by primarily adjusting the axes for space exploration (and by this their outer crown structures), whereas the process of increasing their branching intensity (i.e. adjustments of axes for light exploitation and by this their inner crown structure) will have little impact on CCI. This also explains why TSPs that were more similar in their functional traits benefitted the most (strongest BID - CCI relationship) from increasing differences in branching intensity at low levels of BDD, because changes in inner crown structure (here: branch architecture) can compensate for a lower ability to adjust outer crown structure to reduced canopy space. Consequently, differences in heterospecific TSPs became less evident with increasing BID. These two processes indicate that trees try to balance outer (canopy space occupation, meaning space exploration) and inner (optimisation of canopy space occupation, meaning light exploitation) crown plasticity to use canopy space most efficiently when growing in mixed-species neighbourhoods.

Interestingly, a low FD allowed species pairs that largely differed in BD to achieve highest vertical crown volume overlap between the two neighbouring trees per stratum (indicated by higher CCIs compared with TSP characterised by no or high FD). Next to variation in the plasticity of outer crown structures, this response is most likely the result of variation in the strength of competitive neighbour interactions, as increasing trait divergence between two local species is considered to reduce the intensity of competition (Cahill, Kembel, Lamb, & Keddy, 2008). At high levels of BDD the occupation of the canopy space is sparse due to larger differences in tree height (see above). Consequently, crown competition is relatively low and neither the need for physical niche partitioning nor the potential for strong modular responses at the branch level are given. It is therefore conceivable that a higher intra- and interspecific competition intensity for resources, which should be the result of TSPs becoming more similar in their functional traits and competitive strength, respectively, is needed to trigger morphological adjustments to achieve a high spatial complementarity in canopy space. For TSPs characterised by a large FD, variation in BID may act as an alternative driver for CCI to compensate for their lower interspecific competition intensity. This interpretation is in line with the observed shift in the strength of the BID-CCI relationship along the FD gradient. Moreover, our results show that the responsiveness of conspecific neighbourhoods to changes in BDD or BID was small, but the variation of observed CCIs was relatively large (Fig. 2C). This pattern might be linked to differences in phenotypic plasticity within conspecific TSPs (Valladares, Gianoli, & Gómez, 2007), which we were not able to capture by FD in our study. In this context, it is important to note that the CCI we used in this study reflects the outcome of tree-tree interactions after 10 years of

growth in direct vicinity. These interactions have been present already two years after planting in the BEF-China experiment (Li et al., 2014b) due to the high planting densities (trees were planted at a horizontal distance of 1.29 m on a rectangular grid; Bruelheide et al., 2014) combined with very fast height growth (Li, Kröber, Bruelheide, Härdtle, & von Oheimb, 2017). Given those morphological adjustments of the crown need time to evolve, it takes some time until responses in the complex 3D crown structure to local neighbour interactions emerge. This has been proven to be realised in the BEF-China experiment (Kunz et al., 2019).

In summary, we posit that species mixing allows trees to occupy canopy space more efficiently mainly due to phenotypic changes, which can be brought about by (large) differences in functional diversity (plasticity related to the outer crown structure) or branching intensity (plasticity related to the inner crown structure). The relative importance of these processes driving crown complementarity, however, depend on differences in branch packing (here expressed as BDD). In the context of our analyses the employment of modern TLS technology along with a specifically adjusted scan design allows for a non-destructive acquisition of the 3D architecture of the TSPs at a very high level of resolution, and specifically for analyses of changes in CCI in response to phenotypic plasticity of the inner crown structure. Using this approach our findings provide a better understanding of the mechanisms underlying complementarity effects in forests by showing that the effects of functional diversity and divergences in branch traits on crown complementarity are non-additive. We were able to separate the relative importance of these drivers for spatial aboveground complementarity, and thus to shed light on tree-tree interactions in mixed-species tree communities. Overall, our findings emphasise the need to consider inner crown properties to better understand and predict biodiversity-ecosystem functioning relationships in forest ecosystems.

Declaration of Competing Interest

The authors declare that they have no known competing financial interests or personal relationships that could have appeared to influence the work reported in this paper.

Acknowledgements

We are grateful to the workers who helped to conduct the scans in the field. Moreover, we thank Benjamin Delory for the helpful discussion on branch traits. This study was supported by the International Research Training Group TreeDⁱ jointly funded by the Deutsche

Forschungsgemeinschaft (DFG, German Research Foundation) - 319936945/GRK2324 and the University of Chinese Academy of Sciences (UCAS).

Authorship

GvO, MK, AF and WH conceived the idea of this study. MH, MK and MPG performed the scans, processed the TLS data and computed the tree models and the crown complementarity index. AF analysed the data. MH wrote the first draft of the manuscript and all the authors contributed substantially to the submitted version.

Information about Supplementary materials

Supplementary material associated with this article can be found in the online version at doi:10.1016/j.baae.2021.01.010 and at the end of this dissertation.

References

- Åkerblom, M., Raunonen, P., Mäkipää, R., & Kaasalainen, M. (2017). Automatic tree species recognition with quantitative structure models. *Remote Sensing of Environment*, 191, 1–12. <https://doi.org/10.1016/j.rse.2016.12.002>.
- Ammer, C. (2019). Diversity and forest productivity in a changing climate. *New Phytologist*, 221(1), 50–66. <https://doi.org/10.1111/nph.15263>.
- Barthélémy, D., & Caraglio, Y. (2007). Plant architecture: A dynamic, multilevel and comprehensive approach to plant form, structure and ontogeny. *Annals of Botany*, 99(3), 375–407. <https://doi.org/10.1093/aob/mcl260>.
- Bartoń, K. (2019). MuMIn: Multi-Model Inference. R package version 1.43.15. <https://cran.r-project.org/package=MuMIn>.
- Bell, A. D. (1991). *Plant form: An illustrated guide to flowering plant morphology*. Oxford University Press.
- Bruelheide, H., Nadrowski, K., Assmann, T., Bauhus, J., Both, S., Buscot, F., Chen, X.-Y., Ding, B., Durka, W., Erfmeier, A., Gutknecht, J. L. M., Guo, D., Guo, L.-D., Härdtle, W., He, J.-S., Klein, A.-M., Kühn, P., Liang, Y., Liu, X., ... Schmid, B. (2014). Designing forest biodiversity experiments: General considerations illustrated by a new large experiment in subtropical China. *Methods in Ecology and Evolution*, 5(1), 74–89. <https://doi.org/10.1111/2041-210X.12126>.
- Burnham, K. P., & Anderson, D. R. (2002). *Model selection and multimodel inference: A practical information-theoretic approach* (2nd ed, p. 488). Springer.
- Butterfield, B. J., & Callaway, R. M. (2013). A functional comparative approach to facilitation and its context dependence. *Functional Ecology*, 27(4), 907–917. <https://doi.org/10.1111/1365-2435.12019>.
- Cahill, J. F., Kembel, S. W., Lamb, E. G., & Keddy, P. A. (2008). Does phylogenetic relatedness influence the strength of competition among vascular plants? *Perspectives in Plant Ecology, Evolution and Systematics*, 10(1), 41–50. <https://doi.org/10.1016/j.ppees.2007.10.001>.
- Calders, K., Newnham, G., Burt, A., Murphy, S., Raunonen, P., Herold, M., Culvenor, D., Avitabile, V., Disney, M., Armston, J., & Kaasalainen, M. (2015). Nondestructive estimates of above-ground biomass using terrestrial laser scanning. *Methods in Ecology and Evolution*, 6(2), 198–208. <https://doi.org/10.1111/2041-210X.12301>.

- FAO. (2010). Global Forest Resources Assessment 2010 (No. 163; FAO Forestry Paper). <http://www.fao.org/3/i1757e/i1757e.pdf>.
- FARO Technologies Inc. (2012). FARO Scene5.0—User Manual.
- FARO Technologies Inc. (2015). FARO Laser Scanner Focus 3D x 130.
- Fichtner, A., Härdtle, W., Bruelheide, H., Kunz, M., Li, Y., & Von Oheimb, G. (2018). Neighbourhood interactions drive overyielding in mixed-species tree communities. *Nature Communications*, 9(1). <https://doi.org/10.1038/s41467-018-03529-w>.
- Fichtner, A., Härdtle, W., Li, Y., Bruelheide, H., Kunz, M., & von Oheimb, G. (2017). From competition to facilitation: How tree species respond to neighbourhood diversity. *Ecology Letters*, 20(7), 892–900. <https://doi.org/10.1111/ele.12786>.
- Forrester, D. I., & Bausch, J. (2016). A Review of Processes Behind Diversity—Productivity Relationships in Forests. *Current Forestry Reports*, 2(1), 45–61. <https://doi.org/10.1007/s40725-016-0031-2>.
- Guillemot, J., Kunz, M., Schnabel, F., Fichtner, A., Madsen, C. P., Gebauer, T., Härdtle, W., von Oheimb, G., & Potvin, C. (2020). Neighbourhood-mediated shifts in tree biomass allocation drive overyielding in tropical species mixtures. *New Phytologist*. <https://doi.org/10.1111/nph.16722>.
- Hallé, F., Oldeman, R. A. A., Tomlinson, P. B., & Hallé-Oldeman. (2013). *Tropical trees and forests: An architectural analysis*. Springer.
- Harris, I., Jones, P. D., Osborn, T. J., & Lister, D. H. (2014). Updated high-resolution grids of monthly climatic observations - the CRU TS3.10 Dataset: UPDATED HIGH-RESOLUTION GRIDS OF MONTHLY CLIMATIC OBSERVATIONS. *International Journal of Climatology*, 34(3), 623–642. <https://doi.org/10.1002/joc.3711>.
- Hess, C., Härdtle, W., Kunz, M., Fichtner, A., & von Oheimb, G. (2018). A high-resolution approach for the spatiotemporal analysis of forest canopy space using terrestrial laser scanning data. *Ecology and Evolution*, 8(13), 6800–6811. <https://doi.org/10.1002/ece3.4193>.
- Hothorn, T., Hornik, K., & Zeileis, A. (2006). Unbiased Recursive Partitioning: A Conditional Inference Framework. *Journal of Computational and Graphical Statistics*, 15(3), 651–674. <https://doi.org/10.1198/106186006X133933>.
- Huang, Y., Chen, Y., Castro-Izaguirre, N., Baruffol, M., Brezzi, M., Lang, A., Li, Y., Härdtle, W., Von Oheimb, G., Yang, X., Liu, X., Pei, K., Both, S., Yang, B., Eichenberg, D., Assmann, T., Bauhus, J., Behrens, T., Buscot, F., ... Schmid, B. (2018). Impacts of species richness on productivity in a large-scale subtropical forest experiment. *Science*, 362(6410), 80–83. <https://doi.org/10.1126/science.aat6405>.
- Ishii, H. (2011). How Do Changes in Leaf/Shoot Morphology and Crown Architecture Affect Growth and Physiological Function of Tall Trees? In F. C. Meinzer, B. Lachenbruch, & T. E. Dawson (Eds.), *Size- and Age-Related Changes in Tree Structure and Function* (Vol. 4, pp. 215–232). Springer Netherlands. https://doi.org/10.1007/978-94-007-1242-3_8.
- Ishii, H., & Asano, S. (2010). The role of crown architecture, leaf phenology and photosynthetic activity in promoting complementary use of light among coexisting species in temperate forests. *Ecological Research*, 25(4), 715–722. <https://doi.org/10.1007/s11284-009-0668-4>.
- IUCN. (2020). The Bonn Challenge. <https://www.iucn.org/pt/node/18963>.
- Jucker, T., Bouriaud, O., & Coomes, D. A. (2015). Crown plasticity enables trees to optimize canopy packing in mixed-species forests. *Functional Ecology*, 29(8), 1078–1086. <https://doi.org/10.1111/1365-2435.12428>.
- Kawamura, K. (2010). A conceptual framework for the study of modular responses to local environmental heterogeneity within the plant crown and a review of related concepts. *Ecological Research*, 25(4), 733–744. <https://doi.org/10.1007/s11284-009-0688-0>.
- Kröber, W., Li, Y., Härdtle, W., Ma, K., Schmid, B., Schmidt, K., Scholten, T., Seidler, G., von Oheimb, G., Welk, E., Wirth, C., & Bruelheide, H. (2015). Early subtropical forest growth is driven by community mean trait

- values and functional diversity rather than the abiotic environment. *Ecology and Evolution*, 5(17), 3541–3556. <https://doi.org/10.1002/ece3.1604>
- Kröber, W., Zhang, S., Ehmiq, M., & Bruelheide, H. (2014). Linking Xylem Hydraulic Conductivity and Vulnerability to the Leaf Economics Spectrum—A Cross-Species Study of 39 Evergreen and Deciduous Broadleaved Subtropical Tree Species. *PLoS ONE*, 9(11), e109211. <https://doi.org/10.1371/journal.pone.0109211>.
- Kunstler, G., Falster, D., Coomes, D. A., Hui, F., Kooyman, R. M., Laughlin, D. C., Poorter, L., Vanderwel, M., Vieilledent, G., Wright, S. J., Aiba, M., Baraloto, C., Caspersen, J., Cornelissen, J. H. C., Gourlet-Fleury, S., Hanewinkel, M., Herault, B., Kattge, J., Kurokawa, H., ... Westoby, M. (2016). Plant functional traits have globally consistent effects on competition. *Nature*, 529(7585), 204–207. <https://doi.org/10.1038/nature16476>.
- Kunz, M., Fichtner, A., Härdtle, W., Raunonen, P., Bruelheide, H., & Oheimb, G. (2019). Neighbour species richness and local structural variability modulate aboveground allocation patterns and crown morphology of individual trees. *Ecology Letters*, 22(12), 2130–2140. <https://doi.org/10.1111/ele.13400>.
- Lafarge, T., & Pateiro-Lopez, B. (2017). Implementation of the 3D Alpha-Shape for the Reconstruction of 3D Sets from a Point Cloud. <https://cran.r-project.org/web/packages/alphashape3d/index.html>.
- Lang, A. C., Härdtle, W., Baruffol, M., Böhnke, M., Bruelheide, H., Schmid, B., Wehrden, H., & Oheimb, G. (2012). Mechanisms promoting tree species co-existence: Experimental evidence with saplings of subtropical forest ecosystems of China. *Journal of Vegetation Science*, 23(5), 837–846. <https://doi.org/10.1111/j.1654-1103.2012.01403.x>.
- Lang, A. C., Härdtle, W., Bruelheide, H., Geißler, C., Nadrowski, K., Schuldt, A., Yu, M., & von Oheimb, G. (2010). Tree morphology responds to neighbourhood competition and slope in species-rich forests of subtropical China. *Forest Ecology and Management*, 260(10), 1708–1715. <https://doi.org/10.1016/j.foreco.2010.08.015>.
- Lewis, S. L., Wheeler, C. E., Mitchard, E. T. A., & Koch, A. (2019). Restoring natural forests is the best way to remove atmospheric carbon. *Nature*, 568(7750), 25–28. <https://doi.org/10.1038/d41586-019-01026-8>.
- Li, Y., Härdtle, W., Bruelheide, H., Nadrowski, K., Scholten, T., von Wehrden, H., & von Oheimb, G. (2014b). Site and neighborhood effects on growth of tree saplings in subtropical plantations (China). *Forest Ecology and Management*, 327, 118–127. <https://doi.org/10.1016/j.foreco.2014.04.039>.
- Li, Y., Hess, C., von Wehrden, H., Härdtle, W., & von Oheimb, G. (2014a). Assessing tree dendrometrics in young regenerating plantations using terrestrial laser scanning. *Annals of Forest Science*, 71(4), 453–462. <https://doi.org/10.1007/s13595-014-0358-4>.
- Li, Y., Kröber, W., Bruelheide, H., Härdtle, W., & von Oheimb, G. (2017). Crown and leaf traits as predictors of subtropical tree sapling growth rates. *Journal of Plant Ecology*, 10(1), 136–145. <https://doi.org/10.1093/jpe/rtw041>.
- Liang, J., Crowther, T. W., Picard, N., Wiser, S., Zhou, M., Alberti, G., Schulze, E. D., McGuire, A. D., Bozzato, F., Pretzsch, H., De-Miguel, S., Paquette, A., Héroult, B., Scherer-Lorenzen, M., Barrett, C. B., Glick, H. B., Hengeveld, G. M., Nabuurs, G. J., Pfautsch, S., ... Reich, P. B. (2016). Positive biodiversity-productivity relationship predominant in global forests. *Science*, 354(6309). <https://doi.org/10.1126/science.aaf8957>.
- Liang, X., Kankare, V., Hyypä, J., Wang, Y., Kukko, A., Haggrén, H., Yu, X., Kaartinen, H., Jaakkola, A., Guan, F., Holopainen, M., & Vastaranta, M. (2016). Terrestrial laser scanning in forest inventories. *ISPRS Journal of Photogrammetry and Remote Sensing*, 115, 63–77. <https://doi.org/10.1016/J.ISPRSJPRS.2016.01.006>.
- Liu, X., Trogisch, S., He, J.-S., Niklaus, P. A., Bruelheide, H., Tang, Z., Erfmeier, A., Scherer-Lorenzen, M., Pietsch, K. A., Yang, B., Kühn, P., Scholten, T., Huang, Y., Wang, C., Staab, M., Leppert, K. N., Wirth, C., Schmid, B., & Ma, K. (2018). Tree species richness increases ecosystem carbon storage in subtropical forests. *Proceedings of the Royal Society B: Biological Sciences*, 285(1885), 20181240. <https://doi.org/10.1098/rspb.2018.1240>.

- Niinemets, Ü. (2010). A review of light interception in plant stands from leaf to canopy in different plant functional types and in species with varying shade tolerance. *Ecological Research*, 25(4), 693–714. <https://doi.org/10.1007/s11284-010-0712-4>.
- Pretzsch, H. (2014). Canopy space filling and tree crown morphology in mixed-species stands compared with monocultures. *Forest Ecology and Management*, 327, 251–264. <https://doi.org/10.1016/j.foreco.2014.04.027>.
- R Core Team. (2020). R: A language and environment for statistical computing. R Foundation for Statistical Computing. <https://www.r-project.org/>.
- Raumonen, P., Kaasalainen, M., Åkerblom, M., Kaasalainen, S., Kaartinen, H., Vastaranta, M., Holopainen, M., Disney, M., & Lewis, P. (2013). Fast Automatic Precision Tree Models from Terrestrial Laser Scanner Data. *Remote Sensing*, 5(2), 491–520. <https://doi.org/10.3390/rs5020491>.
- Sapijanskas, J., Paquette, A., Potvin, C., Kunert, N., & Loreau, M. (2014). Tropical tree diversity enhances light capture through crown plasticity and spatial and temporal niche differences. *Ecology*, 95(9), 2479–2492. <https://doi.org/10.1890/13-1366.1>.
- Scholten, T., Goebes, P., Kühn, P., Seitz, S., Assmann, T., Bauhus, J., Bruelheide, H., Buscot, F., Erfmeier, A., Fischer, M., Härdtle, W., He, J.-S., Ma, K., Niklaus, P. A., Scherer-Lorenzen, M., Schmid, B., Shi, X., Song, Z., von Oheimb, G., ... Schmidt, K. (2017). On the combined effect of soil fertility and topography on tree growth in subtropical forest ecosystems—A study from SE China. *Journal of Plant Ecology*, 10(1), 111–127. <https://doi.org/10.1093/jpe/rtw065>.
- Steur, G., Verburg, R. W., Wassen, M. J., & Verweij, P. A. (2020). Shedding light on relationships between plant diversity and tropical forest ecosystem services across spatial scales and plot sizes. *Ecosystem Services*, 43. <https://doi.org/10.1016/j.ecoser.2020.101107>.
- Trogisch, S., Schuldt, A., Bauhus, J., Blum, J. A., Both, S., Buscot, F., Castro-Izaguirre, N., Chesters, D., Durka, W., Eichenberg, D., Erfmeier, A., Fischer, M., Geißler, C., Germany, M. S., Goebes, P., Gutknecht, J., Hahn, C. Z., Haider, S., Härdtle, W., ... Bruelheide, H. (2017). Toward a methodical framework for comprehensively assessing forest multifunctionality. *Ecology and Evolution*, 7(24), 10652–10674. <https://doi.org/10.1002/ece3.3488>.
- Trogisch et al., (202X). The importance of tree-tree interactions for forest ecosystem functioning. *Basic and Applied Ecology*, this issue.
- Valladares, F., Gianoli, E., & Gómez, J. M. (2007). Ecological limits to plant phenotypic plasticity. *New Phytologist*, 176(4), 749–763. <https://doi.org/10.1111/j.1469-8137.2007.02275.x>.
- Van de Peer, T., Verheyen, K., Kint, V., Van Cleemput, E., & Muys, B. (2017). Plasticity of tree architecture through interspecific and intraspecific competition in a young experimental plantation. *Forest Ecology and Management*, 385, 1–9. <https://doi.org/10.1016/j.foreco.2016.11.015>.
- van der Plas, F. (2019). Biodiversity and ecosystem functioning in naturally assembled communities. *Biological Reviews*, 94(4), brv.12499-brv.12499. <https://doi.org/10.1111/brv.12499>.
- Williams, L. J., Paquette, A., Cavender-Bares, J., Messier, C., & Reich, P. B. (2017). Spatial complementarity in tree crowns explains overyielding in species mixtures. *Nature Ecology & Evolution*, 1(4), 63–63. <https://doi.org/10.1038/s41559-016-0063>.
- Wood, S. N. (2017). Generalized additive models: An introduction with R. In Chapman & Hall/CRC texts in statistical science CN - QA274.73. W66 2017 (Second edi, p. 476). CRC Press/Taylor & Francis Group.
- Yang, X., Bauhus, J., Both, S., Fang, T., Härdtle, W., Kröber, W., Ma, K., Nadrowski, K., Pei, K., Scherer-Lorenzen, M., Scholten, T., Seidler, G., Schmid, B., von Oheimb, G., & Bruelheide, H. (2013). Establishment success in a forest biodiversity and ecosystem functioning experiment in subtropical China (BEF-China). *European Journal of Forest Research*, 132(4), 593–606. <https://doi.org/10.1007/s10342-013-0696-z>.
- Zuur, A. F., Ieno, E. N., Walker, N., Saveliev, A. A., & Smith, G. M. (2009). Mixed effects models and extensions in ecology with R. In *Statistics for Biology and Health*. Springer New York. <http://link.springer.com/10.1007/978-0-387-87458-6>.

Chapter IV. Biomass allocation of trees in response to mono- and heterospecific neighbourhoods

Maria D. Perles-Garcia^{1,2*}, Andreas Fichtner³, Sylvia Haider², Hanjiao Gu⁴, Wensheng Bu⁴, Matthias Kunz⁵, Werner Härdtle³, Goddert von Oheimb^{5, 1}

¹ German Centre for Integrative Biodiversity Research (iDiv), Halle-Jena-Leipzig, 04103 Leipzig, Germany

² Institute of Biology / Geobotany and Botanical Garden, Martin Luther University Halle-Wittenberg, Große Steinstr. 79/80, 06108 Halle (Saale), Germany

³ Institute of Ecology, Leuphana University of Lüneburg, Universitätsallee 1, 21335 Lüneburg, Germany

⁴ Jiangxi Provincial Key Laboratory of Silviculture, College of Forestry, Jiangxi Agricultural University, 330045 Nanchang, China

⁵ Institute of General Ecology and Environmental Protection, Technische Universität Dresden, 01737 Tharandt, Germany

* Correspondence: maria_dolores.perles@idiv.de, German Centre for Integrative Biodiversity Research (iDiv), Halle-Jena-Leipzig, 04103 Leipzig, Germany.

Editorial status: Preprint published in bioRxiv (October 2024)

DOI: <https://doi.org/10.1101/2024.10.15.618432>

Abstract

Carbon sequestration by trees is crucial to mitigate the effects of the current climate crisis. The extent to which trees sequester and allocate carbon to above- or belowground structures in turn is mediated by neighbouring species. Although many studies have demonstrated positive effects of diverse neighbourhoods on a tree's productivity, little is known about biomass allocation responses to mono- vs. heterospecific neighbourhoods. In the present study we quantified above- and belowground biomass production and root-to-shoot ratios (RSR) of trees grown in mono- and heterospecific neighbourhoods. To this end we analysed growth of mono- and heterospecific tree species pairs (TSPs) established in a greenhouse and a field experiment. In the greenhouse experiment response variables were measured after one year of growth after sapling harvest. In the field experiment, conducted in the context of a forest biodiversity experiment in subtropical China, we analysed biomass density and RSR over three years using terrestrial laser scanner and minirhizotrons. RSR of trees in heterospecific TSPs were significantly higher than in monospecific TSPs. In the greenhouse experiment, this was related to a stronger below- than aboveground overyielding in heterospecific TSPs. In the field experiment, trees in heterospecific TSPs showed a stronger increase in aboveground investments over time than in monospecific TSPs, indicating that positive diversity effects became stronger for aboveground structures with progressing tree development. Our findings are consistent with the optimal biomass partitioning theory and highlight the importance of tree-tree interactions on biomass allocation. Higher RSR in mixtures further suggest a higher resistance or resilience of tree saplings against environmental stressors related to climate change (drought, heat waves).

Keywords

Aboveground biomass, BEF-China, biodiversity-ecosystem functioning, biomass allocation, minirhizotron, root biomass, root-to-shoot ratio, terrestrial laser scanning

1. Introduction

Mitigating the effects of climate change is one of the major challenges of this century. Forests have the potential to fix CO₂ from the atmosphere and to sequester carbon in the long term in their biomass. As a consequence, afforestation and reforestation measures are widely accepted as one of the most effective strategies to partly compensate for anthropogenic CO₂ emissions (Bastin et al., 2019; Lewis et al., 2019). The acceleration of climate change in recent years has led to an increase in extreme events such as fires,

droughts, floods or plagues (Kirilenko & Sedjo, 2007). Diversifying forests in turn may increase their resilience and their ability to fix carbon (C. L. C. Liu et al., 2018; Piotta, 2008). It is, therefore, important to understand the mechanisms through which the selection and combination of tree species may enhance forest growth and survival, and how these targets may be achieved by means of optimized afforestation strategies and forest restoration on devastated area.

In this context it is vital to know how trees may interact at the local neighbourhood level and in relation to neighbourhood species richness and composition (Fichtner et al., 2017). Several studies have demonstrated that tree growth and biomass allocation to different structures (roots, stems or branches) can vary depending on biotic and abiotic factors (Guillemot et al., 2020; Kunz et al., 2019; Williams et al., 2017). For example, competitive interactions between trees, but also species traits and trait plasticity as well as functional dissimilarity between neighbouring trees may mediate tree crown development and thus aboveground architecture (Guillemot et al., 2020; Hildebrand et al., 2020; Williams et al., 2021). In addition, tree-tree interactions may drive a tree's biomass allocation within and between above- and belowground structures, which in turn affects a tree's ability to compete for light and belowground resources such as nutrients and water (Beugnon et al., 2022; Kunz et al., 2019; Madsen et al., 2020). Even though local tree neighbourhoods have been shown to be one of the main drivers shaping a tree's above- and belowground investments (Lang et al., 2010; Van de Peer et al., 2017; Yang et al., 2019), little is known about the underlying mechanisms and consequences for related traits such as root-to-shoot ratios. Root-to-shoot ratios (RSR), i.e. the ratio of the belowground biomass relative to the aboveground biomass, are measured from a tree individual or a forest stand and may have important implications for a tree's or a stand's ability to cope with environmental stressors such as drought events or heat waves (Qi et al., 2019). Modifying the neighbourhood species richness and composition of a focal tree thus might have consequences for its resistance or resilience to environmental stressors. Besides neighbourhood effects, RSR proved to be related to other factors such as latitude, stand age, nutrient availability, and climate (Qi et al., 2019). In addition, RSR are often used to estimate root biomass density from aboveground biomass, given that environmental factors are accounted for (Annighöfer et al., 2022; Cairns et al., 1997; Singnar et al., 2021).

Destructive methods allow direct measurements of above- and belowground biomass. In contrast, non-destructive methods may be less precise, but allow for continuous observations and longer-term measurements on shifts in allocation patterns in relation to the

drivers of interest (e.g. tree-tree interactions). Non-destructive measures thus account for the dynamics of tree-tree interactions and time-related shifts in tree growth responses to biotic and abiotic environmental conditions (Li et al., 2014). In the present study we applied a combination of both approaches: In a greenhouse experiment tree seedlings were grown under controlled conditions and biomass of aboveground and belowground structures was quantified after sapling harvest one year after planting. In the field experiment we made use of the BEF-China experimental platform (Bruehlheide et al., 2014) and quantified tree growth over three years using inventory and terrestrial laser scanning (TLS) data to quantify aboveground biomass development. In addition we installed minirhizotrons between each of the TSPs selected to examine changes in root biomass density (RBD) over time (Johnson et al., 2001).

The main objective of the present study was to analyse how pairwise interactions between two adjacent, mono- vs. heterospecific trees species (i.e. tree species pairs, hereinafter abbreviated as TSPs) affect the trees' biomass allocation and root-to-shoot ratios. We hypothesize that (i) RSR would be higher in heterospecific TSPs because of relatively higher investments of saplings in belowground biomass, (ii) aboveground biomass investments might become more important over time in heterospecific TSPs, because positive diversity effects might be stronger aboveground with progressing crown development, and (iii) RSR are influenced by species composition and identity.

2. Material and methods

2.1. Greenhouse experiment

In autumn 2018, we collected seeds from eight broadleaved species in the Gutianshan National Nature Reserve (Zhejiang Province) which are also present in the biodiversity-ecosystem functioning experiment BEF China (see section 2.2). In spring 2019, seeds were germinated under controlled conditions in the greenhouse of the botanical garden from the MLU University Halle (Germany). From the individuals germinated 15 were selected by random from each species (8 species \times 15 individuals = 120 individuals in total). In July 2019 the seedlings were measured (height above- and belowground, stem diameter, weight) and transplanted pairwise in 60 PVC tubes of 20 cm in diameter and 100 cm in length (i.e. two individuals per tube). The tubes were cut in two halves and re-assembled again so they could be opened without damaging the roots (Fig S1). We split the species into two sets of four species each and combine them in all possible combinations within the set. In total, 20

different species combinations were used: eight monospecific and 12 heterospecifics (Table S1).

All tubes in which both individuals survived were harvested in September 2020. In total, we analysed 98 trees, 40 and 58 of which grew in monospecific and heterospecific pairs, respectively. Table S1 shows the tree species combinations and the number of pairs that were sampled after one year for each treatment. For analyses, the root biomass was sampled by carefully cleaning roots from adhered soil material. Subsequently, aboveground and belowground biomass was dried at 80°C for 3 days and biomass dry weight of each tree quantified.

2.2. Field experiment (BEF China)

In addition to the one-year greenhouse experiment we used data from the BEF China field experiment. The BEF-China platform represents a Biodiversity–Ecosystem Functioning experiment situated in Jiangxi province (29.08°– 29.11°N, 117.90°– 117.93°E, 100– 300 m a.s.l.; Bruelheide et al., 2014). It has a subtropical climate, the mean temperature is 16,7°C and the mean precipitation is 1821 mm/year (Yang et al., 2013). Site A was planted in 2009. Each plot contains 400 trees planted in a regular grid with a distance between them of 1.29 m. Tree species richness of the plots ranges from monoculture to 24 species mix. TSPs can be monospecific pairs (i.e. both trees belong to the same tree species) or heterospecific pairs (i.e. the two trees belong to different tree species).

In this experiment we applied a non-destructive approach to study the growth behaviour of a total of 94 trees in 47 TSPs from 24 plots (Site A of the BEF-China experiment) over a three-year time period (2014-2016). All trees were identified by species and tree height and stem diameter at ground level were measured annually (between September and October). In addition, terrestrial laser scanning (TLS) was conducted each year in March on 14 of the 24 plots (see description below). Table S2 shows the species combinations, the number of TSPs analysed each year and the number of plots in which each species combination was present. In May 2014 minirhizotrons were installed in the middle of the two trees. From the minirhizotron tube, photos were taken annually to document the trees' rooting pattern (see description below).

2.2.1. Aboveground biomass estimation

TLS was conducted under leaf-off conditions, using the laser scanner FARO Focus S120. The TLS campaigns included 714 trees. We scanned a total of 18 TSPs out of the 47 TSPs

included in this study. We generated quantitative structure models (QSMs) from the point clouds to quantify the wood volume of individual trees. Co-registration and point cloud segmentation were carried out manually using FARO Scene software (V. 5.2.6), RiSCAN PRO (v2.6.2) and Bentley Pointools (v1.5 Pro). For QSMs, we used the TreeQSM software (Åkerblom, 2017; see Kunz et al. 2019 for more details)

To estimate the volume of TSPs that were not scanned and in order to have a consistent data set, we used the random forest algorithm. We used height, stem diameter at ground level and species as explanatory variables and trained the algorithm with a subset of 665 scanned multiple years, $n = 1326$, with the volume derived from TLS as a response. We performed the analysis using R 4.1. and the randomForest package (Liaw & Wiener, 2002). We validated the results with a subsample of 427 trees scanned multiple years, $n = 591$ (RMSE = 5.04, MAE = 2.58, $R^2 = 0.79$), and with the 36 trees from the 18 TSPs included in the study (RMSE = 8.30, MAE = 6.64, $R^2 = 0.77$).

Finally, we used the modelled volume and the wood density of each tree species (taken from Kröber et al., 2014) to calculate the aboveground biomass of each tree.

2.2.2 Belowground biomass estimation

The minirhizotron tubes were installed at a 30° angle to a soil depth of 30 cm (diagonal length of 60 cm). Each minirhizotron was installed in the middle of two neighbouring trees. Before installing the minirhizotrons, we removed understory plants and leaf litter from the ground. Plugs were used to seal the bottom of all pipes, and plastic covers and self-sealing bags were used to seal the top (Fig S2). The sealings were applied to prevent contamination with organic matter and the infiltration of water. Black tapes followed by white tapes were applied to the aboveground part of each tube in order to prevent heat absorption caused by penetrating light (Kou et al., 2018). To minimize soil disturbance, leaf litter was used to cover the ground around the tubes. Root scanning started seven months after installation of the minirhizotrons, to allow stabilization of the soil (Hansson et al., 2013).

To improve fine root turnover analyses, we acquired coloured root images (18 mm × 14 mm) at the same soil depth in November 2014, May 2015 and November 2016. BTC-100 camera system (Bartz Technology, Santa Barbara, Calif.) was used for root images and to document root growth. We collected about 160 images in four directions in each tube. WinRhizo Tron MF (Regent Software, Canada) was used to process the images and to get data on total root length and alive root length. The identification of living and dead roots followed the definition of Wells & Eissenstat (2001), according to which living roots show a white and

brown colour, while dead roots exhibit an exfoliated cortex, wrinkled epidermis, or black colour.

We quantified the following belowground traits: specific root length (SRL), root length density per unit volume (RLD_v), and root biomass density per unit volume (RBD_v). RLD is an important indicator reflecting the below-ground competitiveness of trees. The calculation of RLD_v is as follows:

$$RLD_v \text{ (m}\cdot\text{m}^{-3}\text{)} = L / (A \times DOF) \quad (1),$$

where L is the root length inferred from the minirhizotron images (m), A is an area of minirhizotron image observed, DOF is field depth (m), that was set to 0.002 m (Steele et al., 1997).

For the calculation of SRL, intact fine roots were excavated from the top 30 cm of undisturbed soil through drilled soil samples in each plot and transported to the laboratory in a cooler box with ice packs in September 2015. For each plot, at least 6 individuals per species were sampled in plots with tree species richness of one and 3 individuals per species were sampled in plots with tree species richness greater than one and heterospecific direct neighbours. After gently cleaning the soil and organic particles of the fine roots with tap water, the fine roots were divided into 5 functional groups according to Pregitzer et al. (2002). These five groups were split into two types; that is, the absorptive fine roots (orders 1-3) and transport fine roots (orders 4, and 5). Then, roots of each functional type were scanned by an Epson scanner and analyzed by WinRHIZO (Regent Software, Canada) to get data on total root length and average diameter. After scanning, these samples were dried in an oven at 60°C for over 48 h until they became constant weight and weighed. The calculation of SRL of each order is as follows:

$$SRL \text{ (m}\cdot\text{g}^{-1}\text{)} = L / DW \quad (2),$$

where L is the root length observed in each scanned image (m), DW is the root dry weight (g).

Since minirhizotrons were installed in the middle of two neighbour individuals, the SRL in mixtures represents the mean specific root length of absorptive fine roots of the two species. RBD was estimated in combination with SRL data obtained by soil drilling (Shi et al., 2006). The calculation of RBD_v is as follows:

$$RBD_v = \sum \frac{RLD_i}{SRL_i} \quad (3),$$

where RBD_v is the root biomass density per unit volume ($\text{g}\cdot\text{m}^{-3}$). RLD_i is the RLD_v ($\text{m}\cdot\text{m}^{-3}$) of diameter *i*; and SRL_i is the SRL ($\text{m}\cdot\text{g}^{-1}$) of diameter *i*.

2.3. Statistical analysis

We applied linear mixed-effects models to examine how pairwise tree interactions affect above- and belowground biomass, and RSR, and whether this effect varies over time. Specifically, we analysed the changes depending on whether the trees grew in mono- or heterospecific pairs. We used different approaches:

In the greenhouse experiment, we used the measured dry weight for above- and belowground biomass, and calculated the RSR by dividing the root dry weight of each individual by the dry weight of its shoots. We used TSP species richness (mono- or heterospecific) as predictor and species and neighbour species as random intercepts. We also consider the result of the TSPs as a whole, calculating the sum of the biomass of both trees. In this case, the combination of species was used as a random intercept. The model was fitted separately to predict aboveground biomass weight, belowground biomass weight, and RSR.

In the case of the field experiment, we analysed the response of the TSP: We divided the RBD by the shoot biomass density (SBD), calculated as the biomass (g) divided by two times the distance between the trees and the mean height of the studied trees (2.58 m x 2.58 m x 3.40 m). We fitted different linear mixed-effects models using the RBD, SBD and RSR of the TSP as the response variable and we tested the effect of TSP diversity (mono- or heterospecific), year and the interaction between both. Year 0 was considered the year of the planting of Site A (i.e. 2009). Species combination of a specific TSP and study plot were used as random intercepts. To assure model assumptions (normality, homogeneity and independence; Zuur et al., 2009), we square root transform the dependent variables in both data sets (greenhouse and field experiment data).

All statistical analyses were performed in R 4.0.2 (R Core Team, 2018) using the packages lme4 (Bates et al., 2015), lmerTest (Kuznetsova et al., 2017) and sjPlot (Lüdecke, 2020).

3. Results

Overall, we observed a significant relation between species richness of TSPs and our three response variables (above- and belowground biomass (or biomass density), and RSR; Table 1, Table 2, Fig 1, Fig 2). One year after planting, seedlings from the greenhouse experiment had significantly more biomass above- and belowground in mixtures than in monocultures

(Table 1, Fig 1). In addition, RSR was significantly higher in mixtures (Table 1, Fig 1). However, when we analyse this data grouped by TSPs, the p-value was not significant for any of the three models (Table S3).

Table 1. Results of mixed-effects models for the effects of pairwise species richness (mono- or heterospecific) on the root to shoot ratio (RSR, squared root transformed), aboveground dry biomass (AG_weight, squared root transform), and belowground dry biomass (BG_weight, squared root transform) for 98 trees planted under control conditions in the greenhouse experiment.

Fixed effect	sqrt-RSR				sqrt-AG_weight (g)				sqrt-BG_weight (g)			
	df _{num}	df _{den}	F	p	df _{num}	df _{den}	F	p	df _{num}	df _{den}	F	p
Intercept	-	-	-	< 0.001	-	-	-	< 0.05	-	-	-	< 0.05
Species richness	1	83.391	5.311	< 0.05	1	83.109	8.057	< 0.01	1	83.099	15.389	< 0.001
Marginal R ²	0.027				0.011				0.018			
Conditional R ²	0.512				0.868				0.891			

dfnum, numerator degrees of freedom; dfden, denominator degrees of freedom.

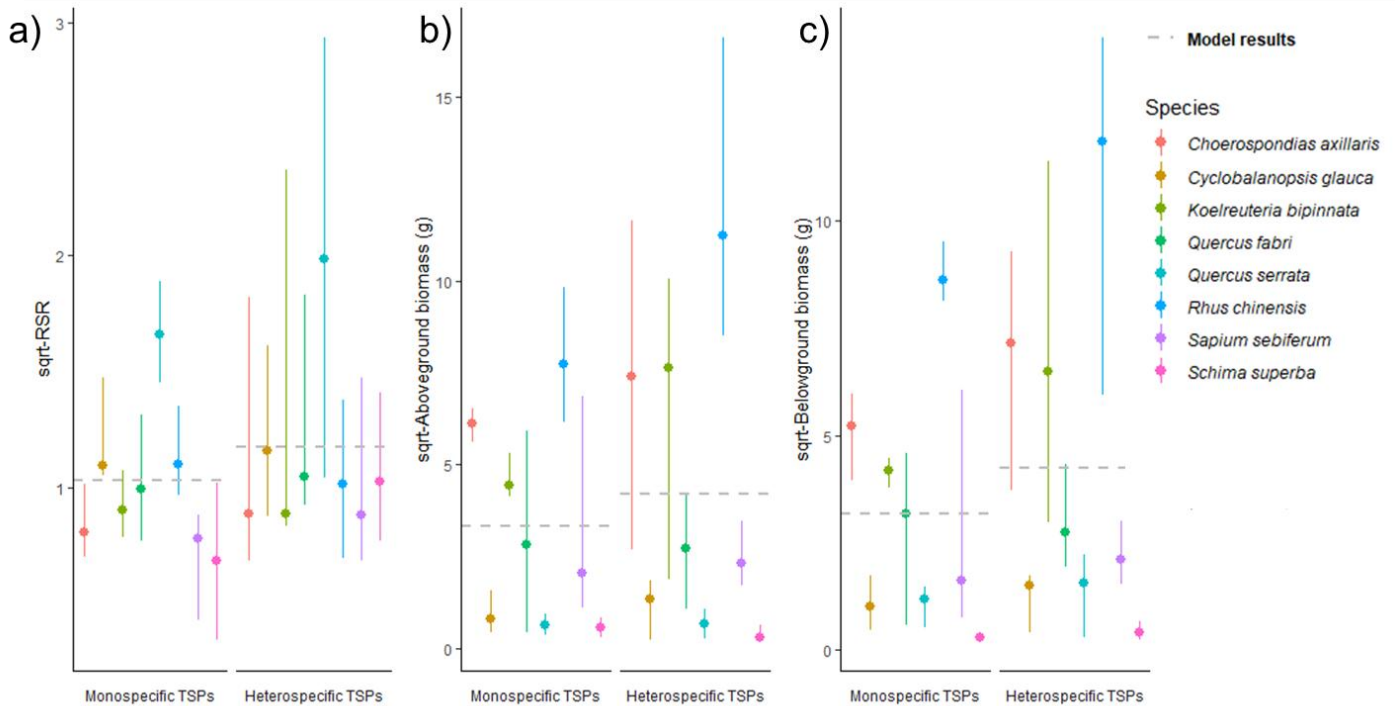


Figure 1. Range bar of observed values and model results for the three response variables measured in the greenhouse: (a) shows root-to-shoot ratio (RSR, squared root transformed), (b) aboveground dry biomass squared root transform, and (c) belowground dry biomass squared root transform. Dots represent the median of the observed values grouped by species and by pairwise diversity. Solid lines represent the range of the results. The grey dashed line represents the predicted values of the models.

We found comparable results in the field experiment in that seedlings showed higher RSR and higher values for SBD in hetero- than in monospecific TSPs, but differences for RBD were not significant (Table 2). In addition, tree growth responses strengthened over time, indicated by a positive and significant “Year”-effect across response variables ($p < 0.05$ for all three variables; Table 2). However, time effects on RSR and SBD were different for

mono- und heterospecific TSPs, indicated by the significant two-way interaction between “Year” and “Species richness”. As shown in Fig 2, trees in heterospecific TSPs showed a stronger increase in aboveground biomass investments over time than in monospecific TSPs. As a result, the increase in RSR over time was stronger in monospecific TSPs (Fig 2a). In contrast, the “Year × Species richness” interaction was not significant for RBD ($p = 0.135$, Table 2).

Table 2. Results of mixed-effects models for the effects of pairwise diversity (mono- or hetero- specific, “Spec_Div”), year and its interaction on the root to shoot ratio (RSR, squared root transformed), shoot biomass density (SBD, squared root transform), and root biomass density (RBD, squared root transform). The model was fitted to 47 TSPs measured during three years (2014, 2015, and 2016), in a total of 126 observations.

Fixed effect	sqrt-RSR			sqrt-SBD (g/m ³)				sqrt-RBD (g/m ³)				
	df _{num}	df _{den}	F	df _{num}	df _{den}	F	p	df _{num}	df _{den}	F	p	
Intercept	-	-	-	< 0.01	-	-	-	< 0.001	-	-	-	< 0.001
Species richness	1	111.188	14.594	< 0.001	1	120.811	8.222	< 0.01	1	85.684	2.7494	0.101
Year	1	81.228	44.481	< 0.001	1	80.177	40.218	< 0.05	1	77.311	98.606	< 0.001
Species richness:Year	1	81.144	12.927	< 0.001	1	80.138	9.146	< 0.01	1	77.33	2.277	0.135
Marginal R ²	0.097			0.061				0.373				
Conditional R ²	0.821			0.922				0.576				

dfnum, numerator degrees of freedom; dfden, denominator degrees of freedom.

Heterospecific TSPs benefit both, above- and belowground over time, with effects being higher for RBD: In 2016 the estimate RBD was 90% higher than in 2014, compared to a 48% increase in SBD. Meanwhile, we estimated a much more pronounced increase of RBD in monospecific TSPs: While its estimated increase in SBD between 2014 and 2016 was 13%, in RBD was 165%

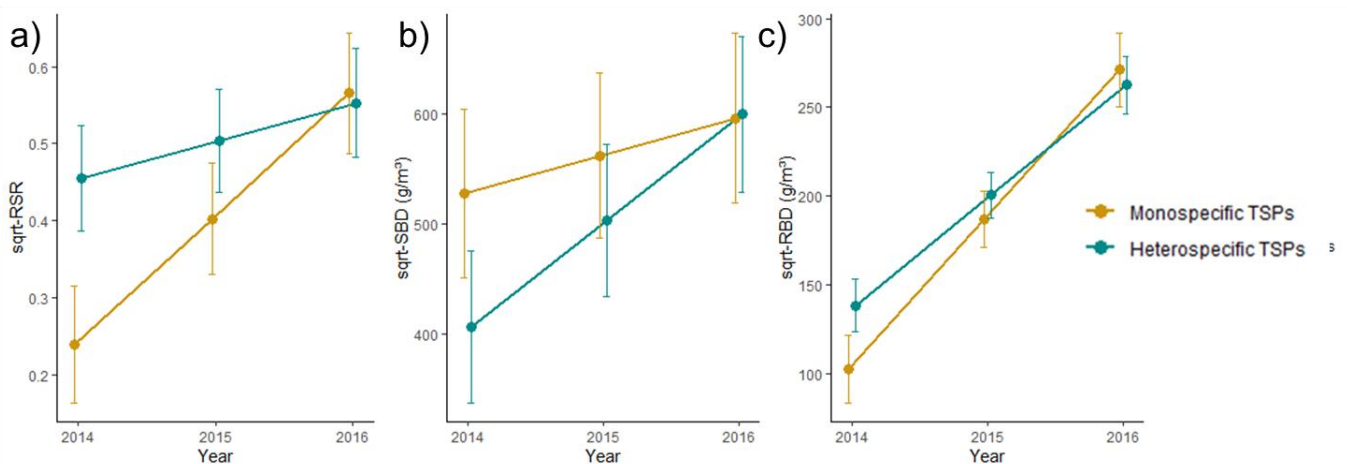


Figure 2. Effects of pairwise species diversity (mono- or hetero- specific pairs) on (a) root to shoot ratio (RSR, squared root transformed), (b) shoot biomass density (SBD, squared root transform), and (c) root biomass density (RBD, squared root transform). Lines represent mixed-effects model fits, dots represent the mean predicted value for each year, and the corresponding standard errors are represented as error bars.

4. Discussion

There is evidence that neighbourhood interactions can modulate the aboveground tree architecture as a result of interspecific differences in morphological and physiological tree traits (Hildebrand et al., 2020; Perles-Garcia et al., 2022; Williams et al., 2017). However, due to sampling difficulties few studies have analysed above- and belowground biomass allocation patterns of trees in relation to con- and heterospecific neighbourhoods. Instead, many studies focused on tree growth responses and crown formation to abiotic factors such as nutrient availability or climate (Y. Liu et al., 2014; Meier & Leuschner, 2008; Trubat et al., 2011; Wright, 2019), or compared estimations of RSR in different biomes (Ma et al., 2021; Mokany et al., 2006; Qi et al., 2019). To address this gap in knowledge, the present study quantified how biomass allocation of different tree species responds to con- and heterospecific neighbourhoods, using two different experimental approaches. Our results evidenced that tree-tree interactions may have significant effects on the biomass allocation of tree individuals, with possible consequences for growth responses to and performance under environmental stressors.

In the greenhouse experiment, trees in heterospecific TSPs showed a higher above- and belowground productivity than trees in monospecific TSPs. This finding is in agreement with previous studies, according to which more diverse forests showoveryielding compared to monocultures, mainly attributable to complementarity between different tree species (Huang et al., 2018; Liang et al., 2016; Paquette & Messier, 2011; van der Plas, 2019). However, this finding became non-significant when comparing TSPs instead of tree individuals, likely indicating a strong effect of the species composition of the respective TSPs. This interpretation is supported by the finding that all models showed distinct differences between R^2_{marginal} and $R^2_{\text{conditional}}$ (see Tables 1 and 2 and further discussion below).

As hypothesized, RSR were higher for saplings in heterospecific than in monospecific TSPs (for both experiments). Since survival of tree seedlings often depends on a rapid development of their root system to ensure a sufficient supply with belowground resources (Grossnickle, 2012), competitive interactions initially might have been stronger belowground, particularly in the greenhouse experiment with limited roots space within the root tubes. This would explain why positive diversity effects for saplings might be stronger belowground, leading to higher biomass production in heterospecific TSPs. Our interpretation is supported by the finding thatoveryielding was stronger for belowground than for aboveground biomass in the greenhouse experiment, probably because of an optimised (complementary) use of resources due to belowground niche differentiation. Our findings are in agreement

with those from Ravenek et al. (2014), who also observed overyielding in root biomass with increasing species richness.

In the field experiment, RSR showed a steady increase over time for trees in both mono- and heterospecific TSPs, attributable to a stronger increase in belowground investments. This plasticity in allocation can be interpreted as a general change in a tree's allometric trajectory with increasing tree age and thus, as allometric growth ("apparent plasticity") in the sense of Weiner (2004). However, as indicated by a significant "Year \times Species richness" interaction, trees in monospecific TSPs showed a significantly stronger increase in their RSR than trees in heterospecific TSPs. Since TSP-related differences in the increase of RBD were non-significant, the weaker increase in RSR observed in heterospecific TSPs is solely caused by a stronger increase in aboveground biomass investments over time. This confirms our second hypothesis that aboveground biomass investments might become more important over time in heterospecific TSPs, because positive diversity effects (e.g. because of niche partitioning and complementary resource use) might be stronger aboveground with progressing crown development (Jucker et al., 2020). As a result, trees grown in heterospecific neighbourhoods may increase their aboveground investments, concomitantly optimize resource acquisition (e.g. light foraging) and minimize interspecific competition. In contrast to heterospecific TSPs and in accordance with the optimal biomass partitioning theory (Bloom & Mooney, 1985), monospecific pairs had higher aboveground investments in 2014, specifically in the elongation of the primary stem, to avoid shading by competing neighbours with similar growth rates. Due to an adjustment of biomass allocation to the most limiting resource (Bloom & Mooney, 1985), trees in monospecific pairs showed an increasing (relative) investment to belowground structures. However, further studies covering longer-time measurement series are required to determine whether this trend persists over time.

Our result that mixtures show lower aboveground biomass values in the early years of development is in agreement with findings from Jucker et al. (2020), but contradicts the findings of Huang et al. (2018), who observed consistent higher productivity at the plot level with increasing tree species richness in the BEF-China experiment for the years 2013-2017. These differences could be due to the fact that we focused on the TSPs between which the minirhizotrons were installed, and we studied the years 2014-2016. Also, SBD accounts for the sum of the biomasses of both trees of the TSP, which could mean that fast-growing species will have lower values when mixed with slow-growing species.

We found that variation in above, below and RSR is largely explained by species identity effects (i.e. species combination of a given TSP) rather than species richness effects (mono- versus heterospecific TSP), which supports our third hypothesis (also see Fig S3 illustrating the biomass of tree individuals from BEF China by species). We assume that the lower values in aboveground biomass in the fifth and sixth year after planting are related to species-specific traits such slow or fast-growing strategies, but also to the fact that other neighbouring trees surrounding the TSPs were not considered (i.e. four of the monospecific TSPs studied were not grown in plots planted as monocultures; this concerns TSPs of *Sapindus mukorossi*, *Castanopsis sclerophylla*, *Cyclobalanopsis glauca*, and *Cyclobalanopsis myrsinifolia*, where one of the TSPs considered as monospecific grew in a plot with tree species richness of two, four, four and four respectively).

In conclusion our findings demonstrate that tree-tree interactions at the neighbourhood level may significantly affect allometric growth of trees in terms of above-and belowground biomass investments, which in turn might influence a tree's growth vigour and performance under shifting environmental conditions. Higher RSR in mixtures suggest a higher resistance or resilience of tree saplings against environmental stressors related to climate change (drought, heat waves). The establishment of diverse tree plantations in the context of afforestation or restoration measures thus might contribute to more stable tree communities under changing climatic conditions.

Acknowledgements

We are grateful to all the students from MLU Halle who helped to establish and measured the greenhouse experiment. Moreover, we thank the students and the workers who contributed in the field campaigns and the processing of the minirhizotron and the TLS data. This study was supported by the International Research Training Group TreeDì jointly funded by the Deutsche Forschungsgemeinschaft (DFG, German Research Foundation) - 319936945/GRK2324 and the University of Chinese Academy of Sciences (UCAS).

References

- Åkerblom, M. (2017). *Inversetampere/Treeqsm: Initial Release*. Zenodo. <https://doi.org/10.5281/ZENODO.844626>
- Annighöfer, P., Mund, M., Seidel, D., Ammer, C., Ameztegui, A., Balandier, P., Bebre, I., Coll, L., Collet, C., Hamm, T., Huth, F., Schneider, H., Kuehne, C., Löf, M., Mary Petritan, A., Catalin Petritan, I., Peter, S., & Jürgen, B. (2022). Examination of aboveground attributes to predict belowground biomass of young trees. *Forest Ecology and Management*, 505(September 2021). <https://doi.org/10.1016/j.foreco.2021.119942>
- Bastin, J.-F., Finegold, Y., Garcia, C., Mollicone, D., Rezende, M., Routh, D., Zohner, C. M., & Crowther, T. W. (2019). The global tree restoration potential. *Science*, 365(6448), 76–79.

<https://doi.org/10.1126/science.aax0848>

- Bates, D., Mächler, M., Bolker, B., & Walker, S. (2015). Fitting Linear Mixed-Effects Models Using {lme4}. *Journal of Statistical Software*, *67*(1), 1–48. <https://doi.org/10.18637/jss.v067.i01>
- Beugnon, R., Bu, W., Bruelheide, H., Davrinche, A., Du, J., Haider, S., Kunz, M., von Oheimb, G., Perles-Garcia, M. D., Saadani, M., Scholten, T., Seitz, S., Singavarapu, B., Trogisch, S., Wang, Y., Wubet, T., Xue, K., Yang, B., Cesarz, S., & Eisenhauer, N. (2022). Abiotic and biotic drivers of scale-dependent tree trait effects on soil microbial biomass and soil carbon concentration. *Manuscript Submitted for Publication*.
- Bloom, A. J., & Mooney, H. A. (1985). *Plants-an Economic Analogy*.
- Bruelheide, H., Nadrowski, K., Assmann, T., Bauhus, J., Both, S., Buscot, F., Chen, X. Y., Ding, B., Durka, W., Erfmeier, A., Gutknecht, J. L. M., Guo, D., Guo, L. D., Härdtle, W., He, J. S., Klein, A. M., Kühn, P., Liang, Y., Liu, X., ... Schmid, B. (2014). Designing forest biodiversity experiments: General considerations illustrated by a new large experiment in subtropical China. *Methods in Ecology and Evolution*, *5*(1), 74–89. <https://doi.org/10.1111/2041-210X.12126>
- Cairns, M. A., Brown, S., Helmer, E. H., & Baumgardner, G. A. (1997). Root biomass allocation in the world's upland forests. *Oecologia*, *111*(1), 1–11. <https://doi.org/10.1007/s004420050201>
- Fichtner, A., Härdtle, W., Li, Y., Bruelheide, H., Kunz, M., & von Oheimb, G. (2017). From competition to facilitation: how tree species respond to neighbourhood diversity. *Ecology Letters*, *20*(7), 892–900. <https://doi.org/10.1111/ele.12786>
- Grossnickle, S. C. (2012). Why seedlings survive: Influence of plant attributes. *New Forests*, *43*(5–6), 711–738. <https://doi.org/10.1007/s11056-012-9336-6>
- Guillemot, J., Kunz, M., Schnabel, F., Fichtner, A., Madsen, C. P., Gebauer, T., Härdtle, W., von Oheimb, G., & Potvin, C. (2020). Neighbourhood-mediated shifts in tree biomass allocation drive overyielding in tropical species mixtures. *New Phytologist*, *228*(4), 1256–1268. <https://doi.org/10.1111/nph.16722>
- Hansson, K., Helmisaari, H. S., Sah, S. P., & Lange, H. (2013). Fine root production and turnover of tree and understorey vegetation in Scots pine, silver birch and Norway spruce stands in SW Sweden. *Forest Ecology and Management*, *309*, 58–65. <https://doi.org/10.1016/j.foreco.2013.01.022>
- Hildebrand, M., Perles-Garcia, M. D., Kunz, M., Härdtle, W., von Oheimb, G., & Fichtner, A. (2020). Tree-tree interactions and crown complementarity: The role of functional diversity and branch traits for canopy packing. *Basic and Applied Ecology*, *50*, 217–227. <https://doi.org/10.1016/j.baae.2020.12.003>
- Huang, Y., Chen, Y., Castro-Izaguirre, N., Baruffol, M., Brezzi, M., Lang, A., Li, Y., Härdtle, W., Von Oheimb, G., Yang, X., Liu, X., Pei, K., Both, S., Yang, B., Eichenberg, D., Assmann, T., Bauhus, J., Behrens, T., Buscot, F., ... Schmid, B. (2018). Impacts of species richness on productivity in a large-scale subtropical forest experiment. *Science*, *362*(6410), 80–83. <https://doi.org/10.1126/science.aat6405>
- Johnson, M. G., Tingey, D. T., Phillips, D. L., & Storm, M. J. (2001). Advancing fine root research with minirhizotrons. *Environmental and Experimental Botany*, *45*(3), 263–289. [https://doi.org/10.1016/S0098-8472\(01\)00077-6](https://doi.org/10.1016/S0098-8472(01)00077-6)
- Jucker, T., Koricheva, J., Finér, L., Bouriaud, O., Iacopetti, G., & Coomes, D. A. (2020). Good things take time—Diversity effects on tree growth shift from negative to positive during stand development in boreal forests. *Journal of Ecology*, *108*(6), 2198–2211. <https://doi.org/10.1111/1365-2745.13464>
- Kirilenko, A. P., & Sedjo, R. A. (2007). Climate change impacts on forestry. *Proceedings of the National Academy of Sciences of the United States of America*, *104*(50), 19697–19702. <https://doi.org/10.1073/pnas.0701424104>
- Kou, L., Jiang, L., Fu, X., Dai, X., Wang, H., & Li, S. (2018). Nitrogen deposition increases root production and turnover but slows root decomposition in *Pinus elliottii* plantations. *New Phytologist*, *218*(4), 1450–1461. <https://doi.org/10.1111/nph.15066>

- Kröber, W., Zhang, S., Ehmiq, M., & Bruelheide, H. (2014). Linking xylem hydraulic conductivity and vulnerability to the leaf economics spectrum - A cross-species study of 39 evergreen and deciduous broadleaved subtropical tree species. *PLoS ONE*, *9*(11), 1–24. <https://doi.org/10.1371/journal.pone.0109211>
- Kunz, M., Fichtner, A., Härdtle, W., Raunonen, P., Bruelheide, H., & Oheimb, G. von. (2019). Neighbour species richness and local structural variability modulate aboveground allocation patterns and crown morphology of individual trees. *Ecology Letters*. <https://doi.org/10.1111/ele.13400>
- Kuznetsova, A., Brockhoff, P. B., & Christensen, R. H. B. (2017). {lmerTest} Package: Tests in Linear Mixed Effects Models. *Journal of Statistical Software*, *82*(13), 1–26. <https://doi.org/10.18637/jss.v082.i13>
- Lang, A. C., Härdtle, W., Bruelheide, H., Geißler, C., Nadrowski, K., Schuldt, A., Yu, M., & von Oheimb, G. (2010). Tree morphology responds to neighbourhood competition and slope in species-rich forests of subtropical China. *Forest Ecology and Management*, *260*(10), 1708–1715. <https://doi.org/10.1016/j.foreco.2010.08.015>
- Lewis, S. L., Wheeler, C. E., Mitchard, E. T. A., & Koch, A. (2019). Restoring natural forests is the best way to remove atmospheric carbon. *Nature*, *568*(7750), 25–28. <https://doi.org/10.1038/d41586-019-01026-8>
- Li, Y., Hess, C., Von Wehrden, H., Härdtle, W., & Von Oheimb, G. (2014). Assessing tree dendrometrics in young regenerating plantations using terrestrial laser scanning. *Annals of Forest Science*, *71*(4), 453–462. <https://doi.org/10.1007/s13595-014-0358-4>
- Liang, J., Crowther, T. W., Picard, N., Wiser, S., Zhou, M., Alberti, G., Schulze, E. D., Mcguire, A. D., Bozzato, F., Pretzsch, H., Paquette, A., Hérault, B., Scherer-Lorenzen, M., Barrett, C. B., Glick, H. B., Hengeveld, G. M., Nabuurs, G. J., Pfautsch, S., Viana, H., ... Reich, P. B. (2016). Positive biodiversity-productivity relationship predominant in global forests. *Science*, *354*(6309). <https://doi.org/10.1126/science.aaf8957>
- Liaw, A., & Wiener, M. (2002). Classification and Regression by randomForest. *R News*, *2*(3), 18–22. <https://cran.r-project.org/doc/Rnews/>
- Liu, C. L. C., Kuchma, O., & Krutovsky, K. V. (2018). Mixed-species versus monocultures in plantation forestry: Development, benefits, ecosystem services and perspectives for the future. *Global Ecology and Conservation*, *15*, e00419. <https://doi.org/10.1016/j.gecco.2018.e00419>
- Liu, Y., Yu, G., Wang, Q., & Zhang, Y. (2014). How temperature, precipitation and stand age control the biomass carbon density of global mature forests. *Global Ecology and Biogeography*, *23*(3), 323–333. <https://doi.org/10.1111/geb.12113>
- Lüdecke, D. (2020). *sjPlot: Data Visualization for Statistics in Social Science*. <https://doi.org/10.5281/zenodo.1308157>
- Madsen, C., Potvin, C., Hall, J., Sinacore, K., Turner, B. L., & Schnabel, F. (2020). Coarse root architecture: Neighbourhood and abiotic environmental effects on five tropical tree species growing in mixtures and monocultures. *Forest Ecology and Management*, *460*(September 2019). <https://doi.org/10.1016/j.foreco.2019.117851>
- Meier, I. C., & Leuschner, C. (2008). Belowground drought response of European beech: Fine root biomass and carbon partitioning in 14 mature stands across a precipitation gradient. *Global Change Biology*, *14*(9), 2081–2095. <https://doi.org/10.1111/j.1365-2486.2008.01634.x>
- Paquette, A., & Messier, C. (2011). The effect of biodiversity on tree productivity: From temperate to boreal forests. *Global Ecology and Biogeography*, *20*(1), 170–180. <https://doi.org/10.1111/j.1466-8238.2010.00592.x>
- Perles-Garcia, M. D., Kunz, M., Fichtner, A., Meyer, N., Härdtle, W., & von Oheimb, G. (2022). Neighbourhood Species Richness Reduces Crown Asymmetry of Subtropical Trees in Sloping Terrain. *Remote Sensing*, *14*(6), 1441. <https://doi.org/10.3390/rs14061441>
- Piotto, D. (2008). A meta-analysis comparing tree growth in monocultures and mixed plantations. *Forest Ecology and Management*, *255*(3–4), 781–786. <https://doi.org/10.1016/j.foreco.2007.09.065>

- Pregitzer, K. S., DeForest, J. L., Burton, A. J., Allen, M. F., Ruess, R. W., & Hendrick, R. L. (2002). Fine Root Architecture of Nine North American Trees. *Ecological Monographs*, *72*(2), 293. <https://doi.org/10.2307/3100029>
- Qi, Y., Wei, W., Chen, C., & Chen, L. (2019). Plant root-shoot biomass allocation over diverse biomes: A global synthesis. *Global Ecology and Conservation*, *18*(18), e00606. <https://doi.org/10.1016/j.gecco.2019.e00606>
- R Core Team. (2018). *R: A Language and Environment for Statistical Computing*. <https://www.r-project.org/>
- Ravenek, J. M., Bessler, H., Engels, C., Scherer-Lorenzen, M., Gessler, A., Gockele, A., de Luca, E., Temperton, V. M., Ebeling, A., Roscher, C., Schmid, B., Weisser, W. W., Wirth, C., De Kroon, H., Weigelt, A., & Liesje, M. J. (2014). Long-term study of root biomass in a biodiversity experiment reveals shifts in diversity effects over time. *Oikos*, *123*(12), 1528–1536. <https://doi.org/10.1111/oik.01502>
- Shi, J., Yu, S., Yu, L., Han, Y., Wang, Z., & Guo, D. (2006). Application of minirhizotron in fine root studies. In *Chinese Journal of Applied Ecology* (Vol. 17, Issue 4, pp. 715–719).
- Singnar, P., Sileshi, G. W., Nath, A., Nath, A. J., & Das, A. K. (2021). Modelling the scaling of belowground biomass with aboveground biomass in tropical bamboos. *Trees, Forests and People*, *3*(August 2020). <https://doi.org/10.1016/j.tfp.2020.100054>
- Steele, S. J., Gower, S. T., Vogel, J. G., & Norman, J. M. (1997). Root mass, net primary production and turnover in aspen, jack pine and black spruce forests in Saskatchewan and Manitoba, Canada. *Tree Physiology*, *17*(8–9), 577–587. <https://doi.org/10.1093/treephys/17.8-9.577>
- Trubat, R., Cortina, J., & Vilagrosa, A. (2011). Nutrient deprivation improves field performance of woody seedlings in a degraded semi-arid shrubland. *Ecological Engineering*, *37*(8), 1164–1173. <https://doi.org/10.1016/j.ecoleng.2011.02.015>
- Van de Peer, T., Verheyen, K., Kint, V., Van Cleemput, E., & Muys, B. (2017). Plasticity of tree architecture through interspecific and intraspecific competition in a young experimental plantation. *Forest Ecology and Management*, *385*, 1–9. <https://doi.org/10.1016/j.foreco.2016.11.015>
- van der Plas, F. (2019). Biodiversity and ecosystem functioning in naturally assembled communities. *Biological Reviews*, *94*(4), 1220–1245. <https://doi.org/10.1111/brv.12499>
- Weiner, J. (2004). Allocation, plasticity and allometry in plants. *Perspectives in Plant Ecology, Evolution and Systematics*, *6*(4), 207–215. <https://doi.org/10.1078/1433-8319-00083>
- Wells, C. E., & Eissenstat, D. M. (2001). Marked differences in survivorship among apple roots of different diameters. *Ecology*, *82*(3), 882–892. [https://doi.org/10.1890/0012-9658\(2001\)082\[0882:MDISAA\]2.0.CO;2](https://doi.org/10.1890/0012-9658(2001)082[0882:MDISAA]2.0.CO;2)
- Williams, L. J., Butler, E. E., Cavender-Bares, J., Stefanski, A., Rice, K. E., Messier, C., Paquette, A., & Reich, P. B. (2021). Enhanced light interception and light use efficiency explain overyielding in young tree communities. *Ecology Letters*, *24*(5), 996–1006. <https://doi.org/10.1111/ele.13717>
- Williams, L. J., Paquette, A., Cavender-Bares, J., Messier, C., & Reich, P. B. (2017). Spatial complementarity in tree crowns explains overyielding in species mixtures. *Methods in Ecology and Evolution*, *1*(February). <https://doi.org/10.1038/s41559-016-0063>
- Wright, S. J. (2019). Plant responses to nutrient addition experiments conducted in tropical forests. *Ecological Monographs*, *89*(4), 1–18. <https://doi.org/10.1002/ecm.1382>
- Yang, X., Bauhus, J., Both, S., Fang, T., Härdtle, W., Kröber, W., Ma, K., Nadrowski, K., Pei, K., Scherer-Lorenzen, M., Scholten, T., Seidler, G., Schmid, B., von Oheimb, G., & Bruelheide, H. (2013). Establishment success in a forest biodiversity and ecosystem functioning experiment in subtropical China (BEF-China). *European Journal of Forest Research*, *132*(4), 593–606. <https://doi.org/10.1007/s10342-013-0696-z>
- Yang, X. zhou, Zhang, W. hui, & He, Q. yue. (2019). Effects of intraspecific competition on growth, architecture and biomass allocation of *Quercus Liaotungensis*. *Journal of Plant Interactions*, *14*(1), 284–294. <https://doi.org/10.1080/17429145.2019.1629656>

Zuur, A. F., Ieno, E. N., Walker, N. S., & Smith, G. M. (2009). Mixed Effects Models and Extensions in Ecology with R. In *Smart Society: A Sociological Perspective on Smart Living*. <https://doi.org/10.4324/9780429201271-2>

Synthesis

Main findings

Subtropical forests are a biodiversity hotspot, and their structure affects ecosystem services. To enhance these ecosystem services in afforestation and reforestation projects, it is important to understand how the choice of tree species affects spatial conditions over time. Despite the importance of these ecosystems, scarce studies have analysed in detail the effect of tree richness on the structure in an accurate and detailed way. In this thesis, I have aimed to deepen the understanding of the mechanisms by which tree diversity in stands affects tree structure per se. Here, I summarize the main findings of the different chapters of this dissertation and illustrate them in Figure 1.

In Chapter I me and my colleagues demonstrate that tree species richness have a positive effect on stand structural complexity, and that this effect became stronger over time. We found consistency across species, that is, none of the species show higher structural complexity in monocultures compare to species mixtures. Importantly, we analyse which element was promoting the increase on complexity, and in this early stage of the development we found that species richness promoted structural complexity via fostering vertical heterogeneity, but did not affect density of structural elements.

In Chapter II, we show that the extension of crown asymmetry was a response of neighbourhood species richness, neighbourhood pressure, tree height and slope inclination. We found that, after the height of the tree itself, neighbour pressure was the strongest predictor of crown asymmetry. This pressure did not show dependence on species richness. However, we showed that high values of species richness were able to reduce asymmetry, and that this effect was stronger on steep slopes. Thus, we found a reduction of up to 33% of crown asymmetry in trees growing on steep slopes but at high levels of species richness compared to monocultures. In addition, we developed a new index to measure the neighbouring force exerted on the tree crown taking into account differences in crown height that may occur due to differences in size between trees or their relative position on the slope.

In Chapter III, we found no evidence that functional dissimilarity resulted in greater tree crown complementarity of tree species pairs. Functional dissimilarity was related to the outer canopy phenotypic plasticity. However, we could explain 70% of the variation of crown complementarity by adding to the model branch trait dissimilarities (branch density and

branch intensity) and their interaction with functional dissimilarity. Therefore, we saw that in order to understand the complementarity of these trees it was necessary to pay attention not only to the outer crown plasticity but also to the inner crown structure.

In Chapter IV, we found differences in biomass allocation patterns above- and belowground between mono- and heterospecific tree species pairs at different stages of their development. We found a greater investment in root biomass in the heterospecific pairs during the early stages of development, but saw this trend change over the years because of a greater aboveground biomass growth compared to the monospecific pairs. We assume that monospecific competition would lead to higher root biomass allocation the roots in response to competition for resources.

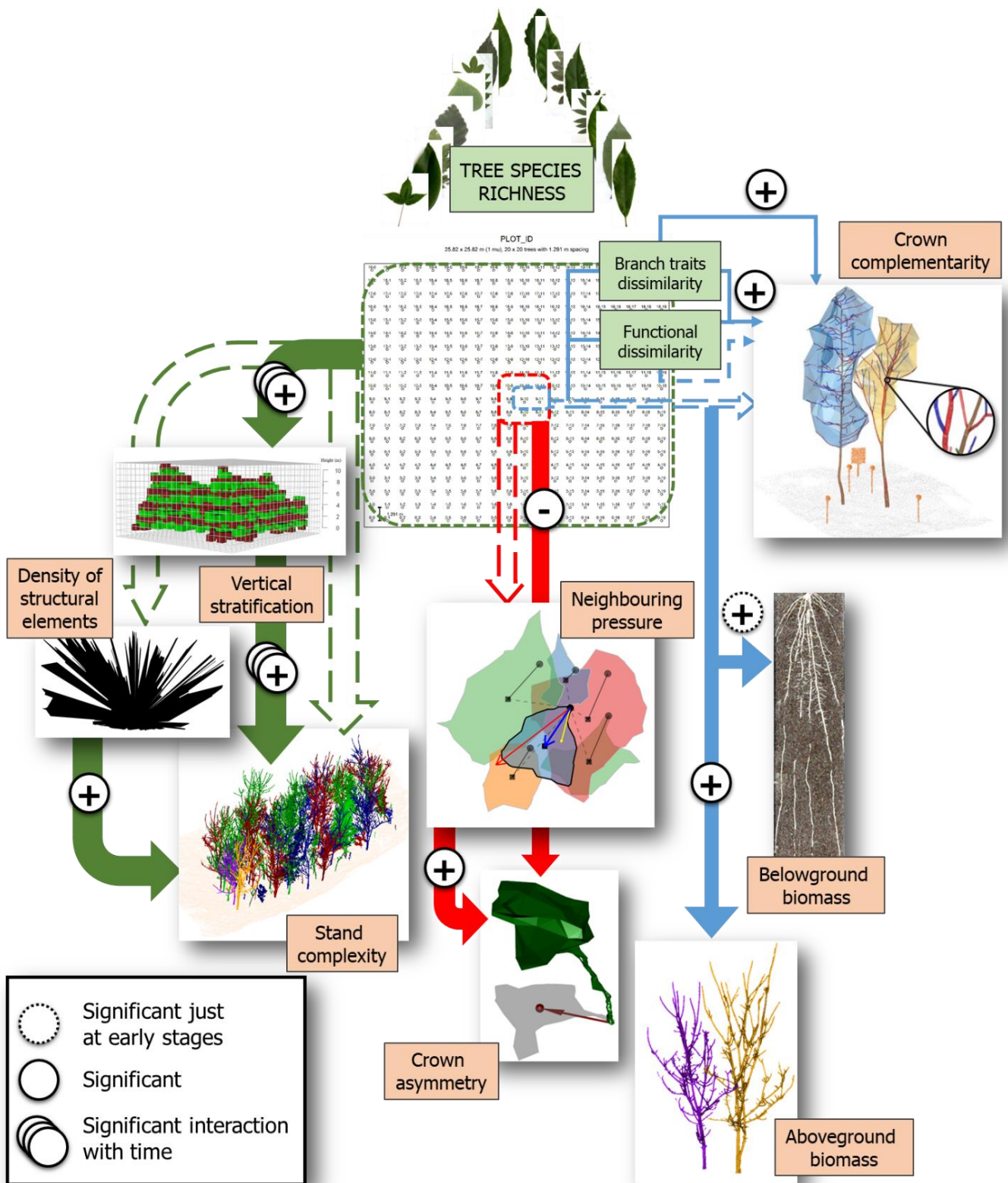


Figure 1. Conceptual figure adapted from Fig. 5: Main findings. Relations between tree species richness (TSR) on different structural parameters. Green arrows represent the path between TSR and structure complexity (vertical stratification and density of structural elements, Chapter I); red arrows represent the path way between TSR, neighbourhood pressure and crown asymmetry (Chapter II); blue arrows represent the path way between TSR and crown complementarity (Chapter III), and above- and belowground biomass (Chapter IV). Solid arrows represent significant relationships, + and - indicate the direction of the effect.

Discussion

Potential drivers of complexity on forest structure

The complexity of a forest can be defined by many attributes that also include understory vegetation or dead wood (McElhinny et al., 2005). However, most studies use measures of tree size variation as a measure of stand structural complexity (Ali, 2019). Tree cover is the defining component of a forest, and is the fundamental element that defines its spatial structure. Conversely, the tree is able to adapt to the forest, being the forest capable of modifying the structure of the tree. Thus, in this dissertation, I have analysed how the trees, in particular the tree species richness, affects the complexity of a forest and how the forest shapes the structure of an individual tree.

When we measured structural complexity in Chapter 1, we compared an index that quantified 3D structural complexity (SSCI) with different indices based on tree size variability: the standard deviation, the coefficient of variation and the Gini coefficient of both tree height and tree diameter. The advantage of the SSCI is that it gives a 3D view of the space and is not based solely on the size distribution of trees. In fact, although the finding that tree species richness enhanced structural complexity was consistent across indices, we observed that results in the inventory-based indices were an effect of species identity, while this relationship was not evident for the SSCI, which in turn was not correlated with the inventory indices. Of course, differences in growth rates between species in an even-aged stand would increase vertical stratification (Laurans et al., 2014), which would be reflected in both inventory-based indices and ENL. But by measuring the structural complexity of space per se, the SSCI was able to register elements that were not only related to the height or diameter of the trees.

ENL increases when the layers are more evenly distributed. This may seem counter-intuitive, as one would expect greater heterogeneity when the difference between layers is higher. However, a high ENL indicates the presence of tree crowns in multiple layers, suggesting higher stratification and canopy packing (Ehbrecht, 2018). In the same way, MeanFrac becomes larger the more structural elements are present. Here, we do not consider the tree as a unit per se, but its traits: We are measuring 3D space with millimetre accuracy, thus the presence of branches of different orders will influence the space occupation. We can therefore assume that the higher the number and density of branches, the greater the ENL and MeanFrac. This also relates to Chapter 3, where we saw that greater dissimilarity in branch density and branching intensity between neighbouring trees presented greater crown

complementarity, and therefore, higher canopy packing. This is in agreement with Seidel et al. (2018), who suggest that branching patterns with a “space-filling character” promoted structural complexity.

We can therefore argue that crown complementarity between trees will positively affect stand structural complexity by achieving greater canopy packing at different vertical layers. We hypothesise that tree species richness has a positive effect in this regard due to niche differentiation between species. Species richness allows for variation in functional traits, for example, it is more likely that trees have different growth rates when we pool many species together. Different tree species have different requirements for light, which is a limiting resource in the canopy (Williams et al., 2021), and therefore may occupy more canopy layers. We were able to observe this in Chapter 2, where we found that as tree species richness increased, crown asymmetry decreased, probably due to different light requirements among species, which allow branches of certain species to grow in the understory without the need to displace their crowns.

Canopy gaps are an important part of the structure of a forest. They can promote multiple ecosystem services, as wild edible plants (Felipe-Lucia et al., 2018) or habitat diversity (Muscolo et al., 2014). They are usually generated by tree mortality. Ehbrecht et al. (2017) mentioned that canopy gaps cause a decrease of MeanFrac because of a decrease of the perimeter in relation with the area. Thus, when studying certain ecosystem function relationships in which canopy gaps play a role, it is important to consider them besides the SSCI results. However, we did not find dependencies of tree mortality on stand structural complexity ($p = 0.29$, Chapter I). The high planting density could be responsible for the absence of canopy gaps even with a relatively high rate of tree mortality. On the other side, we also analysed how tree interactions were able to modify tree architecture. Neighbourhood pressure was the main external driver of crown asymmetry (Chapter 2), and it is reasonable to assume that without this pressure the canopy could spread in all directions covering the gap. In addition, mortality could have favoured vertical stratification, allowing light penetration to lower layers of the forest. And with less competition for belowground resources, more investment could be devoted to aboveground growth (Chapter 4). Thus, we conclude that at this early stage of development of such a densely planted forest, mortality may not have generated canopy gaps, but in the future, it will be necessary to study them separately.

And how has this structural complexity affected tree architecture? Complexifying it: We observed greater investment in aboveground biomass by heterospecific pairs compared to

monospecific (Chapter 4), which could be related to the higher density and intensity of branches in heterospecific pairs observed in Chapter 3. This density appears to be more focused in a single direction in the case of strong neighbour pressure (Chapter 2), but we believe that as neighbour species richness increases, more branches could be spread along the vertical gradient. Thus, we hypothesize that, while trees growing in monospecific environments slow down their growth to invest more in root growth (Chapter 4), perhaps because of nutrient limitation belowground, trees growing in mixtures allocate more biomass to branches. Differences in traits play an important role here. In Chapter 3 we observed how dissimilarities in functional traits were able to explain 70% of the variation in crown complementarity. We find no evidence that dissimilarity in the plasticity of the outer crown structure promotes crown complementarity, but rather that its interaction with dissimilarity in branch traits does.

Trait dissimilarity allows niche differentiation (Wagg et al., 2017). As we already mentioned, differences in shade-tolerance or growth rates can influence vertical stratification and improve canopy packing. Plasticity of the outer crown would allow some species to grow in the direction of the gaps, affecting horizontal stratification. But there are many traits that influence crown complementarity, and with that, canopy packing. When planning a mix plantation, differences in traits between the chosen species should be considered with the main goals of the plantation in mind.

Forest structure and ecosystem functioning

The spatial structure of a forest is dynamic. It varies as the trees grow and even has seasonal changes. The architecture of the forest can be scaled from the branch networks of its trees (West et al., 2009). The heterogeneity of forest architecture has been identified as one of the attributes with a positive effect on ecosystem services (Felipe-Lucia et al., 2018). Thus, in this dissertation I have discussed how tree species richness affects ecosystem functioning by modifying tree structure and, with that, forest architecture.

The structure of the tree is the physical basis of the forest. Trees face many disturbances that can affect their stability. Schnabel et al. (2021) found that tree species richness stabilised forest productivity in the face of drought events. The studies provided by this dissertation emphasise how tree species richness positively affects the mechanical stability of the forest: On the one hand, we found evidence of higher root biomass production in the first year of growth in trees grown with heterospecific neighbours (Chapter 4). Higher root biomass has been associated with greater wind stability (Odrík & Odrík, 2002), resistance to

fires (Azevedo et al., 2013) and greater mechanical stability on slopes (Reubens et al., 2007). In our case, we also found that trees growing in mixtures showed less crown displacement when growing on slopes (Chapter 2). Planting on slopes will contribute to the reduction of erosion, and provides ecosystem services without conflicting with land that could be used for agriculture. Reducing crown asymmetry on slopes reduces the risk of stem breakage and increases forest stability.

Mixtures will also be more stable against plagues and diseases. Saadani et al. (2021) found less foliar fungal infestation on trees with high local tree diversity. Beugnon et al. (2021) observed a positive effect of tree species richness on soil microbial biomass and diversity. Albert et al. (2022) showed in a simulation experiment that herbivory can reduce productivity in monocultures, but this effect is compensated in mixtures due to competing species with resource use complementarity. Schuldt et al. (2019) found that the structural diversity of forests was positively correlated with species richness of forest arthropods. Different structural elements will provide habitats for species with different requirements. In turn, connectivity between branches avoids habitat fragmentation. Predation rates would also be affected by this connectivity and by forest gaps that allow visibility.

The effect of tree species richness also transcends the environmental conditions of the forest. Tree cover has the ability to regulate the microclimate, and tree diversity has been shown to be able to decrease fluctuations and stabilise the microclimate (Gottschall et al., 2019). Beugnon et al. (2022) found that vertical stratification measured with the TLS-based index ENL was negatively related with air temperature. Tree species richness promoted ENL, so we will find fewer heat peaks in mixtures. This is especially relevant with the current climate crisis.

The vertical stratification is produced by a greater presence of branches along the different vertical layers. Higher ENL in mixtures (Chapter 1) and higher density and intensity of branches (Chapter 3) lead to canopy complementarity which in turns will allow greater canopy packing. This effect is the result of increasing carbon sequestration, and with it, higher productivity. Overyielding in mixtures has prompted several interest on outer crown complementarity and niche differentiation (Williams et al., 2017). Liu et al. (2018) found higher carbon stocks and fluxes in species rich stands compare to low-richness. Davrinche et al. (2021) found a shift to a more acquisitive growth strategy in trees growing in mixtures. Schnabel et al. (2019) also report overyielding in mixtures compared to monocultures, and this overyielding was even more noticeable in situations of resource scarcity, in this case due to drought. However, little attention has been paid to inner crown structure and

belowground biomass, which are covered in chapters 3 and 4 of this dissertation. Here we found how shifts in biomass allocation patterns could explainoveryielding: on the one hand, differences in branch traits promoted crown complementarity, and with that, canopy packing (Chapter 3). On the other hand, the higher investment in belowground biomass after a few years of growth with monospecific neighbours decelerated tree growth in monocultures. Therefore, the mixtures will also benefit from increased productivity with all the benefits that this entails.

We would like to conclude by mentioning the finding of Chapter 1 about the fact that tree species richness promotes structural complexity. Because to promote complexity is to promote stability, and with that, ecosystem services.

Limitations

It is worth noting that my dissertation focuses only on the subtropical biome. This biome is characterised by a very high species richness, and subtropical tree species have the capacity to accumulate greater biomass in their canopies (Keeling & Phillips, 2007). To extrapolate the conclusions of my dissertation to other regions it would be necessary to study the specific characteristics, as the positive relationship with the number of tree species could saturate in other biomes.

In addition, this dissertation has analysed a biodiversity experiment. In this experiment, the loss of biodiversity is simulated with random extinction scenarios, and the system is simplified and does not allow the emergence of other species via weeding, which is in contradiction with natural forests (van der Plas, 2019). Moreover, the BEF experiments with trees are still very young, the first one was planted in 1999 (Paquette et al., 2018), so they have not yet reached forest maturity. It would be necessary to go to mature natural forests to understand how these relationships between tree species richness, ecosystem structure and functioning evolve naturally over time.

Future implications

The conclusions of this dissertation can be used in afforestation and reforestation projects in subtropical areas. In the face of the current climate crisis, it is essential to promote plantations that can sequester carbon and withstand the extreme weather events that we are seeing with ever-increasing frequency. Here we provide evidence of how including a large pool of tree species can favour ecosystem functioning at an early stage, particularly on slope terrains. Thus, the inclusion of large numbers of species, or the planting of species

with diversity in their direct neighbours, will enhance forest complexity, tree stability, complementarity and productivity, which can lead to improvements in the provision of ecosystem services. These improvements have even been seen in an even-age plantation planted on a regular grid.

References

- Albert, G., Gauzens, B., Loreau, M., Wang, S., & Brose, U. (2022). The hidden role of multi-trophic interactions in driving diversity–productivity relationships. *Ecology Letters*, *25*(2), 405–415. <https://doi.org/10.1111/ele.13935>
- Ali, A. (2019). Forest stand structure and functioning: Current knowledge and future challenges. *Ecological Indicators*, *98*(January), 665–677. <https://doi.org/10.1016/j.ecolind.2018.11.017>
- Azevedo, J. C., Possacos, A., Aguiar, C. F., Amado, A., Miguel, L., Dias, R., Loureiro, C., & Fernandes, P. M. (2013). The role of holm oak edges in the control of disturbance and conservation of plant diversity in fire-prone landscapes. *Forest Ecology and Management*, *297*, 37–48. <https://doi.org/10.1016/j.foreco.2013.02.007>
- Beugnon, R., Bu, W., Bruelheide, H., Davrinche, A., Du, J., Haider, S., Kunz, M., von Oheimb, G., Perles-Garcia, M. D., Saadani, M., Scholten, T., Seitz, S., Singavarapu, B., Trogisch, S., Wang, Y., Wubet, T., Xue, K., Yang, B., Cesarz, S., & Eisenhauer, N. (2022). Abiotic and biotic drivers of scale-dependent tree trait effects on soil microbial biomass and soil carbon concentration. *Manuscript Submitted for Publication*.
- Beugnon, R., Du, J., Cesarz, S., Jurburg, S. D., Pang, Z., Singavarapu, B., Wubet, T., Xue, K., Wang, Y., & Eisenhauer, N. (2021). Tree diversity and soil chemical properties drive the linkages between soil microbial community and ecosystem functioning. *ISME Communications*, *July*. <https://doi.org/10.1038/s43705-021-00040-0>
- Davrinche, A., & Haider, S. (2021). *Intra-specific leaf trait responses to species richness at two different local scales*. *55*, 20–32. <https://doi.org/https://doi.org/10.1016/j.baae.2021.04.011>
- Ehbrecht, M. (2018). *Quantifying three-dimensional stand structure and its relationship with forest management and microclimate in temperate forest ecosystems*. Georg-August-Universität Göttingen.
- Ehbrecht, M., Schall, P., Ammer, C., & Seidel, D. (2017). Quantifying stand structural complexity and its relationship with forest management, tree species diversity and microclimate. *Agricultural and Forest Meteorology*, *242*(April), 1–9. <https://doi.org/10.1016/j.agrformet.2017.04.012>
- Felipe-Lucia, M. R., Soliveres, S., Penone, C., Manning, P., van der Plas, F., Boch, S., Prati, D., Ammer, C., Schall, P., Gossner, M. M., Bauhus, J., Buscot, F., Blaser, S., Blüthgen, N., de Frutos, A., Ehbrecht, M., Frank, K., Goldmann, K., Hänsel, F., ... Allan, E. (2018). Multiple forest attributes underpin the supply of multiple ecosystem services. *Nature Communications*, *9*(1), 4839. <https://doi.org/10.1038/s41467-018-07082-4>
- Gottschall, F., Cesarz, S., Davids, S., Dous, T. E. N., Auge, H., & Eisenhauer, N. (2019). Tree species identity determines wood decomposition via microclimatic effects. *Ecology and Evolution*, *9*, 12113–12127. <https://doi.org/10.1002/ece3.5665>
- Keeling, H. C., & Phillips, O. L. (2007). The global relationship between forest productivity and biomass. *Global Ecology and Biogeography*, *16*, 618–631. <https://doi.org/10.1111/j.1466-8238.2007.00314.x>
- Laurans, M., Hérault, B., Vieilledent, G., & Vincent, G. (2014). Vertical stratification reduces competition for light in dense tropical forests. *Forest Ecology and Management*, *329*, 79–88. <https://doi.org/10.1016/j.foreco.2014.05.059>

- Liu, X., Trogisch, S., He, J. S., Niklaus, P. A., Bruelheide, H., Tang, Z., Erfmeier, A., Scherer-Lorenzen, M., Pietsch, K. A., Yang, B., Kühn, P., Scholten, T., Huang, Y., Wang, C., Staab, M., Leppert, K. N., Wirth, C., Schmid, B., & Ma, K. (2018). Tree species richness increases ecosystem carbon storage in subtropical forests. *Proceedings of the Royal Society B: Biological Sciences*, *285*(1885). <https://doi.org/10.1098/rspb.2018.1240>
- McElhinny, C., Gibbons, P., Brack, C., & Bauhus, J. (2005). Forest and woodland stand structural complexity: Its definition and measurement. *Forest Ecology and Management*, *218*(1–3), 1–24. <https://doi.org/10.1016/j.foreco.2005.08.034>
- Muscolo, A., Bagnato, S., Sidari, M., & Mercurio, R. (2014). A review of the roles of forest canopy gaps. *Journal of Forestry Research*, *25*(4), 725–736. <https://doi.org/10.1007/s11676-014-0521-7>
- Odrík, J. K., & Odrík, M. K. (2002). *Root biomass of beech as a factor influencing the wind tree stability*. *2002*(12), 549–564.
- Paquette, A., Hector, A., Vanhellefont, M., Koricheva, J., Scherer-Lorenzen, M., Verheyen, K., Abdala-Roberts, L., Auge, H., Barsoum, N., Bauhus, J., Baum, C., Bruelheide, H., Castagneyrol, B., Cavender-Bares, J., Eisenhauer, N., Ferlian, O., Ganade, G., Godbold, D., Gravel, D., ... Zemp, D. C. (2018). A million and more trees for science. *Nature Ecology and Evolution*, *2*(5), 763–766. <https://doi.org/10.1038/s41559-018-0544-0>
- Reubens, B., Poesen, J., Danjon, F., Geudens, G., & Muys, B. (2007). The role of fine and coarse roots in shallow slope stability and soil erosion control with a focus on root system architecture: a review. *Trees*, *21*(4), 385–402. <https://doi.org/10.1007/s00468-007-0132-4>
- Saadani, M., Hönig, L., Bien, S., Koehler, M., Rutten, G., Wubet, T., Braun, U., & Bruelheide, H. (2021). Local tree diversity suppresses foliar fungal infestation and decreases morphological but not molecular richness in a young subtropical forest. *Journal of Fungi*, *7*(3), 1–18. <https://doi.org/10.3390/jof7030173>
- Schnabel, F., Liu, X., Kunz, M., Barry, K. E., Bongers, F. J., Bruelheide, H., Fichtner, A., Härdtle, W., Li, S., Pfaff, C., Schmid, B., Schwarz, J. A., Tang, Z., Yang, B., & Bauhus, J. (2021). Species richness stabilizes productivity via asynchrony and drought-tolerance diversity in a large-scale tree biodiversity experiment. *Science Advances*, *7*(51), 11–13. <https://doi.org/10.1126/sciadv.abk1643>
- Schnabel, F., Schwarz, J. A., Dănescu, A., Fichtner, A., Nock, C. A., Bauhus, J., & Potvin, C. (2019). Drivers of productivity and its temporal stability in a tropical tree diversity experiment. *Global Change Biology*, *May*, 1–16. <https://doi.org/10.1111/gcb.14792>
- Schuldt, A., Ebeling, A., Kunz, M., Staab, M., Guimarães-Steinicke, C., Bachmann, D., Buchmann, N., Durka, W., Fichtner, A., Fornoff, F., Härdtle, W., Hertzog, L. R., Klein, A. M., Roscher, C., Schaller, J., von Oheimb, G., Weigelt, A., Weisser, W., Wirth, C., ... Eisenhauer, N. (2019). Multiple plant diversity components drive consumer communities across ecosystems. *Nature Communications*, *10*(1). <https://doi.org/10.1038/s41467-019-09448-8>
- Seidel, D. (2018). A holistic approach to determine tree structural complexity based on laser scanning data and fractal analysis. *Ecology and Evolution*, *8*(1), 128–134. <https://doi.org/10.1002/ece3.3661>
- van der Plas, F. (2019). Biodiversity and ecosystem functioning in naturally assembled communities. *Biological Reviews*, *94*(4), 1220–1245. <https://doi.org/10.1111/brv.12499>

- Wagg, C., Ebeling, A., Roscher, C., Ravenek, J., Bachmann, D., Eisenhauer, N., Mommer, L., Buchmann, N., Hillebrand, H., Schmid, B., & Weisser, W. W. (2017). Functional trait dissimilarity drives both species complementarity and competitive disparity. *Functional Ecology*, *31*(12), 2320–2329. <https://doi.org/10.1111/1365-2435.12945>
- West, G. B., Enquist, B. J., & Brown, J. H. (2009). *A general quantitative theory of forest structure and dynamics*. <https://doi.org/10.1073/pnas.0812294106>
- Williams, L. J., Butler, E. E., Cavender-Bares, J., Stefanski, A., Rice, K. E., Messier, C., Paquette, A., & Reich, P. B. (2021). Enhanced light interception and light use efficiency explain overyielding in young tree communities. *Ecology Letters*, *24*(5), 996–1006. <https://doi.org/10.1111/ele.13717>
- Williams, L. J., Paquette, A., Cavender-Bares, J., Messier, C., & Reich, P. B. (2017). Spatial complementarity in tree crowns explains overyielding in species mixtures. *Methods in Ecology and Evolution*, *1*(February). <https://doi.org/10.1038/s41559-016-0063>

Acknowledgements

Such a journey, and so many people involved in it that I don't even know where to start.

First of all, I would like to thank the International Research Training Group TreeDì jointly funded by the Deutsche Forschungsgemeinschaft (DFG, German Research Foundation) - 319936945/GRK2324 and the University of Chinese Academy of Sciences (UCAS). Andrea, Florian, Perttu, Mariem, Gonzalo, Bala, Remy, Georg, and Hanjiao, it was nice to start this adventure with you. Also, it has been very exciting to coincide with the new cohort. Tama, I know you will achieve great results and I look forward to supporting you.

Of course I want to thank Goddert von Oheimb for his supervision. Thank you for the freedom and for the advice, for the long discussions and for letting me choose my path but giving me realistic feedback when needed. I don't know what I would have done in the early stages without all the help with TLS from Matthias Kunz. Thank you for the quick feedback and for always sharing your expertise. And from a distance, many thanks to Werner Härdtle and Andreas Fichtner, I have learned a lot from working with you.

Thanks to all the people at Tharandt who have helped me with their advice and to those who have collaborated in processing the data: Norman, Inga, Nora, Louis, Friedrich, Alexandra, and of course Michaela who accompanied me all the way to China. Unfortunately I couldn't come back, but I have very good memories and I want to thank all the people involved on my trip to the BEF China platform: Thanks to the greatest student helper Georg, and to the local workers, especially Mr. Wang, without your help I wouldn't have collected half of the data. And thanks to Yang Bo and Yuxi Xue for helping me in the organisation and answering all my questions, and to Xiaojuan Liu and Wensheng Bu for their collaboration.

Thanks to Stefan Trogisch and to Diana Zellinger for her patience with all the administrative procedures, which have not been few. Stefan, we couldn't imagine a better coordinator than you. And many thanks to the people at iDiv, to everyone with whom I have shared an office (which were quite a few), to the IT support (especially Lucien who has been very patient with my computer) and to Laura Mendez for her support and being my link to other working groups. Thanks to the Eisenhauer lab for lending me another scanner and letting me do tests in MyDiv. Alban and Julius, thanks for organizing it.

And to thank my friends and family, I will switch to my mother tongue:

Gracias a mis amigas y amigos por recordarme que la vida no es solo esto. Muchas gracias a todas las personas que me habéis escuchado alguna vez decir que trabajo con arbolitos y pretendo demostrar que la biodiversidad mola. Me voy a dejar a gente, pero lo voy a intentar:

Gracias a Paula, Clara y Paloma, mis chicas de Alicante, por siempre estar dispuestas a ofrecer un poco de paz mental. A mis compis de ambientales, Pau, Font, Ana R, Vicen, Ana T y Marta, y de aquella casa en el Albayzín, Álvaro, Sara, Tamayo, siento que en el fondo empecé todo esto estudiando y debatiendo con vosotros. A mis compañeros de FIT, especialmente a Sergio, que si me canso de esto de la investigación sé que puedo consultarle, y Rodrigo, que me mandó la oferta de TreeDì y me metió aquí.

A Dani que me convenció de ir a China por primera vez. A Mati, Marta, Sete, Sandra, qué bonito es estar rodeada de mujeres empoderadas. A Daniela, Pilar, Laura, Eli y Tamara, con vosotras descubrí que en Alemania no se estaba tan mal. A la gente de IU Exterior, en especial a Jaime y sus gatos por el espacio de paz que me ofrecieron para terminar el cuarto capítulo. A club mate por las noches de productividad. A quienes me acogieron en Madrid, Javi, gracias por ser mi enciclopedia particular. A la trieja y la Burbuja, que en estos últimos meses me han metido en retos que me han hecho un poco más difícil terminar, pero a la vez hacen que la vida tenga más sentido. Raquel, gracias por acogerme cuando me ha hecho falta, para mi estar contigo es estar en casa, espero colaborar algún día contigo y animar arbolitos 3D. María, gracias de corazón por aguantar mis audios interminables y por hacer reales todas las aventuras que se nos han pasado por la cabeza. Funcionará.

Mucha es la gente que me ha demostrado que Leipzig es un lugar en el que merece la pena vivir. Gracias a mis traductoras favoritas, Claudia, Naty, Antia, Celtia, por vuestro apoyo y vuestra ayuda. A Adrià que me acogió durante la pandemia. A Gregorio y a Sebas por hacer que valga la pena cruzar la ciudad. Y a toda esa gente que en algún momento fue casa. A Anco, Linda, Kuheli y Nutella con las que empecé a formar hogar. Gracias en especial a toda la gente que ha pasado por la Burbuja en el último año, que no es poca. A P. Ost y les Colegues. A Carmen por conseguir mantener el orden en estos meses de ausencia. A Pablo por lo bonito que ha sido vivir juntos este año, el lockdown hubiese sido mucho más oscuro sin ti. A mis vecinos, Nacho, Claudia y Zambra, por dejarme un lugar de calma casi sin salir de casa. A Sara, Mario, Pabel, Jesus, Safa, Karen, Emyd, Luis... Vosotros ya sabeis porqué.

Y a mi familia. Por estar ahí y apoyarme siempre. Sobretudo quiero agradecer a mi madre y a mi abuela, no solo por su apoyo sino también por su ejemplo: Porque estoy tan orgullosa de vosotras que mi gran motivación para terminar esto ha sido que estéis orgullosas de mí.

Supporting information

Chapter 1. Tree species richness promotes an early increase of stand structural complexity in young subtropical plantations

Table of contents

Supporting Methods

- 1. Study plots and experimental design**
- 2. Test for dependency of SSCI values on scanner position and leaf conditions**
- 3. Calculation and slope correction for the ENL**

Supporting Tables

- **Table S1.** Included plots and their characteristics.
- **Table S2.** Names and characteristics of the 16 tree species used in the analysis to test species identity effects on SSCI.
- **Table S3.** Results of the mixed-effects models of a subsample of 30 plots.
- **Table S4.** Results of the mixed-effects models for the effect of tree species richness (TSR), year and their interactions on inventory-based stand structural complexity indices
- **Table S5.** Analysis 1 to test for possible effects of different positions within a plot.
- **Table S6.** Analysis 2: Linear mixed-effects models fitted by REML to analyse the possible effects of leaf-off and leaf-on conditions on SSCI.

Supporting Figures

- **Figure S1.** Examples of cross-sections for the calculation of MeanFrac.
- **Figure S2.** Slope correction for ENL to aligns layers parallel to the ground surface.
- **Figure S3.** Random factors of the linear mix-effects model for SSCI.
- **Figure S4.** Temporal changes in the relationship between tree species richness and different components of stand structural for a subsample of 30 plots.
- **Figure S5.** Temporal changes in the relationship between tree species richness and different inventory-based stand structural complexity indices.
- **Figure S6.** Correlation matrix between stand structural complexity indices measured from 2012 to 2016.

Supporting Methods

Methods S1. Study plots and experimental design

In BEF-China, 40 native broad-leaved tree species were included in the entire species pool (Bruehlheide et al. 2014). To avoid the problem of increasing overlap of species compositions with increasing species richness, random extinction scenarios were used in which three (overlapping) pools of 16 tree species at each site were divided into non-overlapping communities at lower diversities. In addition, an extra-'high' richness level of 24 tree species was included, combining species from the different pools. A set of 32 very intensively studied plots (VIPs) and their replicates (VIPrep, all randomly distributed across the site) was built from one of the three pools of 16 tree species. Tree species composition of the mixtures was determined by randomly assigning (without replacement) each species of the 16-species mixtures to one 8-species mixture, subdividing these sets of 8 tree species to non-overlapping subsets of four species, and the 4-species subsets to non-overlapping 2-species mixtures. The 24-species mixtures were additionally included as an additional high diversity treatment. The total of the 64 plots (32 VIPs and 32 VIPreps) was thus composed of: 32 monocultures, 16 2-species mixtures, 8 4-species mixtures, 4 8-species mixtures, 2 16-species mixtures and 2 24-species mixtures.

Lack of or limited tree establishment (14 plots) and logistical constraints, in particular extremely dense evergreen monocultures (2 plots) and very steep slope inclination (3 plots), limited the set of plots to 45. Four plots were additionally selected to compensate for this, so that the final set of plots amounted to 49 (20 monocultures, 15 2-species mixtures, 6 4-species mixtures, 3 8-species mixtures, 3 16-species mixtures, and 2 24-species mixtures). Slope inclination of plots ranges between 10.5° and 44.8° (Table S1).

Methods S2. Test for dependency of SSCI values on scanner position and leaf conditions

In February-March 2019 we selected 15 plots in which we performed two additional scans from different positions within the plot. Furthermore, we made a single scan at the centre of these 15 plots during the vegetation period (end of April 2019). This was done in order to analyse possible dependence of the stand structural complexity index (SSCI) values on scanner positions or leaf-off / leaf-on conditions. However, no dependence of SSCI values on scanner positions was observed (Table S5), and the best fitting model regarding leaf

conditions was the additive one, indicating that differences in SSCI between leaf-off and leaf-on conditions were constant across all diversity levels (Table S6).

Methods S3. Calculation and slope correction for the ENL

To calculate the effective number of layers (ENL) each point cloud was voxelized. In mature temperate forests, Ehbrecht et al. (2017) used a voxel size of 20 cm and a slice thickness of 1 m. To better account for the young stand age and the size of the planted trees, we applied a voxel size of 5 cm and a slice thickness of 25 cm in our study.

The concept of ENL assumes that the layers are parallel to the ground (Ehbrecht et al., 2016). In sloping terrain, however, this assumption can lead to a bias in the total number of voxels per layer. To deal with this potential bias, we applied a slope correction (Fig. S2) which aligns the layers to be parallel to the local terrain slope. For each scan, we first extracted the ground points within a 3 m radius around the scanner. We then fitted a 3D plane to the ground points, using singular value decomposition with the scan centre at (0,0,0), and derived the surface normal vector of that plane. Finally, we rotated all points onto the normal vector (0,0,1) that is aligned with the vertical Z axis.

Finally, for each slice, represented as green and brown in Fig. S2, the proportion of filled voxels in relation to the total voxels of the slice was quantified, and the ENL was computed using the inverse Simpson-Index: $ENL = 1 / \sum_{i=1}^n p_i^2$, where n refers to the number of slices, calculated as $(\text{height}_{\text{max}} - \text{height}_{\text{min}}) / 25 \text{ cm}$; and p_i is the proportion of filled voxels of the i^{th} slice (Ehbrecht et al., 2016).

Supporting Tables

Table S1. Included plots and their characteristics. Species names follow nomenclature in "The Flora of China" (<http://flora.huh.harvard.edu/china>). An "x" indicates that the plot was scanned in the respective year.

Species Richness	Species	Plot ID	2012	2013	2014	2015	2016	2019	Slope (°)	Mean height (m)	Mortality rate (%)
Monoculture	<i>Castanea henryi</i>	E34	x	x	x	x	x	x	12.2	10.04	44
Monoculture	<i>Castanea henryi</i>	F34	x	x	x	x	x	x	36.0	5.54	25
Monoculture	<i>Castanopsis sclerophylla</i>	G17				x		x	32.5	1.17	25
Monoculture	<i>Castanopsis sclerophylla</i>	L11				x	x	x	30.9	2.17	6
Monoculture	<i>Choerospondias axillaris</i>	L23*	x	x	x	x	x	x	23.6	6.32	8
Monoculture	<i>Choerospondias axillaris</i>	O27*	x	x	x	x	x	x	26.0	9.46	25
Monoculture	<i>Cyclobalanopsis glauca</i>	R14				x		x	33.1	2.03	6
Monoculture	<i>Koelreuteria bipinnata</i>	Q13				x		x	33.4	2.41	33
Monoculture	<i>Liquidambar formosana</i>	E24		x	x	x	x	x	35.3	6.48	3
Monoculture	<i>Liquidambar formosana</i>	I28		x	x	x	x	x	25.7	3.32	0
Monoculture	<i>Lithocarpus glaber</i>	E33		x		x	x	x	26.7	4.86	39
Monoculture	<i>Nyssa sinensis</i>	H25	x	x	x	x	x	x	36.0	6.34	8
Monoculture	<i>Nyssa sinensis</i>	W14			x	x	x	x	35.4	6.01	25
Monoculture	<i>Quercus fabri</i>	E31		x		x	x	x	18.8	2.46	11
Monoculture	<i>Quercus serrata</i>	F21				x	x	x	26.8	1.66	6
Monoculture	<i>Rhus chinensis</i>	N17	x	x		x	x	x	34.2	2.17	69
Monoculture	<i>Sapindus saponaria</i>	N11		x		x	x	x	25.8	2.17	8
Monoculture	<i>Sapindus saponaria</i>	R17	x	x	x	x	x	x	38.0	5.27	0
Monoculture	<i>Triadica sebifera</i>	N13	x	x		x	x	x	33.3	5.19	6
Monoculture	<i>Triadica sebifera</i>	N14*	x	x	x	x	x	x	31.2	5.45	17
2-species	<i>C. axillaris, T. sebifera</i>	I26*	x	x	x	x	x	x	37.7	3.79	22
2-species	<i>C. axillaris, T. sebifera</i>	I27*	x	x		x	x	x	10.5	2.1	11
2-species	<i>C. axillaris, T. sebifera</i>	S18*	x	x	x	x	x	x	30.0	7.33	50
2-species	<i>C. eyrei, C. myrsinifolia</i>	J27				x		x	36.5	2.17	78
2-species	<i>C. glauca, Q. fabri</i>	K3				x		x	35.1	2.07	53
2-species	<i>C. glauca, Q. fabri</i>	Q21				x		x	37.5	2.03	36
2-species	<i>C. henryi, N. sinensis</i>	C32	x	x	x	x	x	x	38.1	8.53	19
2-species	<i>C. henryi, N. sinensis</i>	F22	x	x	x	x		x	44.8	6.19	56
2-species	<i>C. sclerophylla, Q. serrata</i>	P26		x		x	x	x	31.5	2.42	6
2-species	<i>K. bipinnata, L. glaber</i>	J21				x		x	37.7	3.54	33
2-species	<i>K. bipinnata, L. glaber</i>	Q7				x		x	39.7	4.27	56
2-species	<i>L. formosana, S. saponaria</i>	H31		x	x	x	x	x	24.4	4.55	11

Species Richness	Species	Plot ID	2012	2013	2014	2015	2016	2019	Slope (°)	Mean height (m)	Mortality rate (%)
2-species	<i>L. formosana</i> , <i>S. saponaria</i>	T17	x	x	x	x	x	x	33.1	5.86	11
2-species	<i>R. chinensis</i> , <i>S. superba</i>	E23	x					x	37.2	6.65	44
2-species	<i>R. chinensis</i> , <i>S. superba</i>	P23	x					x	28.9	5.81	47
4-species	<i>C. eyrei</i> , <i>C. myrsinifolia</i> , <i>K. bipinnata</i> , <i>L. glaber</i>	F28		x		x		x	16.4	2.51	56
4-species	<i>C. glauca</i> , <i>Q. fabri</i> , <i>R. chinensis</i> , <i>S. superba</i>	N8				x		x	36.6	3.58	40
4-species	<i>C. henryi</i> , <i>L. formosana</i> , <i>N. sinensis</i> , <i>S. saponaria</i>	P19		x		x	x	x	39.9	4.8	15
4-species	<i>C. henryi</i> , <i>L. formosana</i> , <i>N. sinensis</i> , <i>S. saponaria</i>	P29		x	x	x	x	x	22.9	4.53	13
4-species	<i>C. sclerophylla</i> , <i>C. axillaris</i> , <i>Q. serrata</i> , <i>T. sebifera</i>	F27*	x	x	x	x	x	x	33.6	4.02	22
4-species	<i>C. sclerophylla</i> , <i>C. axillaris</i> , <i>Q. serrata</i> , <i>T. sebifera</i>	N20*	x	x		x	x	x	31.0	3.81	12
8-species	<i>C. eyrei</i> , <i>C. glauca</i> , <i>C. myrsinifolia</i> , <i>K. bipinnata</i> , <i>L. glaber</i> , <i>Q. fabri</i> , <i>R. chinensis</i> , <i>S. superba</i>	P27		x				x	33.9	3.30	42
8-species	<i>C. henryi</i> , <i>C. sclerophylla</i> , <i>C. axillaris</i> , <i>L. formosana</i> , <i>N. sinensis</i> , <i>Q. serrata</i> , <i>S. saponaria</i> , <i>T. sebifera</i>	R16*	x	x	x	x	x	x	34.0	5.59	24
8-species	<i>C. henryi</i> , <i>C. sclerophylla</i> , <i>C. axillaris</i> , <i>L. formosana</i> , <i>N. sinensis</i> , <i>Q. serrata</i> , <i>S. saponaria</i> , <i>T. sebifera</i>	S10*	x	x	x	x	x	x	37.7	6.70	33
16-species	<i>C. henryi</i> , <i>C. eyrie</i> , <i>C. sclerophylla</i> , <i>C. axillaris</i> , <i>C. glauca</i> , <i>C. myrsinifolia</i> , <i>K. bipinnata</i> , <i>L. formosana</i> , <i>L. glaber</i> , <i>N. sinensis</i> , <i>Q. fabri</i> , <i>Q. serrata</i> , <i>R. chinensis</i> , <i>S. saponaria</i> , <i>T. sebifera</i> , <i>S. superba</i>	L21		x				x	22.8	3.90	80
16-species	<i>C. henryi</i> , <i>C. eyrei</i> , <i>C. sclerophylla</i> , <i>C. axillaris</i> , <i>C. glauca</i> , <i>C. myrsinifolia</i> , <i>K. bipinnata</i> , <i>L. formosana</i> , <i>L. glaber</i> , <i>N. sinensis</i> , <i>Q. fabri</i> , <i>Q. serrata</i> , <i>R. chinensis</i> , <i>S. saponaria</i> , <i>T. sebifera</i> , <i>S. superba</i>	L22*		x	x	x	x	x	22.8	3.84	31
16-species	<i>C. henryi</i> , <i>C. eyrei</i> , <i>C. sclerophylla</i> , <i>C. axillaris</i> , <i>C. glauca</i> , <i>C. myrsinifolia</i> , <i>K. bipinnata</i> , <i>L. formosana</i> , <i>L. glaber</i> , <i>N. sinensis</i> , <i>Q. fabri</i> , <i>Q. serrata</i> , <i>R. chinensis</i> , <i>S. saponaria</i> , <i>T. sebifera</i> , <i>S. superba</i>	U10*				x		x	40.9	4.92	36
24-species	All 24 species	N9*			x	x		x	27.0	3.68	35
24-species	All 24 species	R18*				x		x	44.7	5.24	47

* indicates that the plot was included in the analysis about the possible dependence of SSCI values on scanner positions or leaf-off / leaf-on conditions. In addition, W13 (monoculture of *Triadica sebifera*) was included in this analysis but it was excluded from the mixed-effects models due to it was just scan in 2019.

C. eyrie refers to *Castanopsis eyrei*, *C. myrsinifolia* refers to *Cyclobalanopsis myrsinifolia*, and *S. superba* refers to *Schima superba*.

24 species: in addition to the tree species in the 16-species mixture these eight species occurred: *Acer davidii*, *Castanopsis carlesii*, *Cinnamomum camphora*, *Daphniphyllum oldhamii*, *Diospyros japonica*, *Melia azedarach*, *Quercus acutissima*, *Triadica cochinchinensis*

Table S2. Names and characteristics of the 16 tree species used in the analysis to test species identity effects on the stand structural complexity index (SSCI). "n" is the number of sampled plots in 2019 with presence of the species. $Avg_{mon} \pm SD$ shows the average and the standard deviation of the monocultures in 2019, where '-' indicates that no monocultures of that species have been measured. p-value refers to the p-value of the model between SSCI and tree species richness (both \log_2 -transformed). RD (%) shows the percentage of the relative difference between the average SSCI of monocultures and the average SSCI in high species mixtures, that is, plots with TSR of 16 or 24. It was calculated as $(Avg_{mon} - Avg_{hsm}) / Avg_{mon} * 100$

Species	Family	n	$Avg_{mon} \pm SD$	p-value	RD (%)
<i>Castanea henryi</i> (Skan) Rehder & E.H. Wilson	Fagaceae	13	9.54 ± 6.8	0.026	106.54
<i>Castanopsis eyree</i> (Champion ex Bentham) Tutcher	Fagaceae	4	-	0.817	-
<i>Castanopsis sclerophylla</i> (Lindley & Paxton) Schottky	Fagaceae	12	14.34 ± 12	0.149	37.38
<i>Choerospondias axillaris</i> (Roxburgh) B. L. Burt & A. W. Hill	Anacardiaceae	14	5.99 ± 2.18	0.000	228.62
<i>Cyclobalanopsis glauca</i> (Thunberg) Oersted	Fagaceae	10	16.47	0.303	19.61
<i>Cyclobalanopsis myrsinifolia</i> (Blume) Oersted	Fagaceae	7	-	0.273	-
<i>Koelreuteria bipinnata</i> Franchet	Sapindaceae	6	5.11	0.408	236.19
<i>Liquidambar formosana</i> Hance	Hamamelidaceae	13	8.82 ± 2.29	0.003	123.22
<i>Lithocarpus glaber</i> (Thunberg) Nakai	Fagaceae	9	17.52	0.752	9.42
<i>Nyssa sinensis</i> Oliver	Nyssaceae	13	8.22 ± 0.44	0.009	139.75
<i>Quercus fabri</i> Hance	Fagaceae	7	11.96	0.111	94.46
<i>Quercus serrata</i> Murray	Fagaceae	12	12.21	0.172	61.25
<i>Rhus chinensis</i> Miller	Anacardiaceae	8	7.37	0.321	160.03
<i>Sapindus saponaria</i> Linnaeus	Sapindaceae	13	5.3 ± 2.91	0.004	271.93
<i>Schima superba</i> Gardner & Champion	Theaceae	9	-	0.405	-
<i>Triadica sebifera</i> (Linnaeus) Small	Euphorbiaceae	13	10.33 ± 0.56	0.003	85.62

Table S3. Results of the mixed-effects models for the effect of tree species richness (TSR; \log_2 -transformed), year and their interaction on different components of stand structural complexity (stand structural complexity index (SSCI), mean fractal dimension (MeanFrac) and effective number of layers (ENL), all \log_2 -transformed), of a subsample of the 30 plots that were consistently scanned in 2013, 2015 and 2019.

Fixed effect	SSCI				MeanFrac				ENL			
	df _{num}	df _{den}	F	p	df _{num}	df _{den}	F	p	df _{num}	df _{den}	F	p
Intercept	-	-	-	< 0.001	-	-	-	< 0.001	-	-	-	< 0.001
TSR	1	70.87	0.94	0.336	1	103.17	1.22	0.272	1	48.35	0.00	0.958
Year	1	53.16	27.92	< 0.001	1	62.90	1.82	0.182	1	105.73	190.84	< 0.001
TSR*Year	1	44.13	4.50	< 0.05	1	53.44	0.75	0.389	1	105.78	5.53	< 0.05

df_{num}, numerator degrees of freedom; df_{den}, denominator degrees of freedom. F and P indicate F ratios and the P value of the significance test, respectively.

Table S4. Results of the mixed-effects models for the effect of tree species richness (TSR; \log_2 -transformed), year and their interactions on inventory-based stand structural complexity indices based on the stem diameter 5 cm above ground (GD) and tree height, all \log_2 -transformed.

Fixed effect	Standard deviation GD				Coefficient of variation GD				Gini coefficient GD			
	df _{num}	df _{den}	F	p	df _{num}	df _{den}	F	p	df _{num}	df _{den}	F	p
Intercept	-	-	-	0.21	-	-	-	< 0.001	-	-	-	< 0.001
TSR	1	58.11	22.20	< 0.001	1	85.99	45.80	< 0.001	1	84.78	45.90	< 0.001
Year	1	25.08	84.72	< 0.001	1	22.10	2.89	0.10	1	18.56	4.04	< 0.1
TSR*Year	1	22.66	0.26	0.62	1	11.70	8.03	< 0.05	1	9.45	7.54	< 0.05

df_{num}, numerator degrees of freedom; df_{den}, denominator degrees of freedom. F and P indicate F ratios and the P value of the significance test, respectively.

Fixed effect	Standard deviation Height				Coefficient of variation Height				Gini coefficient Height			
	df _{num}	df _{den}	F	p	df _{num}	df _{den}	F	p	df _{num}	df _{den}	F	p
Intercept	-	-	-	< 0.001	-	-	-	< 0.001	-	-	-	< 0.001
TSR	1	59.64	7.06	< 0.05	1	53.92	15.33	< 0.001	1	54.38	17.87	< 0.001
Year	1	26.50	111.30	< 0.001	1	14.45	7.20	< 0.05	1	20.33	7.51	< 0.05
TSR*Year	1	23.55	3.04	< 0.1	1	11.63	0.75	0.40	1	17.72	0.93	0.35

df_{num}, numerator degrees of freedom; df_{den}, denominator degrees of freedom. F and P indicate F ratios and the P value of the significance test, respectively.

Table S5. Analysis 1 to test for possible effects of different positions within a plot using multiple comparison of means (Tukey contrast) between scan positions. a, b, and c represent different scan positions within each plot. Each group has $n = 15$.

Group	Mean difference	Std. error	z value	P
b - a	0.018	0.097	0.184	0.982
c - a	-0.022	0.097	-0.228	0.972
c - b	-0.04007	0.097	-0.412	0.911

Table S6. Analysis 2: Linear mixed-effects models fitted by REML to analyse the possible effects of leaf-off and leaf-on conditions and its interaction with tree species richness (TSR) on the stand structural complexity index (SSCI). We use plot as random factor. $n = 30$, where 15 scans were performed in February (leaf-off) and 15 scans in April (leaf-on).

Model	df	R^2_m	ΔAIC
SSCI ~ TSR * Leaf-On	6	0.47	2.69
SSCI ~ TSR + Leaf-On	5	0.46	0.00
SSCI ~ TSR	4	0.32	10.46
SSCI ~ Leaf-On	4	0.14	2.73

df, degrees of freedom; R^2_m , variance explained by the fixed effects alone; AIC is the Akaike information criterion weight; ΔAIC is the difference in AIC with respect to the best-fitting model (lowest value of AIC).

Supporting Figures

Figure S1. Examples of cross-sections for the calculation of the mean fractal dimension (MeanFrac). (a) shows the point cloud of a plot with a representation of different cross-sections. Examples of the resultant polygon for a cross-section of the monoculture O27 (b) and the 24-species mix N9 (c) are shown in (d) and (e) respectively. The fractal dimension is calculated as $2 \times \ln 0.25P / \ln A$, where P is the perimeter and A the area of the resultant polygon for each cross-section. The higher the ratio between perimeter and area, the higher the fractal dimension. In the example, we observed how the perimeter can be much higher than the area in the high-species mix in comparison with monocultures. The MeanFrac is the result of the average of the 2560 fractal dimensions in which each point cloud was divided.

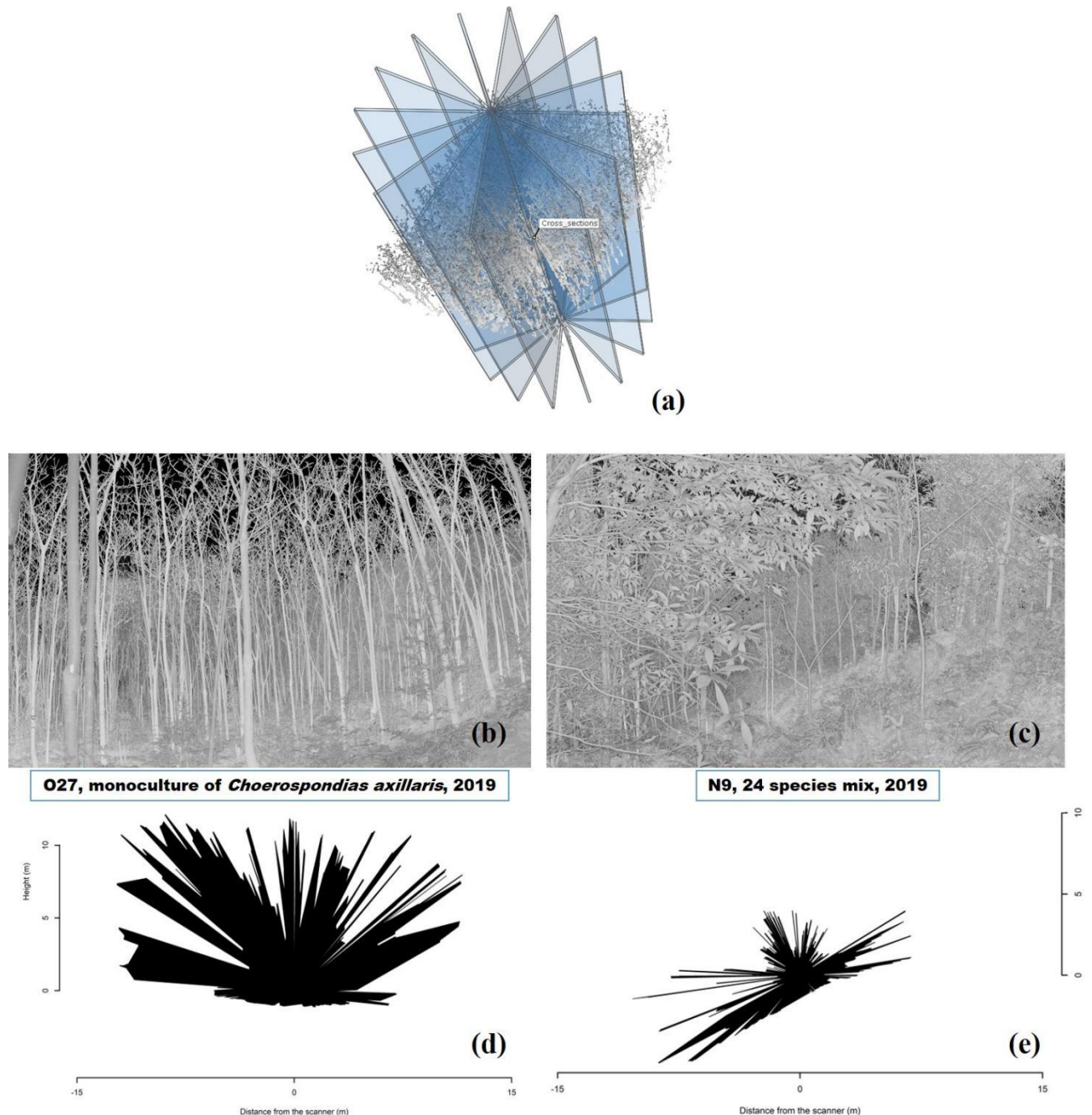


Figure S2. Slope correction for effective number of layers (ENL) to aligns layers parallel to the ground surface. (a) Planar scan view of a single scan in the 24 species plot N9 with a terrain slope of 35° (b) Voxelisation without slope correction (plot N9, ENL = 15.57), (c) Voxelisation after slope correction (plot N9, ENL = 12.05)

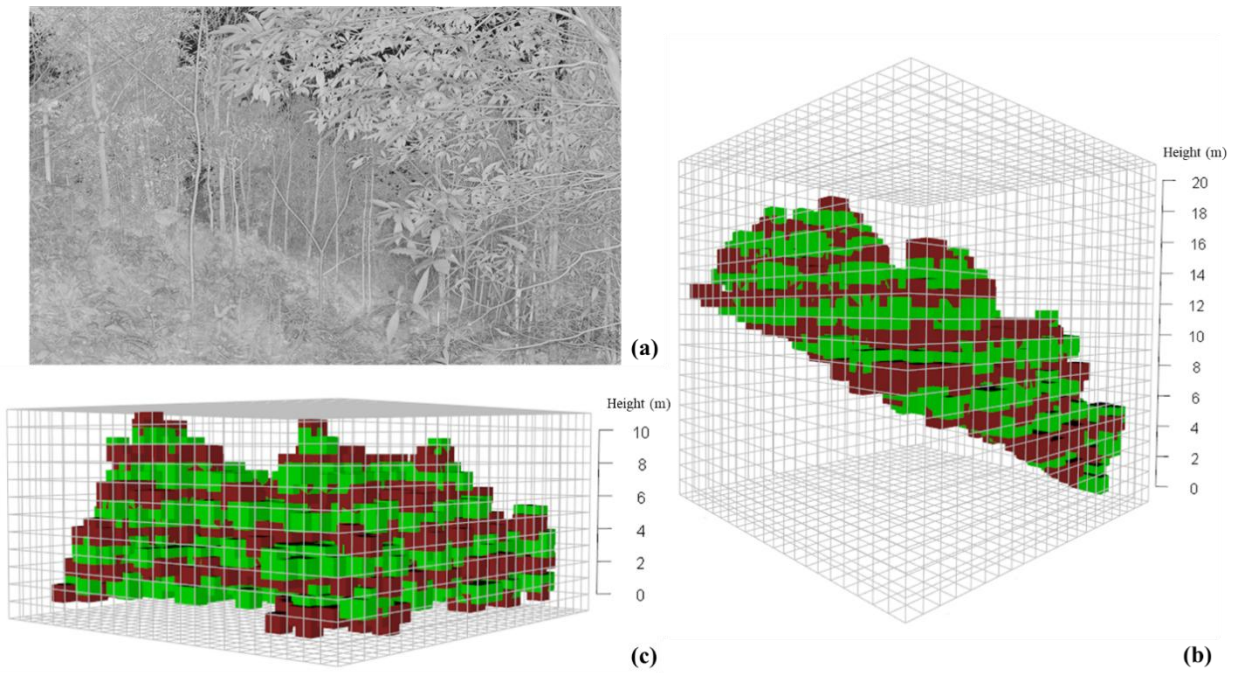


Figure S3. Random factors of the linear mixed-effects model for the stand structural complexity index (SSCI).

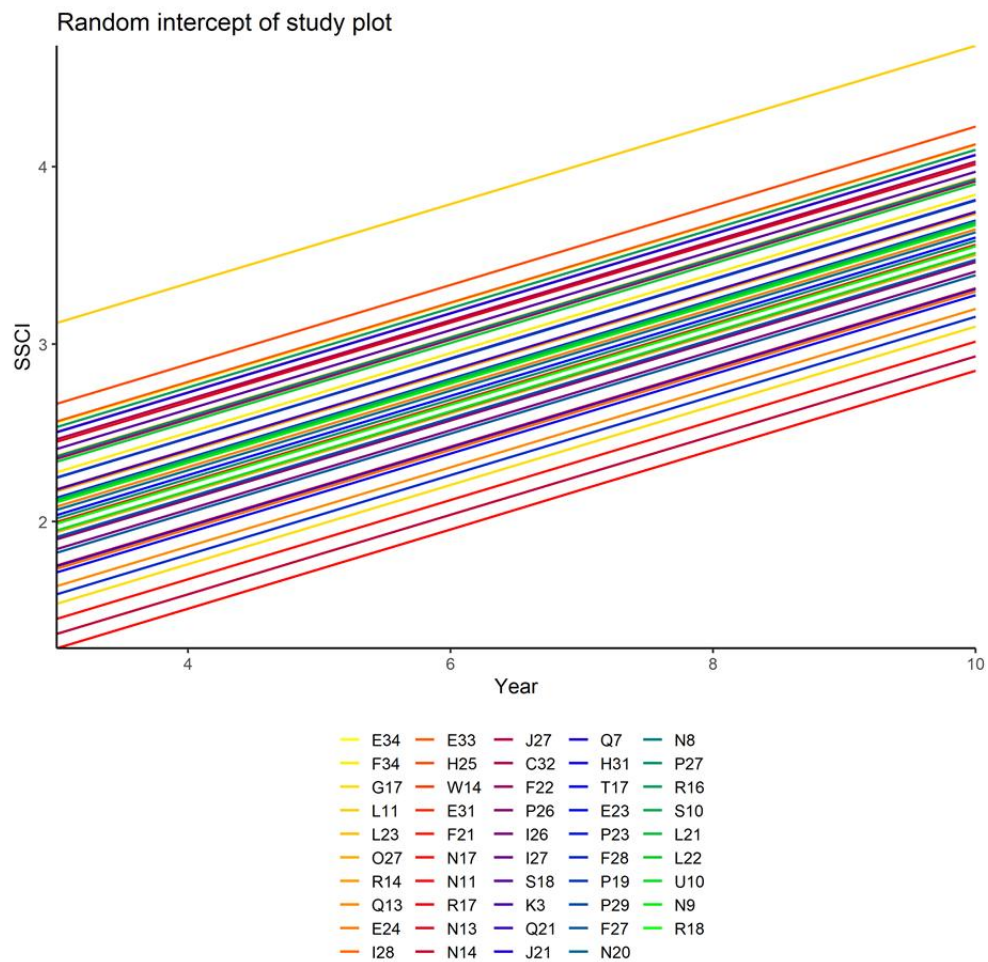
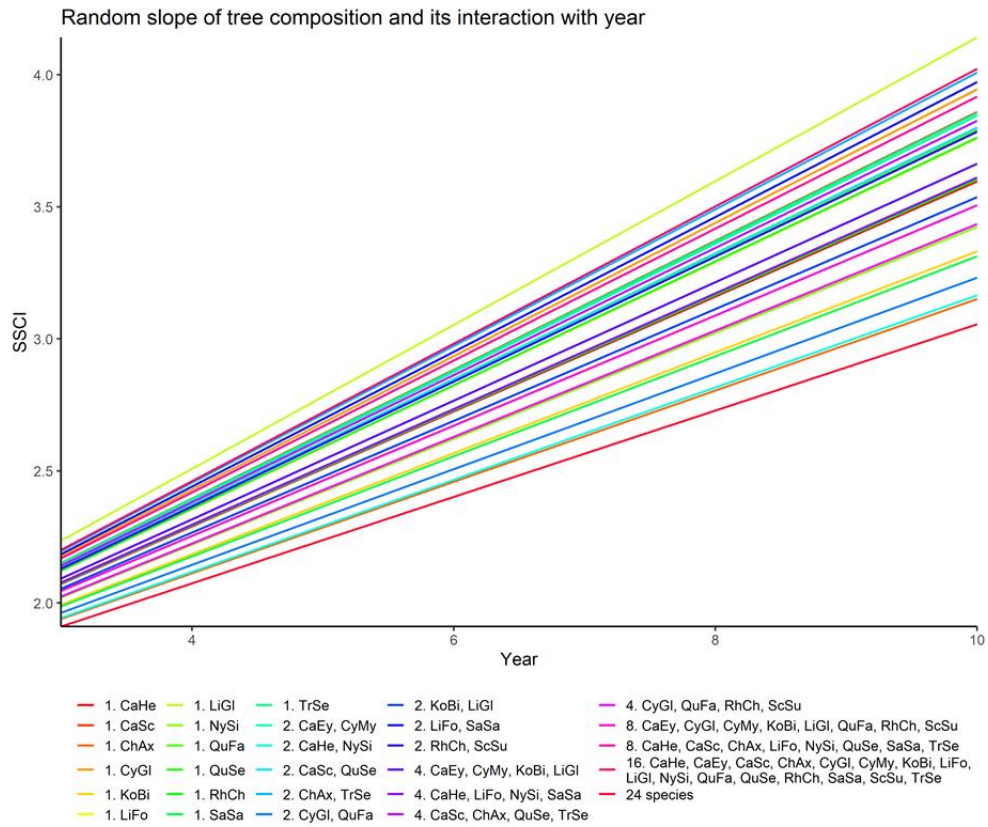


Figure S4. Temporal changes in the relationship between tree species richness and different components of stand structural complexity (a: stand structural complexity index (SSCI); b: mean fractal dimension (MeanFrac); c: effective number of layers (ENL)) for 30 plots that were consistently scanned in 2013, 2015, and 2019. Lines show predictions of linear mixed-effects models, and symbols indicate observed values.

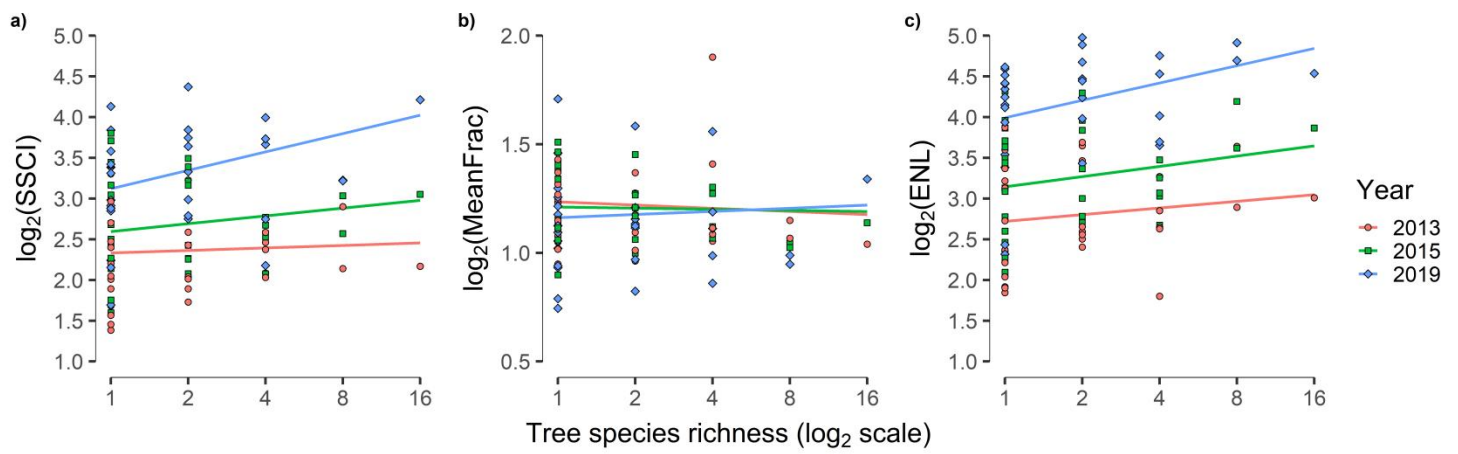


Figure S5. Temporal changes in the relationship between tree species richness and different inventory-based stand structural complexity indices. Lines show predictions of linear mixed-effects models and symbols indicate observed values.

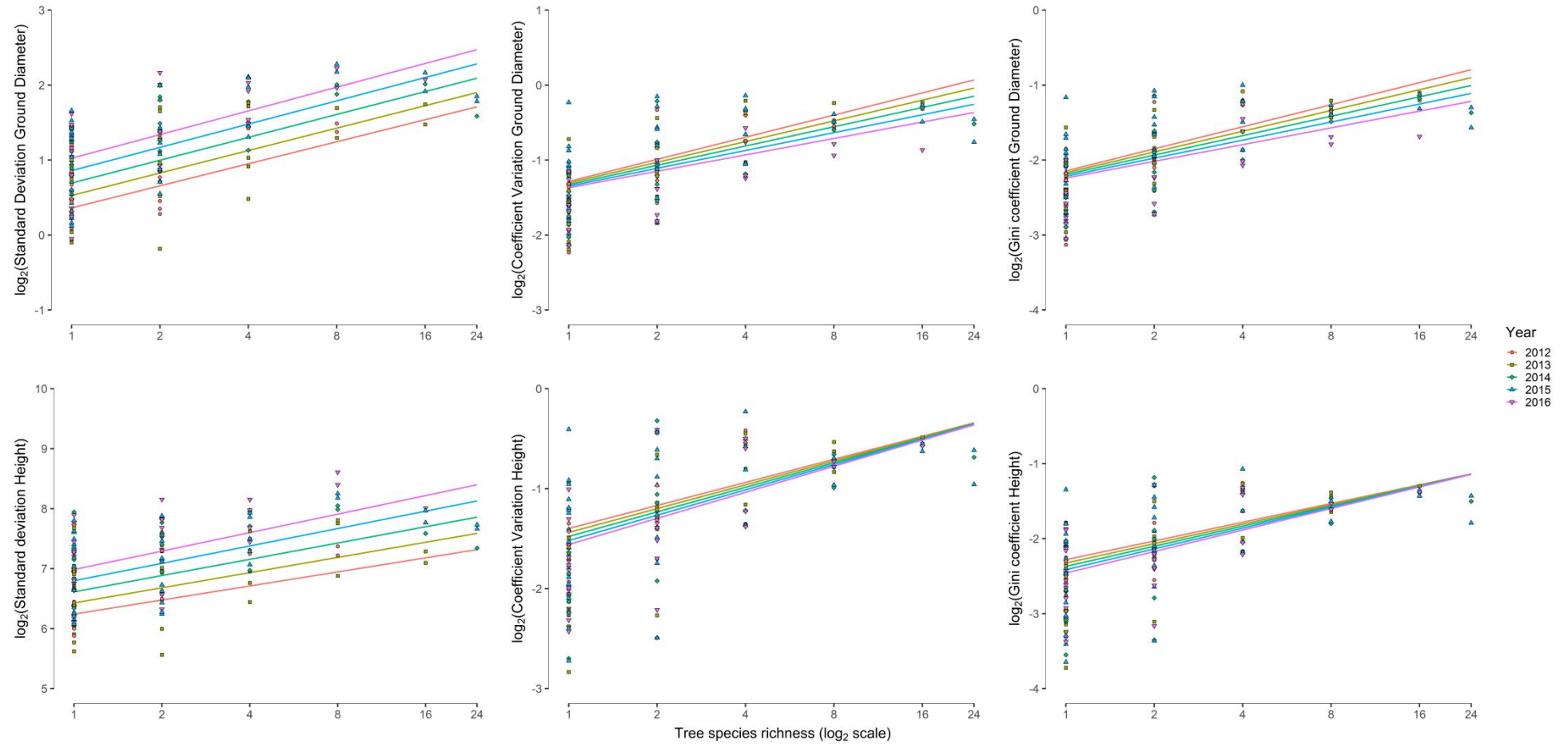
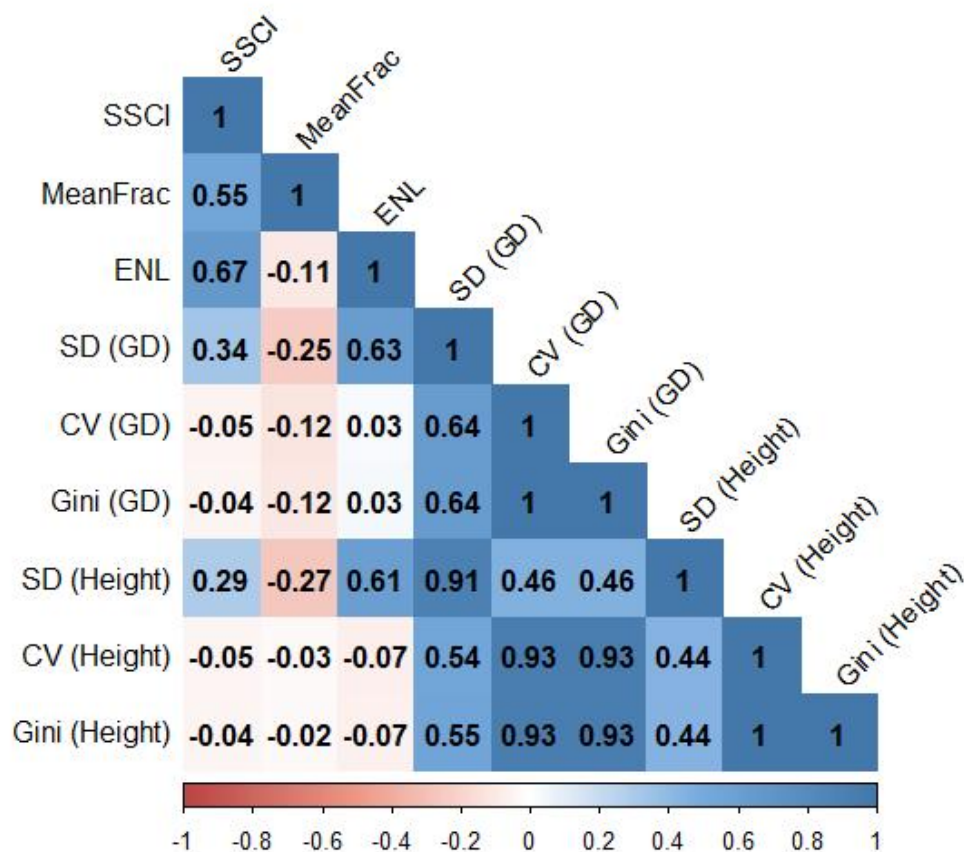


Figure S6. Correlation matrix between stand structural complexity indices measured from 2012 to 2016. The stand structural complexity index (SSCI), mean fractal dimension (MeanFrac) and the effective number of layers (ENL) are based on data from terrestrial laser scanning, whereas the other indices are calculated using inventory-based data of stem diameter 5 cm above ground (ground diameter GD) and total tree height. SD refers to standard deviation, CV to coefficient of variation, and Gini to the Gini-coefficient. The strength of the correlation is indicated by different colour shades (dark red: strong negative correlation, dark blue: strong positive correlation).



References

- Bruelheide, H., Nadrowski, K., Assmann, T., Bauhus, J., Both, S., Buscot, F., ... Schmid, B. (2014). Designing forest biodiversity experiments: General considerations illustrated by a new large experiment in subtropical China. *Methods in Ecology and Evolution*, 5(1), 74–89. <https://doi.org/10.1111/2041-210X.12126>
- Ehbrecht, M., Schall, P., Juchheim, J., Ammer, C., & Seidel, D. (2016). Effective number of layers: A new measure for quantifying three-dimensional stand structure based on sampling with terrestrial LiDAR. *Forest Ecology and Management*, 380, 212–223. <https://doi.org/10.1016/j.foreco.2016.09.003>
- Ehbrecht, M., Schall, P., Ammer, C., & Seidel, D. (2017). Quantifying stand structural complexity and its relationship with forest management, tree species diversity and microclimate. *Agricultural and Forest Meteorology*, 242(April), 1–9. <https://doi.org/10.1016/j.agrformet.2017.04.012>

Chapter 2. Neighbourhood species richness reduces crown asymmetry of subtropical trees in sloping terrain

Table of contents

Supporting Methods

1. Neighbourhood pressure (NP)

Supporting Tables

- **Table S1.** Included plots and their characteristics.
- **Table S2.** Overview of mean file size (and standard deviation) in Mb for each year and plot. In addition the number of scans is given for each plot.
- **Table S3.** Technical specification of the three FARO scanners based on the technical fact sheets by FARO (Korntal-Münchingen, Germany)
- **Table S4.** Model comparison using different calculations of neighbourhood pressure index.

Supporting Figures

- **Fig. S1.** Representation of possible inaccuracies when using (a) crown projection area or (b) height as size measurement for the neighbourhood pressure index.
- **Fig. S2.** Curve of the function for the canopy level index (C_{li}).
- **Fig. S3.** Correlations between the direction of crown displacement (CD), microtopography (MT) and neighbourhood pressure (NP).
- **Fig. S4.** Boxplot showing the relationship between tree height and study year
- **Fig. S5.** Residual plots of the best-fitting model

Supporting Methods

Neighbourhood pressure (NP)

In general, to calculate neighbourhood pressure, a measure of the size of the neighbour is divided by the distance to the target tree. Size of the neighbour can be expressed as height (Umeki, 1995), diameter at breast height (DBH; Brisson, 2001; Seidel et al., 2011) or crown area (CPA; Schröter et al., 2012; Vovides et al., 2018).

However, we observed inaccuracies when applying these methods to a young plantation with steep slopes: When using CPA as size, we found big differences between fast and slow growing species, where a slow growing tree could present higher CPA than a taller tree (Sup. Fig. 1a). When using height, we could see how the topography can situate a smaller tree in the same canopy layer than a taller tree situated in a downhill position (Sup. Fig. 1b).

For this study, we developed an equation to scale the NP depending if both trees are at the same canopy level. The canopy level index (c_{li} , Eq. 1) is a combination between a Gaussian and a Sigmoid function, where a modifies the height of the Gaussian curve's peak, b the width of the Gaussian bell, c the peak of the Sigmoid's curve, and d the position of the centre of the bell. X represents the height difference, calculated as (neighbour altitude + neighbour height) - (target altitude + target height)

$$C_{li} = \frac{a}{1 + e^{-(x+b)}} \cdot e^{-x^2/2 \cdot c^2} + d$$

We look for a function where, if the height difference (taking into account the topography) is 0, it is close to the maximum value (1), if it is negative the effect arrives to 0, and if the positive difference is really high the effect is lower because the target tree could grow in the understorey. We used the parameters $a = 0.5$, $b = 2$, $c = 10$, $d = 1$. Sup. Fig. 2 shows the curve of the c_{li} .

Supporting Tables

Table S1. Plot characteristics and the number of target trees that were scanned and analysed in a given study year. Species names follow nomenclature in "The Flora of China" (<http://flora.huh.harvard.edu/china>).

Species Richness	Species	Plot ID	2012	2013	2014	2015	2016	2019	Mean slope (°)
Monoculture	<i>Castanea henryi</i>	E34	13	11	11	11	11	7	12.2
Monoculture	<i>Castanea henryi</i>	F34	15	14	14	14	14	13	36.0
Monoculture	<i>Castanopsis sclerophylla</i>	G17				9		7	32.5
Monoculture	<i>Castanopsis sclerophylla</i>	L11				16	16	13	30.9
Monoculture	<i>Choerospondias axillaris</i>	L23	15	15	15	15	15	14	23.6
Monoculture	<i>Choerospondias axillaris</i>	O27	14	16	14	13	13	9	26.0
Monoculture	<i>Liquidambar formosana</i>	E24		16	16	16	16	16	35.3
Monoculture	<i>Liquidambar formosana</i>	I28		16	16	16	16	16	25.7
Monoculture	<i>Nyssa sinensis</i>	H25	14	14	14	14	13	12	36.0
Monoculture	<i>Nyssa sinensis</i>	W14			9	9	9	9	35.4
Monoculture	<i>Quercus serrata</i>	F21				15	15	16	26.8
Monoculture	<i>Quercus serrata</i>	G33					8	2	6.1
Monoculture	<i>Sapindus saponaria</i>	N11		15		15	15	14	25.8
Monoculture	<i>Sapindus saponaria</i>	R17	15	15	15	15	15	15	38.0
Monoculture	<i>Triadica sebifera</i>	N13	15	15	16	16	15	15	33.3
Monoculture	<i>Triadica sebifera</i>	N14	15	13	13	13	13	11	31.2
2-species	<i>C. axillaris, T. sebifera</i>	I26	11	11	10	14	14	5	37.7
2-species	<i>C. axillaris, T. sebifera</i>	I27	14	15		15	14	13	10.5
2-species	<i>C. henryi, N. sinensis</i>	C32	14	13	13	12	12	10	38.1
2-species	<i>C. henryi, N. sinensis</i>	F22	12	13	14	14		5	44.8
2-species	<i>C. sclerophylla, Q. serrata</i>	O26				16		12	31.9
2-species	<i>C. sclerophylla, Q. serrata</i>	P26				15	15	15	31.5
2-species	<i>L. formosana, S. saponaria</i>	H31		14	16	14	13	12	24.4
2-species	<i>L. formosana, S. saponaria</i>	T17	13	14	14	15	15	14	33.1
4-species	<i>C. henryi, L. formosana, N. sinensis, S. saponaria</i>	P19		88		87	87	82	39.9
4-species	<i>C. henryi, L. formosana, N. sinensis, S. saponaria</i>	P29		87	86	87	87	83	22.9

Species Richness	Species	Plot ID	2012	2013	2014	2015	2016	2019	Mean slope (°)
4-species	<i>C. sclerophylla, C. axillaris, Q. serrata, T. sebifera</i>	F27	74	75	79	82	85	61	33.6
4-species	<i>C. sclerophylla, C. axillaris, Q. serrata, T. sebifera</i>	N20	81	83		90	91	41	31.0
8-species	<i>C. henryi, C. sclerophylla, C. axillaris, L. formosana, N. sinensis, Q. serrata, S. saponaria, T. sebifera</i>	R16	77	75	75	76	74	66	34.0
8-species	<i>C. henryi, C. sclerophylla, C. axillaris, L. formosana, N. sinensis, Q. serrata, S. saponaria, T. sebifera</i>	S10	76	76	71	70	69	59	37.7

Table S2. Overview of mean file size (and standard deviation) in Mb for each year and plot. In addition the number of scans is given for each plot.

PLOT	Number of scans	2012	2013	2014	2015	2016	2019
E24	9		78.4 ± 0.45	83.6 ± 1.35	87.8 ± 1.01	93.5 ± 1.70	92.0 ± 1.03
E34	9	84.3 ± 0.95	87.9 ± 0.82	92.3 ± 1.14	94.3 ± 0.65	96.6 ± 0.59	97.7 ± 0.77
F21	9				80.9 ± 2.84	80.3 ± 2.45	86.6 ± 2.70
F34	9	80.9 ± 1.03	81.8 ± 0.42	86.2 ± 1.09	90.5 ± 0.71	90.1 ± 0.98	94.0 ± 0.77
G17	9						88.5 ± 3.38
G33	9					79.9 ± 0.95	80.9 ± 0.69
H25	9	84.5 ± 2.05	88.9 ± 1.82	93.7 ± 2.19	00.0 ± 0.05	95.5 ± 1.82	99.9 ± 1.07
I28	9		78.4 ± 0.48	80.8 ± 1.14	83.6 ± 1.32	85.8 ± 1.96	90.5 ± 1.46
L11	9				84.3 ± 2.46	87.9 ± 2.85	94.1 ± 3.97
L23	9	79.7 ± 0.58	81.3 ± 0.74	84.8 ± 1.41	86.4 ± 0.96	86.4 ± 0.97	92.5 ± 1.66
N11	9		76.0 ± 1.17		79.0 ± 1.05	79.3 ± 1.22	81.5 ± 0.93
N13	9	79.9 ± 1.93	81.2 ± 2.94	86.6 ± 3.45	89.0 ± 4.20	90.4 ± 2.79	95.1 ± 1.91
N14	9	77.7 ± 1.02	80.8 ± 1.82	86.1 ± 4.05	88.7 ± 3.65	89.2 ± 3.29	92.7 ± 1.15
O27	9		86.9 ± 0.73	91.4 ± 0.76		92.3 ± 0.97	92.6 ± 0.55
R17	9	78.1 ± 0.96	79.0 ± 1.23		76.7 ± 6.95		89.2 ± 0.71
W14	9			88.5 ± 0.91	89.8 ± 1.10	92.6 ± 0.77	95.2 ± 1.51
C32	9	81.1 ± 1.68	85.9 ± 2.09	90.0 ± 1.64	91.7 ± 0.60	92.1 ± 1.05	93.3 ± 1.13
F22	9	82.2 ± 1.49	85.1 ± 3.06	90.9 ± 2.65	91.2 ± 7.44		92.5 ± 1.25
H31	9		79.6 ± 1.04	83.2 ± 1.76	86.0 ± 1.42	89.4 ± 2.23	91.8 ± 0.96

I26	9	80.1 ± 0.89	80.6 ± 0.91	86.5 ± 0.93	85.7 ± 0.82	78.3 ± 7.70	91.2 ± 0.84
I27	9	74.1 ± 0.72	75.3 ± 1.38		78.1 ± 1.36	79.8 ± 1.35	83.1 ± 1.68
O26	9						95.3 ± 1.58
P26	9				81.4 ± 1.62	84.0 ± 1.91	91.9 ± 3.29
T17	9	76.2 ± 0.41	80.0 ± 1.33	83.9 ± 1.00	88.3 ± 1.40	89.7 ± 0.61	92.3 ± 0.92
F27	16	81.5 ± 0.78	82.3 ± 1.33	86.9 ± 1.45	87.4 ± 1.55	89.0 ± 1.53	93.5 ± 1.38
N20	16	76.5 ± 1.62	79.4 ± 1.67		86.8 ± 2.11	87.5 ± 0.94	89.9 ± 1.08
P19	16		78.8 ± 1.87		85.5 ± 2.14	88.8 ± 1.96	91.7 ± 0.70
P29	16		78.7 ± 1.80	82.0 ± 1.75	83.8 ± 1.92	87.3 ± 1.91	90.4 ± 2.34
R16	16	82.1 ± 2.23	84.5 ± 2.86	88.9 ± 3.56	86.9 ± 1.23	93.8 ± 2.02	96.0 ± 1.11
S10	16	79.1 ± 1.00	82.9 ± 0.91	88.2 ± 1.23	90.8 ± 1.93	91.9 ± 1.24	94.3 ± 1.28

Table S3. Technical specification of the three FARO scanners based on the technical fact sheets by FARO (Korntal-Münchingen, Germany)

Parameters	FARO Photon Scanner	FARO Focus 3D S120	FARO Focus X130
Wavelength	785 nm	905 nm	1550 nm
Step size (V/H)	0.009° / 0.009°	0.009° / 0.009°	0.009° / 0.009°
Range	0.6 – 120m	0.6 – 120m	0.6m – 130m
Field of view (V/H)	320° / 360°	305° / 360°	300° / 360°
Accuracy	± 2 mm	± 2 mm	± 2 mm
Speed	122,000-976,000 points/s	122,000-976,000 points/s	122,000-976,000 points/s
Weight	14.5 kg	5.0 kg	5.2 kg

Table S4. Model comparison using different calculations of neighbourhood pressure index. NP refers to the neighbourhood pressure calculated as described in the supporting methods, VNA refers to the vector of neighbourhood asymmetry (Brisson, 2001; Brisson & Reynolds, 1994). SE: standard error; df: degrees of freedom; SD: standard deviation

	p			p	
MT	0.0609	. [+]	MT	0.0314	. [+]
TH	1.36E-05	*** [+]	TH	1.73E-05	*** [+]
NP	2.20E-16	*** [+]	VNA	2.20E-16	*** [+]
NSR	0.0076	** [-]	NSR	0.0512	. [-]
MT*NSR	0.0375	* [-]	MT*NSR	0.0130	* [-]

	NP	VNA
Marginal R ²	0.606	0.593
Conditional R ²	0.854	0.850
AIC	-4325	-4190

Supporting Figures

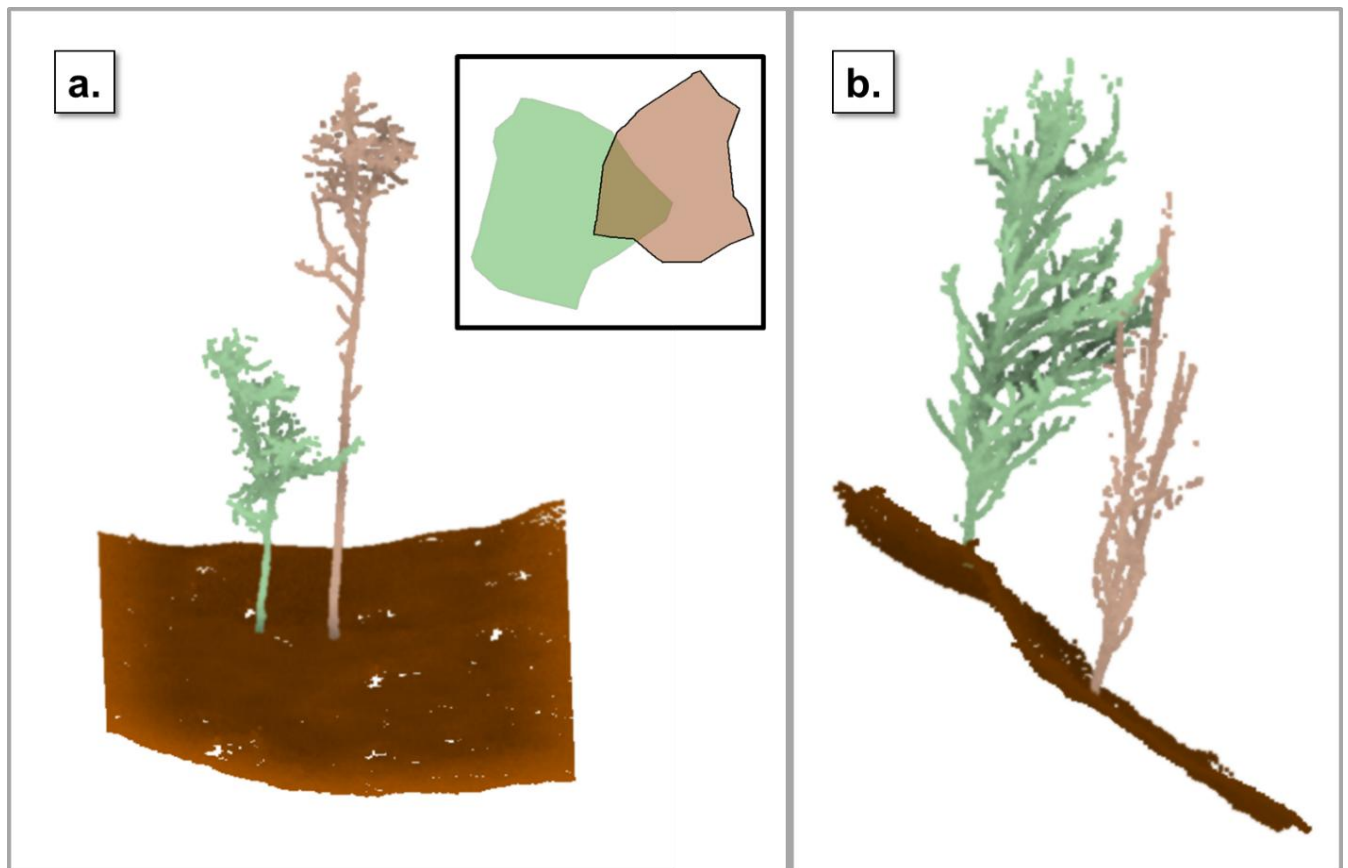


Fig. S1. Representation of possible inaccuracies when using (a) crown projection area or (b) height as size measurement for the neighbourhood pressure index. (a) shows in green a target tree with CPA = 4.5 m² and in coral its neighbour with CPA = 3.5 m². (b) shows in green a target tree situated in an uphill location with height = 5.5 m, and in coral its neighbour with height = 5.5m. Brown represents the terrain.

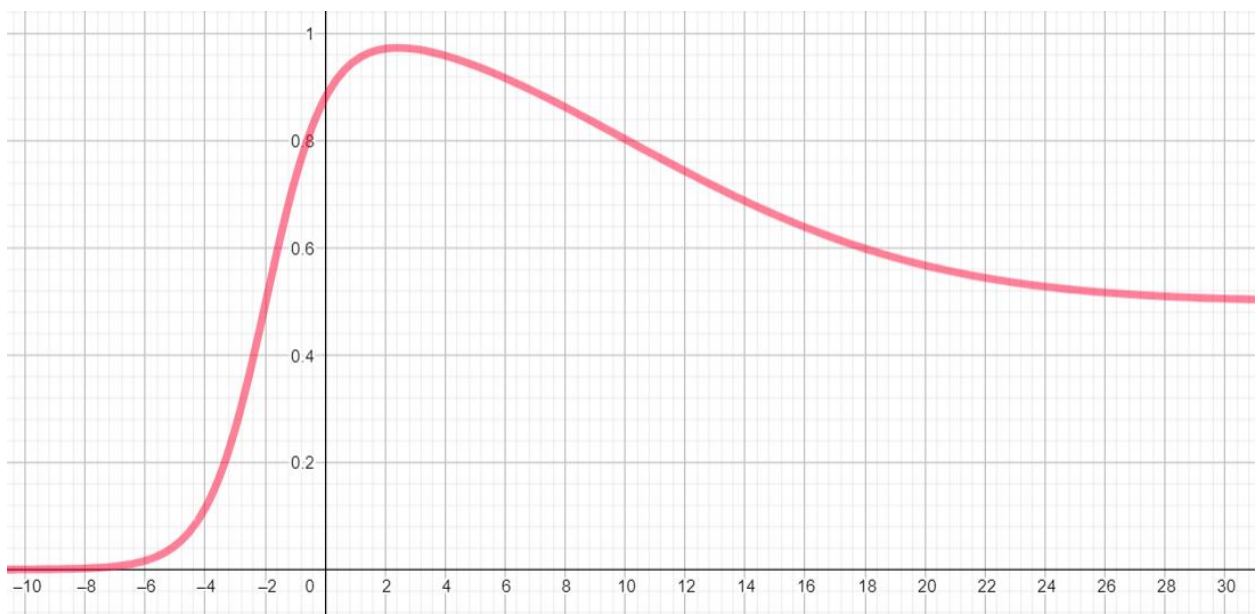


Fig. S2. Curve of the function for the canopy level index (*cli*). X axis represents the height difference between the neighbour and the target tree, including the altitude. Y axis would be the result to apply the *cli* formula to that difference.

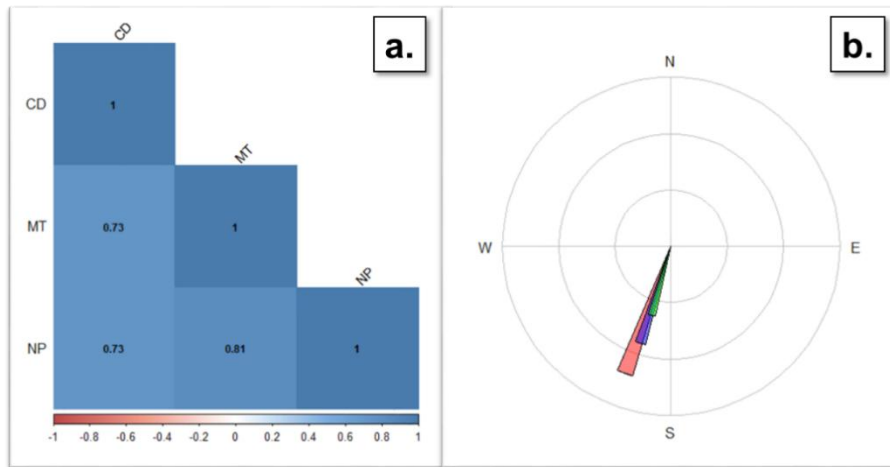


Fig. S3. Correlations between the direction of crown displacement (*CD*), microtopography (*MT*) and neighbourhood pressure (*NP*) (a) and mean direction of *CD* (red), *NP* (blue) and *MT* (green) estimated with the Rayleigh's test for circular data

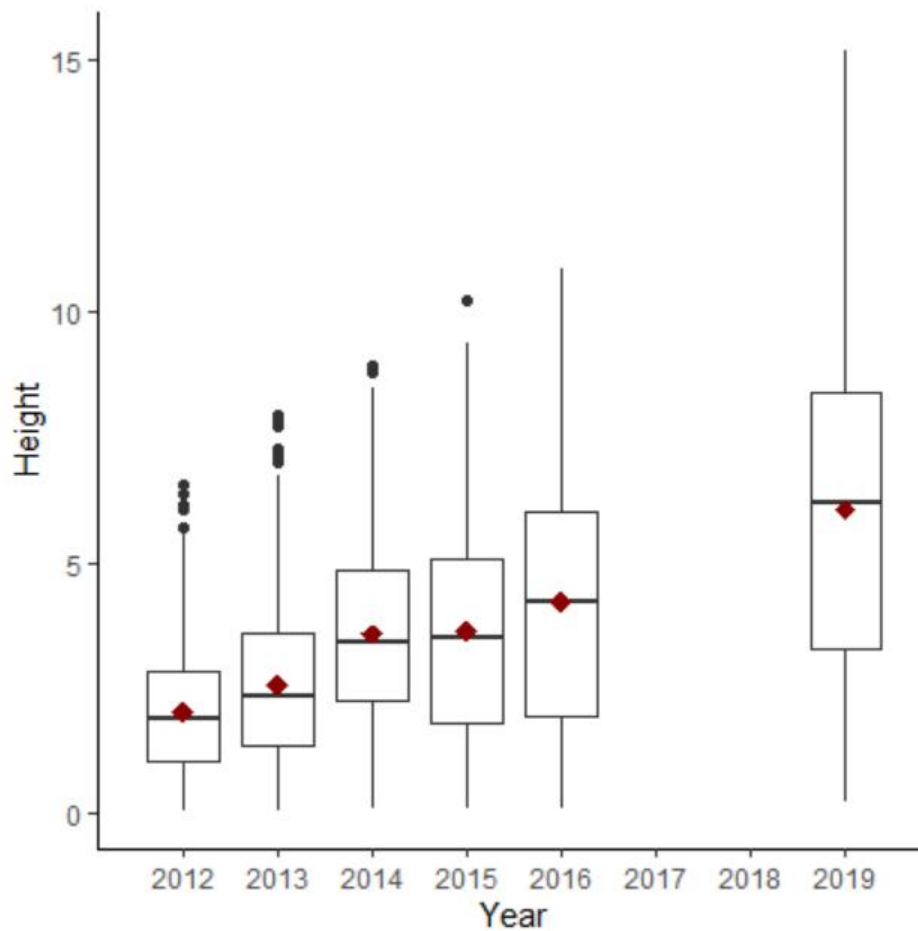


Fig. S4 Boxplot showing the relationship between tree height and study year

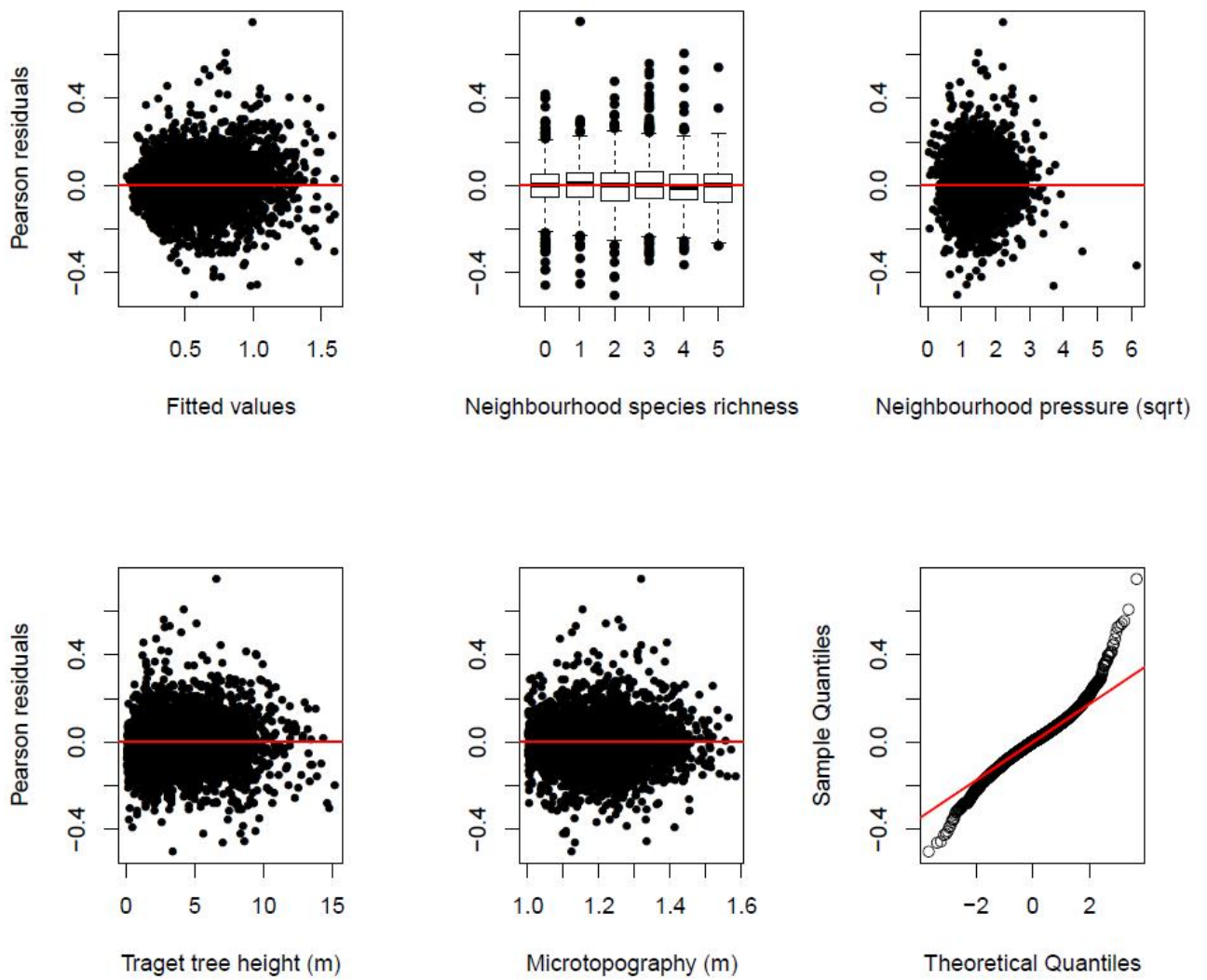


Fig. S56. Residual plots of the best-fitting model

Chapter 3. Tree-tree interactions and crown complementarity: The role of functional diversity and branch traits for canopy packing

Table of contents

Supporting Tables

- **Table S1.** List of values of crown complementarity (CCI), functional dissimilarity (FD) and the sum of morphological flexibility (MF sum) of the tree species pairs (TSPs).
- **Table S2.** Model selection statistics

Supporting Figures

- **Figure S1.** Principal component analysis (PCA) of standardised functional trait values for the six study species.
- **Figure S2.** Model validation plots for the best-fitting generalized additive mixed model.
- **Figure S3.** Relationship between tree height and a) branch density dissimilarity (BDD) and b) branching intensity dissimilarity (BID).

Supporting Tables

Table S1. List of values of crown complementarity (CCI), functional dissimilarity (FD) and the sum of morphological flexibility (MF sum) of the tree species pairs (TSPs). TSP ID contains the name of the pair, which consists of plot number and the local coordinates of the individual trees. To characterise low and high levels of FD, we used the 30% (FD: 0.755) and 70% (FD: 1.271) quantiles of observed FD-values of heterospecific TSPs.

TSP ID	CCI	FD	MF sum
F27_0207.0307	0.577	1.709	1.715
F27_1604.1605	0.995	1.709	1.014
I27_0807.0907	0.198	1.709	1.014
I27_1011.1012	0.307	1.709	1.014
I27_1514.1515	0.970	1.709	1.014
C32_0505.0605	0.521	1.272	1.385
C32_0508.0608	0.605	1.272	1.385
C32_0615.0616	0.452	1.272	1.385
C32_0913.1013	0.688	1.272	1.385
C32_1512.1612	0.948	1.272	1.385
C32_1607.1706	0.664	1.272	1.385
F22_0602.0603	0.525	1.272	1.385
L22_0203.0204	0.406	1.272	1.385
L22_1304.1403	0.061	1.272	1.385
P19_1117.1217	0.575	1.272	1.385
P29_0315.0415	0.583	1.272	1.385
R16_0309.0410	0.729	1.272	1.385
R16_1605.1606	0.624	1.272	1.385
R16_1618.1619	0.961	1.272	1.385
M22_0703.0803	0.989	0.993	0.944
N9_1517.1518	0.708	0.812	1.055
P19_0711.0811	0.909	0.812	1.055
P29_0809.0810	0.201	0.812	1.055
S10_1014.1114	0.864	0.812	1.055
L22_1303.1304	0.623	0.787	0.959
P29_1010.1011	0.181	0.787	0.959
P29_1012.1112	0.982	0.787	0.959
R16_1814.1815	0.901	0.787	0.959
F27_0711.0811	0.982	0.765	1.236
F27_1003.1004	0.372	0.765	1.236
F27_1302.1402	0.920	0.765	1.236
I27_0407.0507	0.592	0.765	1.236
I27_0410.0511	0.685	0.765	1.236
I27_0918.1018	0.864	0.765	1.236
I27_1305.1306	0.914	0.765	1.236

M22_1318.1519	0.315	0.765	1.236
M22_1413.1513	0.978	0.765	1.236
R16_1306.1307	0.946	0.765	1.236
S18_0503.0603	0.925	0.765	1.236
S10_1707.1807	0.605	0.595	0.764
L22_1112.1113	0.429	0.502	1.250
P29_0809.0909	0.325	0.502	1.250
H31_0813.0814	0.738	0.418	0.875
H31_1011.1111	0.790	0.418	0.875
H31_1311.1312	0.457	0.418	0.875
H31_1413.1414	0.719	0.418	0.875
H31_1506.1605	0.902	0.418	0.875
L22_1514.1515	0.377	0.418	0.764
M21_1811.1812	0.574	0.418	0.875
P29_0917.1017	0.566	0.418	0.764
P29_1012.1013	0.794	0.418	0.875
R16_0213.0312	0.819	0.418	0.875
R16_0609.0610	0.699	0.418	0.875
L22_0212.0213	0.935	0.262	1.320
C32_0509.0610	0.630	0	0.944
C32_0813.0913	0.624	0	0.944
C32_1415.1515	0.799	0	0.944
E24_1412.1413	0.369	0	0.584
E34_0210.0211	0.543	0	1.334
E34_0303.0403	0.543	0	1.334
E34_0417.0418	0.832	0	1.334
E34_0708.0709	0.989	0	1.334
E34_1208.1308	0.978	0	1.334
E34_1613.1614	0.788	0	1.334
F22_0802.0803	0.602	0	1.334
F22_0807.0808	0.363	0	1.334
F22_1006.1106	0.407	0	0.944
F27_1404.1504	0.955	0	0.722
H25_0310.0410	0.273	0	0.944
H25_0404.0405	0.812	0	0.944
H25_0415.0416	0.994	0	0.944
H25_0807.0808	0.948	0	0.944
H25_1415.1416	0.832	0	0.944
H31_0505.0605	0.531	0	1.166
H31_0806.0906	0.828	0	0.584
H31_1101.1102	0.426	0	1.166
I12_1106.1107	0.332	0	1.334
I27_0612.0712	0.971	0	1.306
I27_1309.1409	0.898	0	1.306
I27_1406.1407	0.910	0	0.722
I28_0307.0407	0.340	0	0.584

I28_0414.0514	0.880	0	0.584
I28_0509.0609	0.738	0	0.584
I28_1110.1210	0.247	0	0.584
I28_1505.1605	0.667	0	0.584
I28_1514.1614	0.916	0	0.584
L22_0217.0218	0.706	0	1.306
L22_0907.0908	0.389	0	0.584
L23_0405.0505	0.423	0	1.306
N9_1504.1505	0.213	0	1.334
N11_0401.0501	0.970	0	1.166
N11_0404.0504	0.692	0	1.166
N11_0411.0412	0.435	0	1.166
N11_0516.0616	0.545	0	1.166
N11_1111.1112	0.315	0	1.166
N11_1304.1404	0.840	0	1.166
N11_1514.1513	0.477	0	1.166
N13_0306.0406	0.760	0	0.722
N13_0403.0503	0.627	0	0.722
N13_0907.0908	0.371	0	0.722
N13_1412.1513	0.456	0	0.722
N13_1608.1708	0.692	0	0.722
N20_1710.1711	0.649	0	1.306
O27_0508.0509	0.384	0	1.306
O27_0513.0514	0.452	0	1.306
O27_1513.1514	0.717	0	1.306
O27_1712.1713	0.717	0	1.306
P19_1306.1307	0.635	0	1.334
P29_1517.1518	0.697	0	0.584
R16_1611.1711	0.617	0	1.166
R16_1615.1616	0.289	0	0.722
R17_1009.1010	0.378	0	1.166
R18_1505.1605	0.706	0	0.944
S10_0115.0215	0.461	0	0.944
S10_0410.0510	0.884	0	1.306
S10_0504.0604	0.471	0	0.584
S10_1415.1416	0.995	0	1.334
S10_1612.1712	0.840	0	1.334
S18_0415.0515	0.981	0	0.722
T17_0415.0416	0.704	0	0.584
T17_0812.0813	0.943	0	1.166
U10_0913.1013	0.980	0	0.722
U10_1506.1606	0.558	0	1.166
W14_0410.0411	0.780	0	0.944
W14_1111.1112	0.391	0	0.944

Table S2. Model selection statistics. *FD*: functional dissimilarity, *BDD*: branch density dissimilarity, *BID*: branching intensity dissimilarity; *TOPO*: local variation in topography (slope), ΔAIC : difference in AIC (Akaike Information Criterion) with respect to the best-fitting model (lowest value of AIC), w_i : (Akaike weight): relative likelihood of each model being the best-fitting model, given the complete set of candidate models (Burnham and Anderson, 2002). The best-supported model highlighted in bold.

Model	FD	BDD	BID	TOPO	FD x BDD	FD x BID	BDD x BID	FD x BDD x BID	ΔAIC	w_i
1	x	x	x	x	x	x	x	x	1.99	0.204
2	x	x	x		x	x	x	x	0.00	0.552
3	x	x	x		x	x	x		3.06	0.120
4	x	x	x		x	x			4.27	0.065
5	x	x	x			x	x		10.77	0.003
6	x	x	x		x		x		9.89	0.004
7	x	x	x			x			7.77	0.011
8	x	x	x		x				8.37	0.008
9	x	x	x				x		9.58	0.005
10	x	x	x						5.98	0.028

Supporting Figures

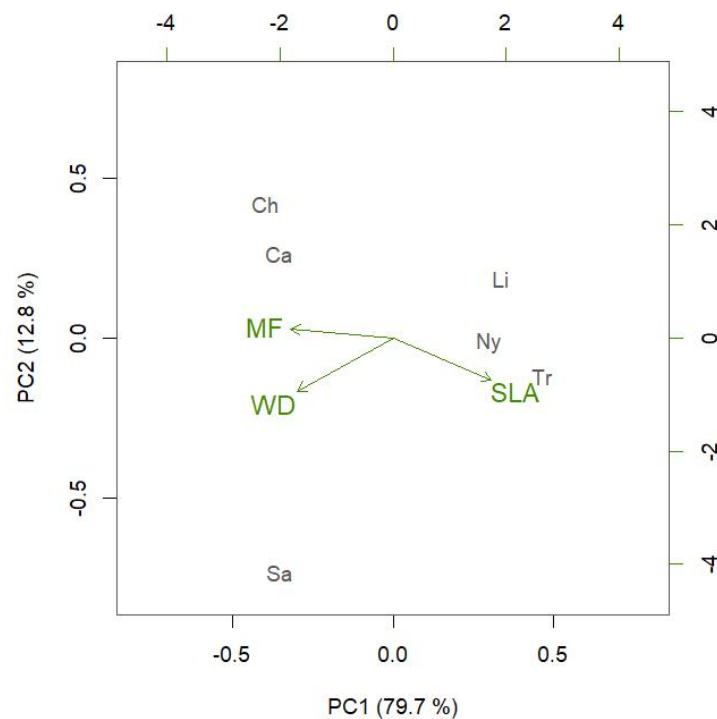


Figure S1. Principal component analysis (PCA) of standardised functional trait values for the six study species. Green arrows indicate significant correlations ($P < 0.001$) between axis scores and functional traits (SLA: specific leaf area; WD: wood density, MF: morphological flexibility). Species abbreviation: Ca: *Castanea.henryi*, Ch: *Choerospondias axillaris*; Li: *Liquidambar formosana*, Ny: *Nyssa.sinensis*, Sa: *Sapindus.saponaria*, Tr: *Triadica.sebifera*.

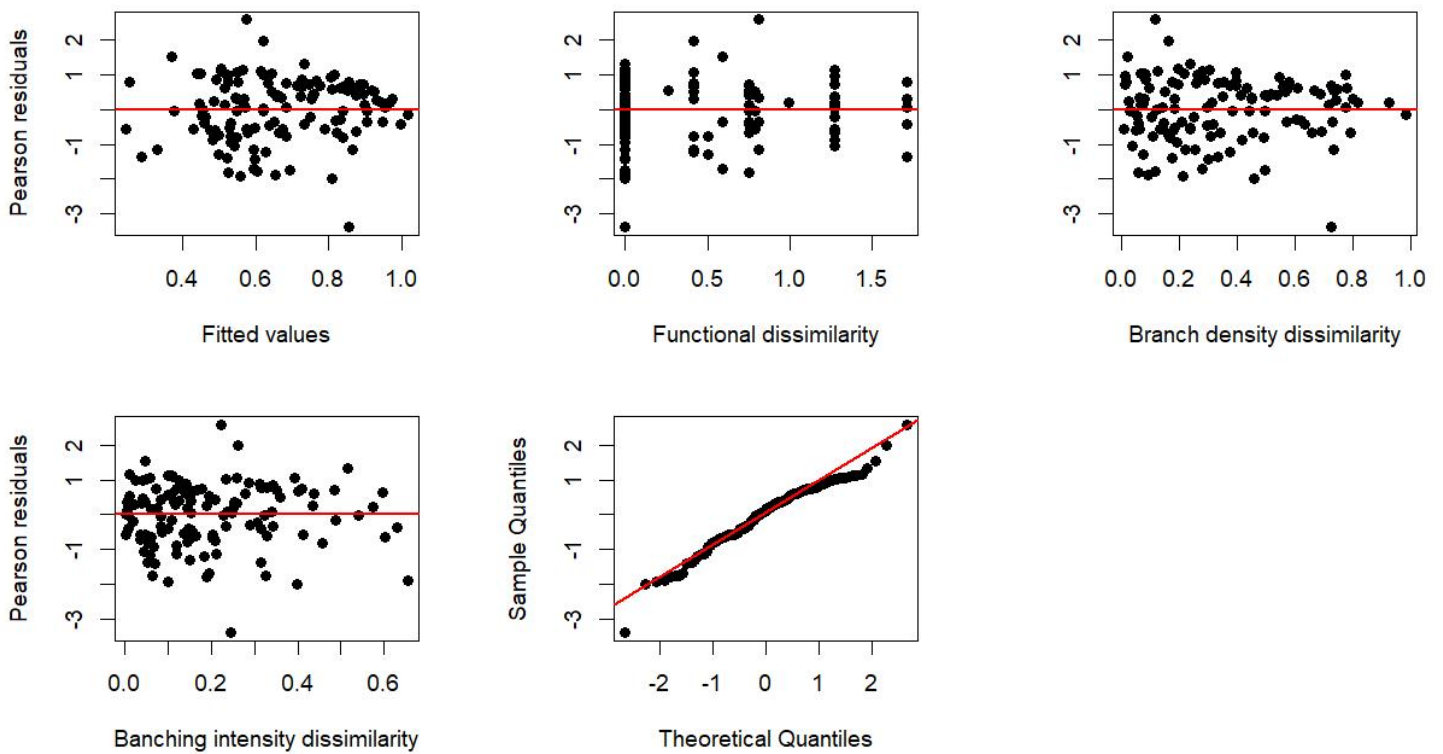


Figure S2. Model validation plots for the best-fitting generalized additive mixed model.

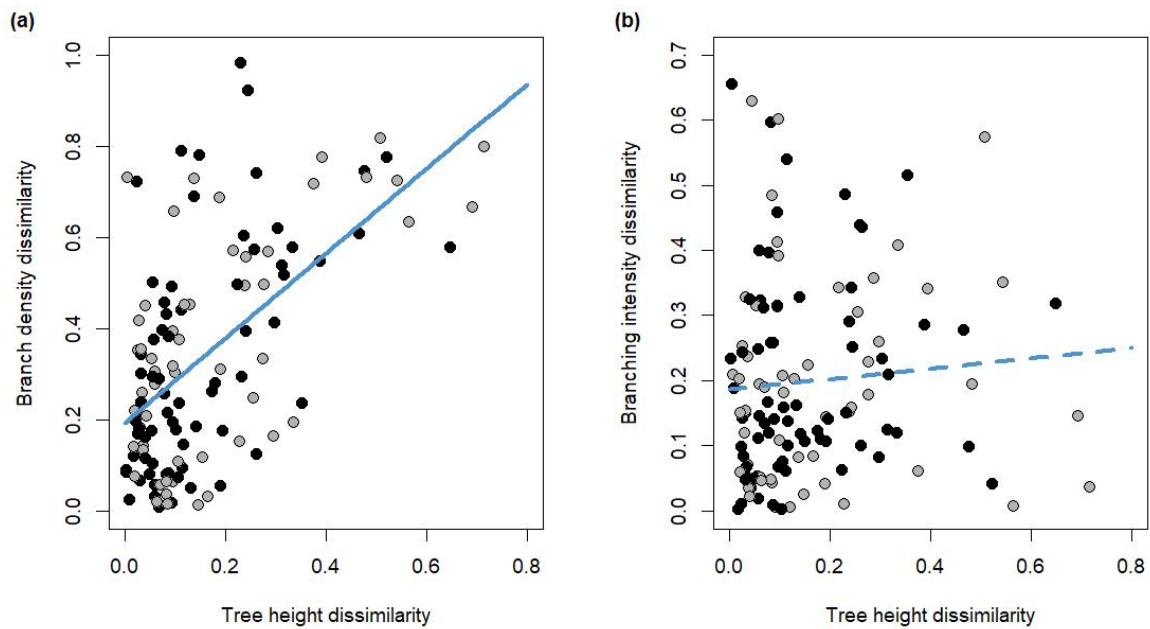


Figure S3. Relationship between tree height and a) branch density dissimilarity (BDD) and b) branching intensity dissimilarity (BID). The solid line correspond to a significant and the dotted line to an insignificant linear model fit (BDD: $r = 0.58$, $P < 0.001$; BID: $r = 0.08$, $P = 0.376$). Dots represent the observed values (dark grey: conspecific tree species pairs, light grey: heterospecific tree species pairs). Tree height dissimilarity was calculated as the absolute differences in tree height divided by the total tree height of a given TSP.

Chapter 4. Biomass allocation of trees in response to mono- and heterospecific neighbourhoods

Table of contents

Supporting Tables

- **Table S1.** Tree species combinations measured in the greenhouse
- **Table S2.** Tree species combinations measured in BEF China
- **Table S3.** Mix-effect model results for the greenhouse data grouped in TSPs

Supporting Figures

- **Fig. S1.** Photograph of the greenhouse experiment
- **Fig. S2.** Photograph of of one minirhizotron installed in BEF China
- **Fig. S3.** Boxplots of estimated biomass of the trees from BEF China by species

Supporting Tables

Table S1. Tree species combinations and the number of pairs that were sampled from the greenhouse experiment.

		Number
<i>Choerospondias axillaris</i> _ <i>Choerospondias axillaris</i>	mono	3
<i>Cyclobalanopsis glauca</i> _ <i>Cyclobalanopsis glauca</i>	mono	3
<i>Koelreuteria bipinnata</i> _ <i>Koelreuteria bipinnata</i>	mono	3
<i>Quercus fabri</i> _ <i>Quercus fabri</i>	mono	3
<i>Quercus serrata</i> _ <i>Quercus serrata</i>	mono	2
<i>Rhus chinensis</i> _ <i>Rhus chinensis</i>	mono	2
<i>Sapium sebiferum</i> _ <i>Sapium sebiferum</i>	mono	3
<i>Schima superba</i> _ <i>Schima superba</i>	mono	1
<i>Choerospondias axillaris</i> _ <i>Koelreuteria bipinnata</i>	mix	3
<i>Choerospondias axillaris</i> _ <i>Quercus serrata</i>	mix	1
<i>Choerospondias axillaris</i> _ <i>Sapium sebiferum</i>	mix	3
<i>Cyclobalanopsis glauca</i> _ <i>Quercus fabri</i>	mix	3
<i>Cyclobalanopsis glauca</i> _ <i>Rhus chinensis</i>	mix	3
<i>Cyclobalanopsis glauca</i> _ <i>Schima superba</i>	mix	2
<i>Koelreuteria bipinnata</i> _ <i>Quercus serrata</i>	mix	2
<i>Koelreuteria bipinnata</i> _ <i>Sapium sebiferum</i>	mix	3
<i>Quercus fabri</i> _ <i>Rhus chinensis</i>	mix	3
<i>Quercus fabri</i> _ <i>Schima superba</i>	mix	2
<i>Quercus serrata</i> _ <i>Sapium sebiferum</i>	mix	1
<i>Rhus chinensis</i> _ <i>Schima superba</i>	mix	3

Table S2. Species combinations, number of TSPs analysed each year, and number of plots from BEF China in which each species combination was present.

		2014	2015	2016	Plots
<i>Castanea henryi</i> _ <i>Castanea henryi</i>	mono	1	0	0	1
<i>Castanopsis sclerophylla</i> _ <i>Castanopsis sclerophylla</i>	mono	2	2	2	2
<i>Choerospondias axillaris</i> _ <i>Choerospondias axillaris</i>	mono	1	1	0	1
<i>Cyclobalanopsis glauca</i> _ <i>Cyclobalanopsis glauca</i>	mono	2	2	2	2
<i>Cyclobalanopsis myrsinifolia</i> _ <i>Cyclobalanopsis myrsinifolia</i>	mono	1	1	1	1
<i>Liquidambar formosana</i> _ <i>Liquidambar formosana</i>	mono	1	1	1	1
<i>Nyssa sinensis</i> _ <i>Nyssa sinensis</i>	mono	1	1	1	1
<i>Quercus fabri</i> _ <i>Quercus fabri</i>	mono	1	1	1	1
<i>Quercus serrata</i> _ <i>Quercus serrata</i>	mono	1	1	0	1
<i>Sapindus mukorossi</i> _ <i>Sapindus mukorossi</i>	mono	2	2	2	2
<i>Sapium sebiferum</i> _ <i>Sapium sebiferum</i>	mono	1	1	1	1
<i>Castanea henryi</i> _ <i>Diospyros glaucifolia</i>	mix	1	1	1	1
<i>Castanea henryi</i> _ <i>Koelreuteria bipinnata</i>	mix	1	1	0	1
<i>Castanea henryi</i> _ <i>Nyssa sinensis</i>	mix	1	1	1	1
<i>Castanopsis sclerophylla</i> _ <i>Choerospondias axillaris</i>	mix	1	1	0	1
<i>Castanopsis sclerophylla</i> _ <i>Cyclobalanopsis myrsinifolia</i>	mix	1	1	1	1
<i>Castanopsis sclerophylla</i> _ <i>Quercus serrata</i>	mix	2	2	1	2
<i>Choerospondias axillaris</i> _ <i>Lithocarpus glaber</i>	mix	1	1	1	1
<i>Choerospondias axillaris</i> _ <i>Quercus serrata</i>	mix	1	1	1	1
<i>Choerospondias axillaris</i> _ <i>Sapium sebiferum</i>	mix	2	2	2	2
<i>Cyclobalanopsis glauca</i> _ <i>Lithocarpus glaber</i>	mix	1	1	1	1
<i>Cyclobalanopsis glauca</i> _ <i>Nyssa sinensis</i>	mix	1	1	1	1
<i>Cyclobalanopsis glauca</i> _ <i>Quercus fabri</i>	mix	1	1	1	1
<i>Cyclobalanopsis glauca</i> _ <i>Schima superba</i>	mix	1	1	1	1
<i>Cyclobalanopsis myrsinifolia</i> _ <i>Lithocarpus glaber</i>	mix	1	1	1	1
<i>Cyclobalanopsis myrsinifolia</i> _ <i>Schima superba</i>	mix	1	1	0	1
<i>Koelreuteria bipinnata</i> _ <i>Lithocarpus glaber</i>	mix	3	3	3	2
<i>Liquidambar formosana</i> _ <i>Lithocarpus glaber</i>	mix	1	1	1	1
<i>Liquidambar formosana</i> _ <i>Quercus serrata</i>	mix	1	1	1	1
<i>Liquidambar formosana</i> _ <i>Sapindus mukorossi</i>	mix	4	4	4	2
<i>Liquidambar formosana</i> _ <i>Sapium sebiferum</i>	mix	1	1	1	1
<i>Lithocarpus glaber</i> _ <i>Quercus fabri</i>	mix	1	1	0	1
<i>Lithocarpus glaber</i> _ <i>Rhus chinensis</i>	mix	1	0	0	1
<i>Quercus fabri</i> _ <i>Sapium sebiferum</i>	mix	1	1	0	1
<i>Quercus fabri</i> _ <i>Schima superba</i>	mix	1	0	0	1

<i>Quercus serrata_Schima superba</i>	mix	1	1	1	1
<i>Rhus chinensis_Schima superba</i>	mix	1	1	0	1
Total:		47	44	35	24

Table S3. Results of mixed-effects models for the effects of pairwise diversity (mono- or hetero- specific, "Spec_Div") on the root to shoot ratio (RSR, squared root transformed), aboveground dry biomass (AG_weight, squared root transform), and belowground dry biomass (BG_weight, squared root transform) for 49 TSPs planted under control conditions in a greenhouse experiment.

Fixed effect	sqrt-RSR				sqrt-AG_weight (g)				sqrt-BG_weight (g)			
	df _m _{nu}	df _{den}	F	p	df _m _{nu}	df _{den}	F	p	df _m _{nu}	df _{den}	F	p
Intercept	-	-	-	< 0.001	-	-	-	< 0.001	-	-	-	< 0.001
Spec_Div	1	10.24	0.827	0.384	1	17.79	2.226	0.1532	1	17.78	2.417	0.1376
Marginal R ²	0.026				0.092				0.101			
Conditional R ²	0.352				0.810				0.837			

dfnum, numerator degrees of freedom; dfden, denominator degrees of freedom.

Supporting Figures



Figure S2. Photograph of the greenhouse experiment: two TSPs in their respective tubes just prior to harvesting (September 2020).



Figure S2. Photographs of one minirhizotron installed in BEF China with a plastic cover (left) and unsealed (right).

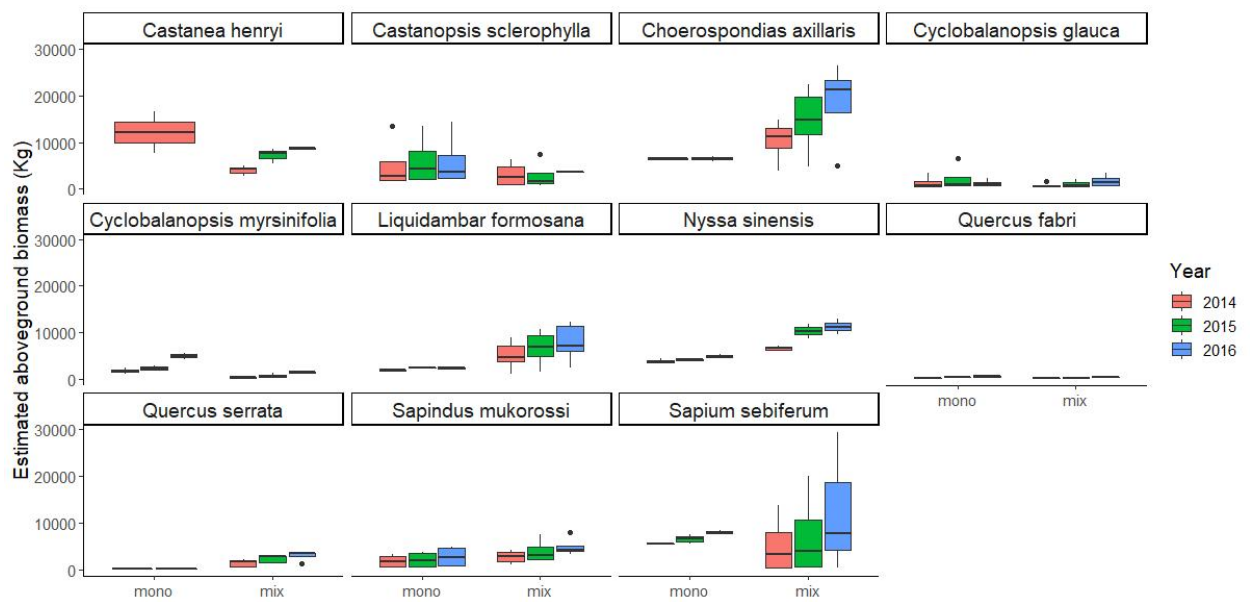


Fig. S3. Boxplot showing the estimated biomass of the trees from BEF China by species

Apendices

Table of contents

- 1. Curriculum vitae***
- 2. List of publications and conference contributions***
- 3. Declaration of originality***

Curriculum vitae

Maria D. Perles-Garcia



EDUCATION

- Doctoral researcher** **2018 – present**
German Centre for Integrative Biodiversity Research (iDiv)/
Martin-Luther-Universität Halle-Wittenberg (MLU)
- Dissertation title: Forest canopies and tree diversity: from stands to tree-tree interactions
 - Principal investigator: Prof. Dr Goddert von Oheimb
- M. Sc. Forest Information Technology** **2015 - 2018**
HNE Eberswalde and University of Life Sciences Warsaw (SGGW)
- B. Sc. and M. Sc. in Environmental Sciences** **2007 - 2013**
University of Granada

PROFESSIONAL EXPERIENCE, GRANTS AND VOLUNTEERING

- Supervision experience** **2019 – 2021**
- Co-supervision of two master thesis
- DAAD STIBET: Internship at World Agroforestry Centre, Kyrgyzstan** **Oct – Nov 2017**
- Field campaign and comparison with satellite image
- Student assistant. HNE Eberswalde** **WS 2016/2017**
- Management and analysis of LiDAR data.
- Internship at Landeskompentzzentrum Forst Eberswalde** **WS 2016/2017**
- Development of an interactive web map
- HNEE-Deutschlandstipendium** **2016 – 2017**
- Grant to particularly successful and committed students.
- Administrative assistant. HM Sanchinarro Hospital, Madrid** **2014 – 2015**
- Statistics, citation, billing and unification of the database
- Volunteering in students' union CSE Granada** **2012 – 2014**
- Development of social and environmental initiatives.
- Student assistant. University of Granada** **2012 – 2013**
- Introducing new ECTS credit system to students
- Volunteering in Tayrona National Park, Colombia** **Dec. 2012**
- Diagnosis of waste management
- Freelance tutor for high school students, Alicante** **2008 - 2010**

- Private teacher for students between 12 and 16 years

Volunteering for Intermon Oxfam and Greenpeace

2006 - 2007

- Informing people of their work

LANGUAGES

Spanish (native speaker level), English (advanced level), Catalan (upper intermediate level), German (intermediate level).

TECHNICAL SKILLS

- Programming skills and mathematical packages: R, MATLAB, Python, Visual Basic, PHP, SPSS.
- ArcGIS (ArcMap, ArcScene, ArcCatalog and ArcOnline), QGIS, GvSIG
- Remote sensing images edition with ERDAS Imagine
- Database management: Git, Access, XAMPP
- LiDAR processing: FARO Scene, RiSCAN Pro, CloudCompare, LAStools, TreeQSM
- Microsoft Office, OpenOffice, R Markdown, LaTeX

ADDITIONAL SKILLS AND INTERESTS

Car owner with full (clean) driving license B.

Extensive international travel background. Travels in Europe, Africa, Asia and Latin America.

Comfortable working with and in different cultures.

List of Publications and conference contributions

PUBLICATIONS

- Hildebrand, M., **Perles-Garcia, M. D.**, Kunz, M., Härdtle, W., von Oheimb, G., & Fichtner, A. (2021). Tree-tree interactions and crown complementarity: The role of functional diversity and branch traits for canopy packing. *Basic and Applied Ecology*, 50, 217–227. <https://doi.org/10.1016/j.baae.2020.12.003>
- Perles-Garcia, M. D.**, Kunz, M., Fichtner, A., Härdtle, W., & von Oheimb, G. (2021). Tree species richness promotes an early increase of stand structural complexity in young subtropical plantations. *Journal of Applied Ecology*, (June), 1–10. <https://doi.org/10.1111/1365-2664.13973>
- Perles-Garcia, M. D.**, Meyer, N., Kunz, M., Fichtner, A., Härdtle, W., & von Oheimb, G. (2022). Neighbourhood species richness reduces crown asymmetry of subtropical trees in sloping terrain. *Remote Sens.*, 14(6), 1441. <https://doi.org/10.3390/rs14061441>
- Perles-Garcia, M. D.**, Fichtner, A., Haider, S., Gu, H., Bu, W., Kunz, M., Härdtle, W., & von Oheimb, G. (2022). Biomass allocation of trees in response to mono- and heterospecific neighbourhoods. Manuscript in preparation
- Koller, A., **Perles-Garcia, M. D.**, Kunz, M., Fichtner, A., Härdtle, W., & von Oheimb, G. (2022). The influence of tree architectural traits and stand characteristics on stand structural complexity in a young biodiversity experiment in subtropical China. Manuscript in preparation.
- Beugnon, R., Bu, W., Bruelheide, H., Davrinche, A., Du, J., Haider, S., Kunz, M., von Oheimb, G., **Perles-Garcia, M. D.**, Saadani, M., Scholten, T., Seitz, S., Singavarapu, B., Trogisch, S., Wang, Y., Wubet, T., Xue, K., Yang, B., Cesarz, S., & Eisenhauer N. (2022). Abiotic and biotic drivers of scale-dependent tree trait effects on soil microbial biomass and soil carbon concentration. Manuscript submitted for publication.
- Schnabel, F., Beugnon, R., Bo, Y., Castro Izaguirre, N. C., Cesarz, S., Eisenhauer, N., **Perles-Garcia, M. D.**, Haehn, G., Härdtle, W., Huang, Y., Kunz, M., Liu, X., Niklaus, P. A., von Oheimb, G., Pietsch, K. A., Richter, R., Schmid, B., Trogisch, S., Wirth, C., Ma, K. & Bruelheide, H. (2022). The role of tree species richness for temperature buffering below forest canopies. Manuscript in preparation.

CONFERENCE PRESENTATIONS

Oral presentations

- “Spatial aboveground complementarity: Spatio-temporal dynamics of canopy space filling”. TreeDì Conference, Beijing, March 2019.
- “Spatio-temporal dynamics of individual-tree crown plasticity as affected by local neighbourhood interaction in BEF-China”. Gesellschaft für Ökologie (GfÖ) conference, Münster, September 2019.

- “Spatial aboveground complementarity - Stand structural complexity and its relationship with tree species richness”. TreeDi seminar series, online, September 2020.
- “Tree canopies and biodiversity: From stands to tree-tree interactions. World Biodiversity Forum (WBF), Davos, June 2022

Poster presentations

- “Spatio-temporal dynamics of individual-tree crown plasticity as affected by local neighborhood interactions in BEF-China”. iDiv conference, Leipzig, August 2019

Declaration of originality - Eigenständigkeitserklärung

Hiermit erkläre ich, dass ich die vorliegende Doktorarbeit mit dem Titel „ Forest canopies and tree diversity: from stands to tree-tree interactions “ eigenständig und ohne fremde Hilfe verfasst sowie keine anderen als die im Text angegebenen Quellen und Hilfsmittel verwendet habe. Textstellen, welche aus verwendeten Werken wörtlich oder inhaltlich übernommen wurden, wurden von mir als solche kenntlich gemacht. Ich erkläre weiterhin, dass ich mich bisher noch nie um einen Doktorgrad beworben habe. Die vorliegende Doktorarbeit wurde bis zu diesem Zeitpunkt weder bei der Naturwissenschaftlichen Fakultät I – Biowissenschaften der Martin-Luther-Universität Halle-Wittenberg noch einer anderen wissenschaftlichen Einrichtung zum Zweck der Promotion vorgelegt.

Maria Dolores Perles Garcia, 14.07.2022